COMPARATIVE ANALYSIS OF LIMITED AND FULLY COMPOSITIONAL SIMULATION OF A NIGER DELTA GAS-CONDENSATE RESERVOIR

A Thesis Submitted to the Faculty at African University of Science and Technology in partial fulfilment of the requirements for the degree of Master of Science in the Department of Petroleum Engineering

By

ALONGE Oluwaseun Tolulope

Supervised by

Professor David Ogbe

Abuja, Nigeria

June 2021

CERTIFICATION

This is to certify that the thesis titled “COMPARATIVE ANALYSIS OF LIMITED AND FULLY COMPOSITIONAL SIMULATION OF A NIGER DELTA GAS CONDENSATE RESERVOIR” submitted to the school of postgraduate studies, African University of Science and Technology (AUST), Abuja, Nigeria for the award of the Master's degree is a record of original research carried out by ALONGE OLUWASEUN TOLULOPE in the Department of Petroleum Engineering.

COMPARATIVE ANALYSIS OF LIMITED AND FULLY COMPOSITIONAL SIMULATION OF A NIGER DELTA GAS-CONDENSATE RESERVOIR

By

ALONGE Oluwaseun Tolulope

A THESIS APPROVED BY THE PETROLEUM ENGINEERING DEPARTMENT

RECOMMENDED:

Supervisor: Prof. David O. Ogbe

.....

Committee: Dr. Alpheus Igbokoyi

.....

Committee: Dr. Saka Matemilola

.....

Head, Department of Petroleum Engineering

APPROVED: .....

Chief Academic Officer

.....

Date

COPYRIGHT

ABSTRACT

Numerical simulators estimate the recovery volumes and the volume of fluids in-place in the reservoir as a function of time and space by solving complex partial differential fluid flow equations. For gas condensate reservoirs, fully compositional modelling is preferred because, in addition to determining fluid saturations, it tracks the compositional changes for each hydrocarbon component. Nonetheless, the complex data requirements, computing memory, costs, and the time required to undertake a fully compositional simulation can be significant. Limited compositional simulation extends the application of conventional black oil models to composition-dependent systems by utilizing modified phase behaviour to determine phase pressures and fluid saturation.

This research work evaluates the performance of a gas condensate reservoir using both fully and limited compositional simulators to investigate the pressure depletion, gas injection, water injection, simultaneous water and gas injection (SWAG), and water-alternating-gas (WAG) injection scenarios. The limited compositional case incorporates a four-component miscible flood model and Todd Longstaff mixing parameter to simulate the recovery schemes. Fluid composition was obtained from a reservoir fluid in the Niger Delta for analysis and tuned to match experimental data using the Peng Robinson EOS, to describe fluid behaviour and generate PVT properties. Comparative studies are conducted for the cumulative condensate and gas production, field water cut, reservoir pressure decline, injectivity, and ultimate recovery of the reservoir for the limited and fully compositional models, respectively.

Results indicate that the limited and fully compositional models give comparable values of the initial fluid-in-place volumes. The fully compositional model always predicts a higher condensate recovery than the limited compositional model for all the recovery schemes. SWAG injection scheme provides the maximum pressure maintenance and recovery of condensate. However, gas injection minimizes water production. The limited compositional simulator can be used as a screening tool and for the rapid evaluation of reservoir performance at the early stages of condensate reservoir development when data is scarce.

Keywords: Fully compositional simulator, limited compositional simulator, gas condensate, reservoir performance, depletion, gas injection, waterflooding, water alternating gas injection, simultaneous water and gas injection, oil recovery optimization

DEDICATION

I dedicate this thesis to God, the Almighty, my dear father, Mr. Folayomi Alonge, and amazing superhuman, Mrs. Alonge, my siblings, and friends who have been an instrumental support system during my graduate studies.

ACKNOWLEDGEMENT

Foremost, my immense gratitude to God Almighty for granting me the grace to accomplish this dream of mine. The prayers, advice, and contributions of my family members are greatly valued.

My appreciation goes to my thesis advisory committee members in the persons of Dr. Alpheus Igbokoyi and Dr. Saka Matemilola. Dr Igbokoyi's fatherly advice and huge support for student's academic, mental, and social welfare during this program were not unnoticed. I appreciate Dr. Saka Matemilola for providing insight on implementing best petroleum industry practices in this thesis. I want to acknowledge the entire academic faculty at the Department of Petroleum Engineering for imparting the technical knowledge and skills which has formed the foundation on which my understanding of petroleum engineering is now based. I am very grateful for the commercial simulation software package and library database that was used and consulted while undertaking this research.

Most especially, I want to appreciate my supervisor, Professor David Ogbe, for his efforts to ensure that successful research work was delivered. He was willing to proffer solutions to challenges that arose along the line despite his other commitments and busy schedule. The consistent weekly meetings and progress reports kept me encouraged, and on track.

A huge thank you to Dr. Petrus Nzerem for believing in me and supporting this dream of mine. Finally, the friendship, support, and kindness of my colleagues, particularly Israel and Awal, as well as my roomie, Halima, were a huge blessing to me during my study. I am grateful to have you all as friends.

TABLE OF CONTENT

LIST OF FIGURES

LIST OF TABLES

CHAPTER ONE: INTRODUCTION

1.1 BACKGROUND OF STUDY

Oil and natural gas extracted from subsurface reservoirs dominate the energy mix for many nations. However, the prevailing low-price environment in the industry requires petroleum companies to make sound engineering decisions to optimize recovery from hydrocarbon reservoirs. The sales price per volume of oil is significantly higher than that of gas, hence, the gas rate and condensate yield from production significantly impacts the financial bottom-line of upstream players operating gas condensate assets (Syzdykov, 2014).

The chemical and physical properties of the hydrocarbon mixture within the reservoir are used to categorize the reservoir fluids. Conventionally, the classification of these reservoir fluids is dependent on their initial state relative to the critical point and the compositional changes that occur within the phase envelope during isothermal depletion (Tarek, 2018). Gas condensate reservoirs lie between the critical point and the cricondentherm and are sources of valuable natural gas liquids, and condensates. At the initial state, gas condensate fluid exists completely in the vapor phase in the reservoir. However, as pressure depletion occurs, liquid begins to condense from the vapor when the dewpoint pressure is reached. Further decline in pressure increases the condensation rate until a maximum liquid dropout level is reached. Usually, this liquid will remain immobile if its critical saturation is not exceeded and cannot be produced. Subsequent depletion of the reservoir pressure will cause the condensates to re-vaporize into the gaseous phase (Tarek, 2018).

There is a high tendency to lose these light-end hydrocarbon liquids if sound reservoir management decisions are not applied. Asides from the loss of valuable liquid production to the reservoir, the gas well productivity is significantly reduced due to condensate blockage, which reduces gas transmissibility through the reservoir pore spaces. Hence, condensate banking has proved to be challenging, especially in today's uncertain market climate where oil price volatility is prevalent. The presence of reservoir heterogeneities and the imbalance between withdrawal and injection rates may cause traditional pressure maintenance techniques such as water flooding or gas cycling to be less effective since the added energy is not instantaneously transmitted from the injector to the producer. Nonetheless, they are still widely employed to optimize reservoir performance and condensate recovery by keeping the reservoir pressure above or close to the dewpoint pressure (Whitson & Brule, 2000).

Reservoir simulation is a versatile tool for modelling and optimizing hydrocarbon recovery from near critical-reservoirs. The black oil model, which is widely applied, produces variable results because it neglects the dependency of fluid properties on the composition of the hydrocarbon system. Limited compositional models incorporate compositional changes that occur during pressure decline while minimizing the run time and costs associated with full compositional models (Bolling, 1987).

1.2 PROBLEM STATEMENT

Pressure depletion using solely the primary energy of a gas condensate reservoir is not advisable. To optimize condensate recovery, reservoir intervention through pressure maintenance methods must be executed in the field.

Numerical simulation enables engineers to evaluate several reservoir management strategies while eliminating the operational costs as well as the financial, safety, and environmental risks associated with undertaking such operations in real-time. The choice of the simulator to use depends on its ability to adequately model the flow mechanics and physics occurring in the reservoir. Black oil models are often too simplistic to capture the flow physics of composition-dependent systems such as gas condensates, near-critical volatile oil, as well as miscible displacement processes (Karacaer, 2014). Phase behaviour and dynamic reservoir modelling of gas condensate reservoirs can be rigorously evaluated using a compositional model and numerical simulation software. Fully compositional models require complex data, significant computing time, and costs during simulation studies, which may not be affordable for marginal field operators. Moreover, although fully compositional models are sophisticated and applicable to any reservoir system, they may not be necessarily required to investigate all reservoir development scenarios. Extended black oil models have increasingly been applied to gas condensate reservoir modelling. In the extended models, the traditional two-phase, three-component model is modified to a three-phase, four-component system using the Todd-Longstaff mixing parameter to achieve varying degrees of miscibility during injection studies (Karacaer, 2014). This allows comprehensive simulation studies of composition-dependent systems to be conducted at a reduced cost and time, without the need for detailed data which fully compositional simulators require.

1.3 JUSTIFICATION OF STUDY

The earliest attempt to evaluate reservoir performance in the oil and gas industry was the use of analogs (Ertekin, Abou-Kassem & King, 2001). Data from a field with similar geologic

characteristics were used to benchmark reservoir management decisions. The process of acquiring this data may be difficult and time-consuming. Since no two reservoirs are entirely the same, the use of analogous data may include inherent errors that may not be foreseen by the reservoir engineer. Decline curve analysis and material balance equations require extensive production data and may not be suitable for field development planning in new frontiers or injection scenarios where no appreciable decline in pressure is observed (Ertekin et al., 2001). Also, decline curve analysis is limited because of the assumption that the pre-existing operational conditions are sustained throughout the life of the reservoir. Material balance calculations are somewhat idealistic, taking no account of geologic complexities that are obtainable in a typical reservoir drained by multiple wells (Ertekin et al., 2001; Ghahri, 2018).

Reservoir simulation utilizes computational algorithms to model reservoir properties and fluid flow processes (Aziz & Settari, 1979). It can be applied to any stage of the reservoir life cycle for optimization purposes. Benefits of reservoir simulation include:

- Reduction of investment risks
- Determination of the best reservoir development plan
- Prediction of reservoir performance and rate under various operational schemes
- Design and optimization of facilities and equipment capacities.
- Identification of new opportunities for incremental recovery of gas and condensates
- Description and characterization of reservoir fluids and reserves distribution.
- Well planning optimization such as the number of wells and location, as well as the sequence of drilling.
- Assessment of interventions that can prolong the reservoir life (Aziz & Settari, 1979; Ghahri, 2018).

1.4 AIM OF STUDY

This study aims to evaluate the recovery performance of gas condensate reservoirs using limited and fully compositional reservoir simulation models. It describes how to improve hydrocarbon recovery and optimize the development of gas condensate reservoirs through four production schemes, i.e., natural depletion, pressure maintenance by gas injection, water-alternating-gas (WAG) injection, and simultaneous water and gas injection (SWAG).

1.5 RESEARCH OBJECTIVES

To achieve the aim of this research, the following objectives will be accomplished:

1. To develop gas condensate reservoir models using both limited compositional and fully compositional simulators.
2. To evaluate the performance of a gas condensate reservoir under four recovery scenarios: primary depletion without any fluid injection, gas injection (GI), water-alternating-gas injection (WAG), and simultaneous water and gas injection (SWAG) scheme.
3. To determine the impact of miscibility, reservoir heterogeneity, and injection parameters on condensate recovery for the full and limited compositional reservoir models.
4. To compare the results between the fully compositional (base case) and limited compositional simulators and perform sensitivity analysis of the effect of subsurface uncertainties on the condensate reservoir performance.
5. To propose the optimal strategy for producing the gas condensate reservoir.

1.6 SCOPE OF STUDY

This research investigates the fully and limited compositional modelling in a Niger-Delta gas condensate reservoir. The dynamic modelling involves limited reservoir development using a few production and injection wells over a 20-year period to determine the reservoir performance and the mechanism of condensate banking. The scope of this study is limited to recovery strategies under natural depletion, water injection, gas injection, water-alternating-gas injection (WAG), and simultaneous water and gas injection (SWAG) scenarios. The reservoir is assumed to be homogenous, and the study does not consider the effect of heterogeneities on reservoir performance. Extensive investigation into injection patterns, WAG ratio and cycles are not explored in this study.

1.7 ORGANIZATION OF THE STUDY

This thesis documenting this research work is presented in five Chapters. Chapter One is an introduction to describe the background, aims and objectives and the scope of work. A literature review of major publications related to this study is presented in Chapter Two to improve our understanding of the challenges and opportunities of producing condensate reservoirs. Chapter Three is the research methodology, and it describes the data collection and quality validation, fluid characterization, model building, and the numerical simulations along with the assumptions made to meet the study objectives. Results obtained from the study are discussed in Chapter Four. It also contains the explanations for the major observations derived from this work. Finally, the conclusions derived from the study and

recommendations proposed for further studies to improve this research are presented in Chapter Five.

CHAPTER TWO: LITERATURE REVIEW

2.1 INTRODUCTION

This chapter explores existing research on reservoir simulation. It discusses theories on gas condensate fluid behaviour, the formulation and application of limited and fully compositional simulators, as well as various reservoir development strategies. It also presents literature on the generation of PVT data and the equation of state to characterize the reservoir fluid. The literature review provides a progression of historical knowledge on the various concepts that form the foundation on which this research work is based. It helps to identify the research gap and motivates to provide a solution to or shed more light on it.

2.2 NIGER DELTA PETROLEUM SYSTEM

The following discussion on the Niger Delta petroleum system is taken primarily from Tuttle et al. (1999). The Niger Delta petroleum system, located in the Gulf of Guinea, is the 12th largest in the world with an estimated proved reserves of 34.5 billion barrels of oil (BBO) and 93.8 trillion cubic feet of gas (TCF) (Doust, 1990; Tuttle et al., 1999). Reserves distribution was bifurcated into a high density, hydrocarbon-prolific region, and a region consisting of fields with sub-commercial accumulation.

Sediments accumulated in five major depobelts of approximate width of 30-60km each, which are bound by a major structural fault to the north, and a counter regional fault in the south of the delta. The geologic strata of the region consist of three main formations, each of distinct lithology. The Akata formation includes marine shales in the lower portion, which are overlain by turbidites as well as minor clay and silt facies in the upper portion (Tuttle et al., 1999). At about 6000m thick, it serves as the source rock for petroleum generation in the province (Edejawe, 1961). The Agbada formation is the hydrocarbon-bearing rock of predominantly deltaic clastic and unconsolidated sandstone facies. The Agbada formation is approximately 4500m thick and characterized by an alternating sequence of intercalated shales that serve as seals (Edejawe, 1961). The net-to-gross ratio is approximately 50% in the lower region of the formation and decreases upwards, with the upper region constituting more sand than shale beds (Tuttle et al., 1999). At the top, the 2000m thick Benin formation functions as the cap-rock, consisting of continental and alluvial sand beds (Edejawe, 1961). The geothermal gradient ranges from 1.0°F/100ft in the Benin formation, 1.5°F/100ft in the Agbada sedimentary sequence, to 3.0°F/100ft in the Akata shales.

Edejawe (1961) noted that the type of hydrocarbon generated was influenced by the nature of the organic matter deposited, thermal conditions, and burial time. Sedimentation of prograded depobelts occurred between the Late Jurassic and Cretaceous, however petroleum generation continues to date. Edejawe et al. (1984) developed a model for the development of the delta by constructing and interpreting oil-genesis monographs using the sediment burial rate, geothermal gradient, and the age of the sedimentary basin. They noted that temperature conditions exerted significant influence on the oil-gas mix in the Niger-Delta. During the period of active deposition and subsidence of the source rocks, the oil generative window occurred at temperatures ranging between 284-295°F and at greater depths (9840-17060ft). The hydrocarbons generated included wet gas, condensates, and dry gas. Post- subsidence, the oil window moved vertically upwards causing oil maturation at shallower depths and lower temperatures. This led to the generation and expulsion of heavier crude fractions in the lower Agbada formation (Edejawe et al., 1984)

Petroleum accumulation in the Agbada formation is aided by the combination of structural and stratigraphic traps. Growth faults, rollover anticlines, clay channels, and collapsed crest structures form the majority of trapping mechanisms in the region closest to the shore. However, stratigraphic traps are more prevalent in the deeper offshore. Pinch out traps originate where the shale sequence graduate into the sand beds, diapirs resulting from an imbalance of gravity forces amongst beds, and shale lenses are commonly found in the province (Tuttle et al., 1999). The reservoirs, when discovered are typically over-pressured with an associated gas cap. The average reservoir thickness is between 10 and 40 meters but could be as high as 100 meters in few cases. Low compactional forces make the porosity and permeability to be as much as 40% and 2 Darcy, respectively (Tuttle et al., 1999). The primary energy drive is through gas cap expansion except in instances where aquifer support is significant. Common technical challenges encountered in the Niger Delta include coning, sand production, wax deposition, and high gas-oil ratios. Fluid properties vary on the reservoir level. However, the oil gravity ranges between 16 – 50°API with low concentrations of sulphur (0.1 – 0.3%), carbon dioxide, and nitrogen. In some cases, trace amounts of metals including Nickel have been observed (Tuttle et al., 1999).

2.3 RETROGRADE GAS CONDENSATE RESERVOIRS

2.3.1 Overview of Gas Condensate Reservoirs in Nigeria

As the world demand for energy increases, there is increased demand to develop petroleum reserves. Nigeria's proved crude (condensate and oil) reserves is estimated to be between 34 and 37 billion barrels, amounting to 25% of its discovered petroleum resources as well as 90% of export revenue (Nwabueze, 2000). However, low oil price and quota cuts stipulated by OPEC can severely impact the Nigerian economy. In addition, the responsibility to leave a low carbon imprint in the environment has made the exploitation and utilization of natural gas more attractive. Natural gas typically exists as a gas at high temperatures and pressures but may exhibit condensate production when pressure conditions decline. Condensates have a higher market value than oil and gas combined. Therefore, condensate production can cushion the impact of production restrictions since it is not regulated by OPEC and also enhance the conservation of oil reserves (Nwabueze, 2000).

2.3.2 Retrograde Gas Condensate Phase Behavior

According to Tarek (2018), the variation in physical and chemical properties and the phase behaviour of a hydrocarbon mixture relative to pressure and temperature changes are used to classify reservoir fluids. Phase diagrams illustrate phase behaviour at the reservoir and surface conditions. Petroleum reservoirs are broadly categorized into oil and gas reservoirs as seen in Figure 2.1. The temperature of an oil reservoir represented by the dashed line KBF, is less than the critical temperature, while natural gas reservoirs have an initial temperature that is greater than the critical temperature. The critical point C denotes a region in which the properties of the liquid and vapor phase cannot be differentiated. The bubble point curve, ABC and the dewpoint curve, CDE separate the liquid phase and the vapor phase from the two-phase region, respectively. The region inside the phase envelope encloses lines of variable liquid and gas saturations existing in equilibrium (Tarek, 2018).

Natural gas reservoirs are further sub-classified into three types. In wet gas reservoirs, the hydrocarbon mixture exists in the gaseous phase in the reservoir irrespective of pressure decline. However, condensate dropout occurs at surface facilities where low pressures and temperature are prevalent (Tarek, 2018). On the other hand, the phase change that occurs in a dry gas reservoir is independent of the operating constraints that are imposed. The reservoir fluid remains in the vapor phase both in the reservoir and at the surface at all pressures (Tarek, 2018). The etymology of retrograde gas condensate reservoirs is derived from their

unusual phase characteristics as pressure decreases. At initial conditions (point L) in Figure 2.1, the reservoir temperature is higher than the critical temperature but less than the cricondentherm, and the fluid is completely gas.

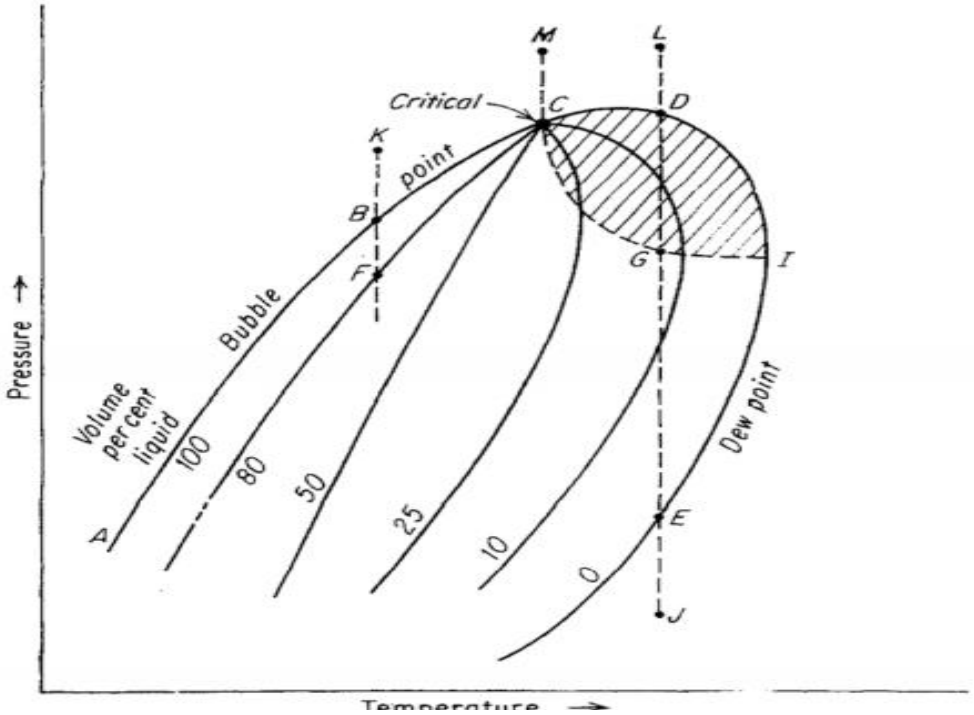

Figure 2-1: P-T phase diagram of a gas condensate reservoir (Tarek, 2018)

During isothermal depletion (line LDGEJ), liquid condenses out of the vapor when the pressure drops to the dewpoint pressure (point D) and below. This retrograde condensation is unusual as it is expected that gas expansion should occur when pressure declines. Tarek (2018) suggests that as the molecules of the light and heavier components of the gas move apart due to expansion, the attraction force between the heavier components becomes stronger, causing them to coalesce and condense out of the vapor phase. The volume of liquid dropout increases as pressure falls until a maximum value is reached before the commencement of re-vaporization of the liquid molecules. At the lower dewpoint pressure (point E), only single-phase fluid will be in the reservoir. Gas condensate reservoirs are typically found at depths between 5000ft to 10,000ft. Initial pressure and temperature occur in the range of 3000psi to 8000psi, and 200^0F and 400^0F, respectively (Tarek, 2018). Gas-oil-ratio in gas condensate wells range between 8,000 to 70,000 scf/STB, and oil gravities of up to 40-60^0 API. The initial condensate gas ratio (CGR) measures the liquid content of the gas condensate fluid and can be as high as 350STB/MMscf for rich condensates (Tarek, 2018). Figure 2.2 summarises the classes of condensate fluids (Nwabueze, 2000).

CLASS	SOURCE	DENSITY RANGE	APPEARANCE	RVP
Heavy	Retrograde Gas Wells	40 – 60 °API	Brown, Orange, Green, Water-White	< 13
Medium	Wet Gas Wells	55 – 75 °API	Water-White	< 14
Light	Dry Gas Wells/Separator Gas	> 75 °API	Water-White	> 14

Figure 2-2:Classes of condensates (Nwabueze, 2000).

2.3.3 Condensate Banking

Condensate production can occur from four sources: volatile oils, wet gas, dry gas, or retrograde gas condensate reservoirs (Nwabueze, 2000). The volume of condensate that drops out in gas condensate reservoirs is a function of the differential between the reservoir pressure and dewpoint pressure. The condensate saturation profile changes with lateral distance from the wellbore, decreasing outwards as the reservoir boundary is approached. Hence, three distinct flow regions within the reservoir are observed. Figure 2.3 is a schematic to show the flow regions (Fan et al., 2005). Two-phase flow of condensate and gas occurs in the first and second regions closest to the well, where the pressure drawdown is highest and below the dewpoint region (Fan et al., 2005), while single-phase gas flow is observed farther away from the wellbore.

In Region 1 of Figure 2.3, the PVT characteristics of the flowing fluid are identical to that of a constant composition expansion zone since the condensate gas ratio is constant (Fan et al., 2005). The condensate saturation is higher than the critical saturation, enabling the simultaneous flow of gas and condensate. The gas permeability declines because of lower saturation conditions, which can restrict the flow of gas towards the wellbore. Increasing the gas production rate may increase the relative permeability, but it will still be lower than the observed relative permeability if condensate build-up did not exist in the region. The first region can extend from 10ft for lean condensates up to 100ft for rich condensates sources (Fan et al., 2005). The boundary between any two regions, which are dynamic and move outwards with time, is estimated by the fluid composition (Fan et al., 2005).

In Region 2, the pressure is below the dew-point but the gas flowing has lesser CGR. The condensate in the second region is immobile and represents somewhat a transition zone of varying gas and condensate saturations. Condensate saturation increases from 0 at the boundary with Region 3, to the critical saturation at the boundary with Region 1. The flowing

gas gets leaner as it approaches the wellbore. If the reservoir is large, the average pressure in the third region will be above the dewpoint and only single-phase gas will flow (Fan et al., 2005).

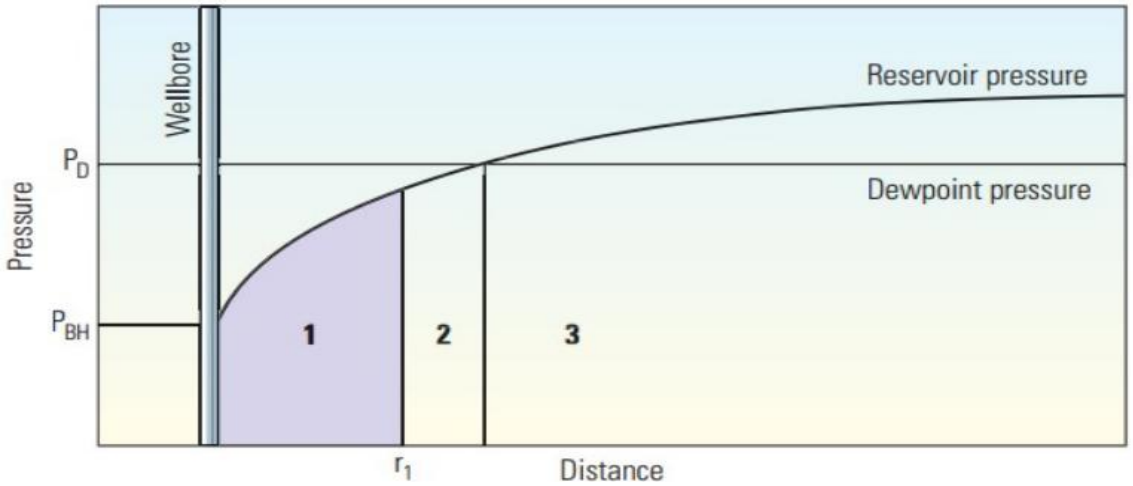

Figure 2-3:Condensate banking profile in a reservoir (Fan et al., 2005)

Condensate banking has been identified as one of the reasons for the low recovery and performance of gas condensate reservoirs. Fan et al. (2005) notes that at high rates, Forcheimer effects may also limit gas relative permeability since the gas molecules slow down after entering a pore throat. Forcheimer effects occur due to the additional pressure drawdown that occur as a result of non-Darcy flow. High flow rates give rise to a rate-dependent skin effect, which leads to higher condensate dropout and lower gas relative permeability. Subsequently, the gas flow rate reduces. Even at low flow rates, the balance between viscous force (arising from high gas velocities) and high capillary forces enables condensate saturation to build up over time in lean condensate reservoirs. Afidick et al. (1994) performed well test analysis and compositional simulation of gas condensate reservoir in the Arun field to determine the effect of condensate dropout on well productivity. They confirmed that condensate blockage can decrease the well productivity by 50% in the wellbore vicinity.

According to Wheaton (2000), the compositional changes that occur in the vicinity of the wellbore are a function of the pressure differential and the type of gas condensate fluid in the reservoir. The molar percentage of the heavier components will increase as pressure continues to fall below the dewpoint. The rate of change in the composition of the pentane plus fraction is faster for a rich gas condensate fluid. Reservoir rock properties also influence condensate drop-out behaviour. Condensate banking is more severe in low permeability reservoirs with rich gas condensate (Wheaton, 2000). Capillary pressure effects can cause

condensate build up to increase even if the offending well is shut in (Wheaton, 2000). Therefore, it is necessary to understand the dynamics of retrograde condensate accumulation for proactive operations management. Sound technical planning and engineering design are required to ensure proper flow assurance through the reservoir, wellbore, and production flowlines (Syzdykov, 2014).

2.4 IMPROVED OIL RECOVERY

Fluid flow towards the wellbore is aided by the pressure difference between the reservoir pressure and the bottom hole pressure. Improved oil recovery (IOR) typically refers to any process or practice that improves oil recovery even though it is often used interchangeably with enhanced oil recovery. Therefore, improved oil recovery includes EOR processes as well as other practices such as waterflooding, pressure maintenance, infill drilling, fracturing, and horizontal wells.

Figure 2-4 adapted from Lake (1989) illustrates the methods of oil recovery. The in-situ energy of the reservoir comes from the combination of reservoir rock and fluid expansion, and gravity forces. This is known as the primary drive mechanism. Although water influx from the adjacent aquifer, the expansion of solution and gas cap gas, gravity segregation, and compaction contribute to the overall displacement process, one of them is usually the dominant drive mechanism during the productive life of a reservoir (Lake, 1989; Tarek, 2018). The ultimate recovery from the reservoir is a function of the drive mechanism. Rock and fluid expansion contribute the least recovery whereas gas cap gas expansion gives a higher recovery efficiency due to the very high compressibility of gas (as high as 60%). As cumulative production increases, the reservoir energy declines until the displacement of hydrocarbons ceases. The primary drive mechanism only recovers 25-30% of the initial oil and gas in place (Zekri et al., 2000). Oil and gas will not flow towards the perforations until pressure assistance is provided to the reservoir through fluid injection.

Secondary recovery, otherwise known as pressure maintenance methods, is conventionally implemented before the reservoir pressure is completed depleted. It involves the injection of gas or water into the reservoir to boost reservoir pressure and sweep residual oil towards the wellbore (Lake, 1989). Gas is injected up structure in the gas cap while water injectors are located below or at the water-oil-contact to maintain the reservoir pressure. Pressure maintenance can provide incremental recovery of oil and gas up to 10 – 15% (Tarek, 2018).

Enhanced oil recovery (EOR) may be initiated at any stage of the reservoir life, depending on the reservoir fluid characteristics (Lake, 1989). The tertiary recovery process utilizes fluids or materials that are not naturally occurring in the reservoir to aid hydrocarbon displacement. It targets specific rock and fluid properties to enhance fluid flow through the reservoir. EOR processes are classified into thermal, chemical, and or biologic methods (Lake, 1989).

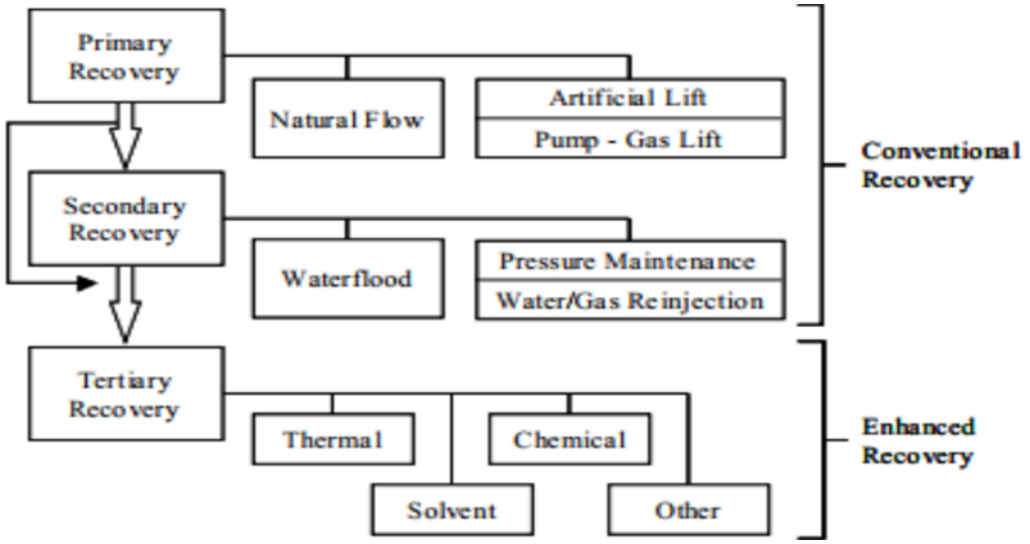

Figure 2-4:Illustration of petroleum recovery methods (Lake, 1989).

Chemical floods include polymer, surfactant, alkaline, or micellar injection. Polymers are added to the displacing fluid to control the mobility ratio and delay the breakthrough of the flood while surfactants lower the interfacial tension between the reservoir and injected fluid (Lake, 1989). Polymer and surfactant flooding are effective methods, but they are susceptible to lost circulation in the reservoir via adsorption, leading to variable injection and displacement efficiency (Lake, 1989; Sanusi, 2017). In addition, surfactant flooding breaks down in the presence of high temperatures and salinities (Green & Willlhite, 1998). Taber et al. (1997) provides one of the screening criteria used in identifying the EOR method applicable to any reservoir given the reservoir and fluid properties.

Chemical Flooding Process	Fluid Properties			Reservoir Properties				
	Gravity (° API)	Viscosity (cp)	Temp. (°F)	Porosity (%)	Perm. (md)	Oil Sat. at start (% PV)	Lithology	Depth (ft)
Polymer/surfactant Flooding	14–34	5–80	80–160	20–30	170–900	60–75	Sandstone	1300–4600
Alkali/Surfactant/ Polymer (ASP) Flooding	14–34	5–80	80–160	20–30	170–900	60–75	Sandstone	1300–4600
Polymer Flooding	14–34	5–80	80–160	20–30	170–900	60–75	Sandstone	1300–4600
Microbial (MEOR)*	—	5–50	< 176	≥20	>50	—	Sandstone or Carbonate	<7700

* Includes water salinity <150,000 ppm.

Figure 2-5:Selection criteria for tertiary recovery methods (Taber et al., 1997)

It should be noted that Thermal EOR methods utilize steam, hot water, or air to facilitate the recovery of highly viscous oil. The increased temperature of the steam or hot air lowers the viscosity of the reservoir fluid, reducing its resistance to flow (Lake, 1989). The potential to recover more condensate is very high with the application of improved oil recovery processes (Alaigba, 2020). However, the decision to undertake secondary and tertiary recovery processes must be underpinned by the technical and economic justifications since the cost of implementing most EOR methods can be prohibitive (Lake, 1989).

2.4.1 Gas Injection or Cycling

Gas injection or cycling is a common improved oil recovery method. Gas injection can occur under miscible or immiscible conditions (Fevang & Whitson, 1999). Miscibility is attained when the composition of the injected fluid is similar to that of the reservoir fluid or when the injection pressure is greater than the minimum miscibility pressure. Operating conditions or capacity of injection facilities may constrain the achievement of minimum miscibility pressure. A flood is miscible when the injection fluid mixes completely with the displaced fluid and form a single phase (Zick et al., 1986). Gas injection is suited to low permeability, high-depth reservoirs. Commonly injected gases include carbon dioxide, nitrogen, flue gas, and hydrocarbon gases. However, various studies have shown that a flue gas (mixture of nitrogen and carbon dioxide injection gas) gives the highest recovery. Nitrogen gas is applicable in light oil reservoirs, readily available, cheap, but requires additional installation costs of the cryogenic unit. Moreover, it requires a higher injection pressure to attain miscibility and poses a corrosion threat to processing equipment (Sanusi, 2017). Carbon

dioxide injection is attractive because it reduces greenhouse gas emissions, is affordable, and promotes recovery of light to medium gravity oils. It works by lowering the oil viscosity and interfacial tension, altering rock wettability to easy oil flow. However, its limited availability, solubility in water, and corrosive properties can be a challenge in EOR applications (Wijaya, 2006). Hydrocarbon gas injection is not as effective as carbon dioxide and nitrogen injection, but it is not difficult to attain miscibility because of its similar composition to that of the reservoir fluid. The leaner the injected hydrocarbon gas becomes, the higher the MMP requirements (Fevang & Whitson, 1999). Elkins et al. (1975) investigated the performance of a gas condensate reservoir under gas injection. They compared simulation results with those of predictive correlations. Their findings indicated that the duration of the injection affects the ultimate recovery of condensates in the reservoir. The location of injection wells and the timing of the onset of the gas cap blowdown is crucial to reduce trapped oil in the reservoir and delay gas breakthrough (Nwonodi et al., 2018).

2.4.2 Water Injection

Most reservoirs are underlain by a column of water contained in aquifer pore spaces. Water influx is the inward movement of water from the adjoining aquifers into the reservoir when the average reservoir pressure decreases (Tarek, 2018). It is triggered when the pressure transient from the producing wells reaches the reservoir boundary or oil-water contact (OWC). However, the influx response may not be sufficient or instantaneous due to the absence of, or small size of the adjoining aquifer, and in low permeability or heterogenous reservoirs. On the other hand, waterflooding is the deliberate injection of water below the OWC or into the aquifer to supplement the declining reservoir pressure.

Several studies have been performed on water injection in oil and gas reservoirs. Cason (1989) reported that water injection in a Louisiana gas condensate reservoir displaced 3% additional residual gas in water drive reservoirs, and an incremental recovery of gas by 16% in volumetric reservoirs. Although water is a cheap and readily available resource, water injection is not an effective option for pressure maintenance in gas condensate reservoirs for several reasons. At high rates, water saturation in the reservoir can build up, bypassing the gas and trapping it in place. Since the gas may contain dissolved oil, condensate recovery therefore decreases (Fishlock & Probert, 1996).

Fishlock and Probert (1996) investigated water injection in the North Sea gas condensate reservoirs. Their results showed that condensed oil reduces the trapped gas saturation and

critical gas saturation. They also noted that a modified set of relative permeability data should be used during blowdown period since gas flow is not immediate after water injection.

According to Ali (2014), the inability to meet contractual sales requirements or delayed earnings may reduce net-present-value (NPV) of a gas condensate asset undergoing gas cycling. Ali (2014) simulated the performance of a gas condensate reservoir under a water injection scheme. He reported that the success of a waterflooding project is influenced by the injection rates, reservoir heterogeneity and permeability, and well spacing. He suggested that to increase condensate recovery, water injection should be done above the dew point pressure. Ali (2014) findings indicate that 50% of the initial gas in place may be trapped during water flooding. At low injection rates, liquid recovery decreases while the gas recovery is increased, and vice versa. He concludes that full pressure maintenance at high water injection rates should be employed early in the reservoir life to increase condensate recovery and the net present value of gas sales. Afterward, the injection rate should be decreased to release trapped gas and delay water breakthrough in the reservoir. Also, as water breaks through at the well, it can pose vertical lift problems in the wellbore, requiring the installation of artificial lift devices.

Udie et al. (2014) developed mathematical models to improve condensate recovery in gas condensate reservoirs. They stated that water injection at the dewpoint leads to an estimated 62-76% of condensate recovered. Udie et al. (2014) noted that injecting high gas rates at the beginning of production when the average reservoir pressure is at or near the dewpoint pressure provide full pressure maintenance and higher gas condensate recoveries. However, breakthrough occurs earlier and the producing wells may be shut-in at higher abandonment pressures. If field water cut is controlled, the overall gas recovery does not change with higher injection rates and the incremental recovery may be insignificant except in low permeability reservoir studies.

2.4.3 Water-Alternating Gas Injection (WAG)

Water-alternating-gas injection involves the injection of slugs of water and gas into the reservoir in an alternating sequence. Only one fluid is injected at a particular period called a cycle. The first fluid is injected for a chosen duration of time before the second fluid is introduced into the reservoir for the same length of time as the first fluid. Figure 2-6 is a schematic of water-alternating-gas injection process (Nangacovié, 2012). Some studies have predicted up to 64% recovery in mature Norwegian fields using the WAG technique

(Nangacovié, 2012). WAG injection exploits the individual advantages of gas and water injection to optimize recovery. It provides mobility control, reduces gas injection and processing requirements, and improves condensate recovery.

Several factors influencing the design consideration for the WAG technique include reservoir rock and fluid properties, availability and composition of injecting gas, the WAG cycle, WAG ratio, injection pattern, and time to initiate WAG (Nangacovié, 2012). Reservoir wettability affects flow parameters such as relative permeability and capillary pressure. High permeability zones promote the channeling of the displacing fluid, reducing the sweep efficiency. In reservoirs with high vertical permeability, crossflow may occur between layers due to density differences between the fluids. However, a low vertical-horizontal permeability ratio boosts hydrocarbon recoveries in condensate reservoirs. Availability of the injection gas helps to underpin the decision to adopt the WAG technique or not. When the injection gas volume is not readily available, or the supply from the production platform is remote, it may lead to additional acquisition and transportation costs. Economic constraints determine the capacity of the surface facilities that are installed to implement the WAG technique (Nangacovié, 2012).

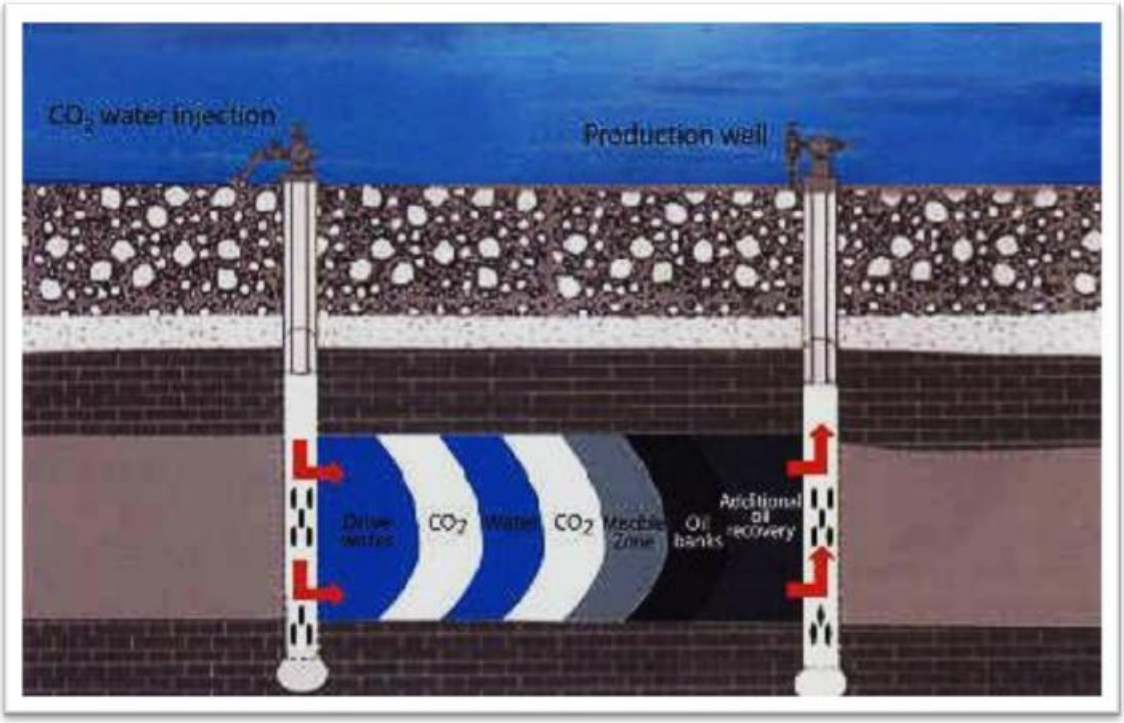

Figure 2-6:Schematic of water-alternating-gas injection technique (Nangacovié, 1997).

The supply of injection gas influences the WAG ratio, which determines the miscibility during the gas displacement cycle. Sensitivity analysis must be conducted on the WAG ratio

to determine the optimal choice for the reservoir being developed. High WAG ratios cause considerable trapping of the condensate as water bypasses the oil, preventing proper contact between the injected gas or solvent and the oil. This results in the production performance of the WAG flood being identical to that of a waterflood. On the other hand, low WAG ratios cause gas to channel and break through early at the producing wells like in a gas flood.

The WAG cycle is the duration for which each fluid is injected into the reservoir. Ramachandran (2010) performed sensitivity analysis on the WAG cycle effect on oil recovery indicated that using a WAG ratio of 1:2 and a six-month cycle combination achieves better performance in WAG applications. The five-spot injection pattern is commonly applied in WAG studies, however recent findings show that the 4-spot pattern gives a higher recovery. Better performance is achieved when a combination of horizontal injectors and vertical producers are used, as well as maintaining a moderate distance between the injection and producer wells (Nangacovié, 2012).

Nangacovié (2012) performed various sensitivity on the WAG ratio, WAG cycle, as well as the injection rate and pattern of the Norne-E reservoir. She concludes that the WAG cycle has negligible significance on incremental recovery at low injection rates. She proposes a 3-month injection cycle be used at high injection rates to achieve better performance.

2.4.4 Simultaneous Water and Gas Injection (SWAG)

Simultaneous water and gas injection entail the injection of water and gas at the same time through an injection well after mixing at the surface. The conventional SWAG involves mixing the liquid and gas phases at the surface before injection. A special type of SWAG technique has been applied to field applications where the gas and water are not mixed at the surface but injected through separate completion intervals simultaneously into the reservoir. The factors that affect WAG performance are valid for the SWAG technique. Hence, extensive sensitivity analysis must be done to determine the optimum choice of injection ratio and pattern. Nangacovié (2012) results indicate recoveries of up to 73% using a 1:3 SWAG ratio at high injection rates, which is 10% higher than the WAG recovery factor of 63%. Perforating a new completion in addition to drilling a new injection well adds to the cumulative oil recovered.

2.5 RESERVOIR SIMULATION

Reservoir modelling involves the use of computerized flow equations to describe actual fluid flow processes (Aziz & Settari, 1979). The purpose of modelling is to evaluate the

performance of the reservoir under one or more production strategies. It is the aim of every upstream operator to maximize the profitability of their investment. Subsurface geologic uncertainties present huge risks to the profitability of oil and gas companies. Thus, it is economically, technically, and environmentally efficient to carry out several simulation scenarios to assist in making the best management decisions (Ertekin et al., 2001). Reservoir simulation applies to any stage of the reservoir life for field development planning, facilities design considerations, history matching, and enhanced oil recovery. The choice of the simulator to use depends on the complexity of the fluid composition and processes to be investigated (Aziz & Settari, 1979). It is common to classify a simulator as black-oil, full compositional or limited compositional (also called modified black-oil) model. These models are described in the following section.

2.5.1 Black Oil Models

The earliest attempts at reservoir modelling incorporated the use of black oil models. It was applied to solve most natural depletion and pressure maintenance problems (Aziz & Settari, 1979). In the black oil model, reservoir fluid consists of two components: surface gas and stock tank oil. The surface gas has no liquid components, and its properties are identical to that of the reservoir gas. The hydrocarbons are insoluble in the water phase and the injected gas must have the same properties as the reservoir gas. The composition of the surface oil and gas remains constant throughout pressure decline. Black oil models are suitable for simulating heavy hydrocarbons, production above the bubble point pressure, waterflooding, and gas injection. The formation volume factors (Bo, Bg), solution gas-oil ratios (Rs, Rv), fluid densities, and viscosities are functions of pressure only. Although, they are preferred for their ease of use, less complicated data requirements, and lower run time, black oil simulators are too simplistic to capture the complexities of composition-dependent systems (Aziz & Settari, 1979).

2.5.2 Fully Compositional Simulators

A fully compositional model treats fluid properties as a function of both pressure and composition. It utilizes flash calculations to account for the mass transfer between the liquid and vapor phase and equilibrium ratios at each pressure step. Compositional models are more prone to numerical dispersion effect, and the use of coarse grids may be inadequate to capture the influence of heterogeneities on fluid flow dynamics. The assumption of instantaneous equilibrium conditions within the reservoir may overestimate the performance of miscibility

studies. The memory, data, costs, and time associated with compositional simulation can be huge as the flow physics becomes more complicated (Aziz &s Settari, 1979).

2.5.3 Limited Compositional Models

The drawbacks associated with fully compositional models necessitate the development of alternatives. Limited compositional models, also known as Extended or modified black-oil models provide an alternative to the drawbacks of black oil and a fully compositional model. It utilizes pressure-dependent equilibrium ratios to determine phase properties and compositions. Pressure equations are iterated using the Newton Raphson technique to solve for grid block pressures. Oil saturation is calculated explicitly after phase pressures have been solved. Todd-Longstaff (1972) mixing parameter is used to extend miscibility and viscous fingering effects to the reservoir fluid system by way of 4 pseudo components: oil, gas, water, and solvent. This application is very useful when simulating gas or chemical flooding scenarios. The solvent and reservoir gas are immiscible unless the minimum miscibility pressure is attained (Aziz & Settari, 1979).

2.5.4 PVT Modeling

PVT data is obtained by performing the experiments on collected fluid samples. Fevang and Whitson (1999) note that the cost and difficulty associated with obtaining representative bottomhole samples at high pressures and temperatures make the use of recombined surface separator samples preferrable to obtain fluid compositions even though the latter procedure is susceptible to inaccurate predictions. Typically, PVT data are measured in the laboratory. However, the data calculated by the PVT software package may deviate from the measure data.

2.5.4.1 Compositional Gradient and Saturation Pressure Experiment

The saturation pressure experiment is conducted to ascertain the dewpoint pressure (Psat) of the reservoir fluid. The compositional gradient experiment helps to determine the change in fluid composition with depth. In steeply dipping reservoirs, gravity segregation effects may be significant and the liquid and vapor fractions of each component of the reservoir fluid may vary with depth (Fevang & Whitson, 1999).

2.5.4.2 Constant Composition Expansion (CCE) Experiment

This experiment is used to determine the pressure-volume relationship of the fluid sample. The experiment involves the thermal expansion of the reservoir fluid to a pressure followed by consequent pressure depletion (Whitson & Brule, 2000). It measures the dewpoint,

relative volume, and the liquid dropout in the fluid sample. These properties are then used to determine the gas deviation factor, density, and dew point pressure using the real gas law. The fluid is placed in a PVT cell, and charged to a pressure greater than the dewpoint pressure while maintaining the cell temperature at the reservoir temperature. The cell pressure is then reduced stepwise (isothermally) until the dewpoint pressure is observed (Ahmed, 2018).

2.5.4.3 Constant Volume Depletion (CVD) Experiment

The constant volume depletion experiment involves a series of pressure expansions and constant volume displacement to maintain the sample in a constant PVT cell volume that is equal to the volume the fluid occupies at the dew point (Whitson & Brule, 2000). This experiment simulates the natural depletion process that occurs within the reservoir and measures the compositional changes of the produced gas (Whitson & Brule, 2000). A measured fluid sample is placed in a PVT cell and charged to the dewpoint pressure. The fluid volume (Vsat) and gas deviation factor at this pressure is recorded as the reference values. The cell pressure is then gradually decreased to a lower pressure P1, by withdrawing mercury from the PVT cell. The total volume (liquid and gas) at this pressure is measured and recorded. Mercury is then reinjected into the PVT cell while simultaneously removing an equivalent gas volume from the cell until Vsat is reached. The volume of the removed gas and the condensed liquid is measured. These records are then used to calculate the moles of gas, two-phase z-factor, gas deviation factor, and liquid dropout (%). The process is repeated stepwise until abandonment pressure (Whitson & Brule, 2000; Ahmed, 2018).

2.5.5 Equation of State (EOS)

An equation of state (EOS) describes the pressure-volume-temperature behaviour of hydrocarbon fluids using mathematical correlations (Whitson & Brule, 2000). Phase equilibrium and transfer between (from) the liquid and vapor phase of the hydrocarbon components is established from flash calculations. Several EOS have been developed in literature. The Soave, Redlich, and Kwong (SRK) equation is one of the most widely used EOS because of its simplicity. Although it underestimates the liquid densities and overpredicts the liquid volumes of petroleum mixtures, it gives accurate predictions of vapor-liquid equilibria and vapor properties (Whitson & Brule, 2000). Zudkevich and Joffe presented an equation of state that better predicts liquid and vapor densities, but the EOS requires the use of convoluted temperature-dependent functions to modify the EOS constants. They noted that adjusting the EOS constants and vapor fugacity would improve the

volumetric predictions compared to the SRK equation of state (Whitson & Brule, 20000. Peng Robinson developed an EOS that provides accurate description of liquid density in the critical region. Initially, a 2-parameter EOS which utilizes critical temperature and pressure to describe the density of saturated fluids, was proposed but results indicated significant inaccuracies in the saturated liquid density (Whitson & Brule, 2000). He further developed a 3-parameter EOS which utilizes the acentric factor in addition to the critical properties. Later on, Peng Robinson proposed a four-parameter EOS which incorporates an additional volume correction parameter for better volumetric predictions (Whitson & Brule, 2000).

Crude oil consists of several hydrocarbon compounds. For compositional simulation, the computing time and requirements can become significant since material balance and flow equations must be solved for each of the individual components in the liquid and vapor phase for accurate estimation of phase pressures, saturations, and composition at each timestep and grid location (Aziz & Settari, 1979). The original fluid components can be lumped together, using established lumping procedures, to a smaller number of pseudo-components, which allows for shorter run times. The pseudo-components are formed in such a way that the critical properties such as the critical pressure and temperature, binary interaction coefficients provide an accurate match with the measured properties of the original fluid (Whitson & Brule, 2000). Once the EOS is tuned to match the experimental data, it was then used to predict the fluid behaviour at any given pressure and temperature.

$$P = \frac{RT}{v-b} - \frac{a}{v(v+b)+b(v-b)} \tag{2.1}$$

$$a = \Omega_a^0 \frac{R^2 T_c^2}{P_c} \alpha \; ; \; \Omega_a^0 = 0.45724 \tag{2.2}$$

$$b = \Omega_b^0 \frac{RT_c}{P_c} \; ; \; \Omega_b^0 = 0.07780 \tag{2.3}$$

$$\alpha = \left[1 + m(1 - \sqrt{T_r})\right]^2 \tag{2.4}$$

$$m = 0.37464 + 1.54226\omega - 0.26992\omega^2 \tag{2.5}$$

$$for\ \omega > 0.49;\ m = 0.3796 + 1.485\omega - 0.1644\omega^2 + 0.01667\omega^3 \quad (2.6)$$

Efforts to improve energy supply, utilization, and reduce carbon emissions have made gas production to become more eminent in Nigeria's energy mix. Currently, gas contributes 80% of the energy required for power generation (International Energy Agency, 2019). By 2040, gas demand is expected to rise to 35MTOE, and approximately 82 billion dollars of investment is required to meet the estimated gas forecast. As a result, the exploration and production of gas reservoirs will be further intensified to boost the economy. Gas condensate reservoirs provide additional value through the export of condensate volumes which are not restricted by OPEC quota cuts. Condensate banking remains the biggest challenge in producing a gas condensate reservoir. It has been established that depleting such a reservoir using its primary energy will lead to loss of condensate reservoir. Gas injection remains the most widely used pressure maintenance technique compared to WAG and SWAG injection. Literature suggest that carbon-dioxide or nitrogen injection are more efficient for condensate recovery, however hydrocarbon gas cycling is investigated in this study because it is readily available in the field and the cost of acquiring or processing carbon-dioxide or nitrogen is eliminated. Although, gas injection is proposed to be more efficient when it is done above the dew-point pressure, this condition may not be fulfilled for every gas condensate reservoir since it may take some time to build up to the required gas reinjection volume for a virgin reservoir.

WAG injection is considered a better option than continuous gas injection because it provides better sweep efficiency and makes more gas available for immediate sales during the water injection cycle thereby, mitigating the effect of delayed gas sales on the net present value of production. However, the injected water may not sustain reservoir pressure before aquifer response kicks in, leading to more condensate dropout. Even if lower WAG ratios are used to improve the flood efficiency, the alternating sequence of fluid injection may cause gravity effects to be exaggerated in the reservoir. Hence, gas injection may only provide better sweep efficiency in the upper layers due to its low density, while water injection will only improve displacement in the lower layers for longer WAG cycles. SWAG injection is thus investigated to determine if hydrocarbon recovery is improved since the gas and water are injected concurrently. Injecting both fluids at the same times ensures that pressure is always maintained throughout the injection period. Better mobility ratio is achieved because the

injected water preferentially fills the highly permeable zones, while the injected gas fills up the pore spaces left. Crossflow due to gravity improves the process.

Often, fully compositional modelling is employed to simulate the fluid flow physics and development concepts for a reservoir but it is associated with huge computing time and costs. This makes limited compositional modelling an attractive option to simulate complex reservoir scenarios. The low price of gas requires upstream companies, especially marginal operators, to be economically prudent when deciding on the choice of pressure maintenance project or technical intervention.

CHAPTER THREE: RESEARCH METHODOLOGY

In this chapter, the sequence of steps utilized to attain the desired research objectives is discussed elaborately. The workflow for the study methodology is presented below in Figure 3.1. The major steps in the workflow include data gathering and data quality validation, development of the simulation models, simulation of methods for condensate recovery, sensitivity analysis, and comparison of limited vs. fully compositional simulation for modelling condensate reservoirs. Proposed workflow is described in the following section.

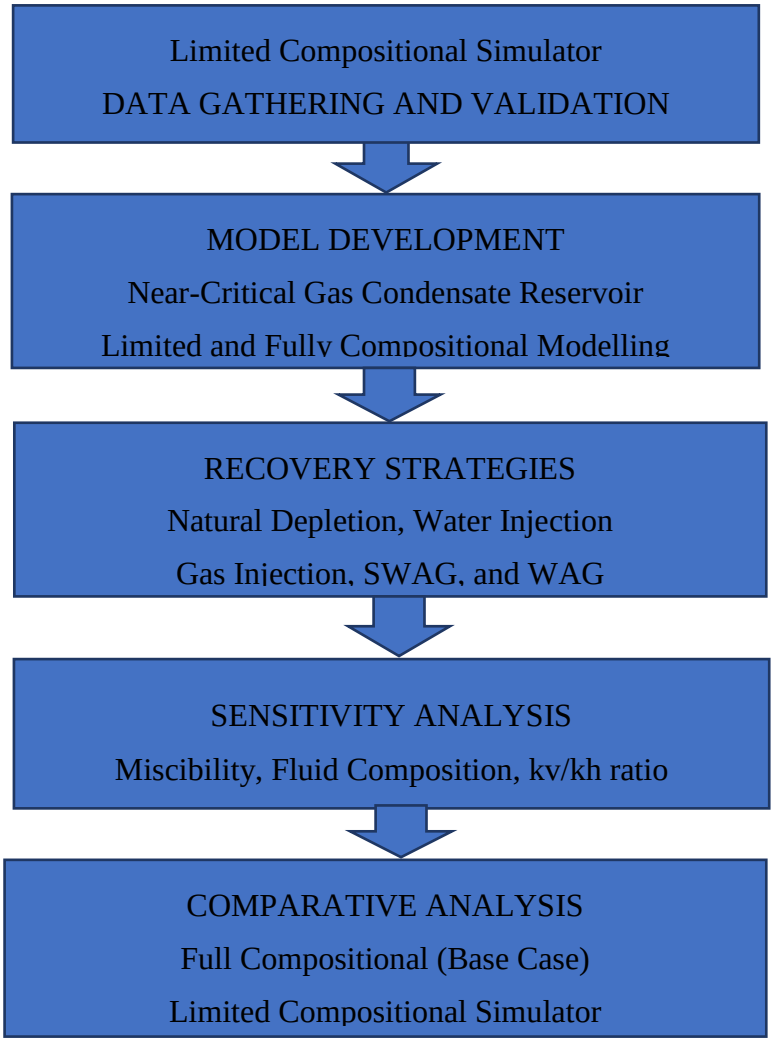

Figure 3-1:Flowchart of project methodology

3.1 DATA GATHERING AND VALIDATION

The reservoir data for this research work is collated from published articles on studies conducted on Niger Delta gas condensate reservoirs. The data gathered include reservoir rock and fluid data, reservoir management strategies, as well as industry best practices. Table 3-1 summarizes the reservoir and rock-fluid properties used in the Niger-Delta Case study. Care

is taken to ensure that the quality of the data is representative of the Niger-Delta oil province to obtain accurate results from the simulator. The accuracy of the results obtained from a reservoir simulation process depends on the quality of input data used.

The reservoir is situated between 10,100 ft and 10,300 ft below sea level. The reservoir structure is an undulating anticline producing hydrocarbons in two regions--the North-West and the South-East regions. The reservoir has an average initial pressure of 4191psia and porosity of 18%. It is bounded by three aquifers, two in the North-Western region and one in the South-Eastern region. Fluid contacts are established using equilibration data. The fluid contacts are assumed to be horizontal and reservoir properties are homogeneous in the reservoir.

Table 3-1:Reservoir and Rock-Fluid Properties of a Niger Delta Case Study

PARAMETERS	VALUE	UNIT
Rock Properties		
Lithology	Unconsolidated Sandstone	
Porosity	0.18	
Dewpoint Pressure	4191	psia
Reservoir Temperature	176.6	0F
Perm X	910	mD
Perm Y	910	mD
Perm Z	91	mD
Rock Compressibility	4 x 10-6	1/psia
Water Properties		
Water Reference pressure	4300	psia
Water Formation volume factor	1.0	
Water compressibility	3.6 x 10-6	1/psia
Water viscosity	0.31	cp
Water density	62.4	lb/ft3
Hydrocarbon fluid properties		
Gas density	0.0505	lb/ft3
Oil Density	49.54	lb/ft3
Solvent Density	0.0505	lb/ft3

3.1.1 Aquifer Data

Most petroleum reservoirs are adjoined by an aquifer. Aquifers are distinct geologic formations bearing water which may charge or support the reservoir as it is depleted. Several models have been developed to estimate water influx for various aquifer types based on a predetermined set of initial and boundary conditions, and assumptions (Aziz & Settari, 1979). In this research, three adjacent aquifers are adjoined to the reservoir, at varying encroachment angles. The water influx was modelled using the Carter-Tracy aquifer model (Carter & Tracy, 1960). The aquifer data can be seen in Table 3-2.

Table 3-2:Reservoir Model Aquifer Properties

Aquifer Properties	Value	Unit
Type of Aquifer	Carter-Tracy	
Number of Aquifers	3	
Porosity	21	%
Permeability	1000	mD
Datum Depth	10224	ft
Initial Pressure	4300	psia
Total compressibility	5.89 x 10-6	1/psia
Aquifer Internal Diameter	2318	ft
Encroachment Angle	Aquifer 1= 180, Aquifer 2= 90, Aquifer 3= 180	degrees

3.1.2 Fluid Contacts Initialization

The reservoir model consists of two hydrocarbon producing regions--the North-West and the South-East regions. Model initialization for the two regions is carried out using the data listed in Table 3-3. For the fully compositional case, in addition to the fluid contact depths, the compositional gradient data (Appendix A) is used to initialize the reservoir and determine the fluid volumes in place as well as the fluid composition with depth. On the other hand, for the limited compositional case the oil-gas ratio and the gas-oil-ratio versus depth data are used to estimate the oil and gas initially in place. The model initialization data is obtained by exporting the PVT data file using keywords that can be applied in the limited compositional simulator.

Table 3-3:Niger Delta Model Initialization Data

NORTH-WEST REGION		
Datum depth	10250	ft
Initial pressure	4200	Psia
Oil gas contact	10140	ft
Water oil contact	10300	ft
SOUTH-EAST REGION		
Datum depth	10224	ft
Initial pressure	4191	Psia
Oil gas contact	10124	ft
Water-oil contact	10300	ft

3.2 RESERVOIR SIMULATION MODEL DEVELOPMENT

The well stream composition of the Niger-Delta gas condensate fluid was acquired from literature. The reservoir fluid composition consists of 11 components. The composition of the reservoir fluid is shown in Table 3-4 which presents an overview of the molar proportions of the liquid and vapor phase for each component.

Table 3-4:Composition of the Niger Delta reservoir fluid (Akpabio et al., 2015).

Components	**Liquid mol %, xi**	**Vapor mol %, yi**	**Reservoir Fluid mol %, zi**
N2	0	0.15	0.14
CO2	0	0.18	0.18
C1	0	87.98	87.98
C2	0.1	5.29	5.29
C3	0.07	2.83	2.83
IC4	0.06	0.68	0.68
NC4	0.13	0.91	0.91
IC5	0.21	0.41	0.41
NC5	0.25	0.31	0.31
C6	1.73	0.56	0.56
C7+	97.45	0.7	0.7
TOTAL	**100**	**100**	**100**
Liquid Density, lb/ft3	50.067		
Liquid Mol. Wt.		156.37	
Gas Gravity	0.807		
GOR (scf/bbl)			82918.7

3.2.1 PVT Modeling

A commercial PVT modelling software package was utilized to perform component lumping and simulate the fluid experiments used to generate the PVT data for the limited and fully compositional models. The approach for the fluid characterization largely follows the methodology proposed by Whitson et al. (1999). The characterized fluid, shown in Table 3-4, consists of 11-components. These components were lumped into 7 pseudo-components to reduce computing time. Several fluid experiments were simulated to obtain the fluid critical properties. These experiments include the Constant Composition Expansion (CCE), Constant Volume Depletion (CVD), Saturation Pressure, and Compositional Gradient experiments. The results of the simulations were matched with the experimental data through a regression process. The saturation pressure data was matched to obtain a value close to the experimental results. Following this, the relative volume from the CCE and CVD experiments were matched by adjusting some of the critical properties of the C7+ fractions (Appendix A.1-A.3).

3.2.2 Equation of State (EOS)

An equation of state (EOS) describes the pressure-volume-temperature behaviour of hydrocarbon fluids using mathematical correlations (Whitson & Brule, 2000). Phase equilibrium and transfer between (from) the liquid and vapor phase of the hydrocarbon components is established from flash calculations. The Peng Robinson equation of state was utilized in this research to establish the pressure-volume-temperature behaviour of the reservoir fluid. This includes the critical properties, acentric factor, as well as the binary interaction parameters utilized in the fully compositional model (Whitson & Brule, 2000). The pseudo-components are formed in such a way that the critical properties such as the critical pressure and temperature, binary interaction coefficients provide an accurate match with the measured properties of the original fluid. Once the EOS was tuned to match the experimental data, it was then used to predict the fluid behaviour at any given pressure and temperature.

3.2.3 Relative Permeability Data

Permeability is the measure of the ability of a reservoir rock to transmit fluids in the direction of a given pressure differential. The absolute permeability is measured when the rock is completely saturated with a single fluid. In a petroleum reservoir, more than one fluid is typically present within the pore spaces. The effective permeability measures the capacity of

the rock to preferentially transmit a fluid when the rock is saturated with one or more fluids (Ahmed, 2018). The relative permeability is the ratio of the effective permeability to the absolute permeability. It is often determined from core measurements in the laboratory as two sets of two-phase relative permeability data for the oil- water system and gas-oil system (Aziz & Settari, 1979). Above the dew-point pressure, a gas condensate reservoir is a two-phase system consisting of gas and water. As liquid dropout occurs below the dew point, multiphase flow within the reservoir is better represented with a three-fluid system of oil (condensate, gas, and water). Hence, there is need to estimate the three-phase relative permeability data such that,

$$For\ oil - water\ system;\ k_{row} = f(S_w) \tag{3.1}$$

$$For\ oil - gas\ system;\ k_{row} = f(S_g) \tag{3.2}$$

In this study, the two-phase relative permeability data was modelled using the Wyllie and Gardener correlation for the well-sorted unconsolidated sandstone. Connate water saturation is assumed to be 20%. Connate gas saturation is 10%, and the residual oil saturation is 16%. Capillary pressure was assumed to be zero.

Oil-Water System

$$K_{ro} = (1 - S_w^*)^3;\ K_{rw} = (S_w^*)^3 \tag{3.3}$$

Gas-Oil System

$$K_{rg} = (1 - S_o^*)^3;\ K_{ro} = (S_o^*)^3 \tag{3.4}$$

where,

$$S_o^* = \frac{S_o}{1-S_{wc}}; S_w^* = \frac{S_w - S_{wc}}{1-S_{wc}};\ S_g^* = \frac{S_g}{1-S_{wc}} \tag{3.5}$$

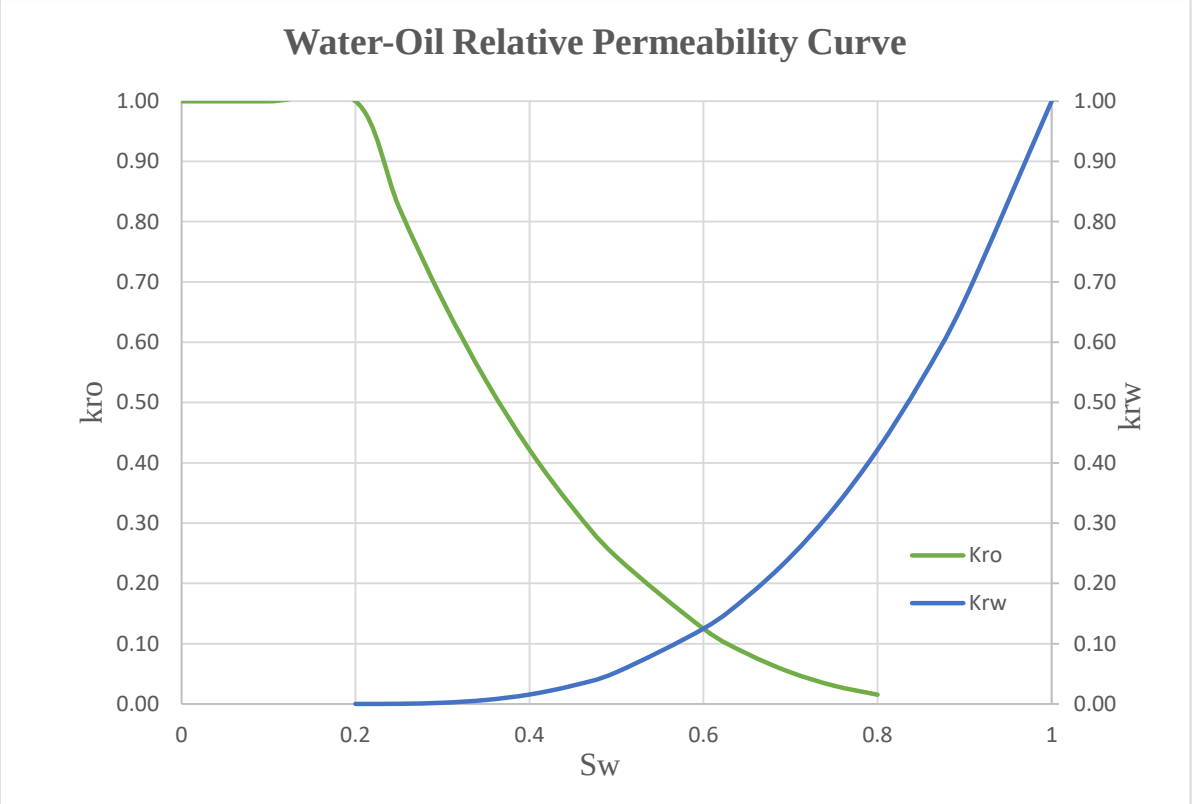

Figure 3-2:Water-oil relative permeability curves.

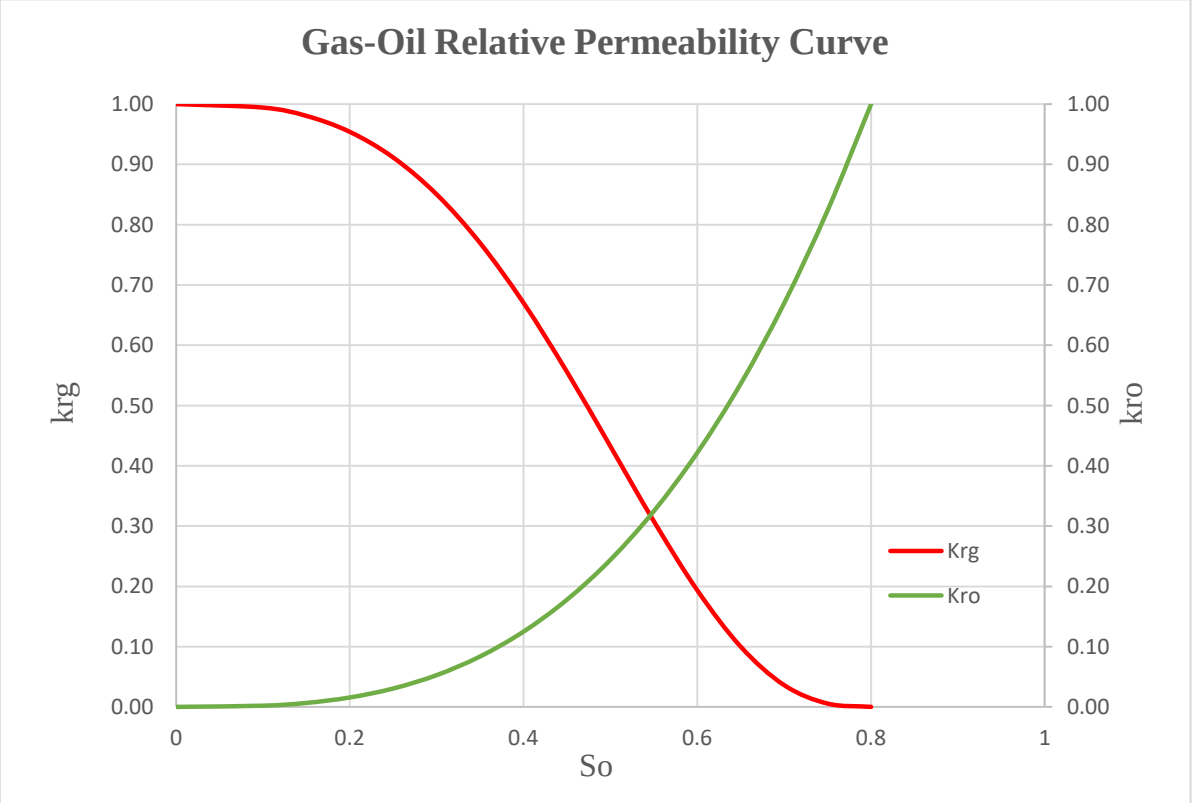

Figure 3-3:Gas-oil relative permeability curves.

3.3 SIMULATION OF CONDENSATE RECOVERY METHODS

A static reservoir model was built using a 3-D corner-point grid with dimensions (48×31×3). Table 3-5 summarizes the grid properties used in the reservoir model.

Table 3-5:Reservoir grid dimensions and properties.

Grid Properties	Value	Unit
No of cells in X Direction	48	
No of cells in Y Direction	31	
No of cells in Z Direction	3	
Delta X	900	ft
Delta Y	900	ft
Delta Z	34	ft

The limited and fully compositional simulation models were run for the gas condensate reservoir under five production strategies, namely, natural depletion (DEP), gas injection (GI), water injection (WI), water-alternating-gas injection (WAG), and simultaneous water-and-gas injection (SWAG). The natural depletion strategy produces the reservoir using its primary energy mechanism (gas cap gas expansion and water influx) for a duration of 20 years. Subsequently, to maintain the reservoir pressure and optimally recover valuable condensates from the reservoir, several improved oil recovery methods are investigated. The second production scheme is gas injection. Produced gas is re-injected into the two reservoir regions to displace condensate towards the producing wells. The third scenario is the water injection, which entails injecting produced water into the two regions of the reservoir. The recovery of the oil and gas was then recorded. In addition, the water-alternating gas injection scenario was simulated. It involved alternatively injecting water and gas into the reservoir, with individual fluid injection cycle spanning a period of 1 year. Lastly, the simultaneous injection of water and gas into the reservoir was studied. Operating constraints were applied to the gas, water, and oil phases, as shown in Table 3-6.

Table 3-6:Operating constraints.

Well Constraints	Value	Unit
Minimum oil rate	100	STB/D
Minimum gas rate	50	MSCF/D
Maximum water cut	0.95	

3.3.1 Depletion

Three (3) vertical wells were drilled in the North-west region, with an average of a 3-month drilling period between each new well. After a year, the south-eastern region was developed with two (2) horizontal wells to increase field rate as shown in Figure 3.1. Field gas rates were built up from 7MMscf/D to a peak value of value of 31MMscf/D. Multi-rate depletion sensitivity was conducted to determine the optimal production rate for each well.

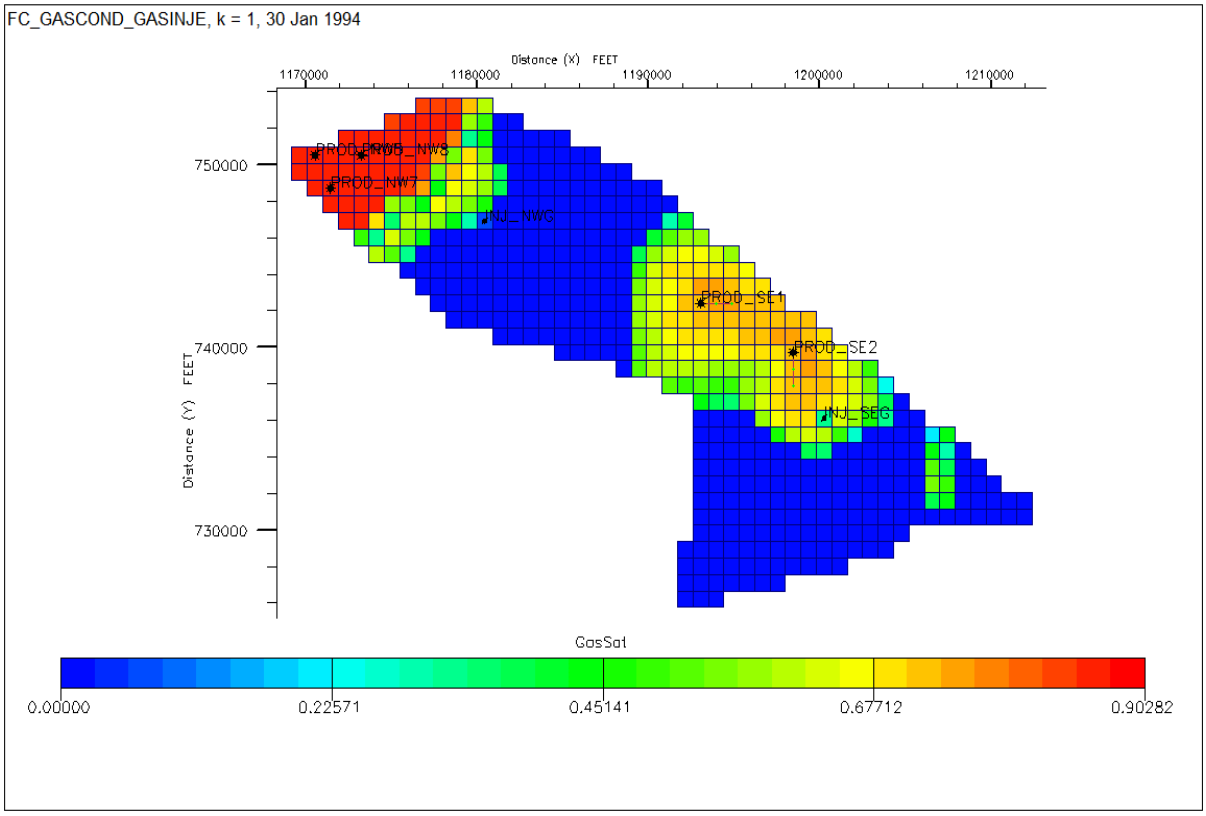

Figure 3-4:Schematic illustrating the reservoir grid and the location of wells.

3.3.2 Gas Injection

Fluid injection began in the 2nd year after the reservoir pressure had dropped by 10% from its initial level and to account for the drilling and installation of gas processing and injecting facilities. A maximum of two injection wells were drilled, one for each region as seen in Figure 3.1 The reservoir gas is recycled through an injection well completed in the first and second layer of the grid (peripheral injection). A multi-rate injection sensitivity (Appendix C) is performed in the limited compositional and full compositional model to determine the optimal re-injection fraction. after determining the minimum miscibility pressure to be 5500psia. Gas injection volume of 12MMscf/D, which accounts for about 40% of the total gas production is chosen to investigate gas injection scenario. In the limited compositional model, the Todd Longstaff Parameter(ω) is incorporated to simulate the miscibility of the

displacement process. After a sensitivity analysis on the mixing parameter was conducted, and the optimal mixing parameter was determined to be 0.85.

3.3.3 Water Injection

To make results comparable, the same number of injection wells are used for all the injection schemes. Water injectors were completed below the OWC in both regions. A sensitivity analysis of water injection ratio for the two regions was conducted to determine the optimum surface injection rate of 4000stb/day. An injection ratio of 3:2 was applied to the North and South regions respectively to manage the field water production profile. This is because, the aquifer in the SE is highly active compared to the aquifers in the NW. Thus, 2600STB/D was injected in the North-western region and 1400STB/D was injected in the South-eastern region.

3.3.4 Water-Alternating-Gas Injection

For the water-alternating-gas (WAG) scheme, water was injected at 2400STB/D, with a gas injection rate of 8MMscf/D in the North-West while the water and gas injection rates of 1600stb/d and 4MMscf/D, respectively, are used in the South-East. The cycle length for each injection fluid is 6 months. Sensitivity analysis on the WAG cycle, and the injection pattern (well location) was carried out to determine the optimum slug injection period.

3.3.5 Simultaneous Water and Gas Injection

For the SWAG scheme, 4000STB/D of water and 12MMSTB/D of gas were injected at the same time into the reservoir. Gas was injected in the upper layers while the water was injected into the lower layers using a single injection well in each region. The injection rates for the gas and water were unchanged to provide a basis for comparison of the injection schemes explored in this research.

The results obtained from execution of the proposed research methodology are presented in the next chapter.

CHAPTER FOUR: RESULTS AND DISCUSSION

4.1 INTRODUCTION

The findings of this research work are presented in this chapter. The discussions include key field performance indicators including pressure, water cut, cumulative oil production, cumulative gas produced trends as a function of time. Simulations were performed for the natural depletion and injection schemes in a gas condensate reservoir with both fully compositional and limited compositional models. For both the limited and full compositional simulations, five recovery strategies are evaluated over a 20-year period. The fully compositional model is considered the base case for the study and compared with the limited compositional model by evaluating the effect of the following parameters on reservoir performance:

- Initialization with a compositional gradient in the fully compositional model, and correspondingly with gas-oil ratio (R_s) and the oil-gas ratio (R_v) versus depth for the limited compositional model.
- Natural pressure depletion
- Injection schemes – Gas Injection (GI), Water Injection, Water-Alternating-Gas Injection (WAG), and Simultaneous Water-and-Gas Injection (SWAG)
- Production and Injection rates
- Sensitivity analyses on kv/kh ratio, WAG Cycle, Todd-Longstaff mixing parameter.

The total field production rate is 31,000MSCF/D, with the wells in the North-western and South-eastern region delivering a production target of 15,000MSCF/D and 16,000MSCF/D, respectively. When the minimum bottomhole pressure of 1000psia is reached, the pressure constraint takes precedence over the rate target. The limited compositional model is initialized with oil-gas ratio versus depth tables, which correspond to fluid composition at a reference depth of 10,140 ft. During natural depletion, the reservoir energy is supported solely by the expansion of the in-situ fluid and rock. Four fluid injection schemes are then initiated to maintain reservoir pressure. The effects of gas injection (GI), water injection (WI), and water-alternating-gas injection (WAG) are examined to determine the optimum injection plan. Fluid injection is initiated after 2years of primary depletion, after which injection program runs over a time of 15 years followed by a reservoir blowdown in 3 years. The late timing of the gas cap blowdown is chosen to optimize gas and condensate recovery. Nwonodi et al. (2018) note that the early onset of gas cap blowdown significantly reduces

production performance. The upward movement of the gas-oil contact and water-oil due to the simultaneous production of gas and water encroachment from the adjoining aquifer causes oil smearing in the gas cap and trapped gas in the reservoir. According to El- Banbi et al. (2000), reservoir blowdown helps to re-mobilize gas trapped by the injected fluids or the aquifer influx. Sensitivity analysis on the effect of varying the Todd-Longstaff mixing parameter, water injection ratio, WAG cycle, WAG ratio, number of WAG injection wells on the condensate recovery was also evaluated. The results of the sensitivity analysis are discussed in this chapter. For easy cross reference, each of the recovery scheme is colour-marked.

4.2 FULLY COMPOSITIONAL SIMULATION RESULTS

4.2.1 Field Pressure

The average reservoir pressures for the five prediction strategies (i.e., natural depletion (DEP), water injection (WI), gas injection (GI), water-alternating-gas (WAG) injection, and simultaneous water and gas injection (SWAG) are presented in Figure 4.1 for the fully compositional case. The SWAG injection scheme provided the best pressure maintenance followed by the gas injection, WAG injection, water injection, and depletion strategies, respectively. The pressure decline is highest in the natural depletion scheme with a pressure falling to about 1590psia after 20 years of production. Water injection gave negligible incremental pressure to the reservoir (El-Banbi et al., 2000). After the end of the simulation run, the final reservoir pressure was about 1600psia after the 20-year simulation. The pre-injection and post-injection pressure decline slopes are not identical for all the injection cases. In Year 9, there was a noticeable increase in pressure for the depletion case due to pressure support from the aquifer. The aquifer response was delayed for the WAG and gas injection scenarios. With gas injection, there was significant pressure increment in the reservoir due to the compressibility of the injected gas, and pressure decline was not as rapid as observed for the WAG scenario (Cobanoglu et al., 2018). Although, WAG injection should benefit from the gas compressibility and mobility ratio of the injected water, it does not sustain the field pressure (1800psia) due to the low WAG ratio. The SWAG injection scheme provides the best pressure support after producing for 20 years. There was a smaller pressure drop during the SWAG injection process, and the final average reservoir pressure was estimated to be 2500 psia.

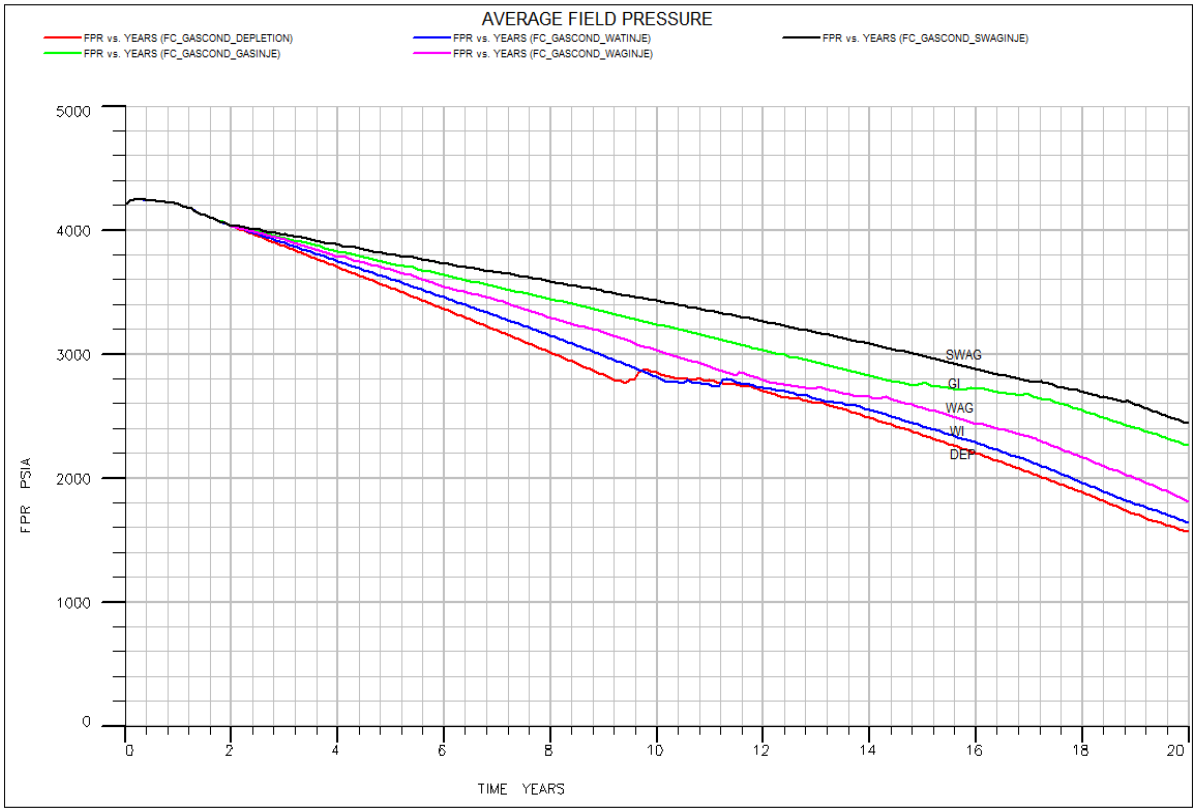

Figure 4-1:Reservoir pressure profile versus time (fully compositional case).

4.2.2 Field Water Cut

Figure 4.2 shows the results of field water cut from the full compositional simulation. The water cut for the natural depletion, water injection, WAG, and SWAG schemes were 74%, 77%, 72%, and 85%, respectively. The gas injection scheme showed the least increase in water cut during the duration of injection (~65%). The expansion of gas in the reservoir provided support and delayed the influx of water from the aquifer The WAG injection scheme has a 'slug' effect on the field water cut profile between Year 4 and Year 8. The water cut is usually maintained during the gas injection cycle of the WAG scheme, but increases during the water injection cycle, However, it shows an overall upward trend as the injected water displaces the previously injected gas, in addition to water influx from the aquifer. The final water cut from WAG was higher than that of gas injection but slightly lower than the natural depletion and water injection schemes (Cobanoglu et al., 2018). The SWAG scheme has the highest fractional water flow (85%) due to the cumulative volume of water from the aquifer and the injection well. Since gas is being injected simultaneously, it expands and propels the water towards the producer. Essentially, the WAG, natural depletion, and water injection schemes show similar water cut profiles for the field unlike the gas injection and SWAG scheme.

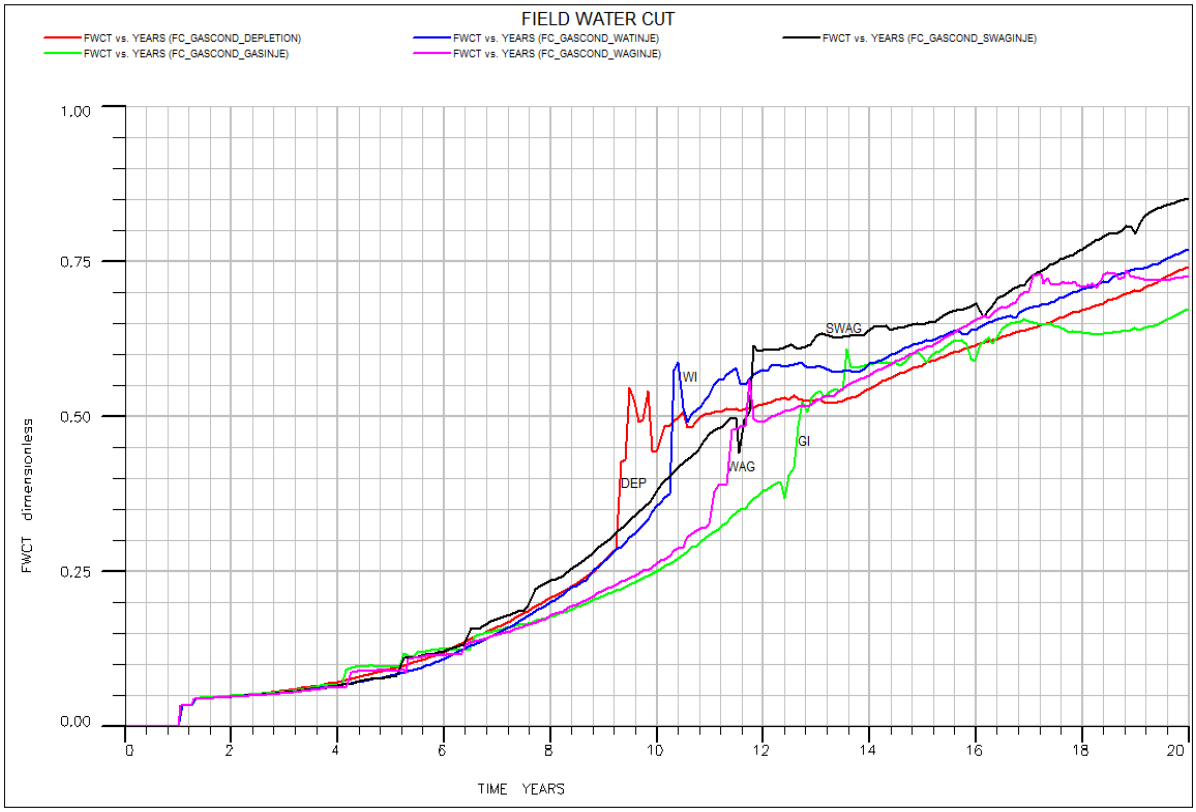

Figure 4-2:Reservoir water cut (fully compositional case).

4.2.3 Cumulative Gas Produced and Field Gas Production Rates

The plot shown in Figure 4.3 indicates the trend of the cumulative gas production for the various injection schemes. The base case (depletion) recovers 216.19BCF of gas. The primary drive mechanism is a combination of the gas expansion and water influx from the aquifer.

Continuous gas injection gave the third highest recovery (218.63BCF). The injected gas closely followed the in-situ gas condensate, revaporises the heavier hydrocarbon components in the reservoir, reducing the condensate saturation. The WAG injection scheme has the highest gas recovery (218.83BCF). After the end of a gas injection cycle, the injected water provides a favourable mobility ratio and displaces any condensate bypassed by the already injected gas. The SWAG injection case has the second highest gas recovery (218.72BCF) of all injection schemes. The favourable mobility ratio and additional pressure support from the injected water mitigates retrograde condensation, while displacing liquid that has already condensed in the reservoir (Cobanoglu et al., 2018). Water injection reduces the ultimate gas recovery (215.25BCF) because the volume of water moving towards the producers increases, trapping the gas behind. These observations agreed with field gas production rates shown in Figure 4.4.

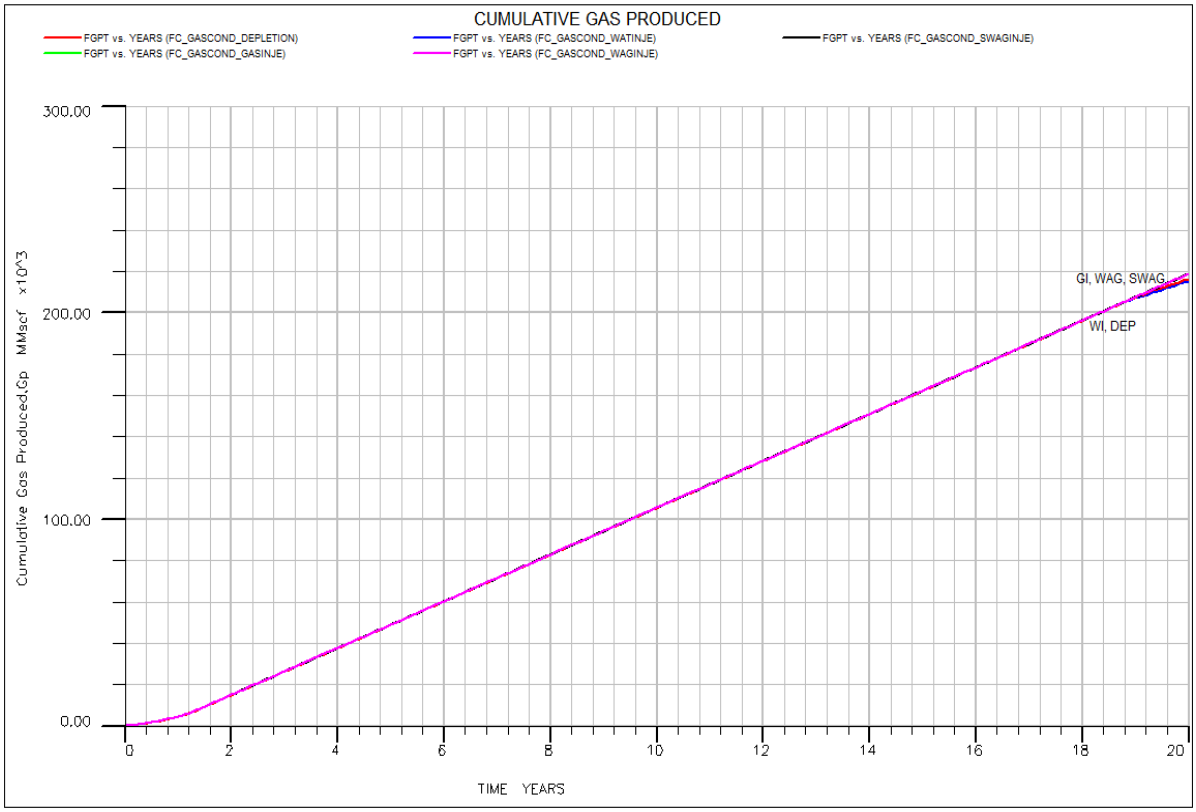

Figure 4-3:Cumulative gas produced (fully compositional case).

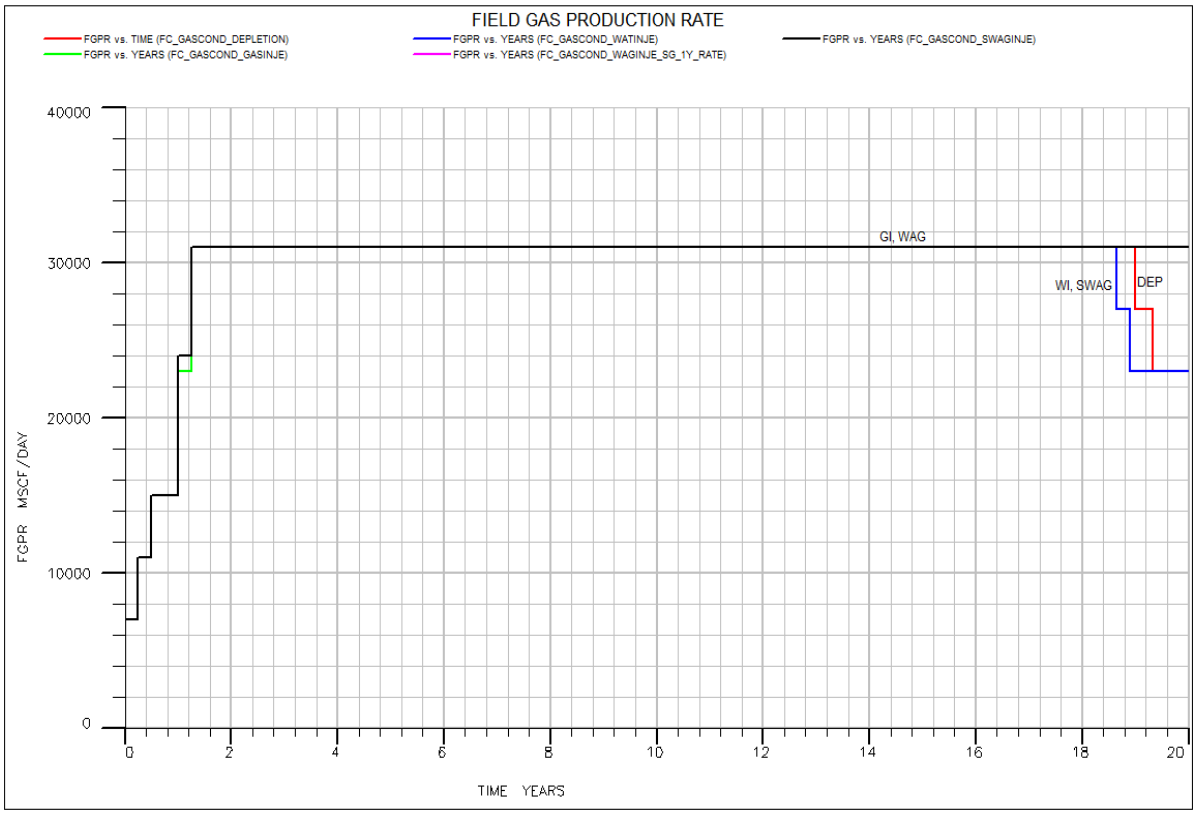

Figure 4-4:Field gas production rate (fully compositional case).

4.2.4 Cumulative Oil Produced and Field Oil Production Rates

In this study, gas production rate slowly increased as more wells were drilled and brought on-stream. Pressure maintenance commenced in Year 2, when the reservoir pressure has fallen considerably below the dew-point. The ultimate recovery of condensate is low due to the late onset of fluid injection and relatively short duration of pressure maintenance (Table 4-2). Figure 4.5 shows the cumulative oil production for the recovery strategies considered. The natural depletion recovery is the smallest at 41MMSTB of oil. This is due to significant condensate banking in the reservoir. Water injection rate of 4000STB/D gives a slightly higher cumulative condensate production (45.6MMSTB), compared to natural depletion. Water injection is an immiscible displacement mechanism; hence the efficiency of the process depends on the mobility ratio of the water relative to the mobility of oil and gas. Waterflooding boosts the reservoir pressure, thereby decreasing the condensate dropout rate, and it also sweeps any condensate pools that have already formed towards the producing well. However, viscous fingering effects eventually cause the water to bypass the oil, and breakthrough at the producer (El-Banbi et al., 2002; Ali, 2014).

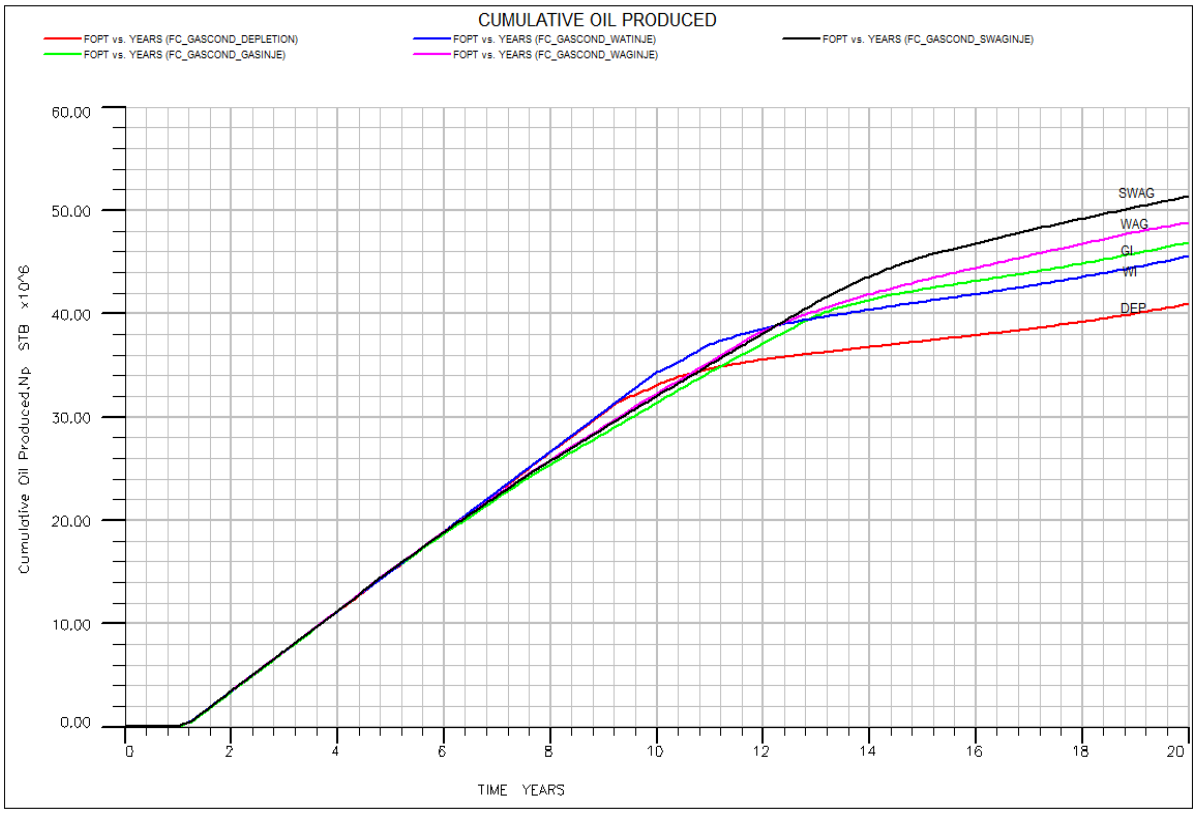

Figure 4-5:Cumulative oil produced (fully compositional case).

During WAG displacement, the miscibility and pressure maintenance of the injected gas aids the displacement process and leads to increase in cumulative oil production up to 49MMSTB

after 20 years. This is a significant improvement compared to water injection scheme. The injected gas mixes with the reservoir fluid, causes it to move quickly towards the reservoir, reduces the residual oil/condensate saturation while the injected water aids mobility control. The continuous gas injection scheme recovers approximately 47MMSTB. Injecting solely gas into the reservoir eliminates the impact that water injection has on the recovery since the water cut will be drastically reduced in the long run. The trend of the field oil production rate in Figure 4.6 illustrates that the SWAG injection yields a highest condensate recovery (51.3MMSTB).

The timing of the fluid injection strategies influences the cumulative condensate that can be recovered from the reservoir. As pressure declines, condensate dropout occurs within the reservoir. This condensate remains immobile unless the critical saturation is exceeded, leading to an initial low condensate-gas ratio (CGR) at the surface. Condensate recovery is more efficient when pressure maintenance commences at the early stages of reservoir development. At field pressures above or near the dewpoint pressure, full pressure maintenance will give 100% recovery of the condensate-in-place, since it is still dissolved in the gas-phase (Whitson et al., 1999). This technique may require the availability of makeup gas or water to meet injection requirements and maintain pressure (El-Banbi et al., 2000). In frontier or extremely remote gas condensate reservoirs, the use of make-up gas or water may be prohibitive due to inaccessibility or high transportation costs. Fluid injection is therefore delayed because a high gas or water production rate must be attained before water reinjection/gas cycling commences. As a result, the condensate bank will continue to increase as pressure declines below the dew-point. By the time pressure maintenance commences, the condensate fractions that remain in the gas phase will be completely produced at the surface. Whereas, the recovery of the condensate that has dropped out in the reservoir depends on the sweep efficiency of the displacement. It is impossible to completely re-vaporize or displace the condensate in the reservoir due to irreducible saturation (Cobanoglu, 2018). The difference between the condensate saturation at any given time and the value of the irreducible oil saturation will determine the ultimate condensate recovery at the end of the flood.

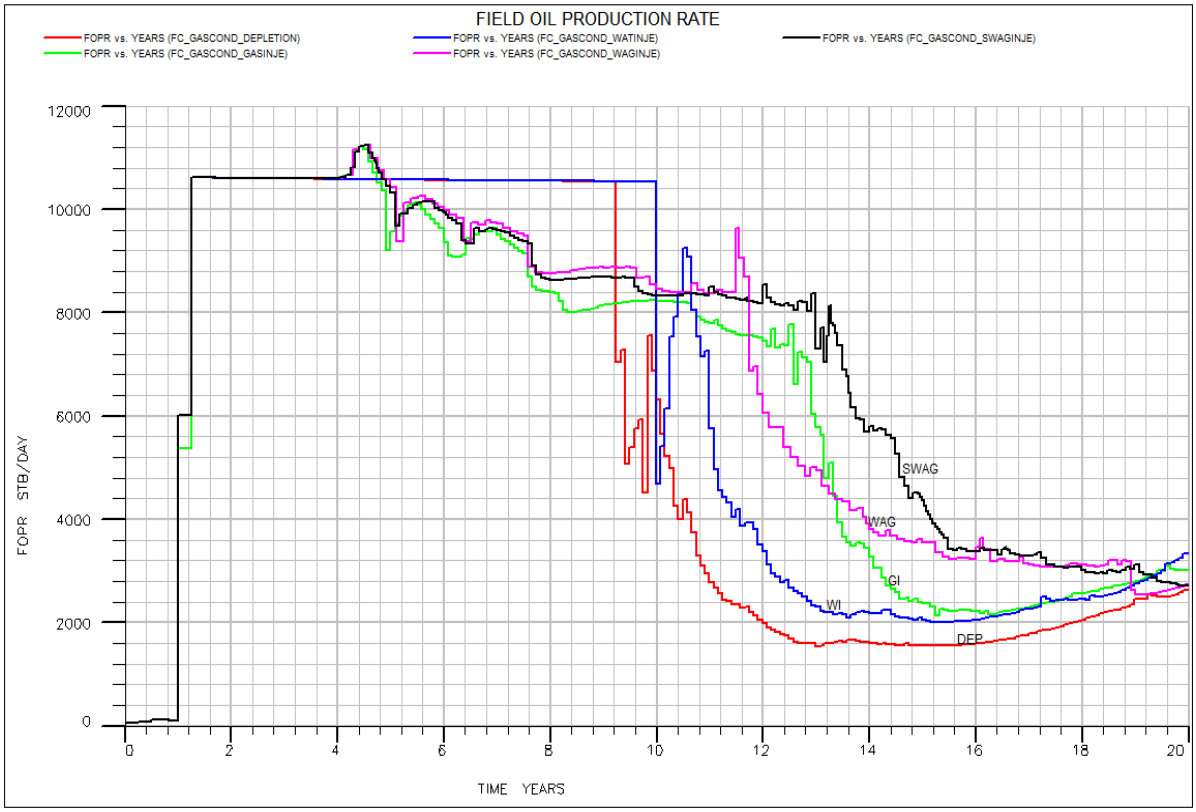

Figure 4-6:Field oil production rate (fully compositional case).

4.3 LIMITED COMPOSITIONAL SIMULATION RESULTS

4.3.1 Field Pressure

An illustration depicting the reservoir pressure for the primary production and injection cases is presented in Figure 4.7. Pressure drop during natural depletion is most severe (down to 1500 psia) because of the high production rate. However, the high compressibility and small molecule size of the injected gas increase its mobility, making it an effective displacement fluid that can maintain the reservoir pressure at 2400 after gas cap blowdown. The WAG injection provides an intermediate degree of pressure maintenance with the average reservoir pressure of 2080 psia after 20 years. The process combines the high gas compressibility with the mobility control of water to give a low pressure drop during the reservoir production. As shown in Figure 4.7, the pressure trend for the gas and WAG injection scenario deviates from that of water injection around Year 5 and Year 6, respectively. It can be noted that after injection, the pressure trend tends to approach its pre-injection decline slope. This phenomenon is negligible in the water injection case, but it is observed in any form of process that incorporated gas in the injection mixture. SWAG injection showed the best pressure maintenance during the miscible displacement process (Hernandez et al., 1999; Nangacovic, 2012).

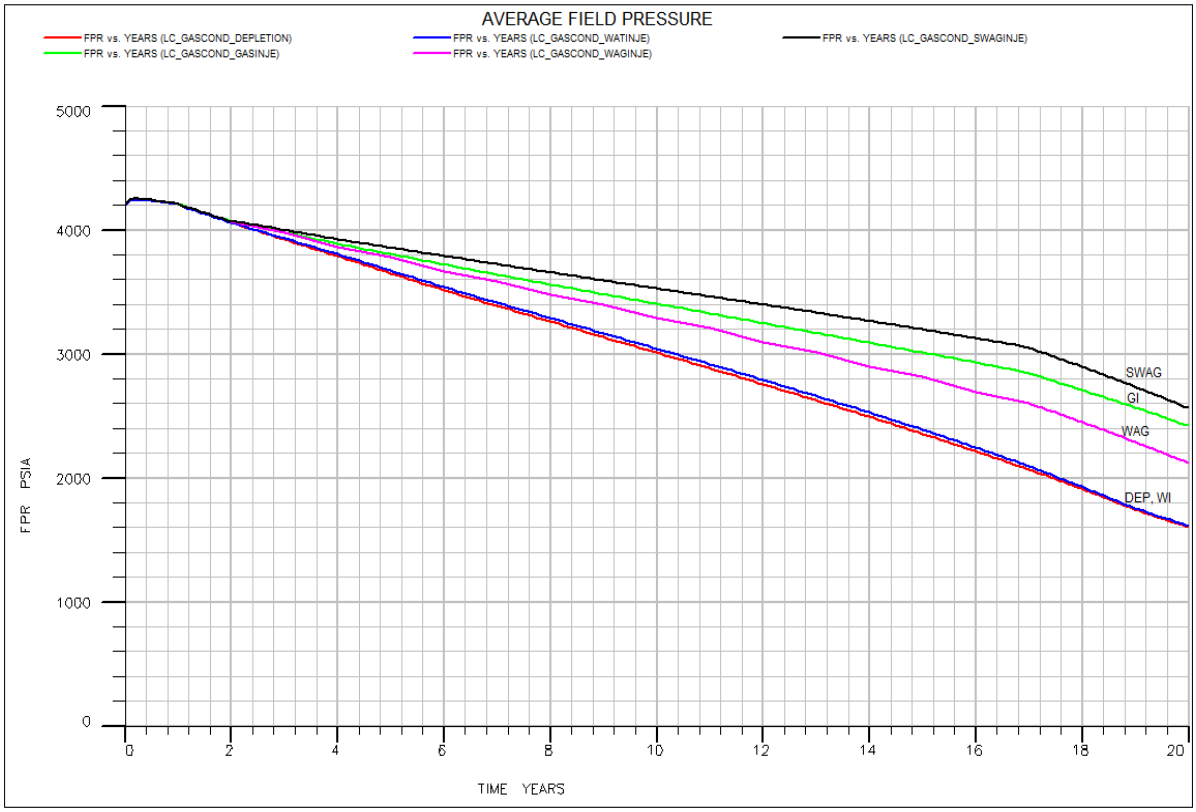

Figure 4-7:Field pressure profile as a function of time (limited compositional case).

4.3.2 Field Water Cut

The remarkably high water cut of 90% is observed for the natural depletion case due to the influx of water into the wells in the south-eastern (SE) region of the reservoir from the adjoining aquifers. Figure 4-8 shows the water cut profiles for the 20-year simulations. The limited compositional model identifies the fluid within the region to be oil. Therefore, the pressure energy comes from the expansion of the gas dissolved in the oil. This solution gas expansion may be insufficient to maintain reservoir pressure. Also, the withdrawal rates of the wells in the SE region are higher. Injection of water into the reservoir only adds to the excessive water production in some of the wells, hence the highest water cut is recorded in this case. The water cut gradient is very steep because it is an aggregate of the aquifer influx and injection rate. The gas injection case significantly reduces the field water cut to about 53%. Gas can move quicker and saturate the pore spaces before the aquifer can respond to the production voidage. The WAG process helps to lower the fraction water flow to around 62%. This value is higher than that of the gas injection process due to the water been pumped into the reservoir alongside the gas. The final water cut from SWAG injection process is 76%. The water injection and natural depletion cases show a similar profile until the 6th year, where the water cut rises steeply as the cumulative water injection increases (Cobanoglu et al., 2018). On the other hand, the WAG and gas injection profile only become distinct after

injection totally ceases in the 11th year, with the WAG water cut rising higher above that of gas injection. At the end of the simulation, there water cut by gas injection and WAG are 77% and 64%, respectively.

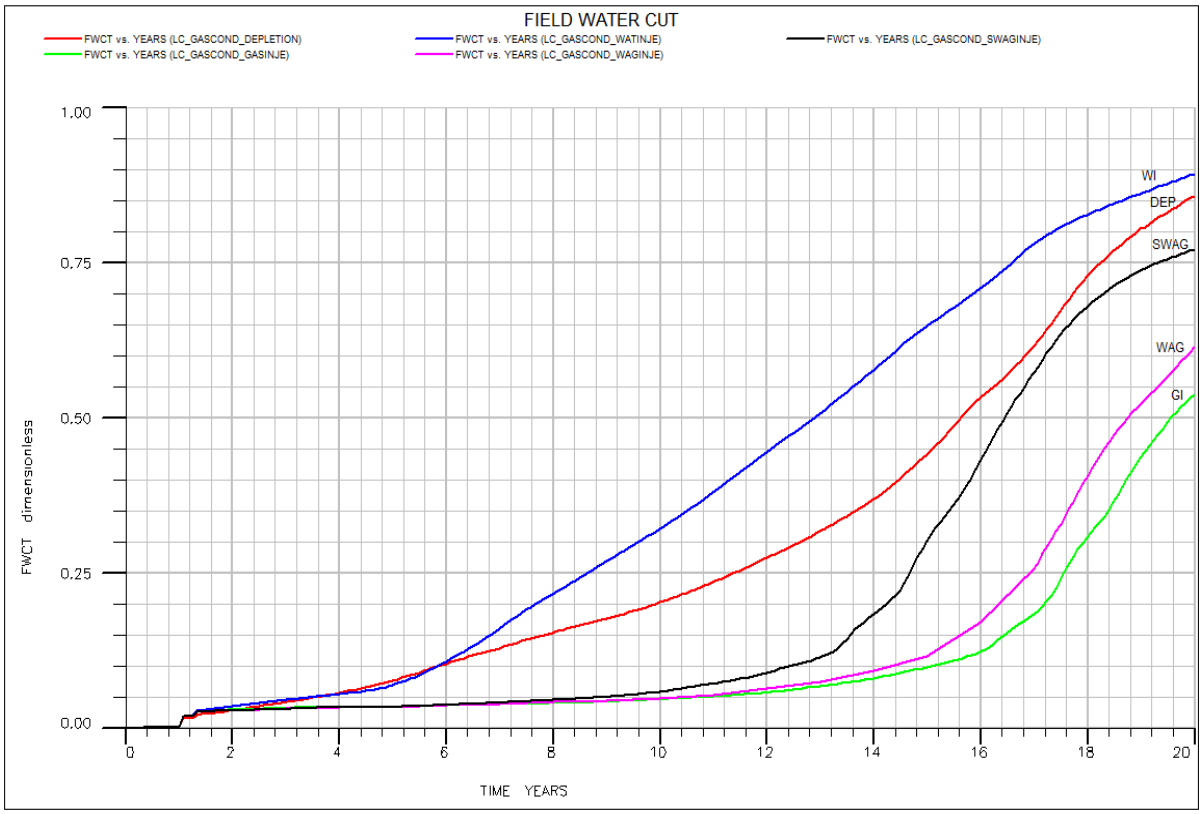

Figure 4-8:Field water cut versus time (limited compositional case).

4.3.3 Cumulative Gas Production and Field Gas Production Rates

For the limited compositional model, the WAG, SWAG, and gas injection processes gave identical cumulative recovery of gas as in the fully compositional model (Figure 4.9 vs. Figure 4.3). However, the cumulative gas recovery for the water injection and depletion strategy are higher in the limited compositional model than the fully compositional model. (The cumulative gas production under water injection is the lowest (216.03 BCF), followed by the depletion strategy (216.31BCF).

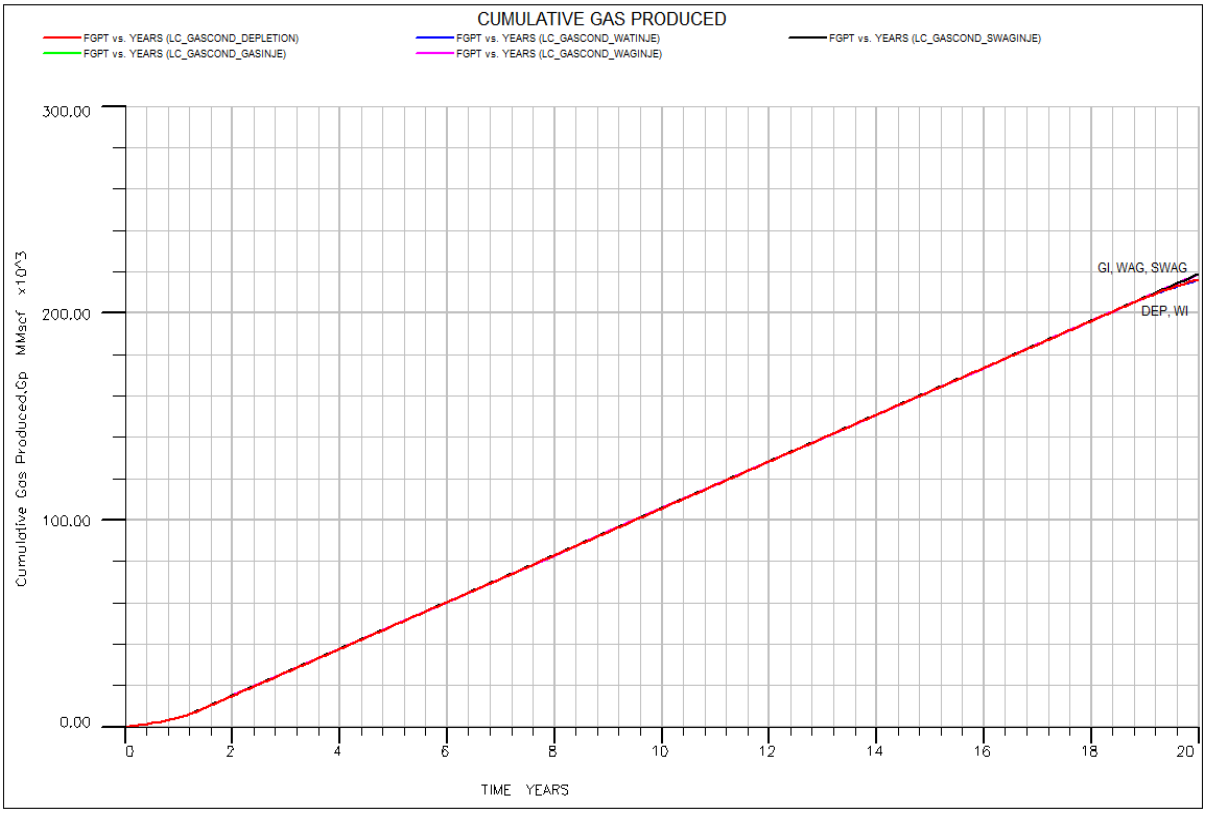

Figure 4-9:Cumulative gas produced (limited compositional case).

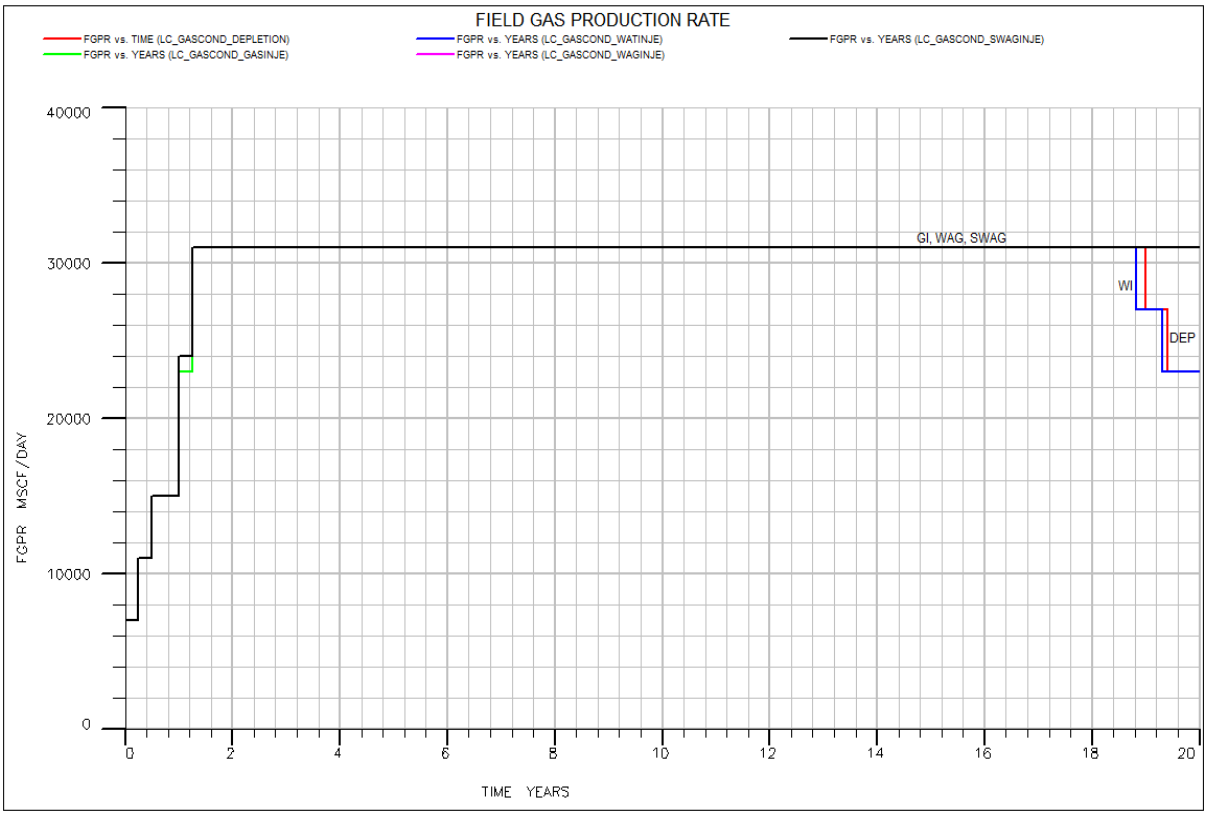

Figure 4-10:Field gas production rates (limited compositional case).

Figure 4.10 displays the gas production rate versus time. The results indicated the duration for which the producing wells were able to deliver the target rates while satisfying the operational constraints. It was observed that for the depletion case, production dropped from 31MMSCF to 25MMSCF in the Year 19.5. Similarly, the production decline was observed earlier in the water injection strategy in Year 19. The reason for this is because wells PROD_SE1, PROD_NW7, and PROD_NW8 (Figure 3.3) were shut-in after exceeding the maximum water cut (95%).

4.3.4 Cumulative Oil Production

The results of the cumulative oil produced are presented in Figure 4-11. The injection cases (GI, WI, WAG, and SWAG) exhibit varying degree of influence on the recovery of the oil in place. In terms of incremental oil recovery, the SWAG injection (45.07MMSTB) recovers the highest volume of oil, followed by the WAG (43.07MMSTB) and gas injection (39.67MMSTB) schemes, respectively. Under natural depletion, the wells recovered 33.30MMSTB of oil after 20 years production, while water injection predicted the oil recovery of 36.67MMSTB. The water injection recovery strategy follows the same slope in cumulative oil production as with the natural depletion case before it overtakes the latter in the Year 4. Although, the slope of the SWAG injection case is not as sharp as the aforementioned (i.e., natural depletion and WI), it overtakes the natural in the 10^{th} year. The condensate recovery due to WAG and gas injection surpass the base case in the Year 12 and Year 14, respectively.

The field oil production rate profiles plotted in Figure 4-12 show that oil rates build up to a peak value before a gradual oil rate decline is observed. The duration and amount of the peak production for each of the five recovery strategies differ. However, the results of the water injection are similar to those from natural depletion cases. We can also observe the similarity in results from the WAG and gas injections schemes. The maximum build up rate begins at 9,000 STB/D until a peak production rate of 11,250 STB/D is reached for WI and natural depletion in Year 3 and Year 5. The peak production for the SWAG, WAG, and gas injection is identical (10,000 STB/D).

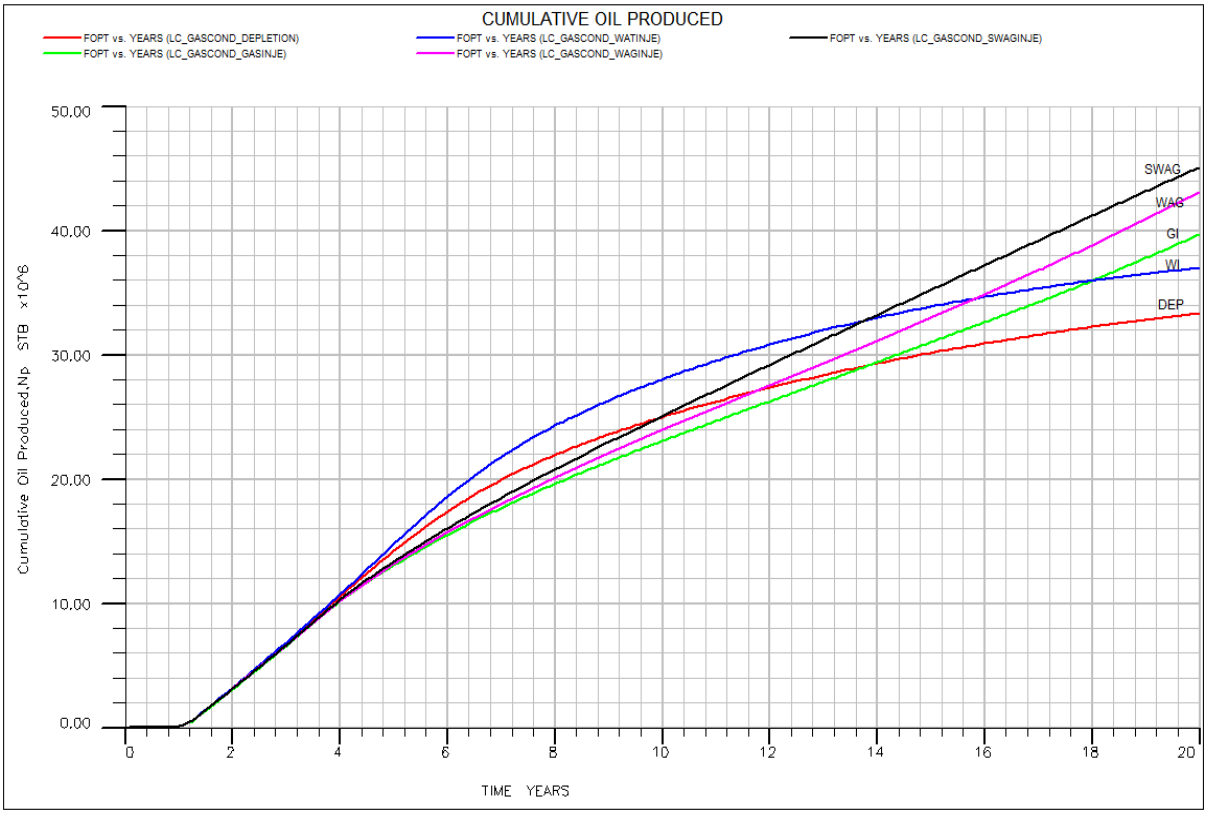

Figure 4-11:Cumulative oil produced (limited compositional case).

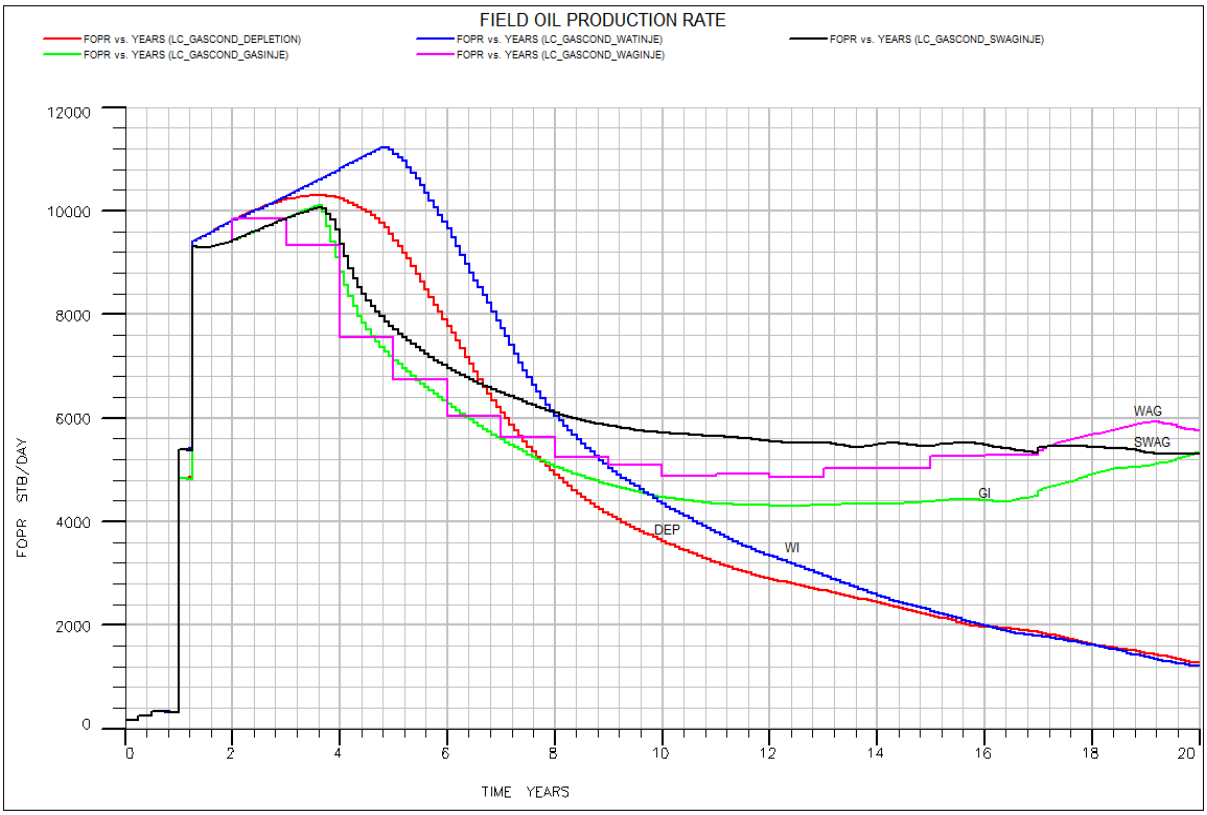

Figure 4-12:Field oil production rates (limited compositional case).

The SWAG injection scheme shows an overall improvement in oil rates as it overtakes the natural and water injection in Year 7 and 8. At the end of the simulation run, the field oil rates are highest in the WAG case, closely followed by gas and SWAG injection, pressure depletion, and water injection, in that order.

4.4 COMPARATIVE ANALYSIS BETWEEN THE LIMITED AND FULLY COMPOSITIONAL MODELS

4.4.1 Fluid-in-Place Volumes

At the beginning of the study, the fully and limited compositional models are initialized to estimate the initial fluids in place. Although the depth of the oil-water/gas-oil contact are used to determine the pay-zone thickness, it may not be sufficient to accurately predict the hydrocarbon volumes. The reservoir fluid is made up of components of varying molecular weights, and as the pressure-temperature conditions permit, component segregation may occur due to gravity effect in steeply dipping reservoirs. Hence, the initial reservoir fluid composition may be either constant with depth or exhibit a vertical compositional gradient.

To begin this study, both the fully compositional and limited compositional models were run with vertical compositional gradients. The fully compositional model was initialized with a composition versus depth table, while the limited compositional model was initialized with solution gas-oil and oil-gas ratio versus depth tables to represent the compositional gradient. Figure 4.13 shows comparison of the fluid in-place volume for the fully compositional and limited compositional models. The fully compositional model predicts a lower value of FGIIP than the limited compositional model (Fevang et al., 1999). This is because the simulator can determine that the molar composition of the intermediate to heavier fractions in the liquid phase is higher than that in the gas phase. Subsequently, the fully compositional model predicted a higher value of oil initially in place than the limited compositional model as shown in Figure 4.14 (Fevang et al., 1999)

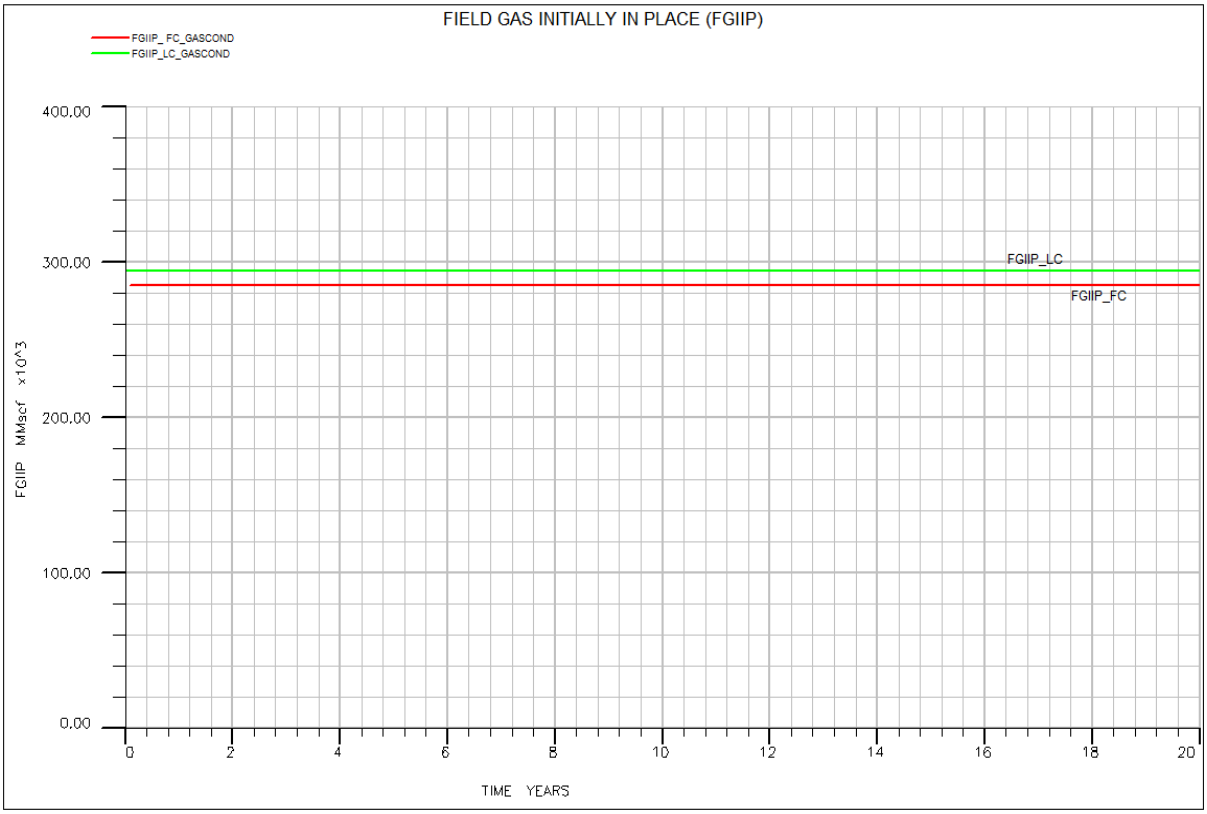

Figure 4-13:Initial gas in place for limited and fully compositional case.

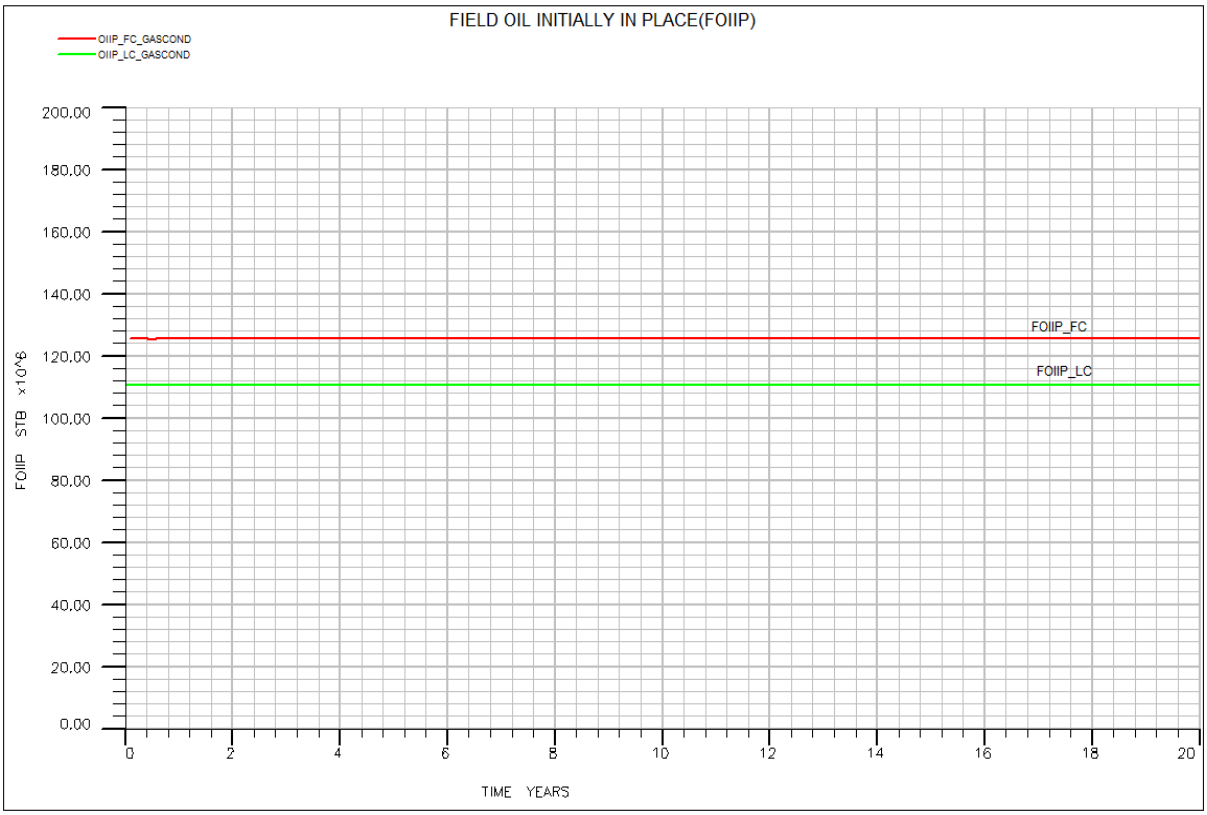

Figure 4-14:Initial oil in place for limited and fully compositional case.

4.4.2 Reservoir Performance and Recovery Efficiency

The results of the comparative analysis between the limited and fully compositional simulations are summarised in Tables 4-1 through 4-3.

The cumulative gas production for the five recovery schemes are presented in Table 4-1 for the fully and limited compositional cases respectively. Although the same volume of gas production is obtained for the fully and limited compositional simulators for the GI, WAG, and SWAG scheme, the limited compositional model reported a higher cumulative production for gas compared to the fully compositional model for the WI scheme. Generally, the cumulative production of condensate for the fully compositional case is higher than that calculated for the limited compositional scenario.

Even though the cumulative volumes for the reservoir fluids produced are identical for some of the recovery strategies that were investigated, it is essential to distinguish the performance of each scheme based on the calculated values of GIIP and OIIP for the fully and limited compositional models respectively. The limited and fully compositional model results reported 74-76%, 74-77%, 75-77%, and 75-77% of GIIP for the DEP/WI, GI, WAG, and SWAG injection respectively. Water flooding reduced gas recovery due to high water production and early well abandonment (Cobanoglu et al., 2018; Tran et al., 2018).

The condensate recovery efficiency of the production strategies is stated in ascending order. Waterflooding of gas condensate reservoir recovers efficiency of 33-36% of OIIP (Ali, 2014; Udie et al., 2014). For the GI scheme, recovery efficiency is `36-37% of OIIP due to partial pressure maintenance (Cobanoglu et al., 2018. WAG injection improves recovery to 39% of OIIP, while SWAG injection gives 41% of OIIP.

For the fully compositional model (as shown in Table 4-2), the incremental condensate recovery was maximum for the SWAG injection scheme (8.29%), followed by the WAG (6.32%), GI (4.77%), and least performance by WI (3.72%) in comparison to depletion without any form of injection. The incremental result of the SWAG scheme over WAG and GI scheme were 1.97% and 3.52% respectively (Hernandez et al, 1999). For the limited compositional case, SWAG provided the best additive recovery of condensate (10.63%), followed by WAG (8.82%), GI (5.75%), and WI (3.31%), compared to the conventional depletion strategy

.

Table 4-1:Comparative analysis of reservoir performance between the limited and fully compositional models.

PARAMETERS	GAS (BCF)			OIL (MMSTB)		
	FC	LC	Difference	FC	LC	Difference
Fluid In Place	284.57	293.64	+3.19%	125.40	110.68	+11.74%
RECOVERY SCHEMES						
Depletion	216.19	216.31	+0.06%	40.91	33.30	+18.6%
WI	215.25	216.03	+0.36%	45.57	36.97	+18.87%
GI	218.63	218.63	0%	46.89	39.67	+15.39%
WAG	218.83	218.83	0%	48.83	43.07	+11.81%
SWAG	218.72	218.72	0%	51.30	45.07	+12.14%

Table 4-2:Comparative analysis of the oil and gas recovery factors.

RECOVERY EFFICIENCY				
	GAS		CONDENSATE	
	Fully Compositional (Base case)	Limited Compositional	Fully Compositional (Base case)	Limited Compositional
Depletion	75.97%	73.67%	32.62%	30.09%
WI	75.6%	73.57%	36.34%	33.40%
GI	76.83%	74.46%	37.39%	35.84%
WAG	76.89%	74.52%	38.94%	38.91%
SWAG	76.86%	74.49%	40.91%	40.72%

Table 4-3:Comparative analysis of the average reservoir pressures and field water cut.

	FIELD PRESSURE (psia)		WATER CUT	
	Fully Compositional (Base case)	Limited Compositional	Fully Compositional (Base case)	Limited Compositional
Depletion	1563	1600	73.9%	86%
WI	1637	1620	76.85%	89%
GI	2263	2400	67.21%	53%
WAG	1811.4	2180	73.39%	62%
SWAG	2439	2600	85.03%	77%

4.5 CONDENSATE BANKING

In this section, condensate banking phenomena is investigated for the various injection cases. A time lapse (using a 5-year interval) of pressure, gas saturation, and oil saturation is

presented here for the fully compositional case under the depletion, gas injection, WAG, and SWAG schemes. A similar set of time-lapse profiles for the limited compositional model is covered in Appendix B (Figures B-7 - B-65)

4.5.1 Depletion Scheme

4.5.1.1 Pressure

The pressure distribution generally decreases with time due to continuous fluid withdrawal. The reservoir is produced from two major regions in the North-west and South-east respectively. Since the wells in the South-east are horizontal, pressure declines more rapidly in the region than the North-western part due to higher production rate targets. At initial conditions (t=0 year), the reservoir pressure is above the dewpoint pressure (Figure 4-15). Subsequently, pressure declines in the reservoir with time as shown in Figures 4-16 – 4-19, with the highest pressure drop occurring in the vicinity of the wells, but increasing outwards towards the aquifer boundaries.

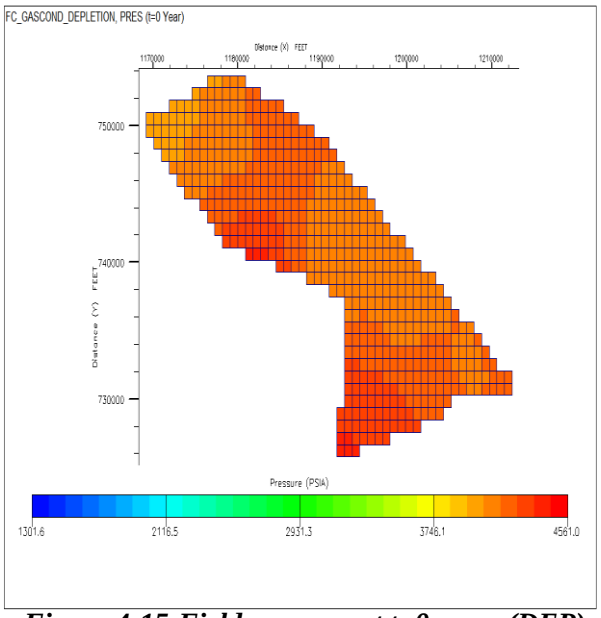

Figure 4-15:Field pressure at t=0 years (DEP).

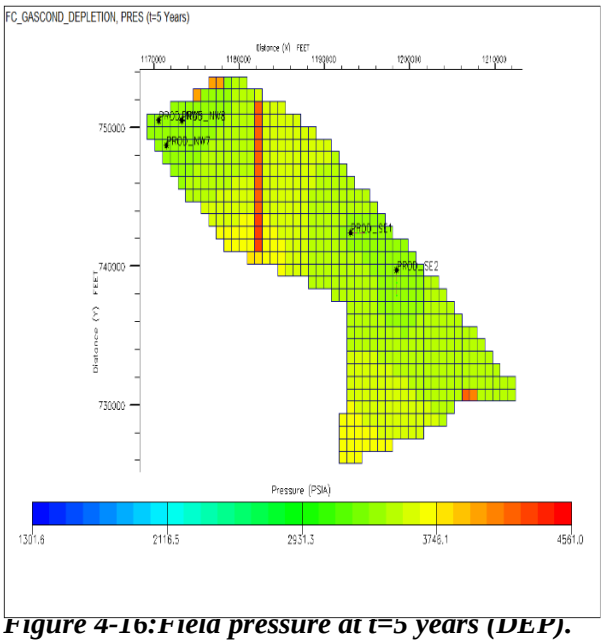

Figure 4-16:Field pressure at t=5 years (DEP).

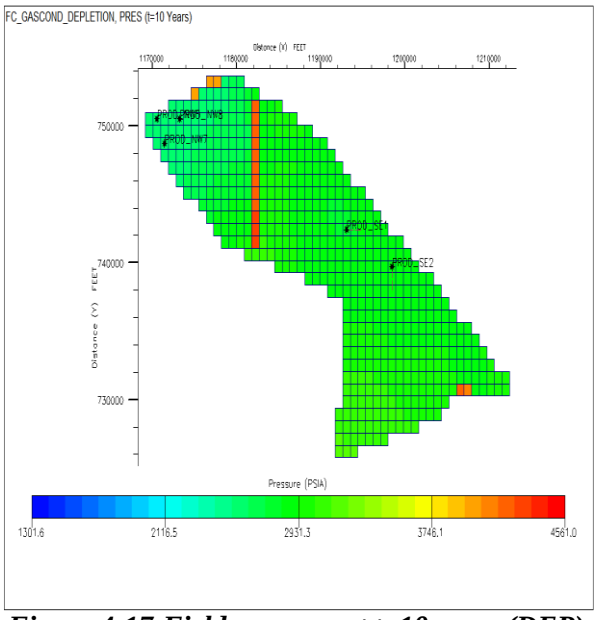

Figure 4-17:Field pressure at t=10 years (DEP).

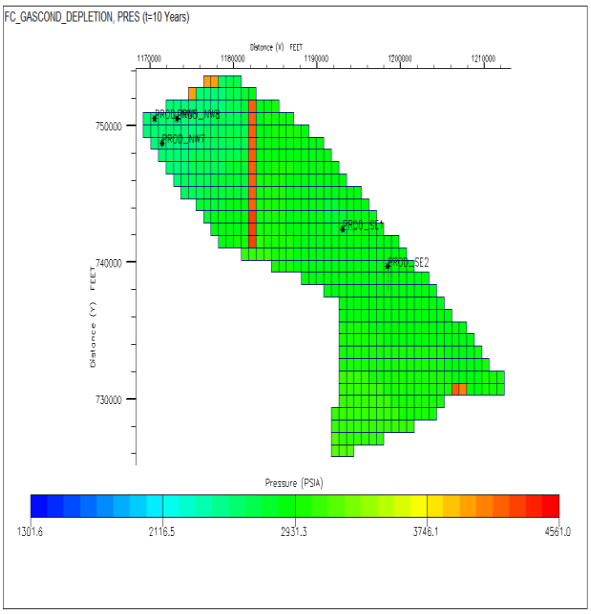

Figure 4-18:Field pressure at t=15 years (DEP).

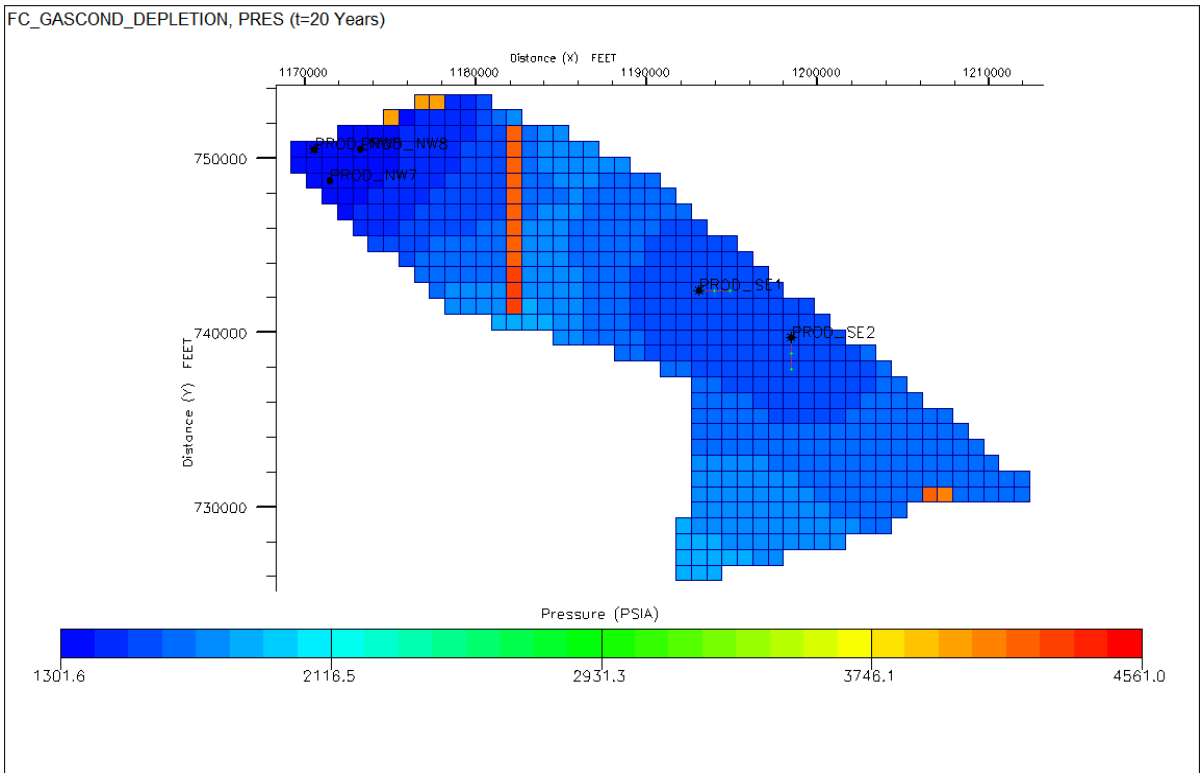

Figure 4-19:Field pressure at t=20 years (DEP).

4.5.1.2 Gas Saturation

The gas saturation distribution of the field at throughout the simulation period are presented in Figures 4-20 – 4.24 respectively. Initially, the gas saturation in the Northwest was at a maximum of 80%, and it decreases down structure towards the OWC (Figure 4-20). The South east region has a slightly lesser gas saturation at Year 0 (Figure 4-20). The North-west

producers (PROD_NW5, NW7, & NW8) show negligible change in gas saturation with time compared to PROD_SE1 and PROD_SE2. As production progresses, the gas saturation decreases for grid cells located at higher depths and closest to the wells. Nonetheless, gas saturation declines throughout the reservoir the reservoir wellbore had the highest reduction profile and this was due to fluid withdrawal. There appears to be stranded hydrocarbons farther away from the two main reservoir sands. The gas saturation at this location remains the same and suggests non-communication with the existing wells. Thus, additional wells may be required to drain the area.

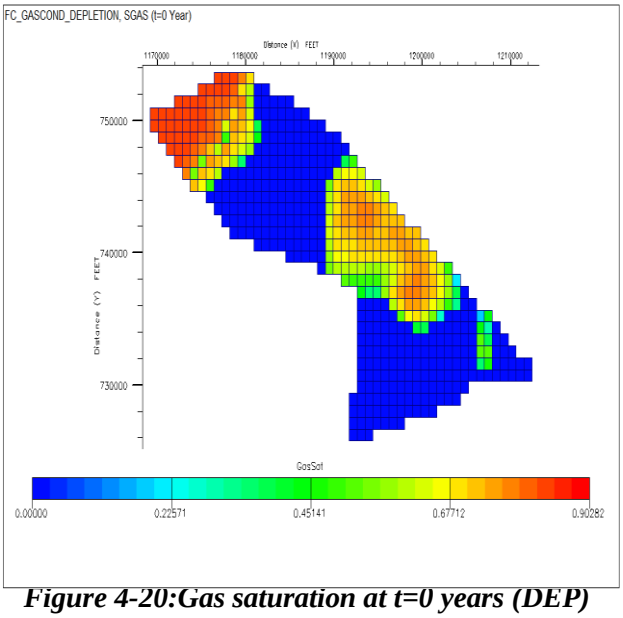

Figure 4-20:Gas saturation at t=0 years (DEP)

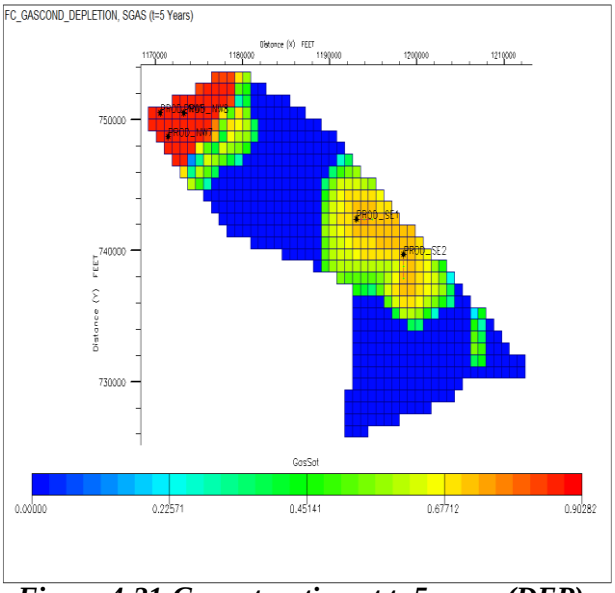

Figure 4-21:Gas saturation at t=5 years (DEP).

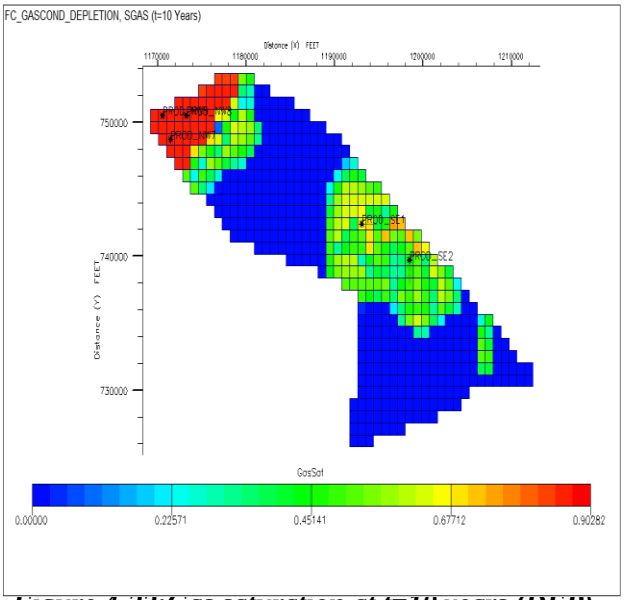

Figure 4-22:Gas saturation at t=10 years (DEP).

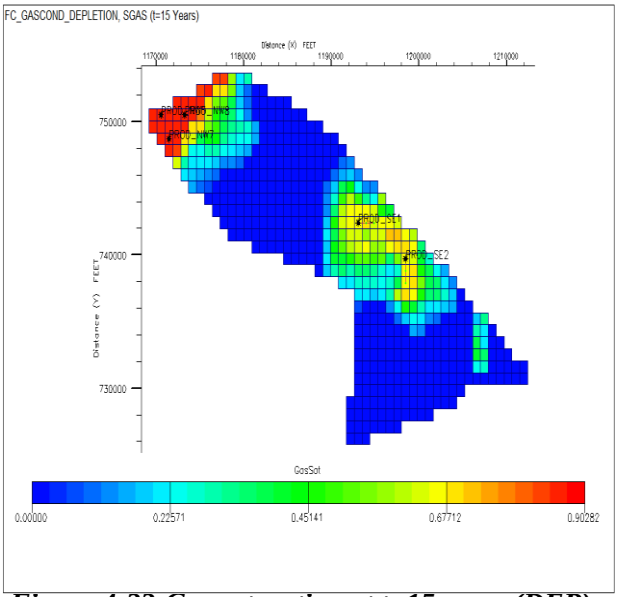

Figure 4-23:Gas saturation at t=15 years (DEP).

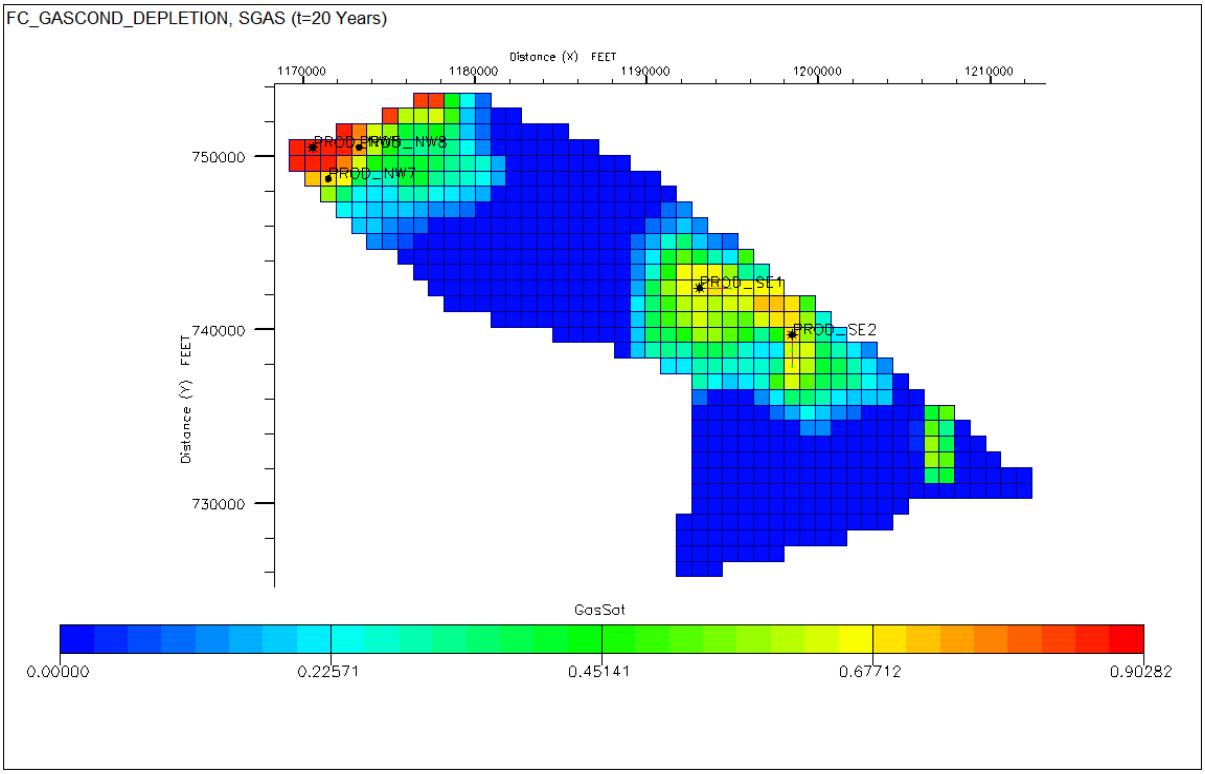

Figure 4-24:Gas saturation at t=20 years (DEP).

4.5.1.3 Oil Saturation

The oil saturation distribution of the field at different times of production is discussed in Figures 4-25, 4-26, 4-27, 4-28, and 4.29 respectively. At Year 0, the oil saturation in the entire field was essentially zero since the reservoir pressure was the same as the dew point pressure, except in the North-western region where small condensate drop out has occurred at higher depth due to gravity segregation of the heavier components (but oil saturation is lesser than the critical oil saturation). In Year 5, as pressure declines, more condensate build-up is observed in the Northwest but no condensate drop out occurs in the south-east. With continued production, considerable condensate production is observed closest to the wellbore as the condensate saturation exceeds critical saturation and becomes more mobile (Figure 2-27). In Figure 4-28 and 4-29, it is observed that the condensate saturation has drastically reduced to the residual oil saturation around the wellbore. However, since the reservoir pressure generally decreases, condensate dropout reaches a significant saturation at even farther distances from the well completions at the end of the simulation.

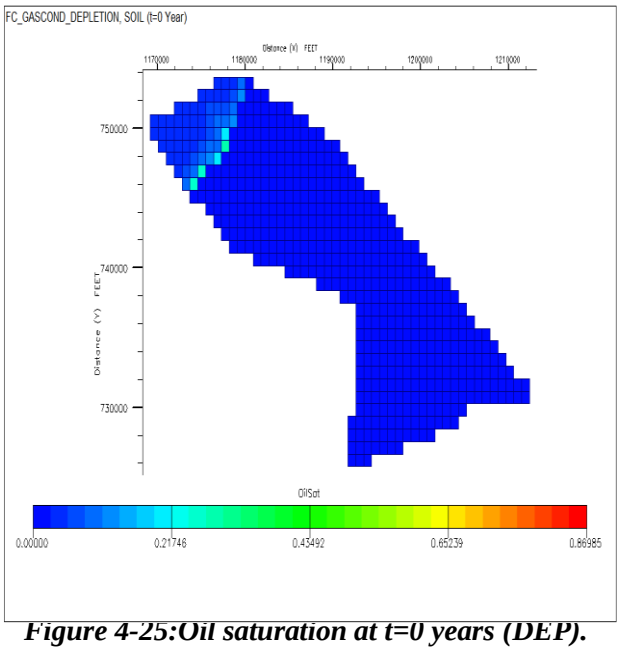

Figure 4-25:Oil saturation at t=0 years (DEP).

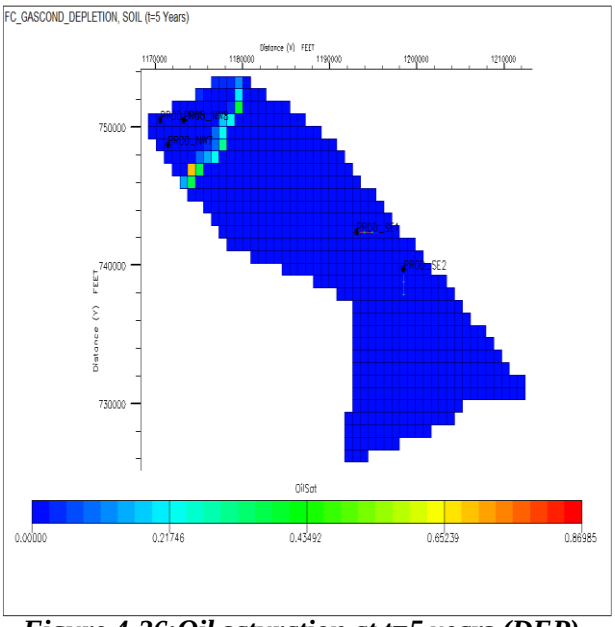

Figure 4-26:Oil saturation at t=5 years (DEP).

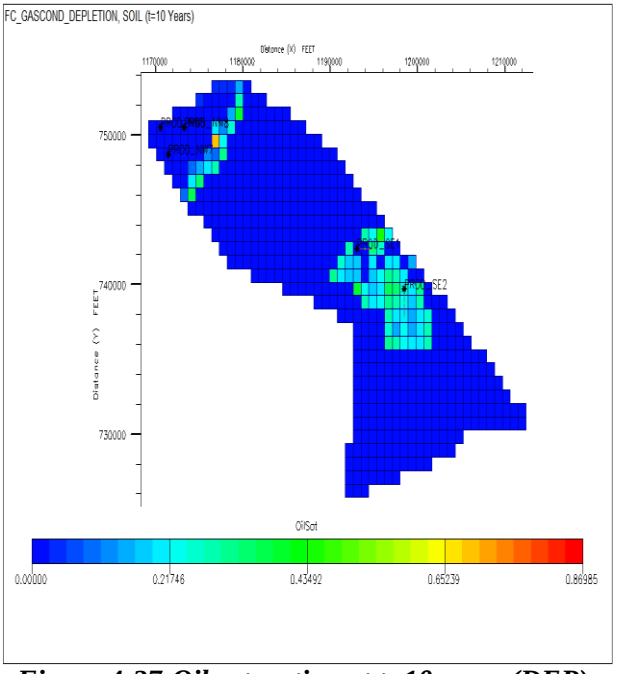

Figure 4-27:Oil saturation at t=10 years (DEP).

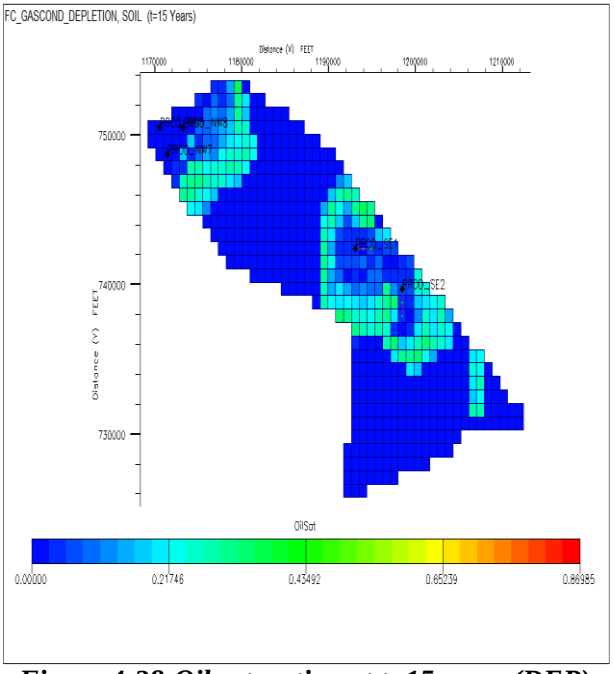

Figure 4-28:Oil saturation at t=15 years (DEP)

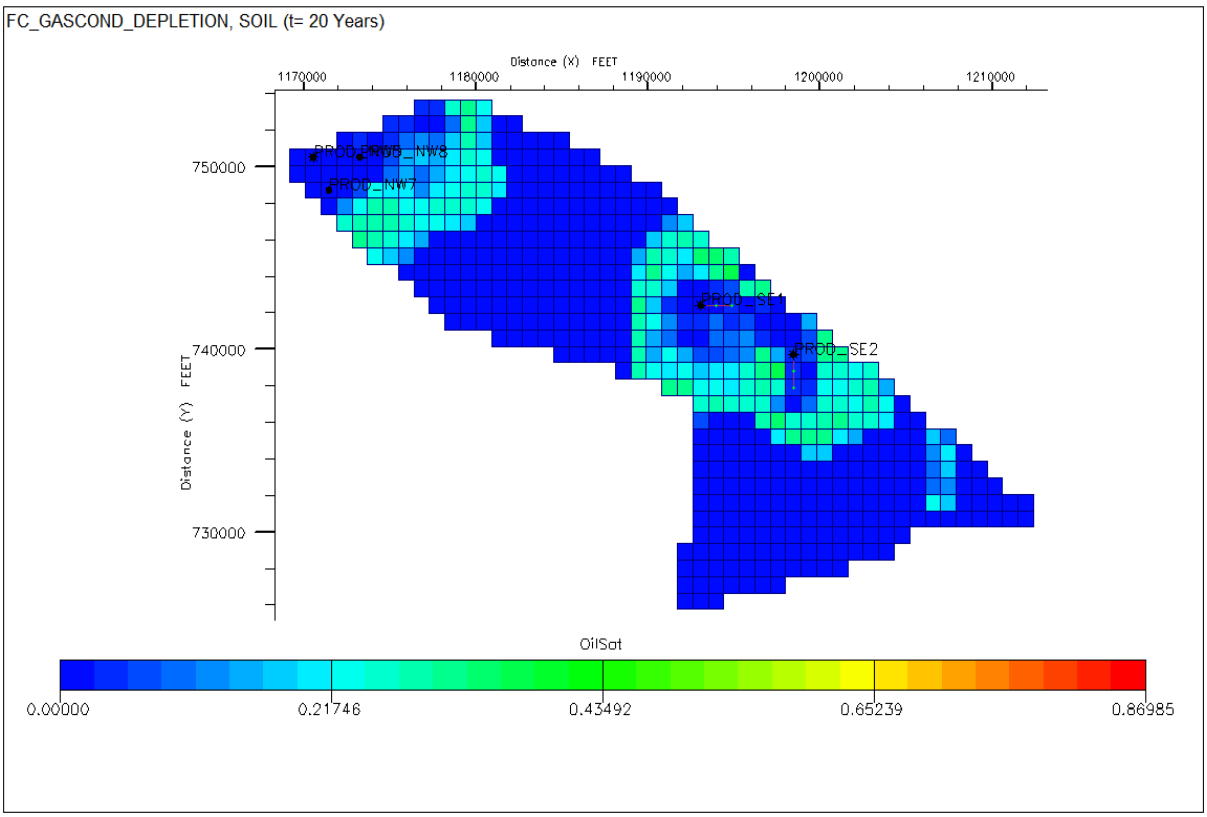

Figure 4-29:Oil saturation at t=20 years (DEP).

4.5.2 Gas Injection

4.5.2.1 Pressure

The pressure distribution at different stages of production during gas cycling. Initial pressure conditions are the same as that in the natural depletion scheme (Figure 4-30). In Year 5, the reservoir pressure declines due to partial gas re-injection, although less rapidly compared to the natural depletion case (Figure 4-31). However, the Northwest is maintained at a slightly higher pressure than the Southeast. The pressure around the injector wells is greater compared to the grid pressures surrounding the producers. At Year 10 and Year 15, the reservoir pressure approaches equilibrium as the aquifer influx compensates for the pressure deficit in each region (Figure 4-32, 4-33). At the end of the simulation period, the average field pressure has decreased due to gas cap blowdown (Figure 4-34).

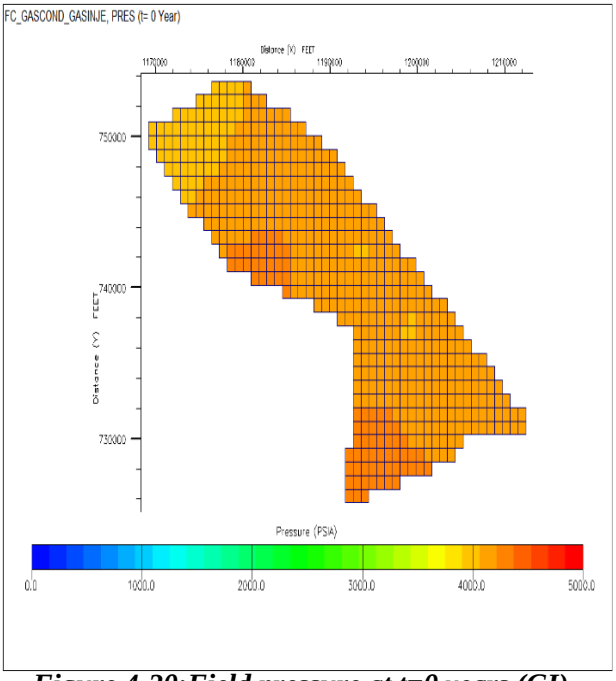

Figure 4-30:Field pressure at t=0 years (GI).

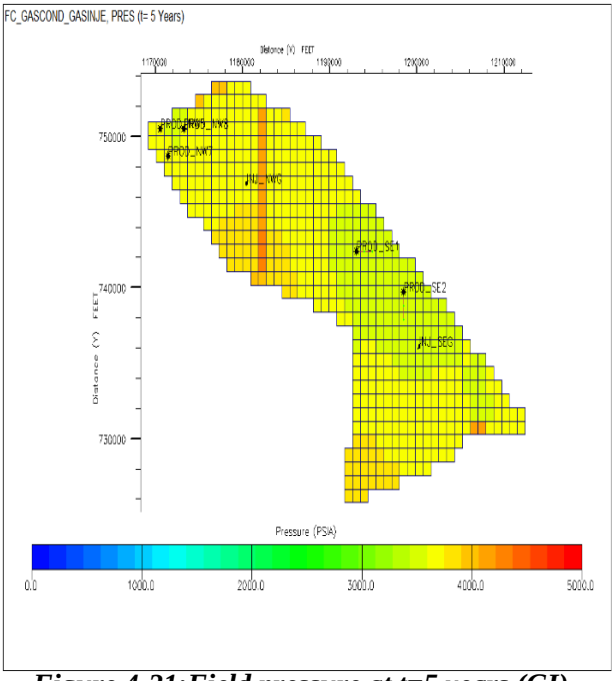

Figure 4-31:Field pressure at t=5 years (GI).

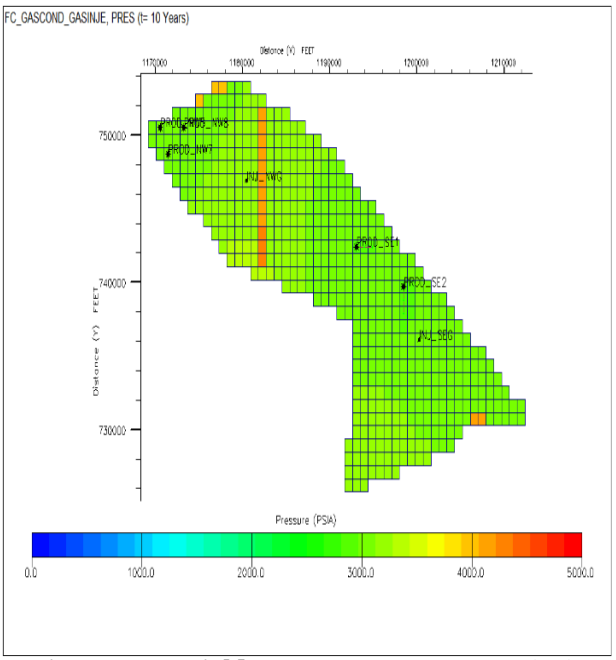

Figure 4-32:Field pressure at t=10 years (GI).

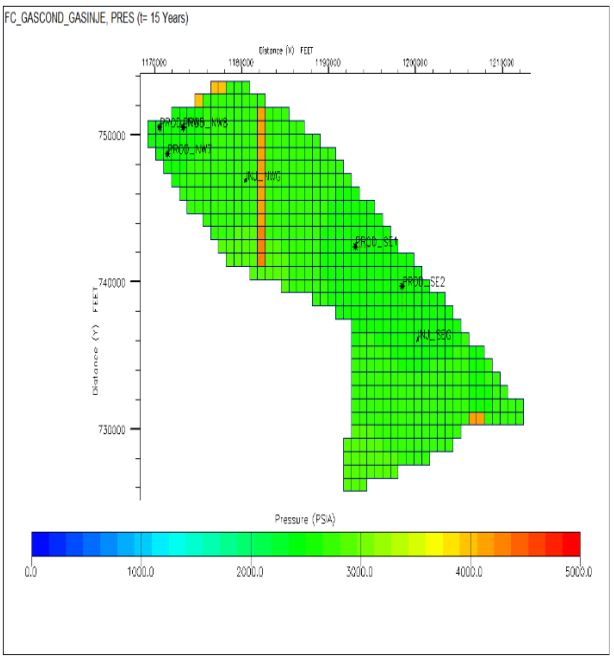

Figure 4-33:Field pressure at t=15 years (GI).

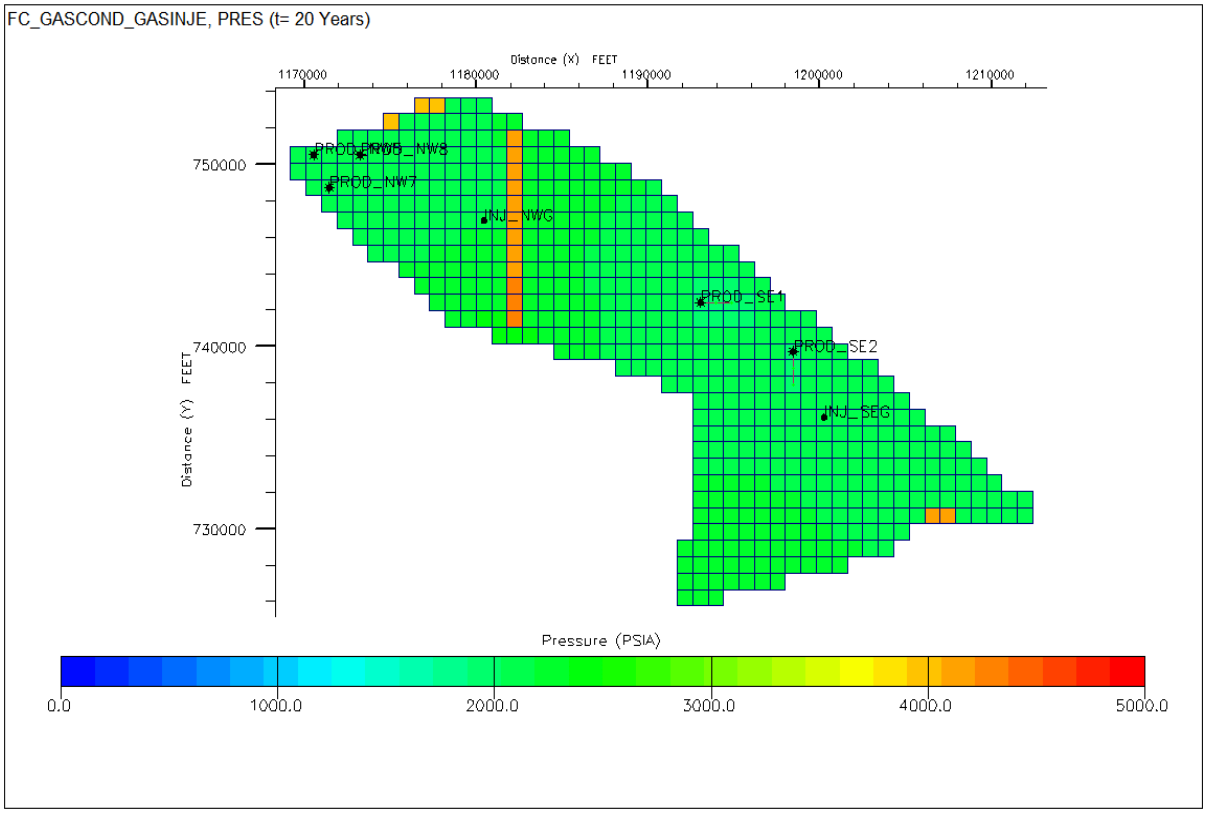

Figure 4-34:Field pressure at t=20 years (GI).

4.5.2.2 Gas Saturation

At initial conditions, the gas saturation is similar to that in the depletion scenario. Before injection begins and during the early stages of gas reinjection, gas saturation decreases slightly around the wellbores because the injected gas has not reached the producers. For the horizontal wells, decline in gas saturation is more prominent at the heel of the well compared to the toe. However, the saturation of gas at the injector wells are maintained at a value of ~75% (Figure 4-36). As injection continues, it is observed that gas saturation continues to increase in the Northwest because a higher fraction of the produced gas is reinjected. The opposite trend is noted in the Southeast because a small fraction of gas is reinjected in Year 10 and Year 15 (Figure 4-38, 4-38). Nonetheless, the gas saturation generally decreases as injection ceases and more gas is being produced (Figure 4-39).

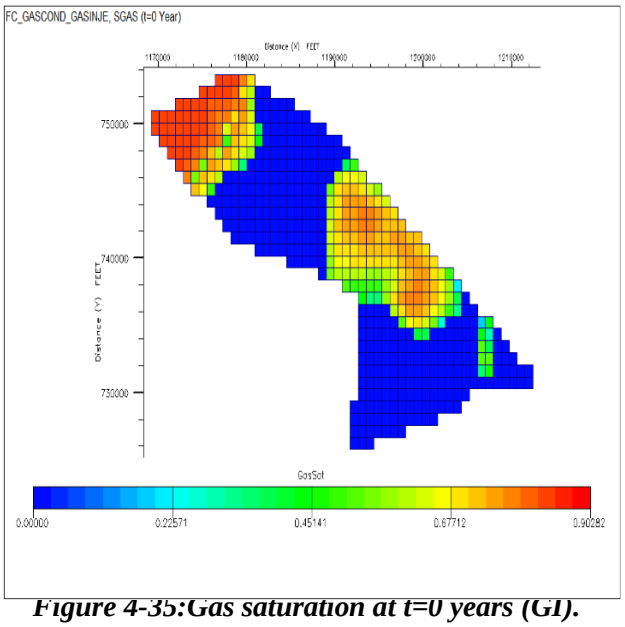

Figure 4-35:Gas saturation at t=0 years (GI).

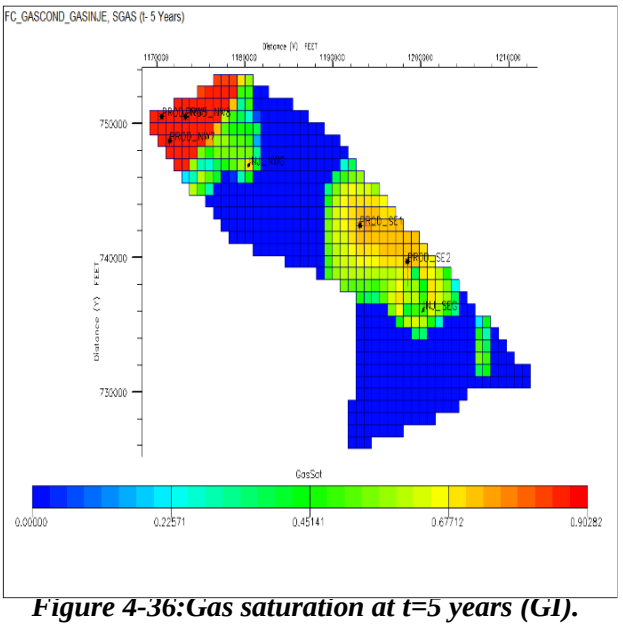

Figure 4-36:Gas saturation at t=5 years (GI).

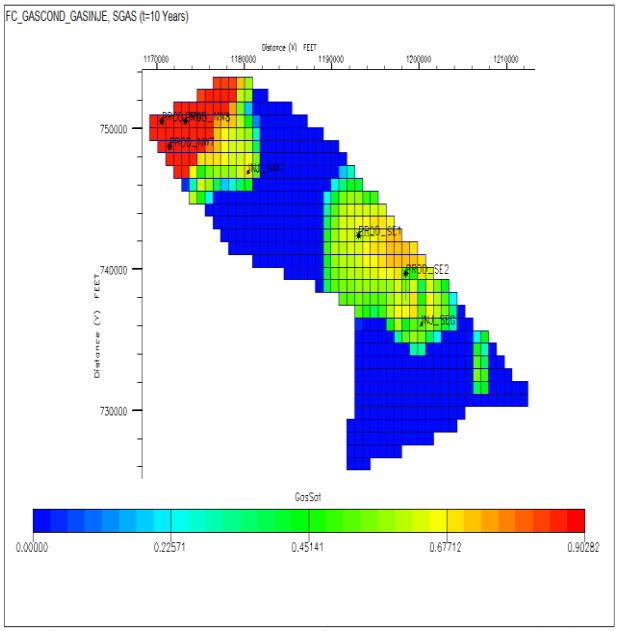

Figure 4-37:Gas saturation at t=10 years (GI).

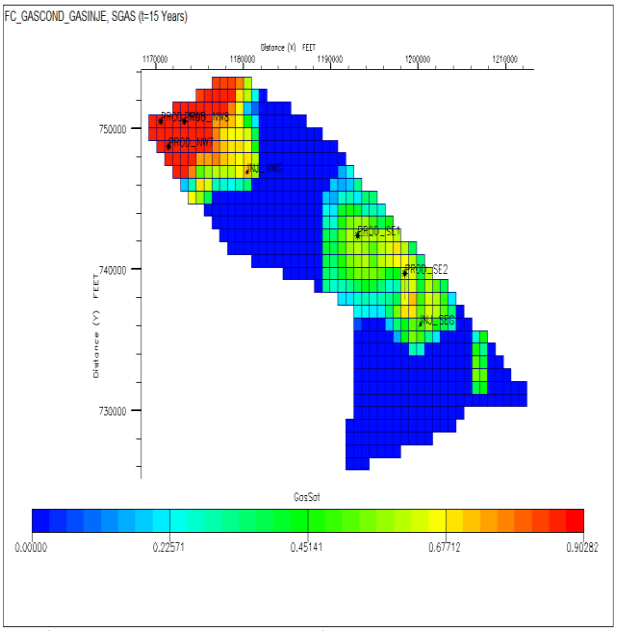

Figure 4-38:Gas saturation at t=15 years (GI).

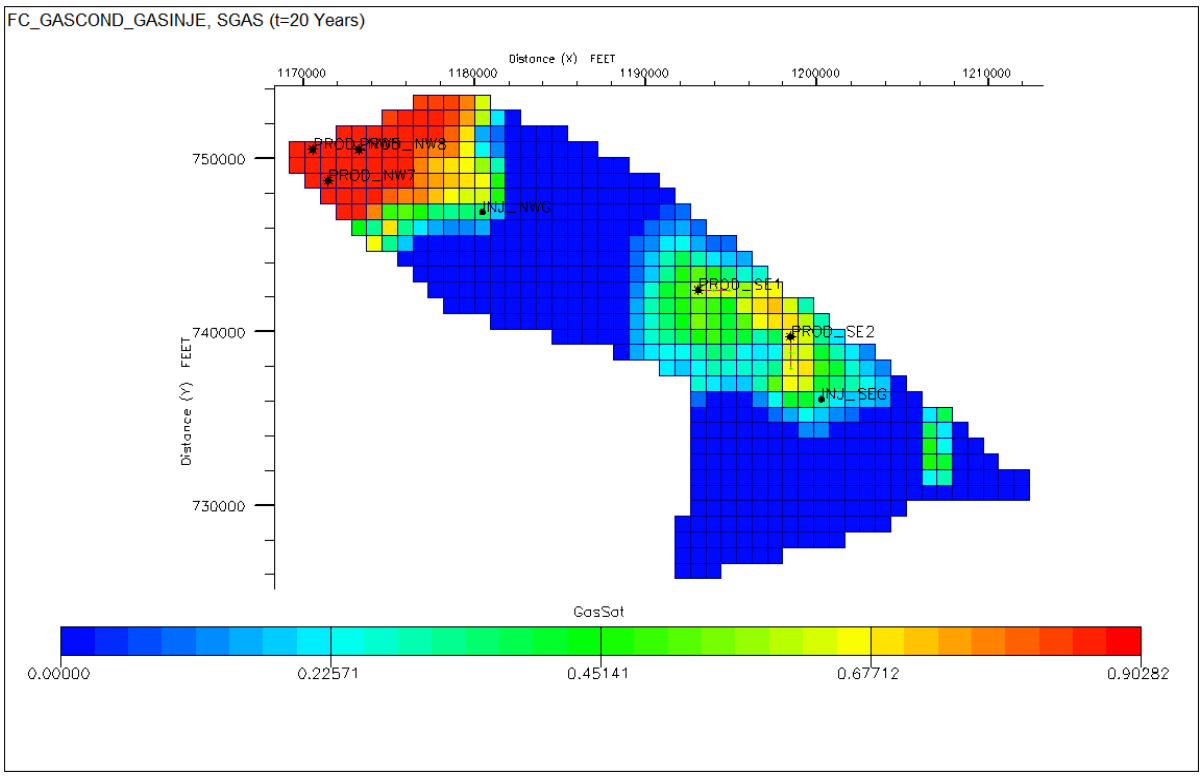

Figure 4-39: Gas saturation at t=20 years (GI).

4.5.2.3 Oil Saturation

The oil saturation is at connate levels at initial time. When injection begins, since pressure is not fully maintained due to partial reinjection, some condensate dropout occurs but the injected gas helps to revaporise the intermediate components for better displacement towards the producers. In the Southeast, oil saturation is significant around the toe of the horizontal wells (Figure 4-40, 4-41). In Year 10, and Year 15, the gas sweep efficiency increases and more condensate is produced at the surface (Figure 4-42, 4-43). Nonetheless, since full pressure maintenance is not achieved, condensate drop out away from the wellbore vicinity increases to considerable saturation levels (Figure 4-44).

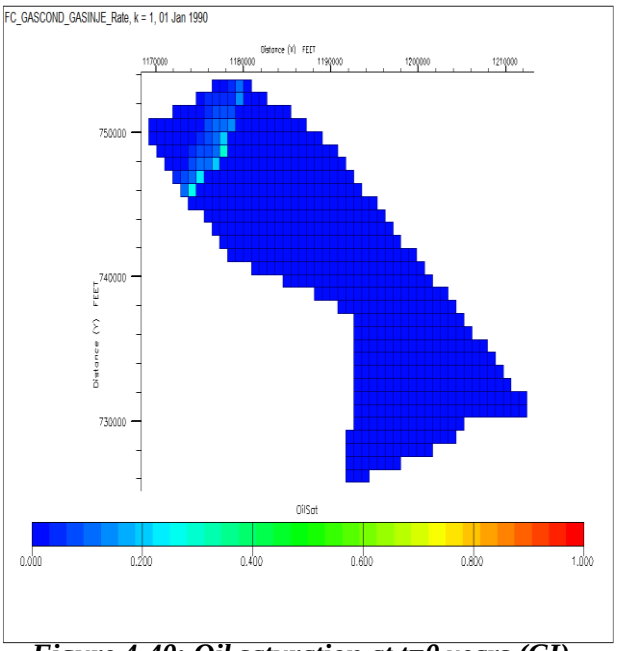

Figure 4-40: Oil saturation at t=0 years (GI).

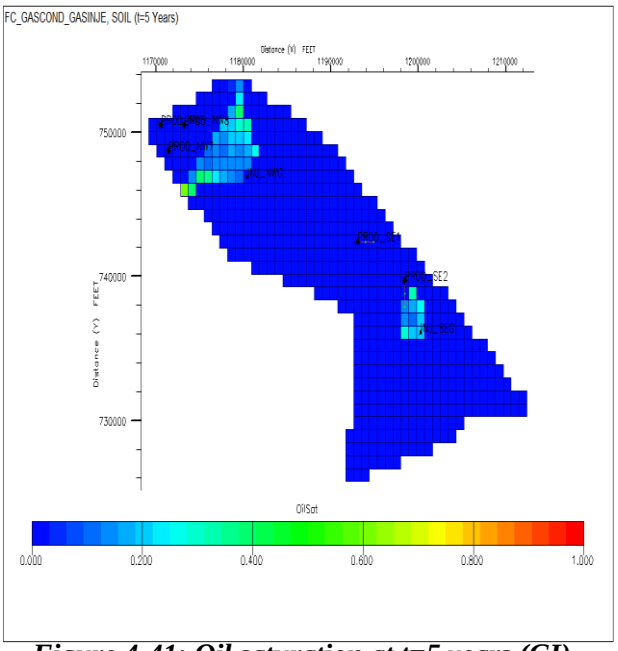

Figure 4-41: Oil saturation at t=5 years (GI).

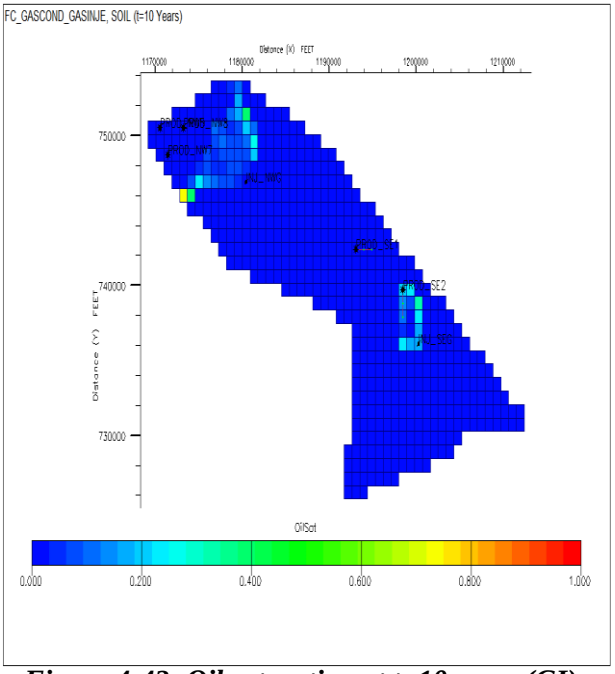

Figure 4-42: Oil saturation at t=10 years (GI).

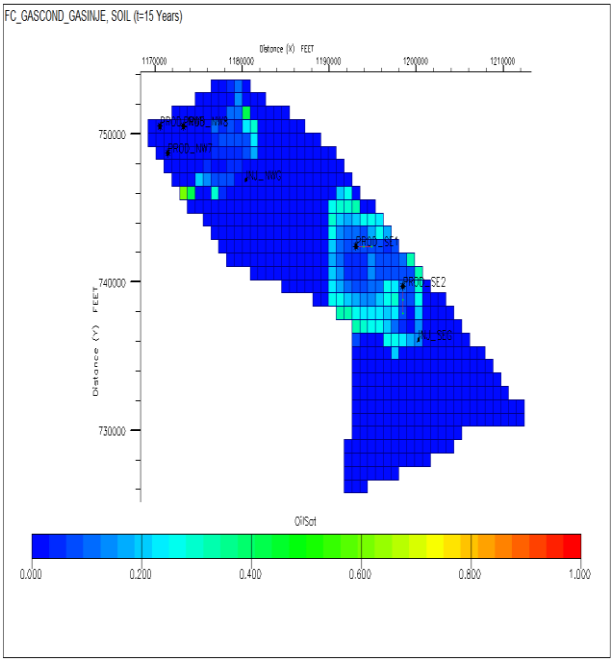

Figure 4-43: Oil saturation at t=15 years (GI).

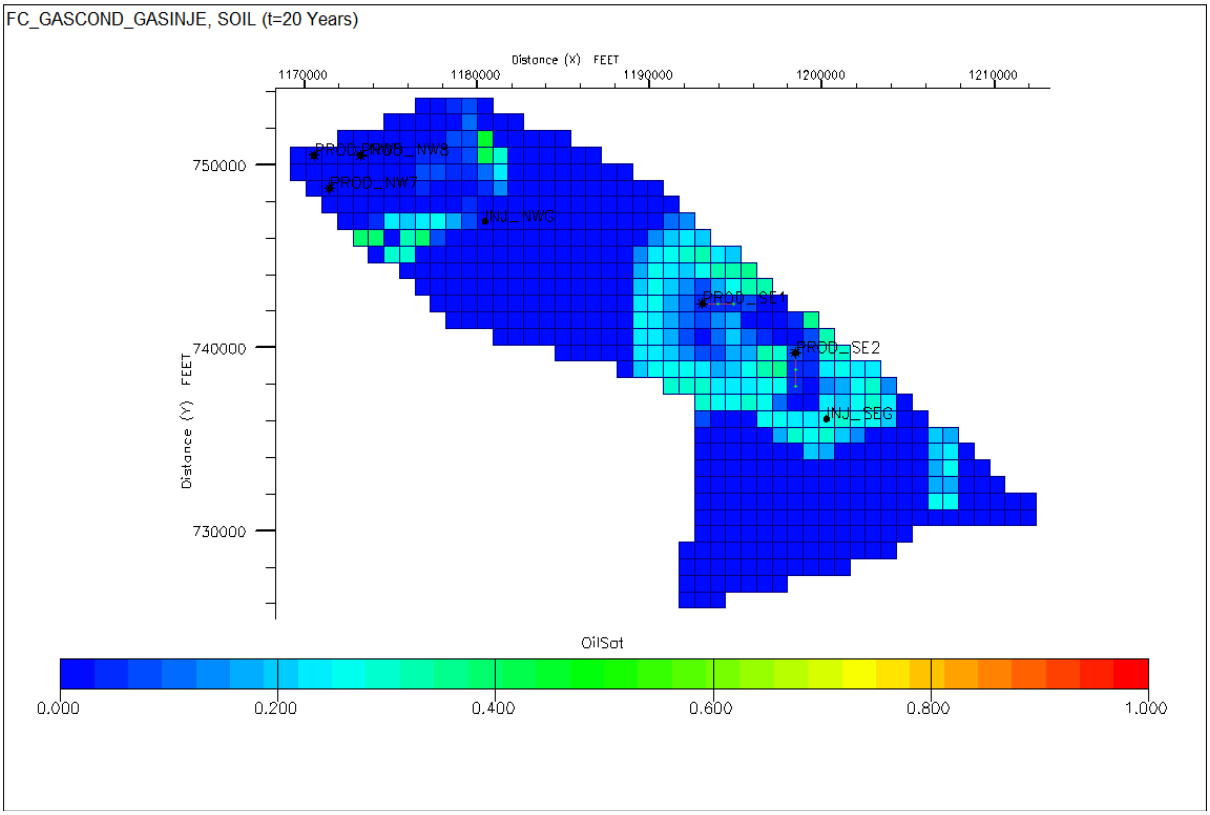

Figure 4-44: Oil saturation at t=20 years (GI).

4.5.3 WAG Injection

4.5.3.1 Pressure

After 5 years of production, the reservoir pressure has declined to about 3200psia (Figure 4-47, 4-48). The pressure decline is more observable around the producing wells but it increases outwards towards the area surrounding the injector wells (Figure 4-49). In fifteen years, the reservoir pressure is completely stabilized as equilibrium is reached between the pressure drawdown of the wells, the pressure of the injected fluids, and the aquifer support (Figure 4-50). It is noted that the reservoir pressure declines more rapidly during the water injection cycle of the WAG scheme as a result of the low WAG ratio utilized in this study. After the end of injection, reservoir pressure declines rapidly to a level much lower than that obtained in gas injection scheme (Figure 4-51).

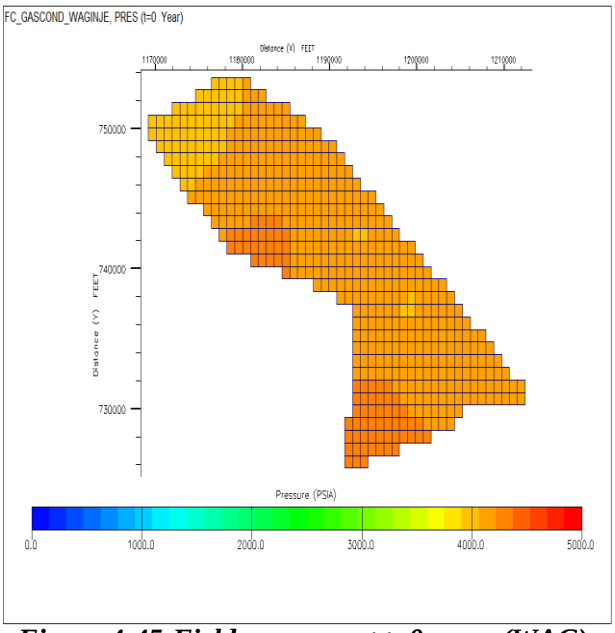

Figure 4-45:Field pressure at t=0 years (WAG).

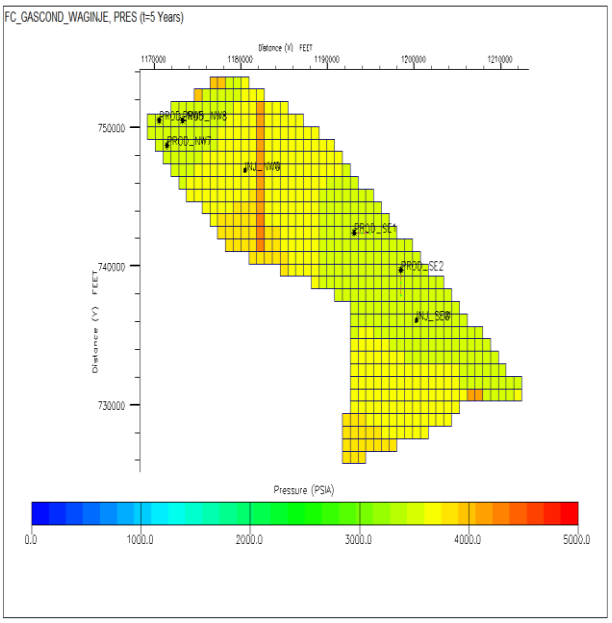

Figure 4-46:Field pressure at t=5 years (WAG).

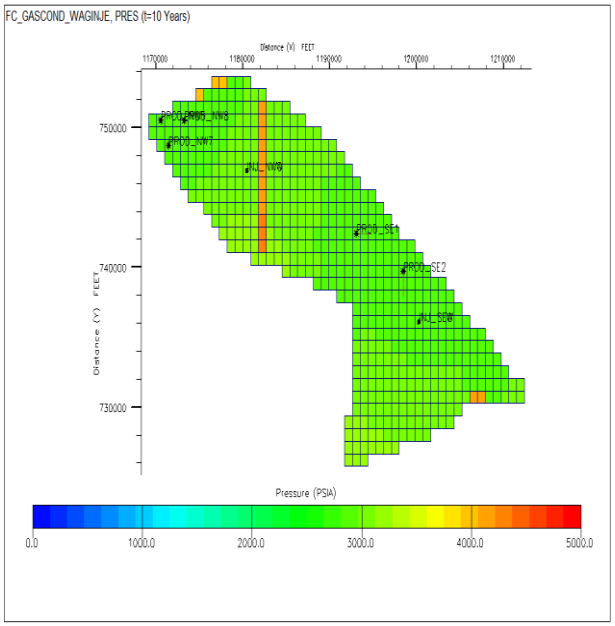

Figure 4-47:Field pressure at t=10 years (WAG).

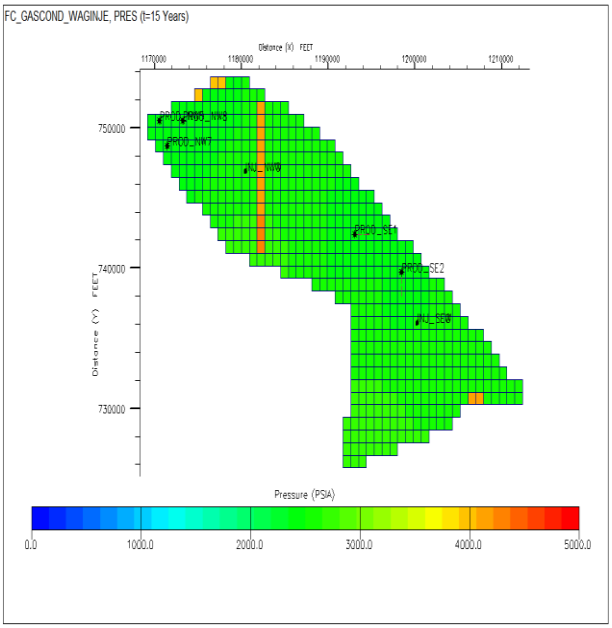

Figure 4-48:Field pressure at t=15 years (WAG).

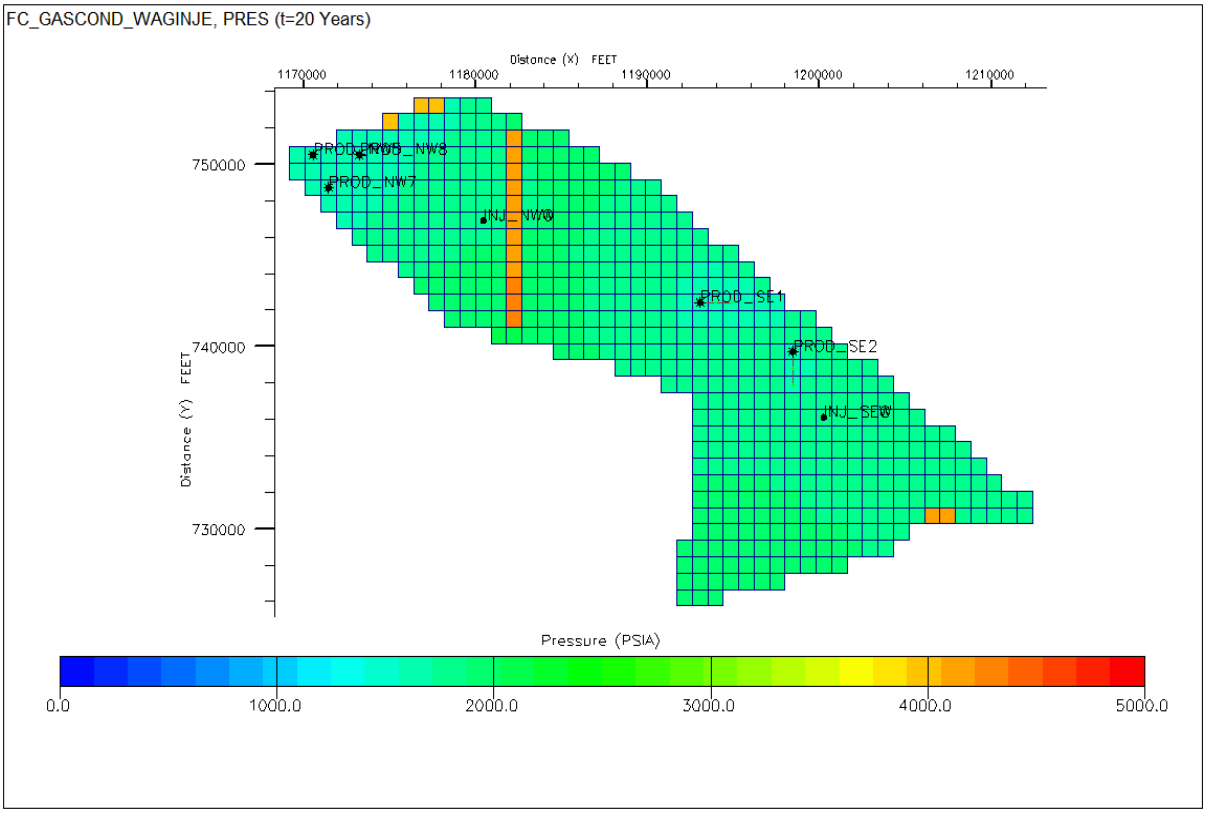

Figure 4-49:Field pressure at t=20 years (WAG).

4.5.3.2 Gas Saturation

Initial conditions are not sustained as gas saturation increases in the Northwest and South east regions, especially around the producers and injectors (Figure 4-50 – 4-51). With continued production, gas saturation continues to decrease. Farther from the well completions and at higher depths, the gas saturation reduces because the low density of gas cause it to preferentially move in the upper layers (Figure 4-52, 4-53). The gas saturation around the injectors also reduces during the water injection cycle of the WAG scheme. Eventually, gas saturation keeps decreasing with more fluid withdrawal (Figure 4-54).

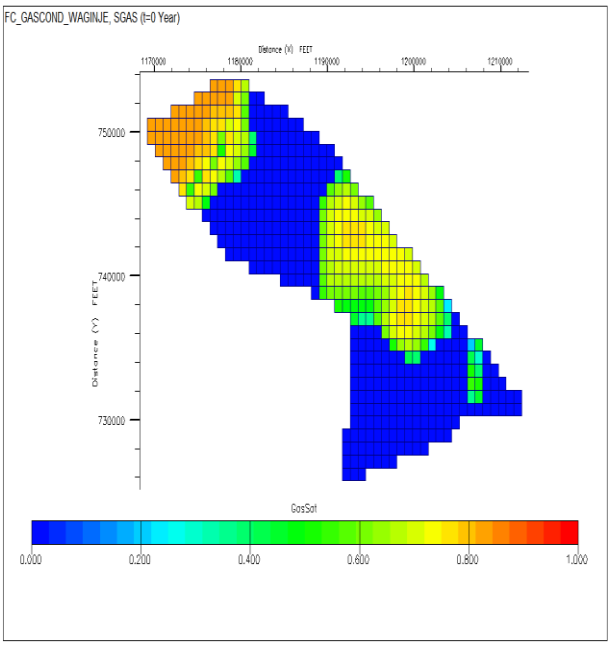

Figure 4-50: Gas saturation at t=0 years (WAG).

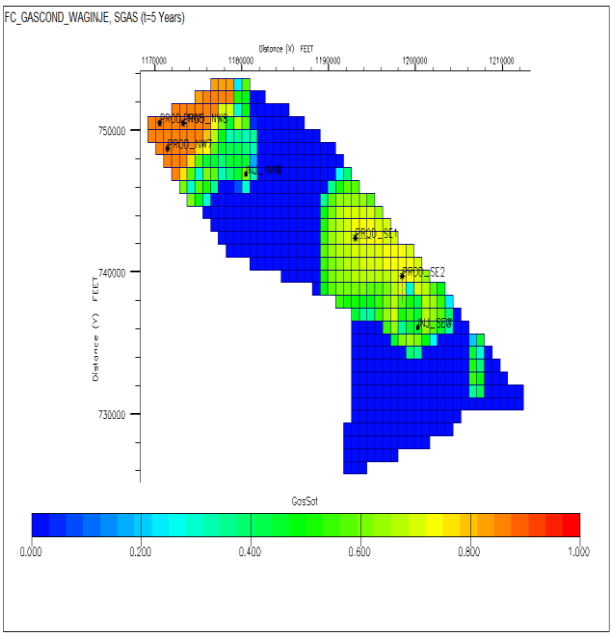

Figure 4-51: Gas saturation at t=5 years (WAG).

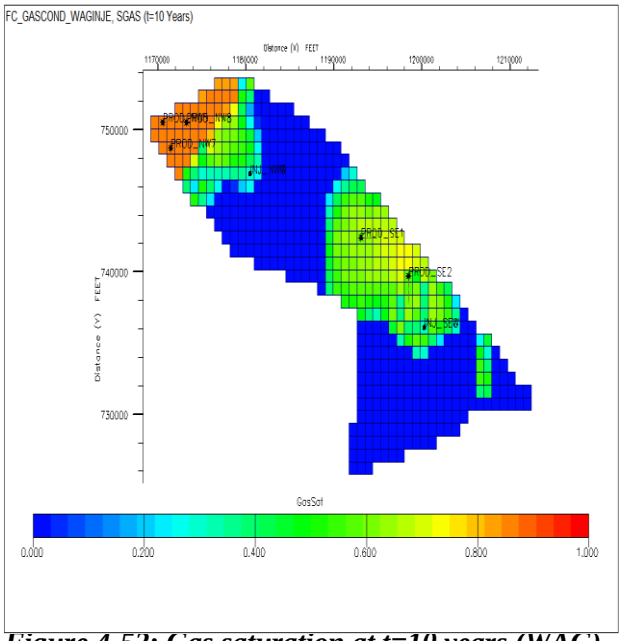

Figure 4-52: Gas saturation at t=10 years (WAG).

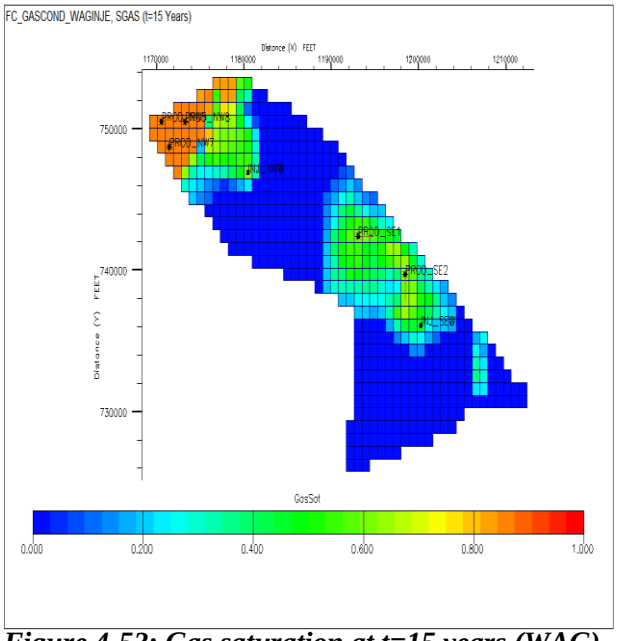

Figure 4-53: Gas saturation at t=15 years (WAG).

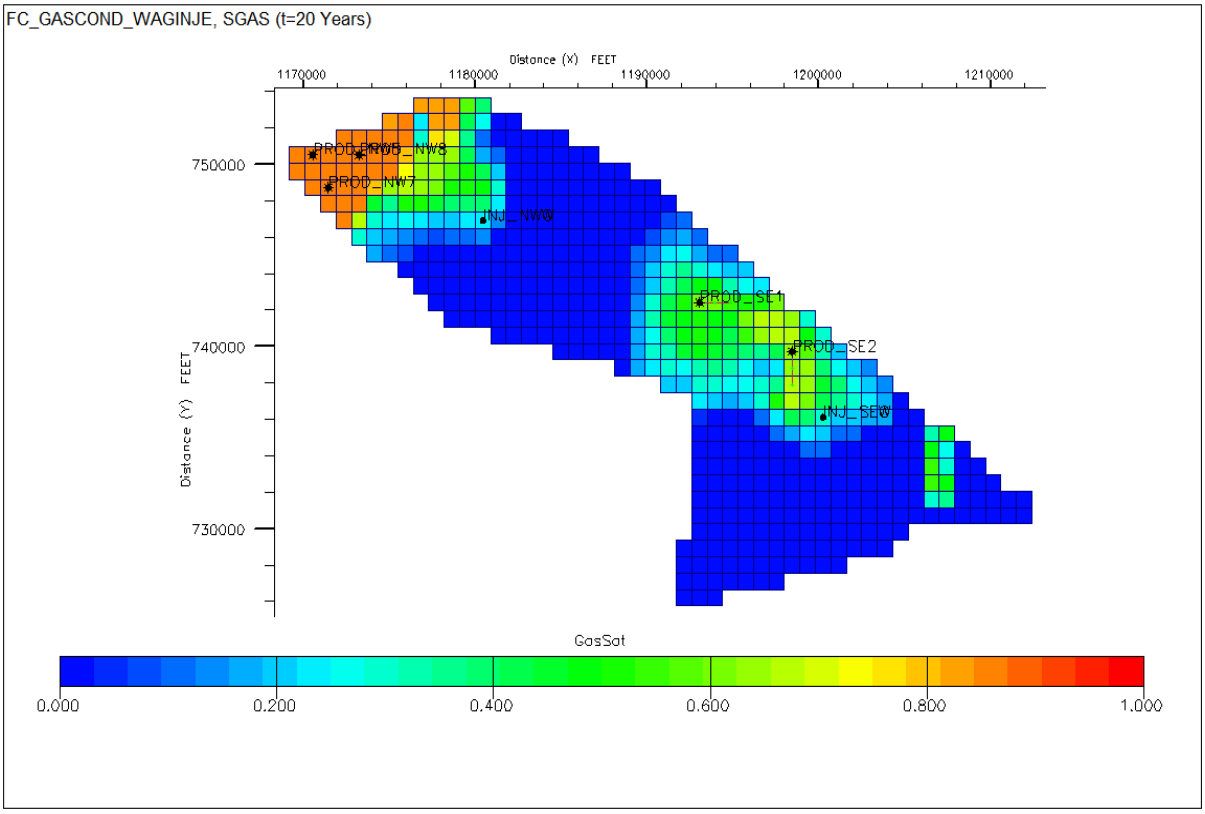

Figure 4-54:WAG injection Gas saturation at t=20 years (WAG).

4.5.3.3 Oil Saturation

Negligible condensate saturation is noticed in the entire reservoir at the start of the simulation run (Figure 4-55). After 5 years, more condensate buildup occurs in the reservoir, especially in the North-eastern region due to insufficient pressure maintenance during the water injection phase of the WAG scheme (Figure 4-56). Similarly, some condensate saturation has started to develop at the toe of PROD_SE2. The oil saturation around the injectors INJ_NWG and INJ_SEW are slightly above the critical saturation (Figure 4-57). More condensate is formed with time, but the WAG scheme provides favorable displacement towards the producers (Figure 4-58). Horizontal wells provide better drainage of the condensate compared to the vertical producers. Away from the wells, the condensate buildup is observable over a wilder area in the reservoir as the pressure declines (Figure 4-59).

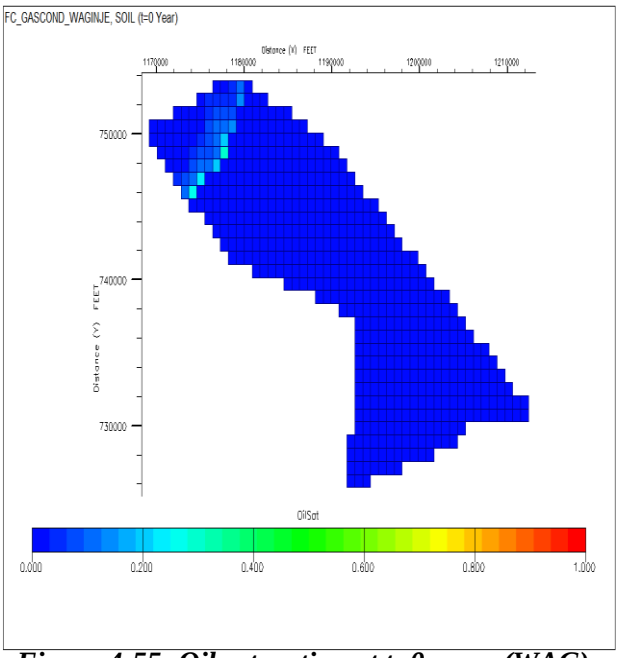

Figure 4-55: Oil saturation at t=0 years (WAG).

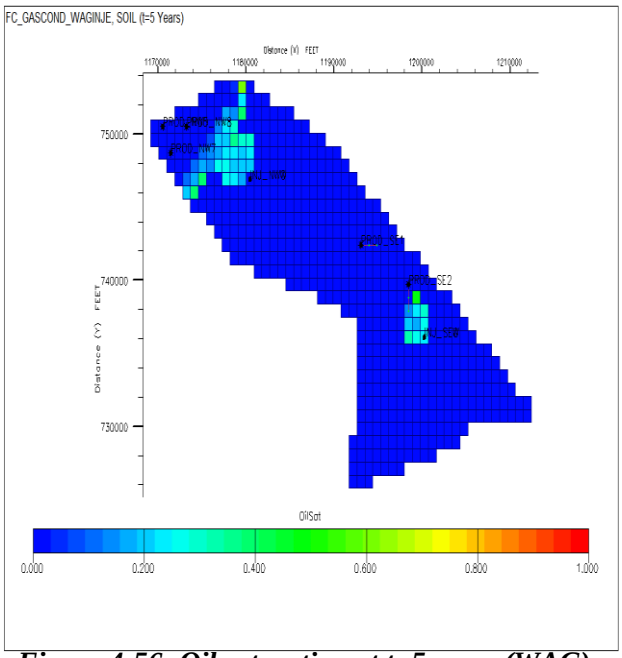

Figure 4-56: Oil saturation at t=5 years (WAG).

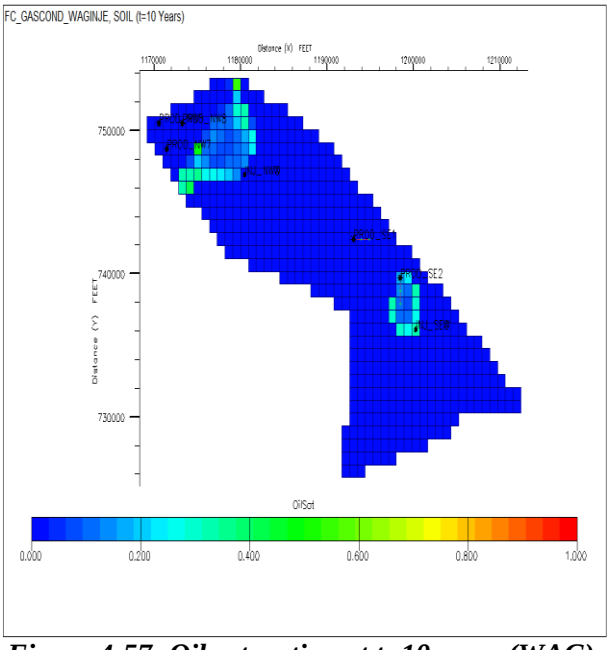

Figure 4-57: Oil saturation at t=10 years (WAG).

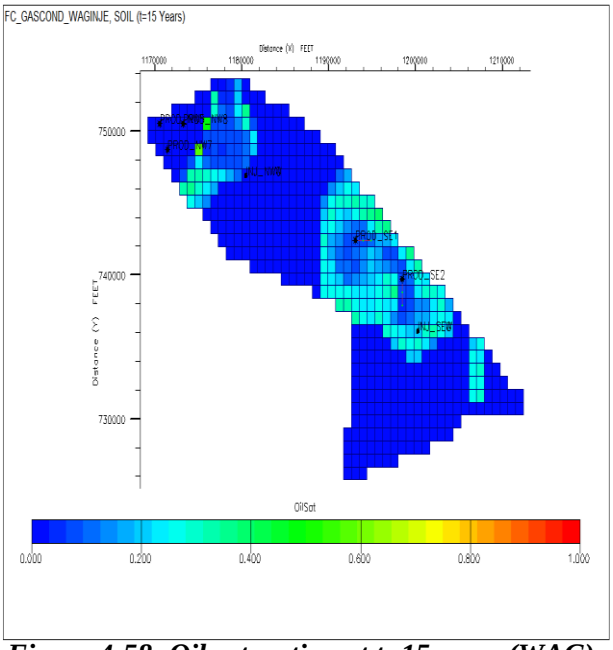

Figure 4-58: Oil saturation at t=15 years (WAG).

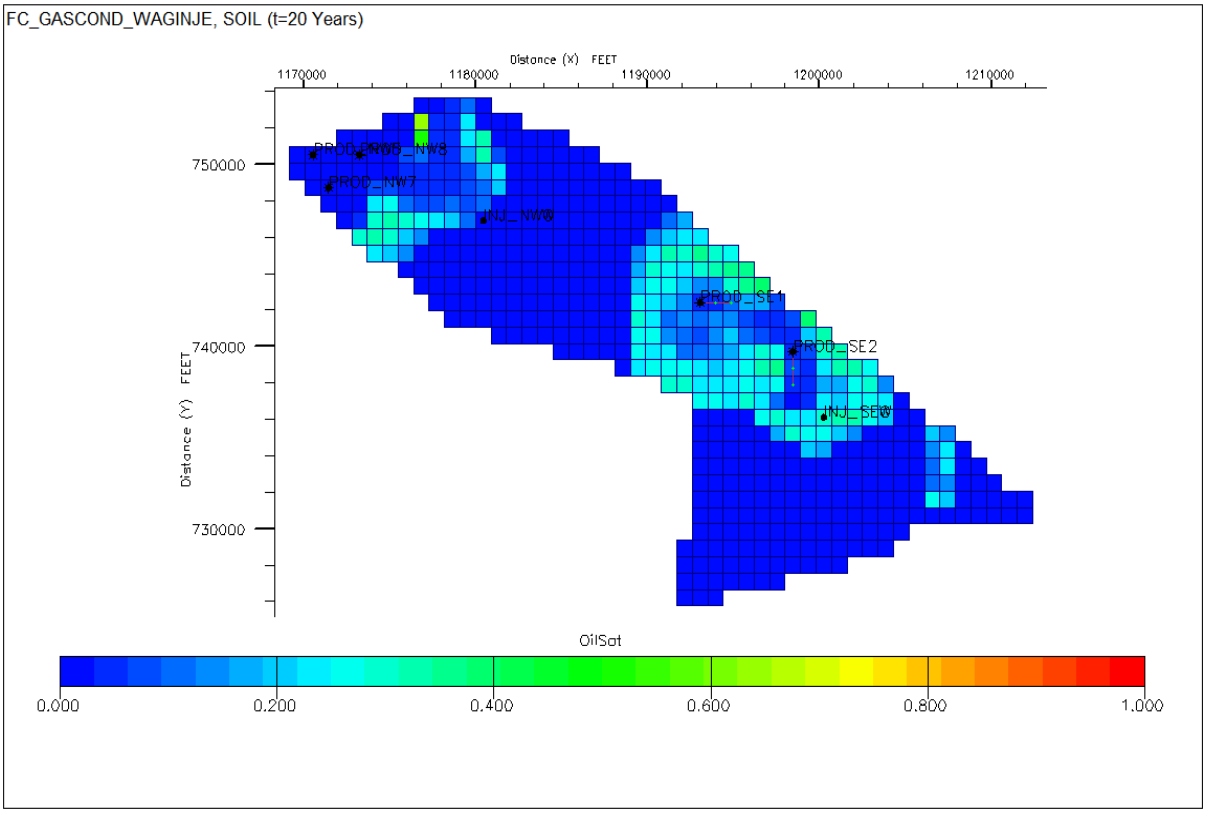

Figure 4-59: Oil saturation at t=20 years (WAG).

4.5.4 SWAG Injection

4.5.4.1 Pressure

In Year 0, the average field pressure is greater than 4000psia. The Southeast region has a slightly higher pressure than the Northwest because it is at a higher depth, and the fluid composition is more of the intermediate-heavy components (Figure 4-60). After 5 years of production, the reservoir pressure has declined by 12%, to about 3700psia (Figure 4-61). The pressure decline is more observable around the producing wells but it increases outwards towards the area surrounding the injector wells (Figure 4-62). In fifteen years, the reservoir pressure is completely stabilized as equilibrium is reached between the pressure drawdown of the wells, the pressure of the injected fluids, and the aquifer support (Figure 4-63). It is noted that the reservoir pressure declines less rapidly compared to the WAG and gas injection scheme. After the end of injection, reservoir pressure declines at a higher rate but the final reservoir pressure is maintained at pressure greater than 2500psia, which corresponds to 50% of the initial (Figure 4-64).

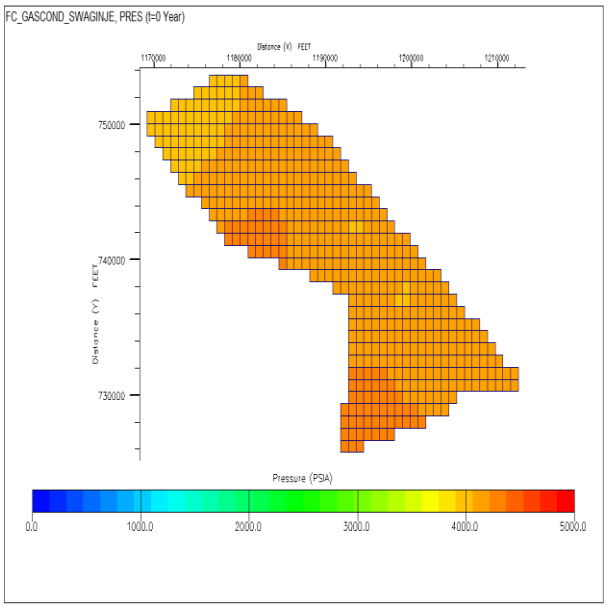

Figure 4-60:Field pressure at t=0 years (SWAG).

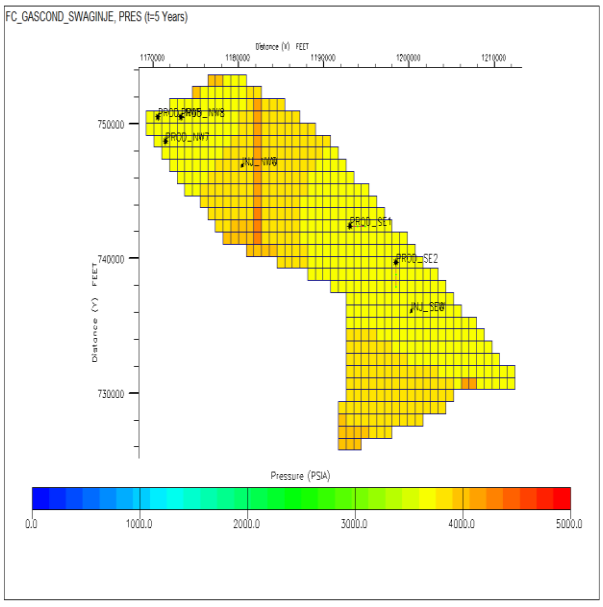

Figure 4-61:Field pressure at t=5 years (SWAG).

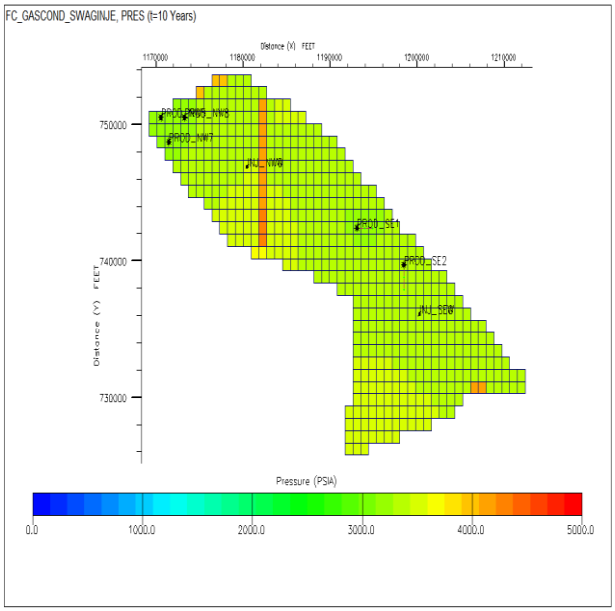

Figure 4-62:Field pressure at t=10 years (SWAG).

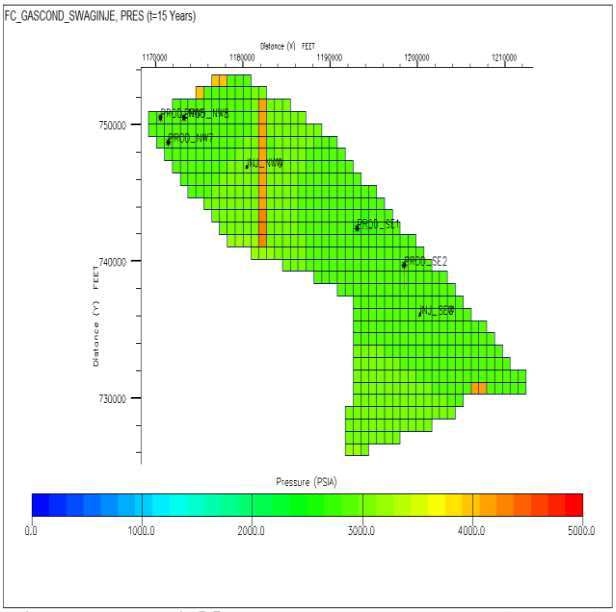

Figure 4-63:Field pressure at t=15 years (SWAG).

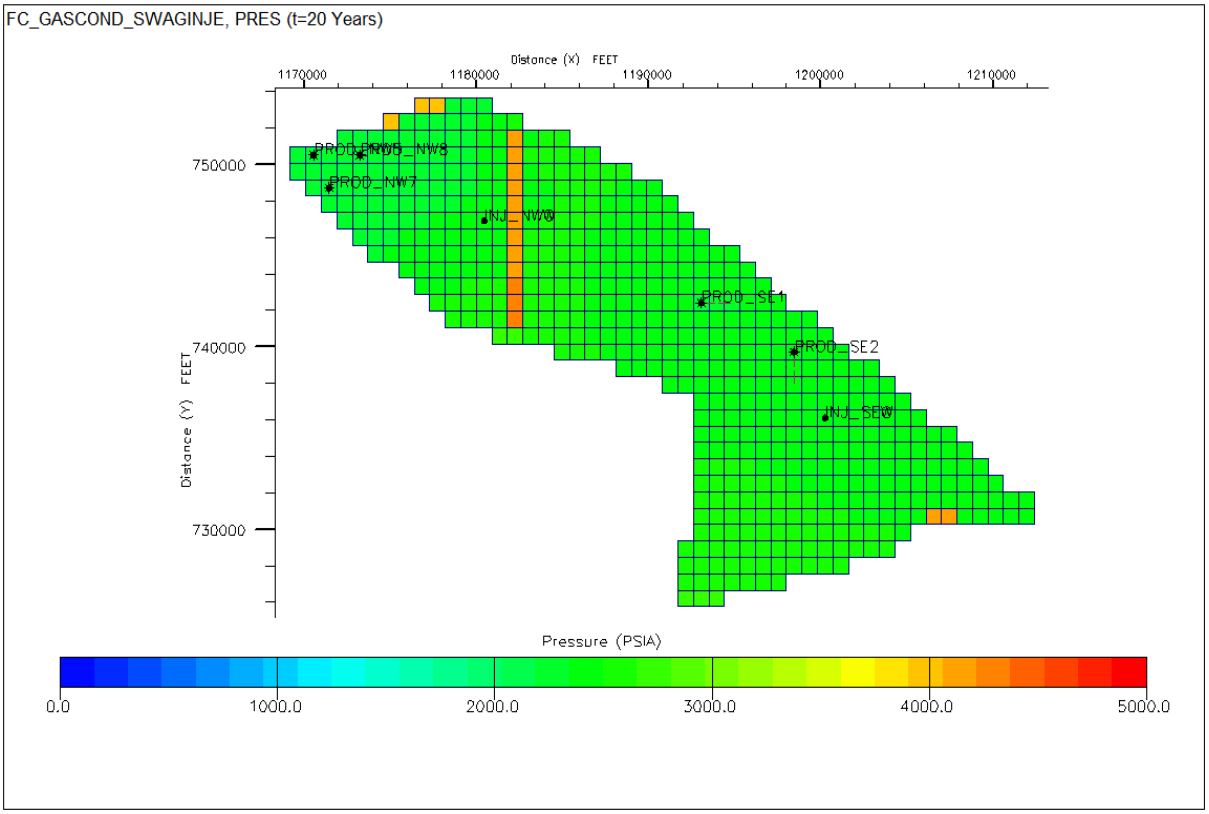

Figure 4-64:Field pressure at t=20 years (SWAG).

4.5.4.2 Gas Saturation

Initial saturation conditions change as soon as injection begins. Gas saturation increases in the Northwest and South east regions, especially around the producers and injectors (Figure 4-65, Figure 4-66). With continued production, there is negligible decrease in gas saturation in the Northwest because pressure is maintained and condensate drop out is mitigated. Farther from the well completions and at higher depths, the gas saturation reduces because the low density of gas cause it to preferentially move in the upper layers (Figure 4-67, 4-68). On the contrary, decline in gas saturation is more considerable in the Southeast due to the higher withdrawal rate and lower gas reinjection fraction. At the end of injection, the gas saturation around the injectors reduces but PROD_SE1 has a higher gas saturation than PROD_SE2 because it is closer to the injector well with more fluid withdrawal (Figure 4-69).

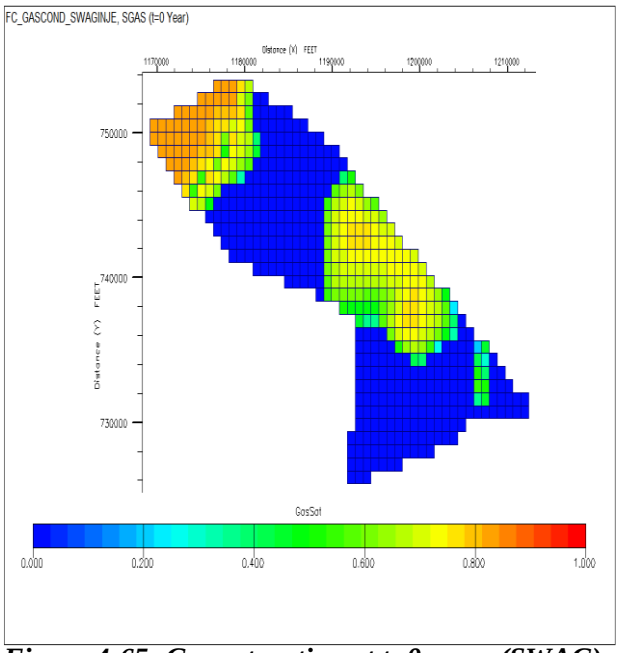

Figure 4-65: Gas saturation at t=0 years (SWAG).

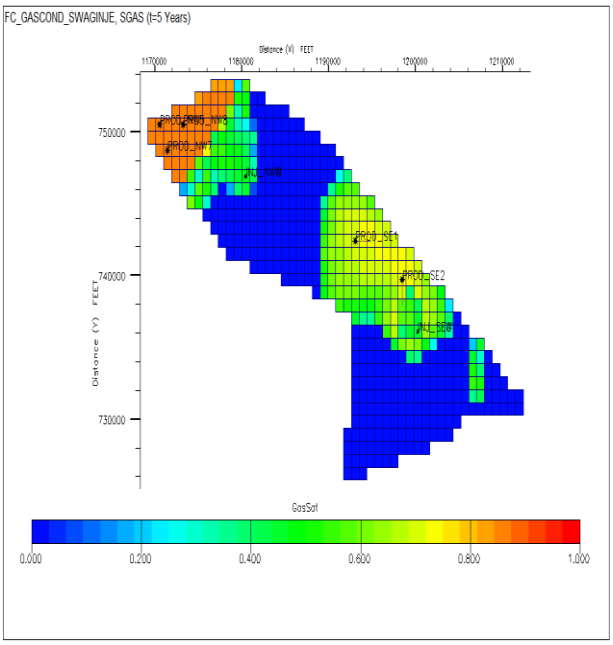

Figure 4-66: Gas saturation at t=5 years (SWAG).

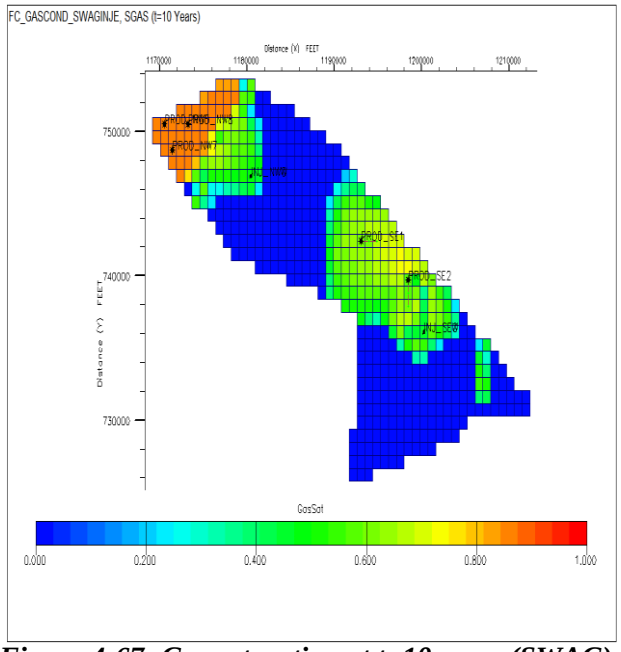

Figure 4-67: Gas saturation at t=10 years (SWAG).

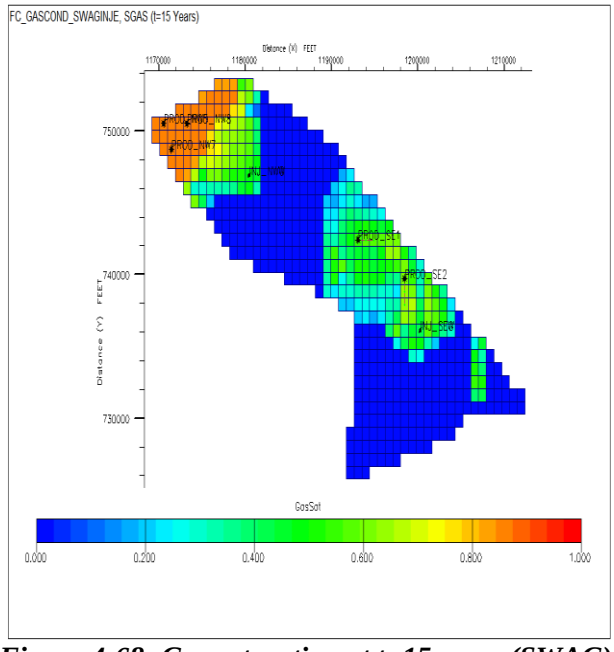

Figure 4-68: Gas saturation at t=15 years (SWAG).

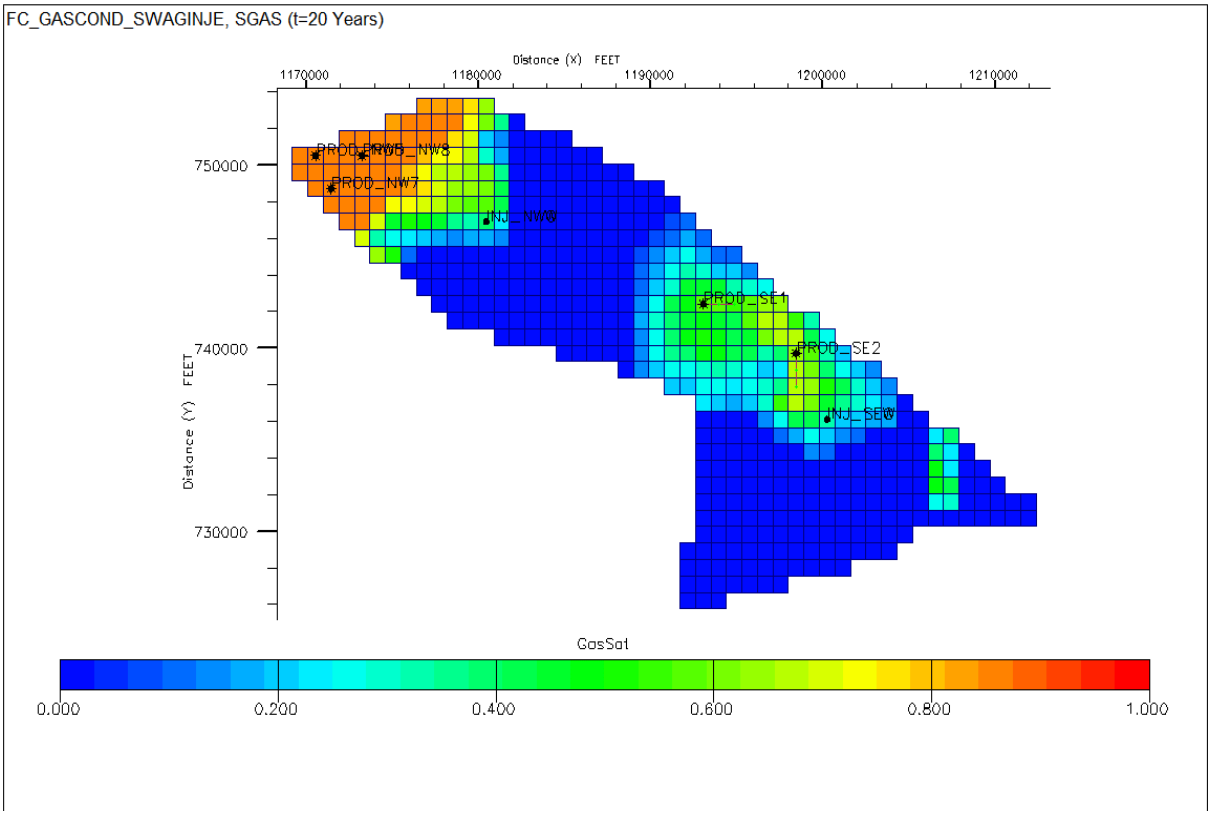

Figure 4-69: Gas saturation at t=20 years (SWAG).

4.5.4.3 Oil Saturation

Negligible condensate saturation is noticed in the entire reservoir at the start of the simulation run (Figure 4-70). After 5 years, slight condensate buildup occurs in the reservoir, especially in the North-eastern region due to partial pressure maintenance of the SWAG scheme (Figure 4-71). The oil saturation around the injectors INJ_NWG and INJ_SEW are near the critical saturation (Figure 4-72). More condensate is formed with time, but the SWAG scheme provides favorable displacement towards the producers (Figure 4-73). Horizontal wells provide better drainage of the condensate compared to the vertical producers. Away from the wells, the condensate buildup is observable over a wider area in the reservoir as the pressure declines. However, since water is being injected continuously into the reservoir, water traps some of the condensate behind, and breakthrough at the well much earlier (Figure 74).

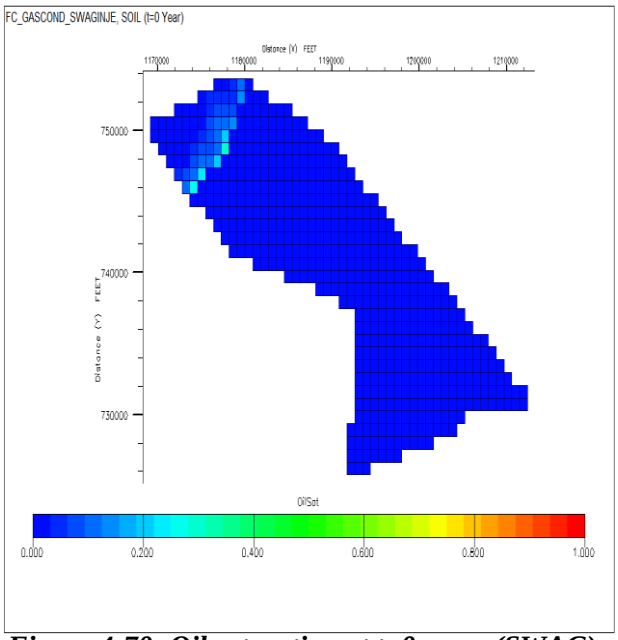

Figure 4-70: Oil saturation at t=0 years (SWAG).

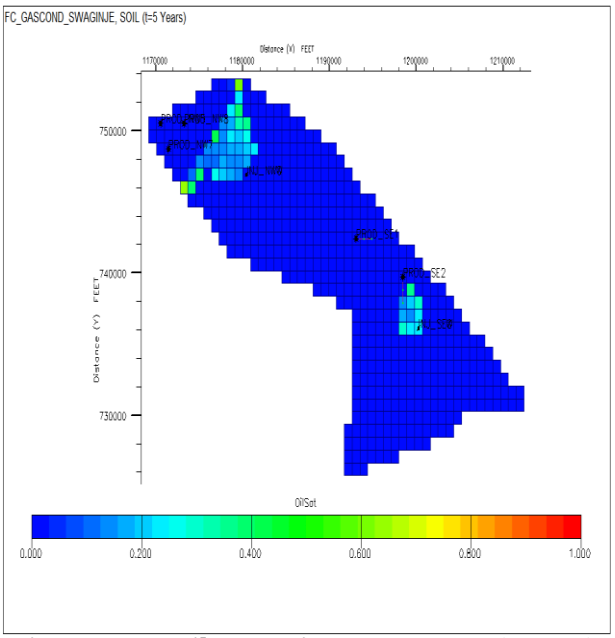

Figure 4-71: Oil saturation at t=5 years (SWAG).

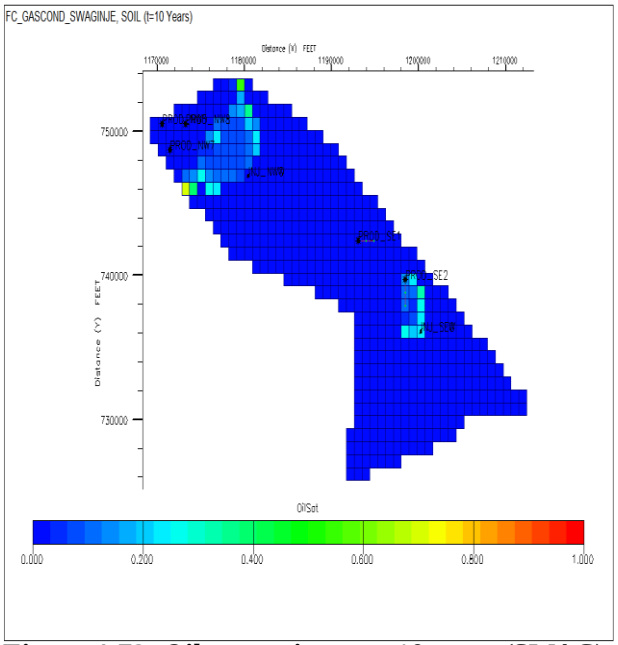

Figure 4-72: Oil saturation at t=10 years (SWAG).

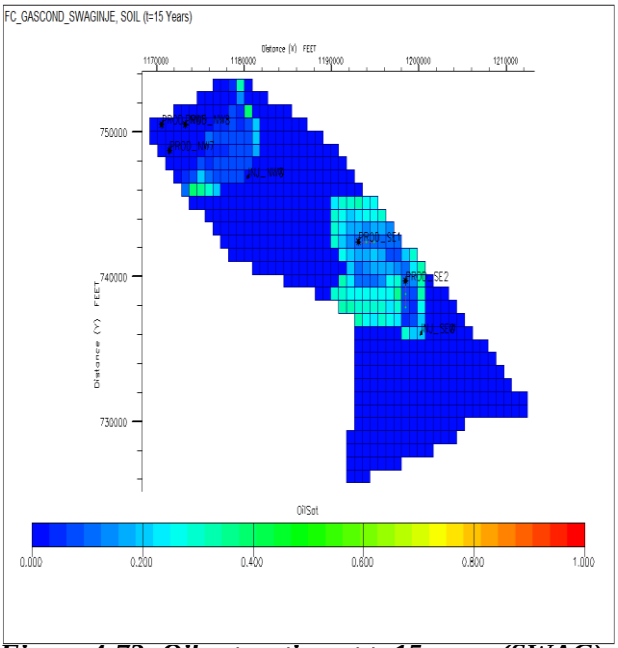

Figure 4-73: Oil saturation at t=15 years (SWAG).

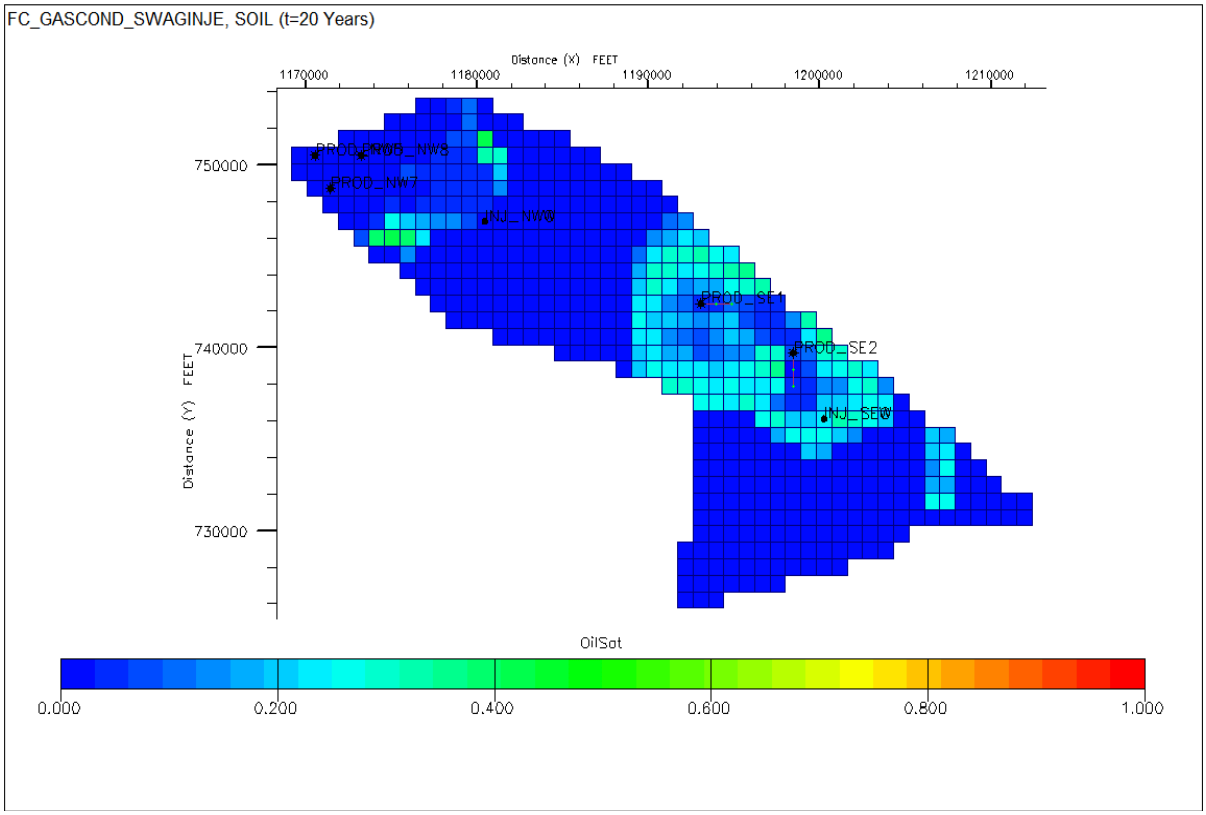

Figure 4-74: Oil saturation at t=20 years (SWAG).

4.5.5 Water Injection

4.5.5.1 Pressure

Since the wells in the South-east are horizontal, pressure declines more rapidly in the region than the North-western part due to higher production rate targets. At initial conditions (Year 0), the reservoir pressure is above the dewpoint pressure (Figure 4-75). Subsequently, pressure declines rapidly in the reservoir with time as shown in Figure 4-76 and Figure 4-77, with the highest pressure drop occurring in the vicinity of the wells, but increasing outwards towards the aquifer boundaries. The injector wells were sustained at a higher pressure than the reservoir (Figure 4-78). Pressure maintenance via water injection is inefficient and aquifer support is activated until pressure stabilization is reached in the reservoir (Figure 4-79).

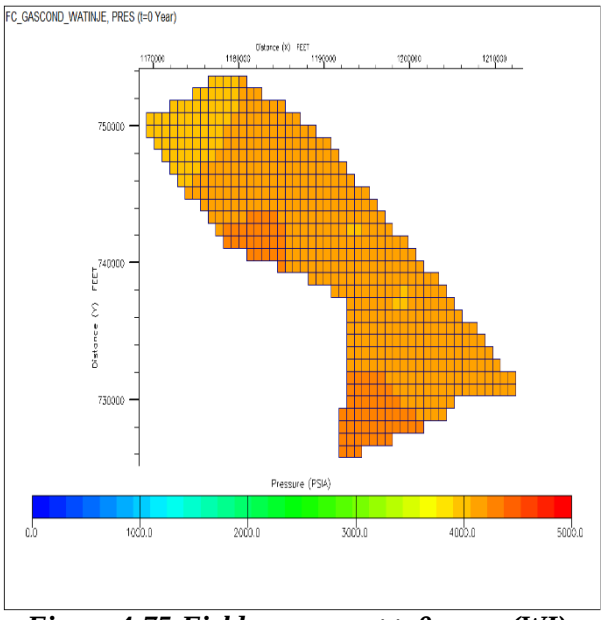

Figure 4-75:Field pressure at t=0 years (WI).

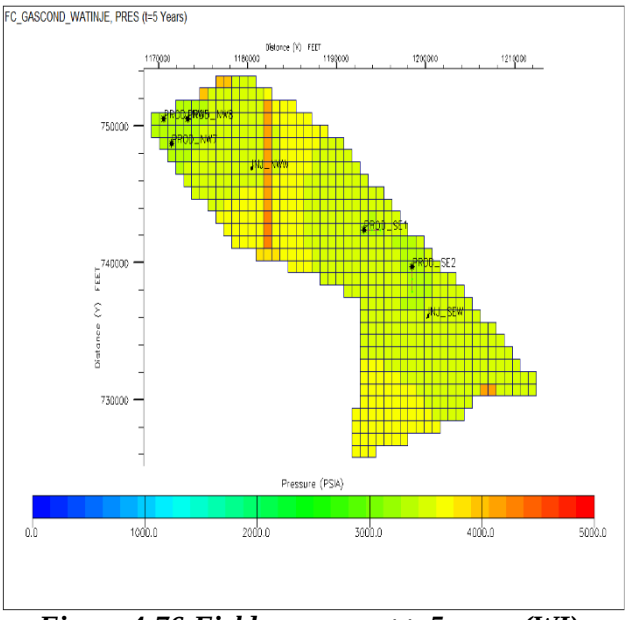

Figure 4-76:Field pressure at t=5 years (WI).

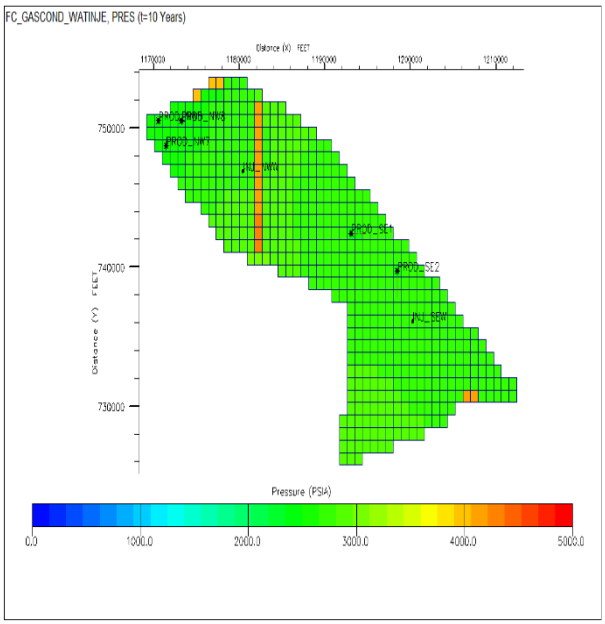

Figure 4-77:Field pressure at t=10 years (WI).

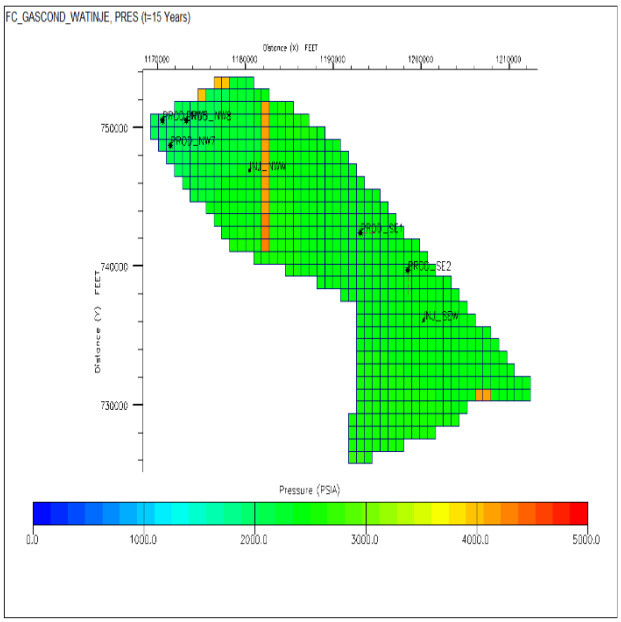

Figure 4-78:Field pressure at t=15 years (WI).

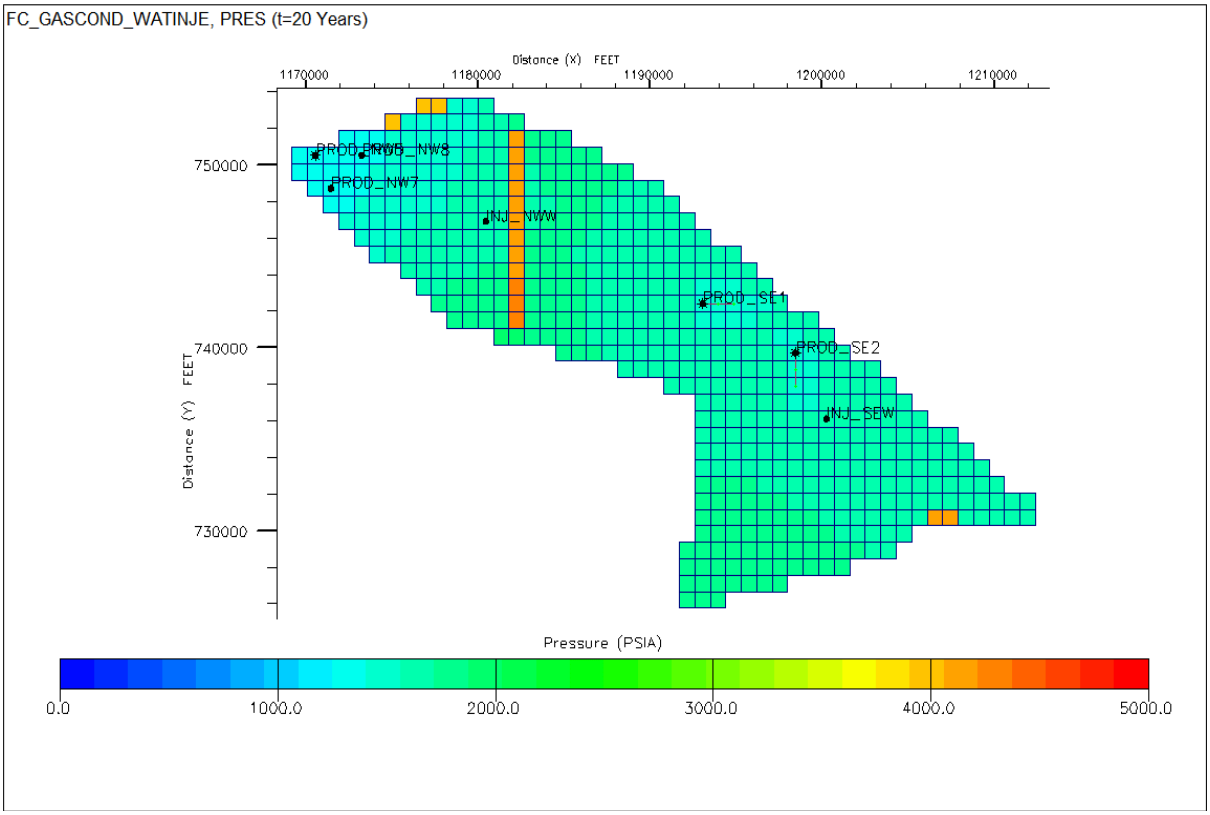

Figure 4-79:Field pressure at t=20 years (WI).

4.5.5.2 Gas Saturation

The gas saturation distribution of the field throughout the simulation period are presented in Figures 4-20 – 4.24 respectively. Initially, the gas saturation in the Northwest was at a maximum of 80%, and it decreases down structure towards the OWC (Figure 4-80). The South east region has a slightly lesser gas saturation at Year 0 (Figure 4-80). The North-west producers (PROD_NW5, NW7, & NW8) show lesser change in gas saturation decline with time compared to PROD_SE1 and PROD_SE2. As production progresses, the gas saturation decreases for grid cells located at higher depths and closest to the wells (Figure 4-81). Gas saturation declines throughout the reservoir. The wellbore had the highest reduction profile and this was due to fluid withdrawal. In Figure 4-82, gas saturation decreases significantly due to insufficient pressure maintenance and the increased water encroachment towards the producers (due to aquifer and injected water). The injected water initially displaces the gas in the pore spaces. However, by the end of Year 20, water breakthroughs at the completion, with more gas trapped behind the flood front (Figure 8-83).

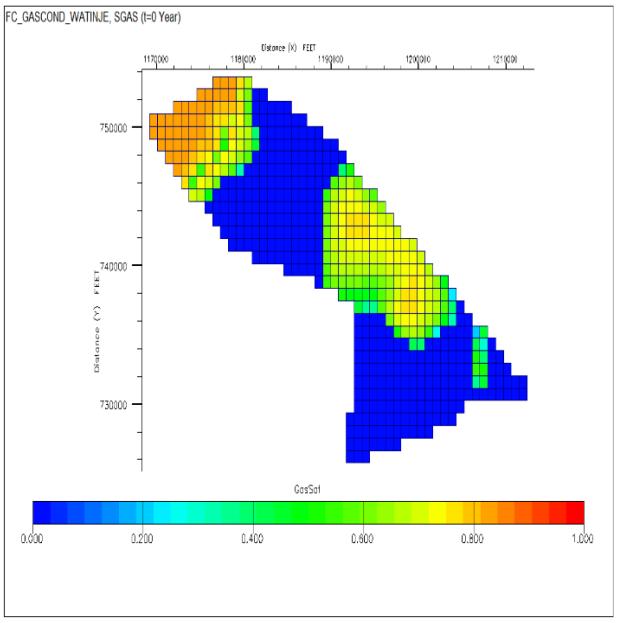

Figure 4-80:Gas saturation at t=0 years (WI).

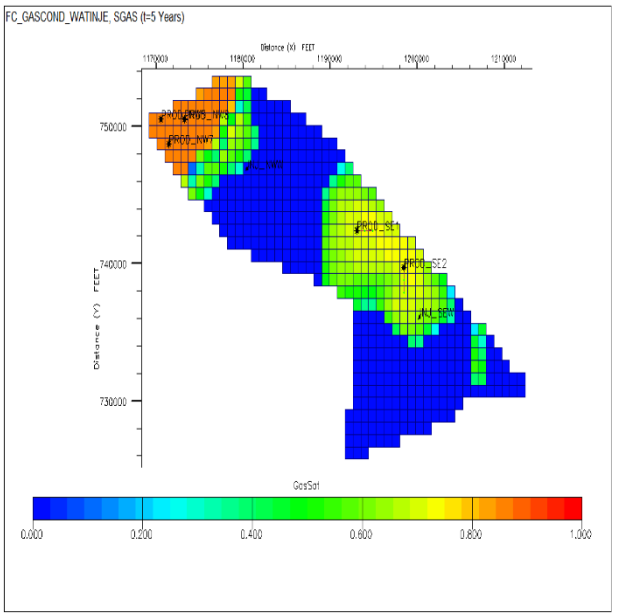

Figure 4-81: Gas saturation at t=5 years (WI).

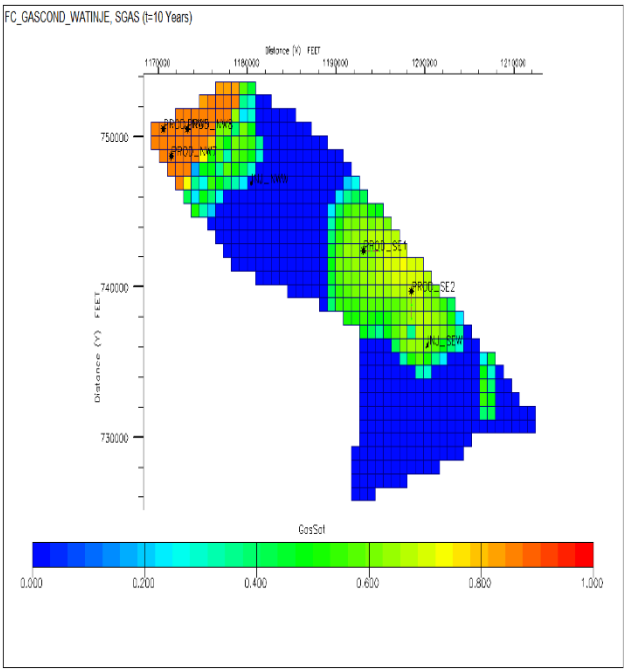

Figure 4-82: Gas saturation at t=10 years (WI).

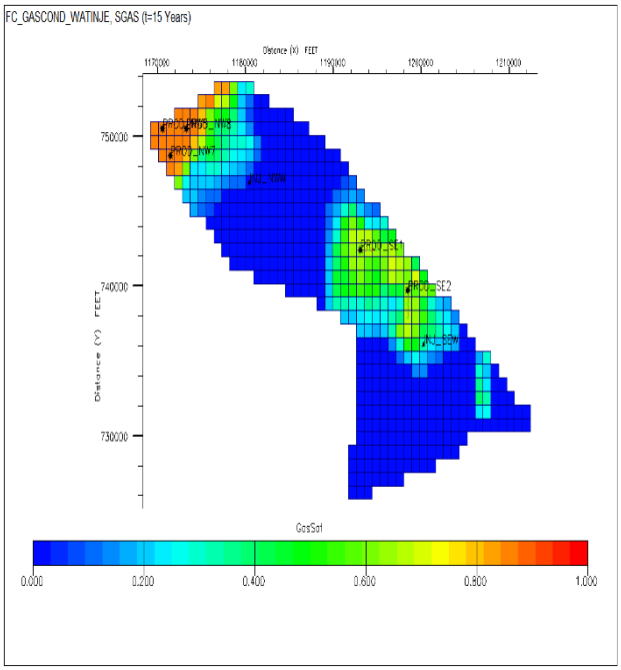

Figure 4-83:Gas saturation at t=15 years (WI).

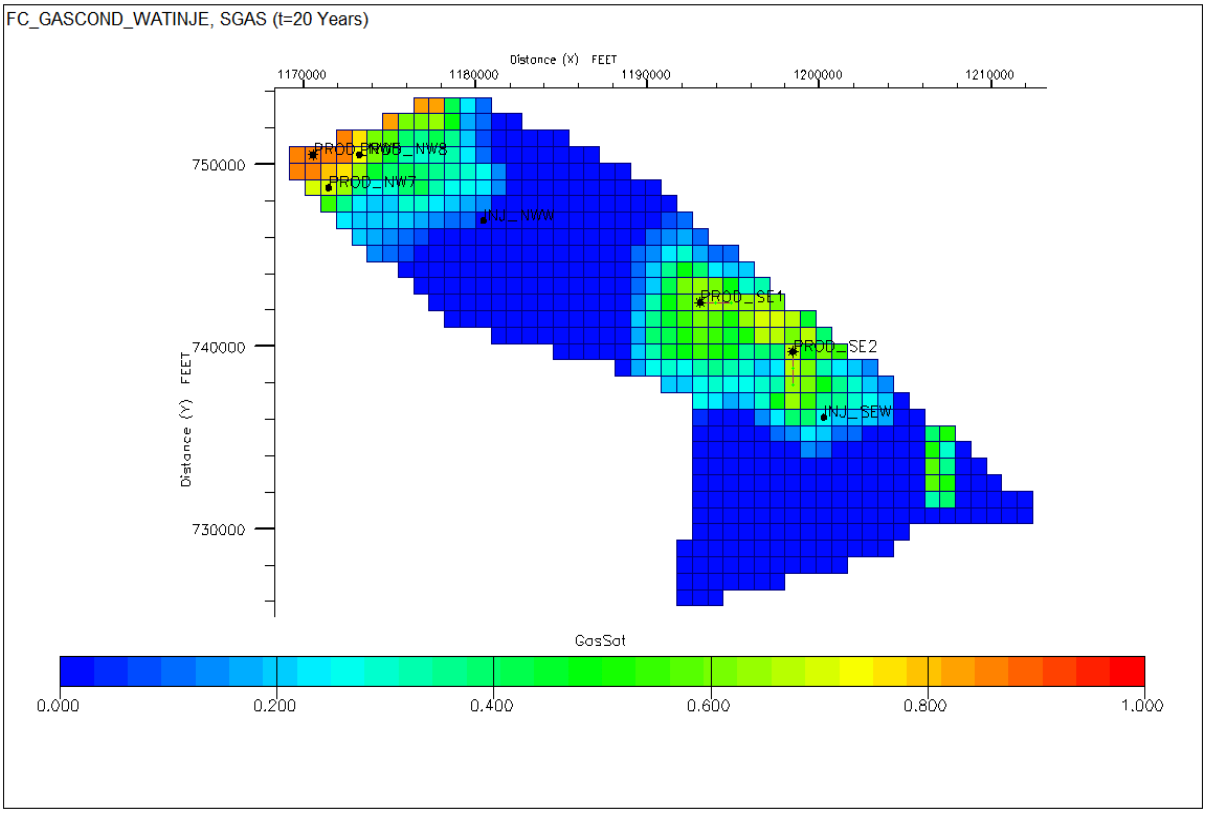

Figure 4-84:Gas saturation at t=20 years (WI).

4.5.5.3 Oil Saturation

The oil saturation distribution of the field at different times of production is illustrated in Figures 4-85, 4-86, 4-87, 4-88, and 4.89 respectively. At Year 0, the oil saturation in the entire field was essentially zero since the reservoir pressure was the same as the dew point pressure, except in the North-western region where small condensate drop out has occurred at higher depth due to gravity segregation of the heavier components (but the oil saturation is lesser than the critical oil saturation). In Year 5, as pressure declines, more condensate build-up is observed in the Northwest but no condensate drop out occurs in the south-east. With continued production, considerable condensate production is observed closest to the wellbore as the condensate saturation exceeds critical saturation and becomes more mobile (Figure 4-87). In Figure 4-88, it is observed that the condensate saturation has drastically reduced around the wellbore. Nonetheless, this saturation is higher because the displacement advantage provided by the favourable mobility ratio of the injected water is countered by the increasing injection volume, causing the producers to be shut in very early. Since the reservoir pressure generally decreases, condensate dropout reaches a significant saturation at even farther distances from the well completions at the end of the simulation (Figure 4.89).

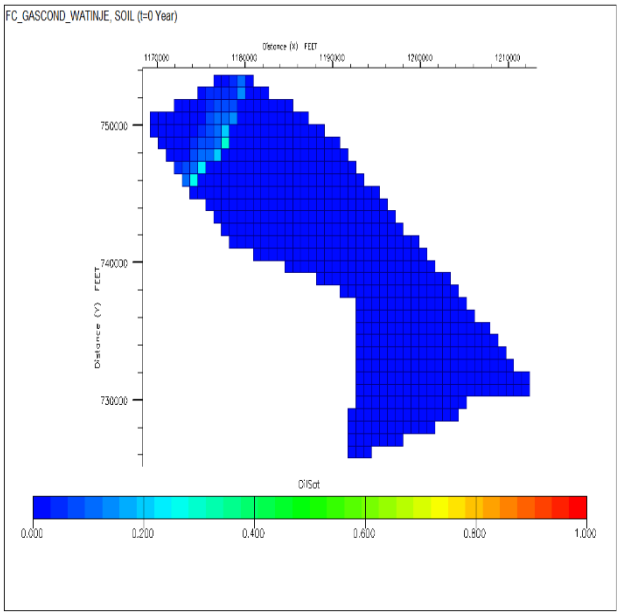

Figure 4-85: Oil saturation at t=0 years (WI).

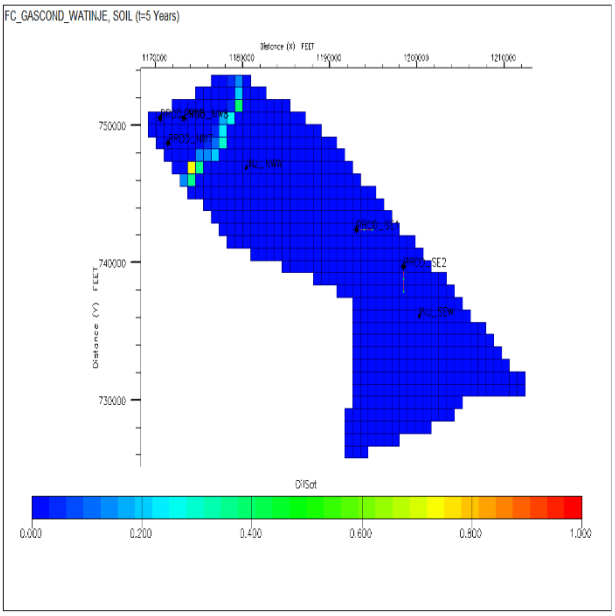

Figure 4-86: Oil saturation at t=5 years (WI).

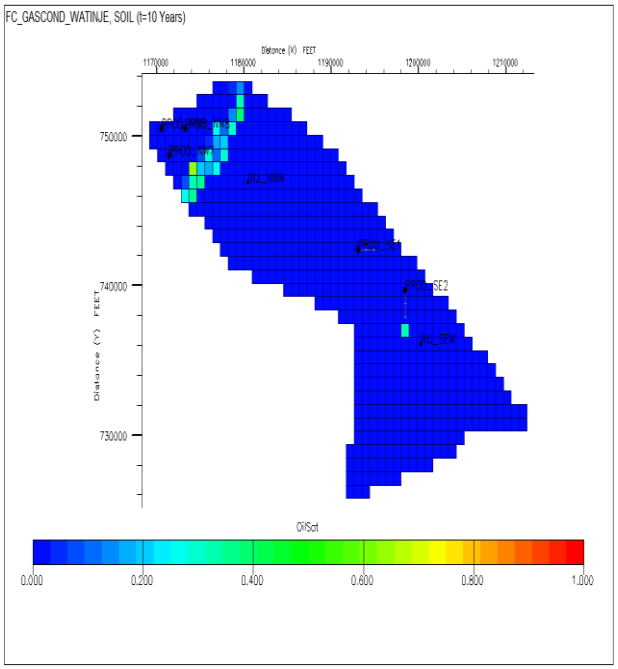

Figure 4-87: Oil saturation at t=10 years (WI).

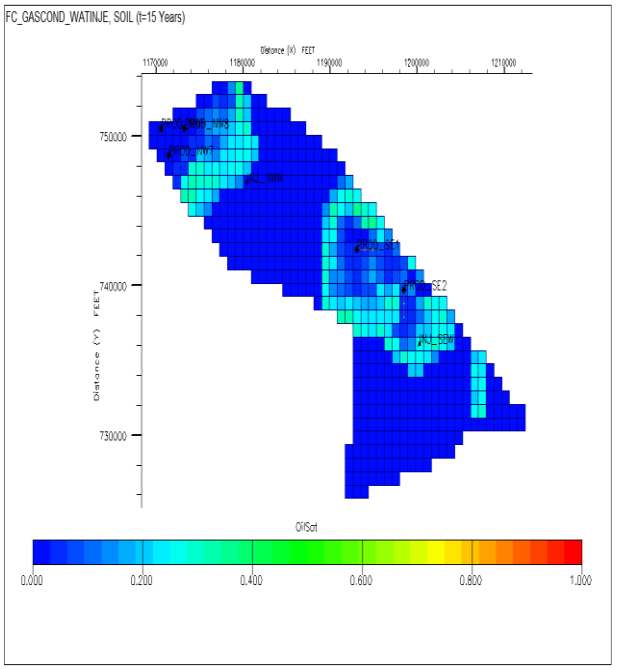

Figure 4-88:Oil saturation at t=15 years (WI).

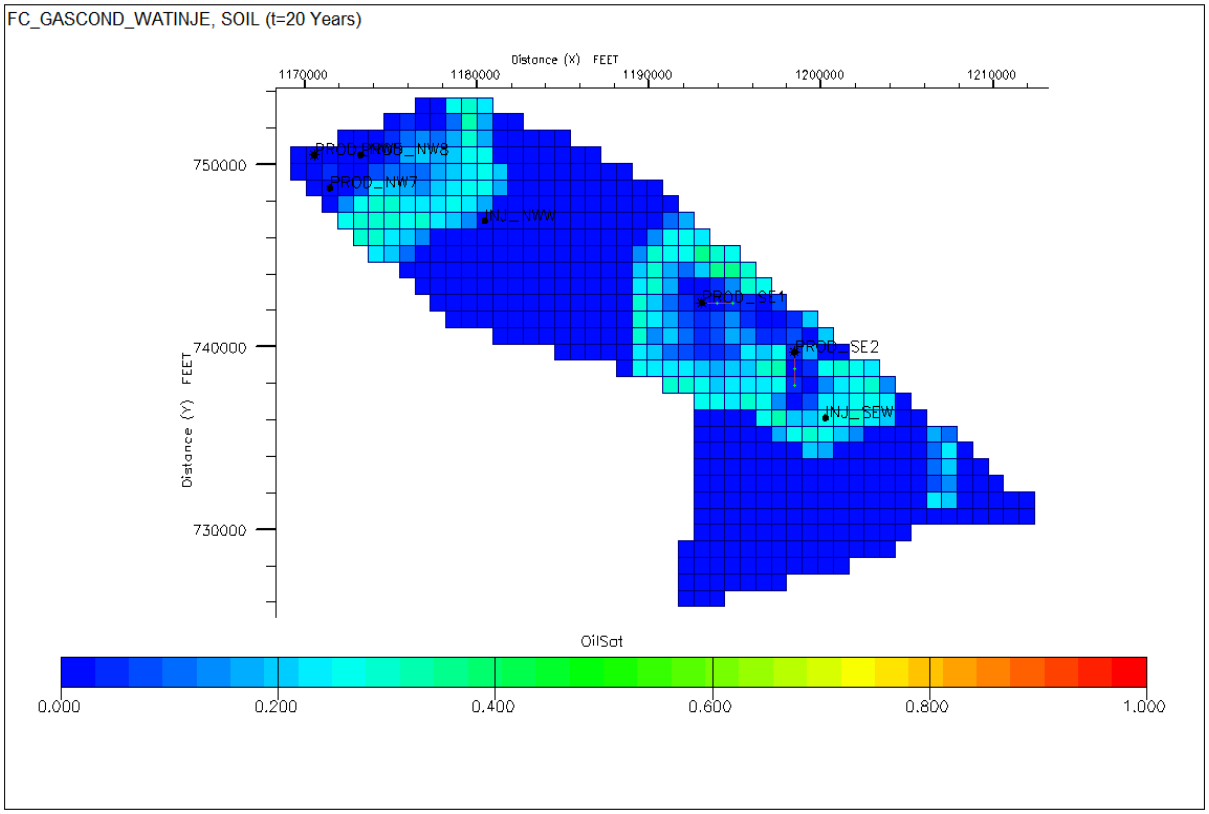

Figure 4-89:Oil saturation at t=20 years (WI).

4.6 SENSITIVITY ANALYSIS

Sensitivity analysis is carried out on several parameters to understand their impact on field performance and guide decision making process during the project. The results are presented below.

4.6.1 Gas Reinjection Fraction

When gas injection in a gas condensate reservoir is being investigated, one must consider the displacement efficiency and pressure maintenance capacity of the process. A high injection rate will provide necessary pressure support in the reservoir, however early gas breakthrough may occur as the injected gas channels through the condensate bank in the reservoir. On the contrary, a low injection volume may maximize condensate recovery but provide insufficient pressure boost to prevent further liquid dropout in the reservoir. Sensitivity analysis was conducted on the gas reinjection fraction to determine the optimum gas injection rate for the reservoir. In Figures 4.15 through Figure 4.17, the gas reinjection fraction is between 0.2 and 0.4. Approximately 40% of the field gas production rate is reinjected into the reservoir. This

reinjection ratio allows for the field to meet its fuel or sales requirements, enhance condensate recovery, and provide some pressure support.

At reinjection fractions greater than 0.6, gas displacement process becomes disadvantageous because the mobile gas bypasses the condensate. The results presented here are for the fully compositional model only. Figure 4.16 illustrates the relationship between the volume of injected gas and the reservoir pressure. As the gas injection rate increases, the reservoir pressure becomes higher, and vice versa. The gas molecules increase and can replace the voidage created by fluid withdrawal from the reservoir. The limited compositional model results are presented in Appendix B and they show the same trend with the fully compositional model.

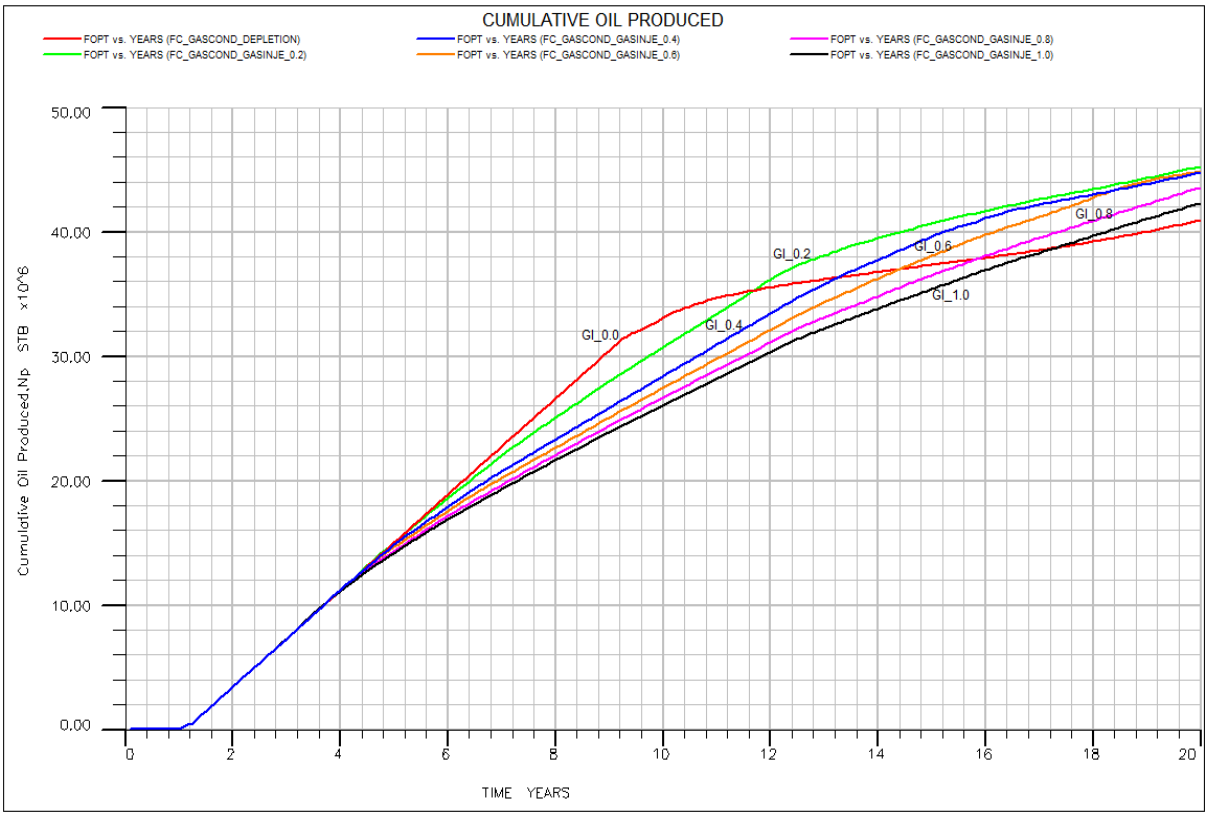

Figure 4-90:Sensitivity analysis of cumulative oil produced per gas re-injection fraction (fully compositional case).

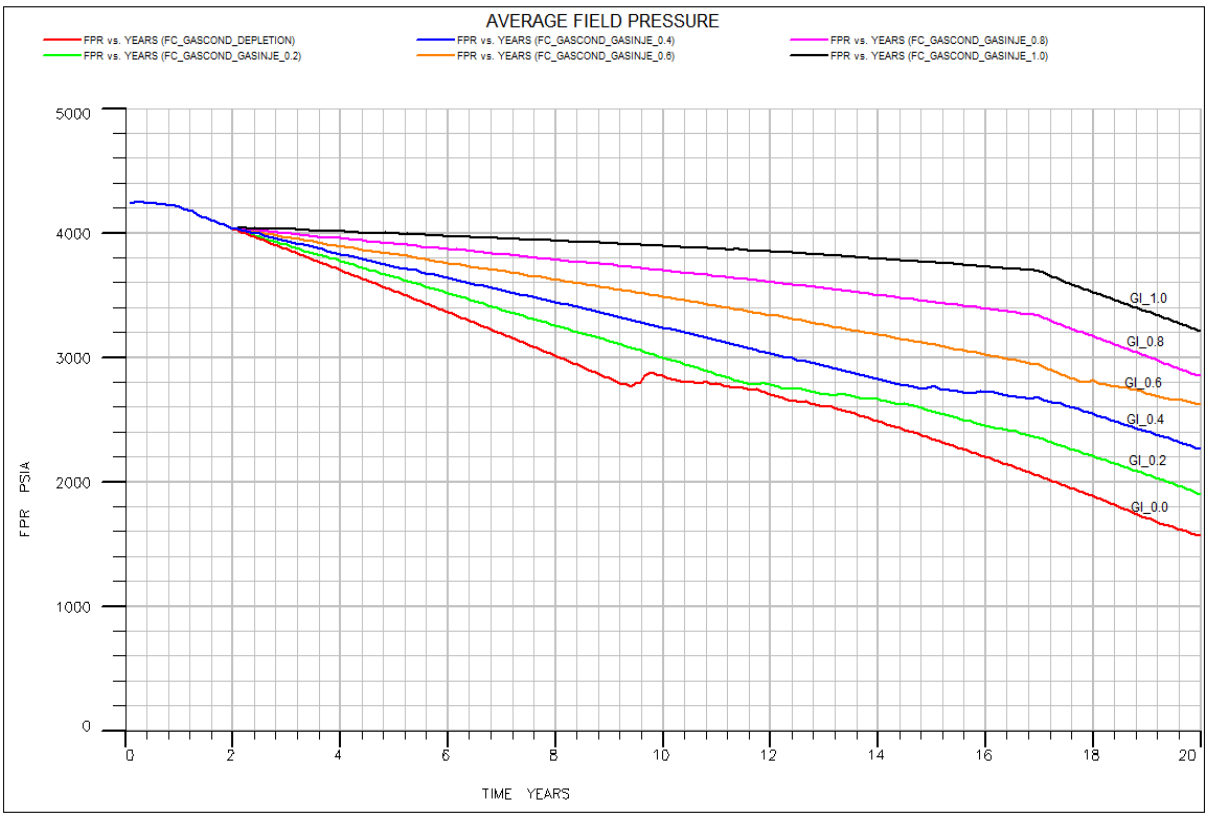

Figure 4-91:Sensitivity analysis of average reservoir pressure per gas re-injection fraction (fully compositional case).

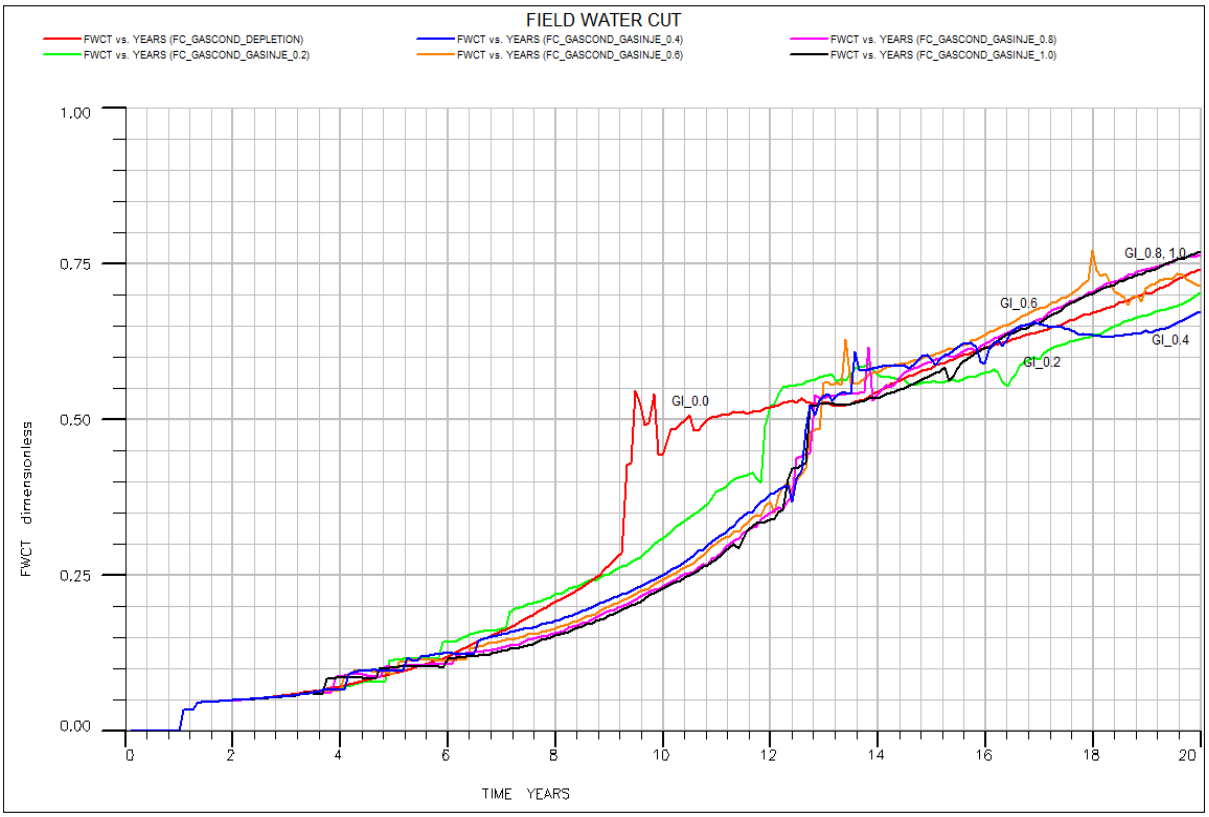

Figure 4-92:Sensitivity analysis of field water cut per gas re-injection fraction (fully compositional case).

4.6.2 Todd Longstaff Mixing Parameter

To simulate miscible displacement processes in the reservoir, the limited compositional simulator utilizes the Todd-Longstaff mixing parameter ω, to establish the degree of miscibility between the displacing and displaced fluid (Todd & Longstaff, 1972). In this study, the reinjected gas is obtained from the produced gas well stream before being diverted for pressure maintenance. Therefore, it is inherently assumed that both the injected and reservoir gas have almost identical composition. However, to incorporate the viscous fingering and dispersion effect in the limited compositional model, the Todd-Longstaff mixing parameter is varied to obtain optimum miscibility in case first contact miscibility between the injected gas and reservoir fluid was not established or where the injection pressure may be less than the MMP. Results shown in Figures 4.16 through 4.18 indicate that the any value of the Todd Longstaff mixing parameter between 0.8 and 1.0 provides the best displacement conditions because the cumulative oil recovery is higher, and the field water cut is lower as the value of ω approaches 1. On the contrary, the field pressure decreases as ω increases in the simulations using any value of the Todd Longstaff mixing parameter between 0.8 and 1.0.

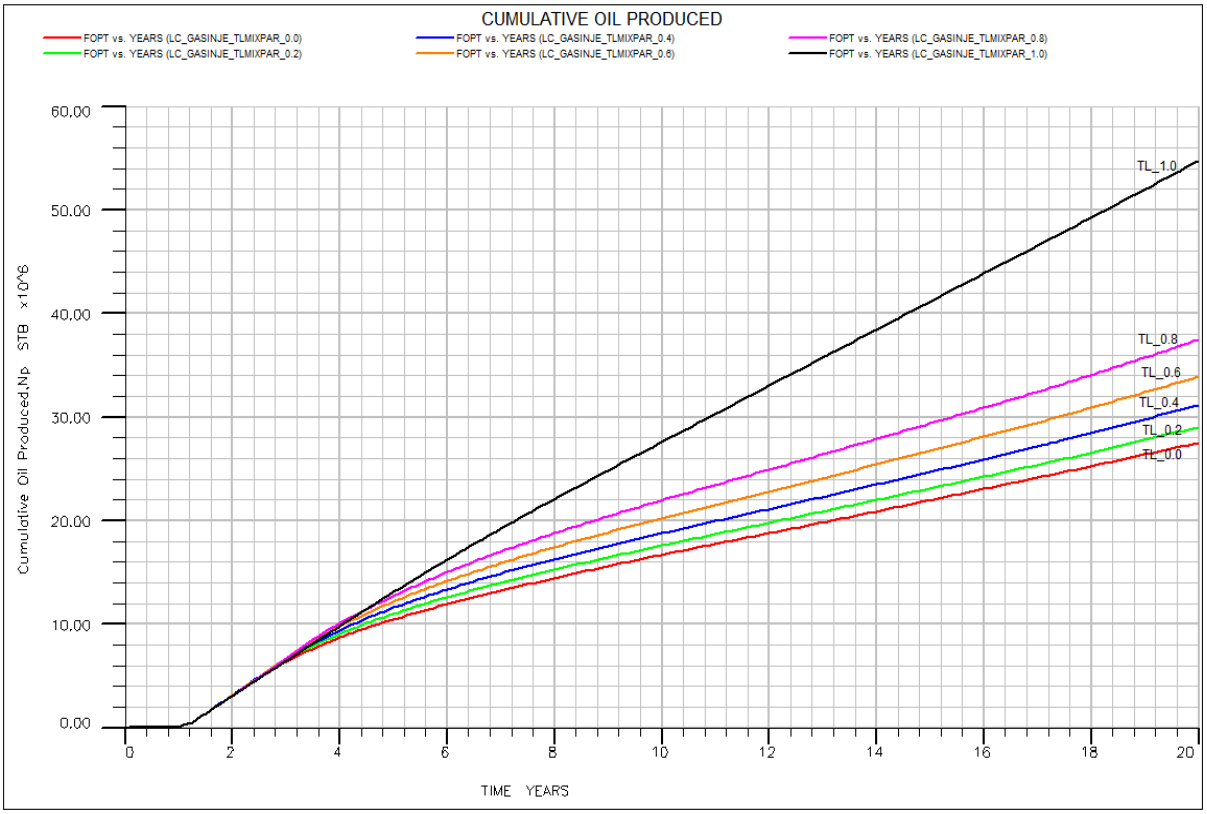

Figure 4-93:Sensitivity analysis of Todd Longstaff mixing parameter on field cumulative oil recovery (limited compositional case).

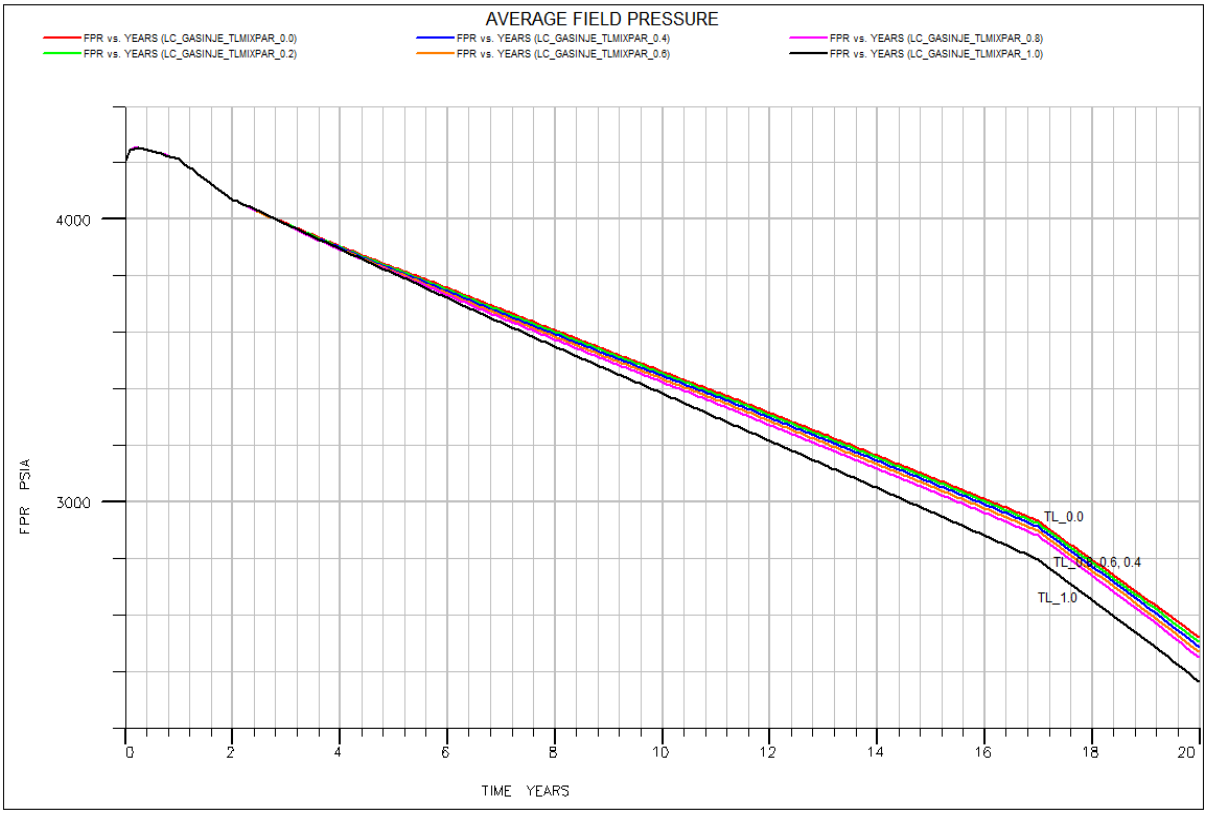

Figure 4-94:Sensitivity analysis of Todd Longstaff mixing parameter on field water cut (limited compositional case).

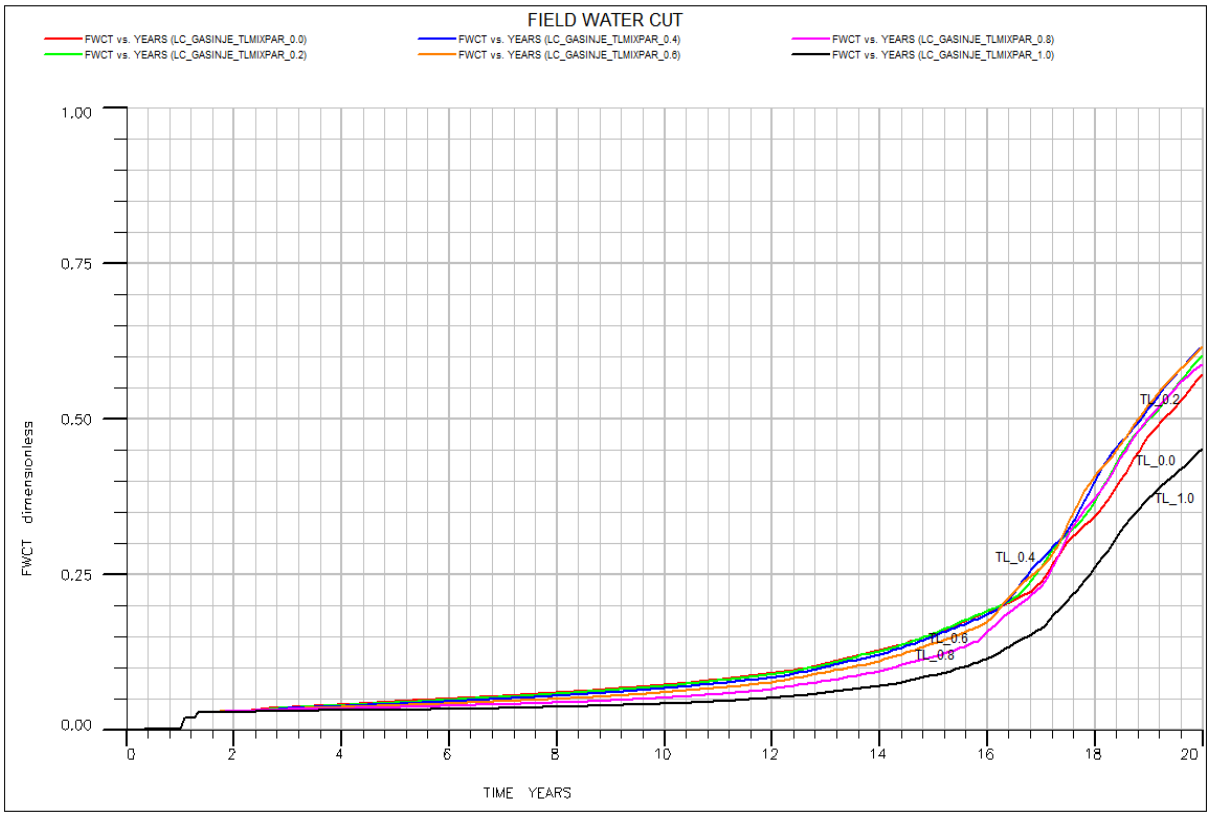

Figure 4-95:Sensitivity analysis of Todd Longstaff mixing parameter on field water cut (f compositional case).

4.6.3 WAG Cycle

Most WAG studies examined the impact of the duration of the injection cycle on the performance of the WAG process. In this research, sensitivity has been carried out to determine the optimum cycle to use in the simulation studies. Four cycles considered are the 3-month WAG, 6-month WAG, 1-year WAG, and 3-year WAG cycle. It is observed that for higher cycling times (1-Year WAG, 3-Year WAG), the condensate recovery was higher than for the lower WAG cycles (Figure 4.19). During the injection duration, there was negligible changes in the degree of pressure maintenance for the various WAG cycles. However, care must be taken to choose the optimum cycle as it appears that the field water cut is higher for longer WAG cycles For the limited compositional model, the length of the injection cycle does not have significant effect on the condensate recovery, field pressure, or final water cut (Appendix B). The effect of WAG cycle may be more evident for higher WAG ratios or WAG cycling times (5-year WAG), and this should be investigated in a future study.

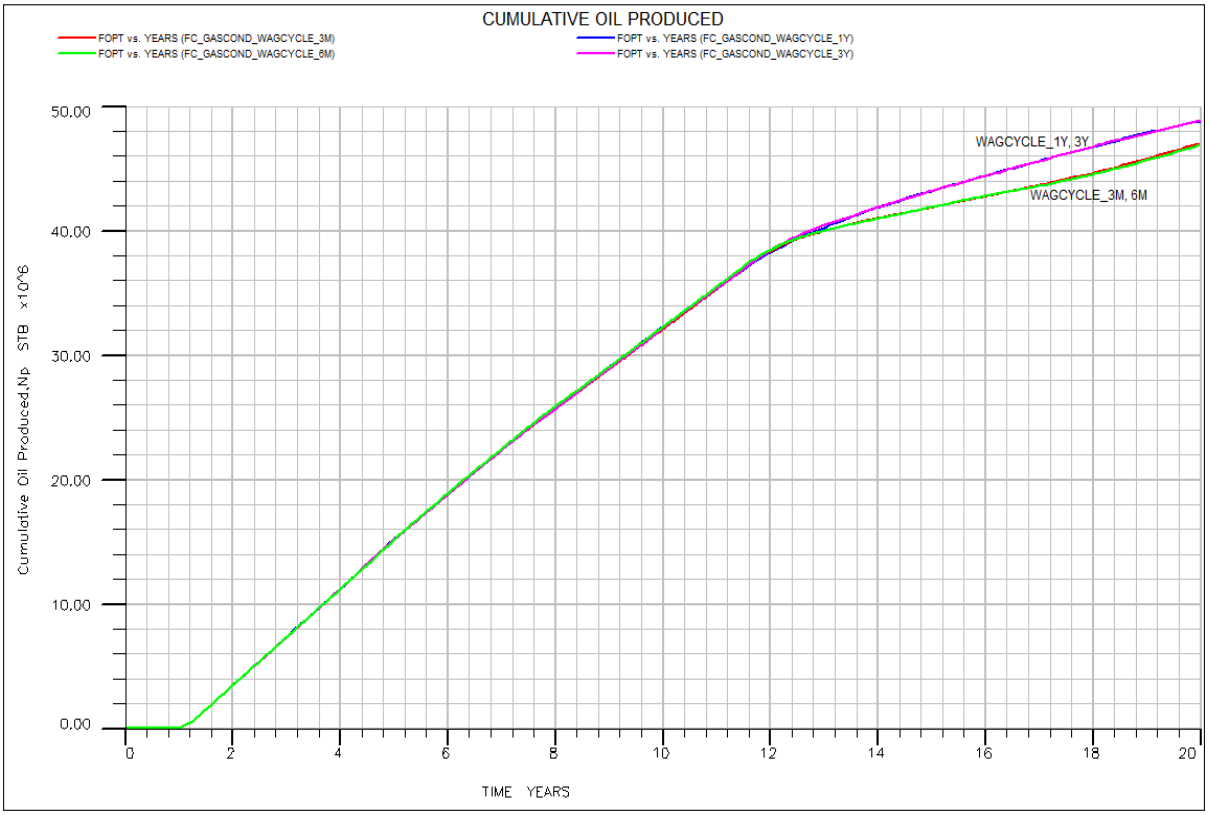

Figure 4-96:Sensitivity analysis of WAG cycle on cumulative oil produced (fully compositional case).

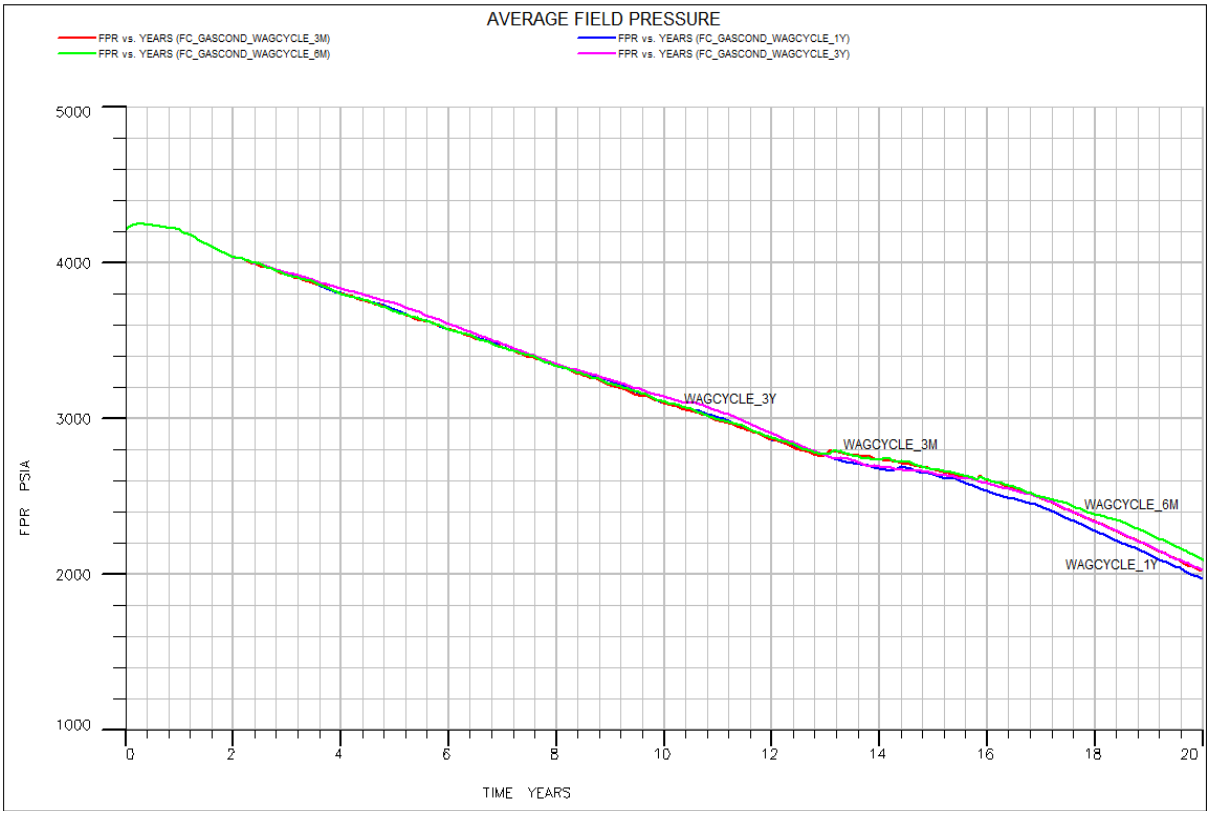

Figure 4-97:Sensitivity analysis of WAG cycle on average field pressure (fully compositional case).

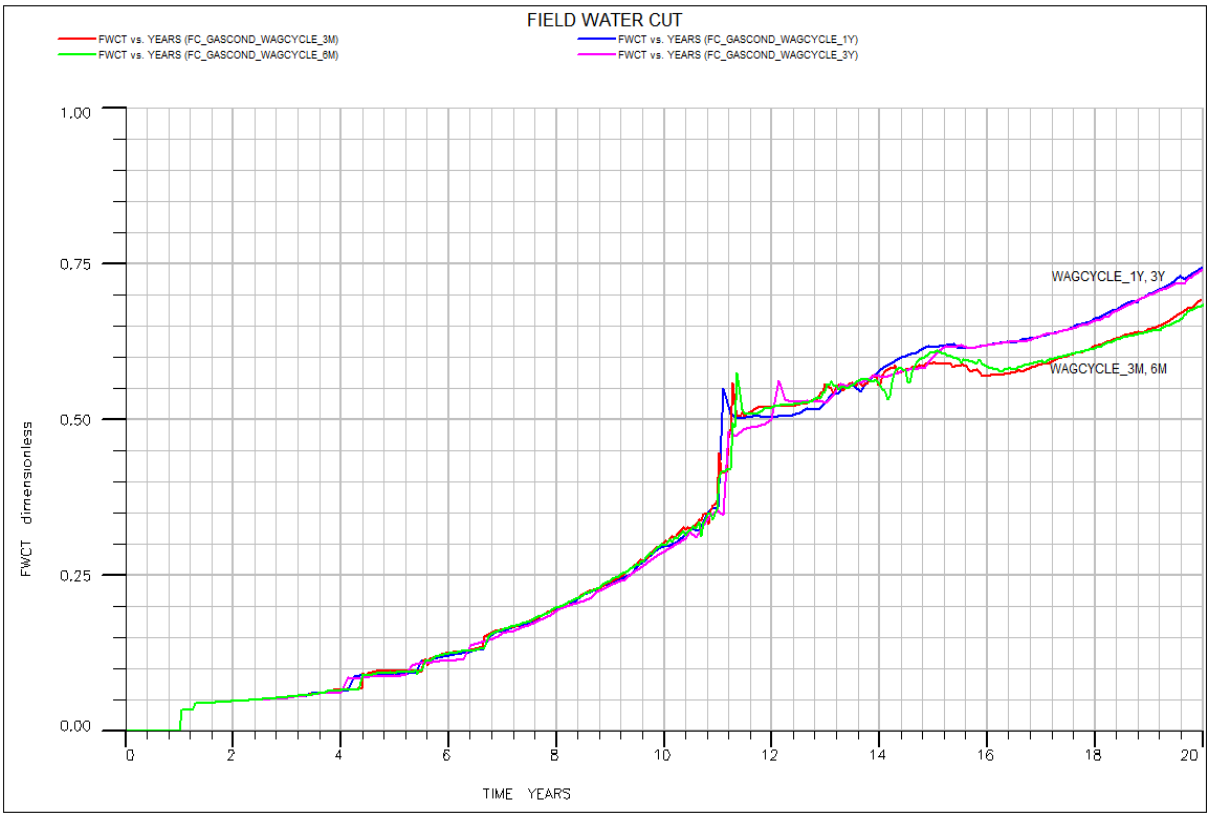

Figure 4-98:Sensitivity analysis of WAG cycle on field water cut (fully compositional case).

4.6.4 Vertical Communication (kv/kh Ratio)

To investigate the effect of reduced communication between layers, kv/kh ratio was reduced from a base value of 0.1 to 0.0001. Average field pressure from both models has the same trend as the previous cases investigated but the decline is higher due to reduced communication between the layers (Appendix C-13). It takes time for pressure transient from the aquifer to move further into the reservoir for each individual layer. This movement is also restricted by the condensate accumulation around the wellbore.

As the communication between the layers is reduced, it is clearly observed that compositional and the modified black-oil (MBO) models showed closer performances for gas recovery. The gas recovery reduced with increasing kv/kh ratio for the five recovery strategies that were investigated (Table 4-4, Table 4-5, Table 4-6, and Table 4-7).

Table 4-4:Effect of kv/kh ratio on gas recovery (fully compositional model).

Gas Recovery (BCF)				
Recovery Schemes	**Kv/kh Ratio**			
	0.1	**0.01**	**0.001**	**0.0001**
DEP	216.19	214.85	214.85	211.89
GI	218.63	217.77	218.63	218.15
WI	215.31	213.73	212.36	210.09
WAG	218.83	218.83	218.83	217.30
SWAG	218.72	216.24	215.71	217.12

From the oil production rate plot, it can also be seen that the time of constant oil production rate became shorter as the vertical communication is reduced (Appendix C-12). Since the condensation and consequent vaporization processes are controlled by pressure dependent functions, the reduction in pressure drop caused a delay in condensate drop-out for the depletion, water injection, and gas injection in MBO model unlike the fully compositional model. For the WAG and SWAG injection, the limited compositional model predicted a higher condensate recovery than the limited compositional model (Table 4-7). Reduced vertical communication prevents the mixing of leaner reservoir gas (relative to initial conditions) with oil formed after condensation. Also, the accumulated condensate is not able to settle in lower layers under the effect of gravity forces. So, each individual layer condensation and vaporization process becomes proportional to that layer's content of heavy and light component fractions (Bulent, 2000).

The findings from this research indicate that the fully compositional model predicts a higher condensate recovery than the limited compositional model because it accounts for the compositional changes as pressure declines. The cumulative gas produced predicted by the fully and limited compositional model are comparable for all the recovery schemes investigated. However, the fully compositional model predicts a higher condensate recovery than the limited compositional model. For the fully and limited compositional model, WAG injection gives the highest gas recovery. Based on the observation of the performance of the five recovery schemes, it can be concluded that the SWAG injection provides the highest condensate recovery, followed by WAG and gas injection, respectively. Reduced vertical communication reduces the gas recovery for the depletion and water injection scenarios, whereas the condensate recovery during injection processes increases as the vertical permeability is reduced

Table 4-5:Effect of kv/kh ratio on condensate recovery (fully compositional model).

Condensate Recovery (MMSTB)				
Recovery Schemes	**kv/kh Ratio**			
	0.1	**0.01**	**0.001**	**0.0001**
DEP	40.91	41.19	41.19	43.44
GI	46.89	46.75	47.37	46.67
WI	45.57	43.93	45.64	45.43
WAG	48.83	46.66	47.23	46.49
SWAG	51.3	49.34	49.36	48.95

Table 4-6:Effect of kv/kh ratio on gas recovery (limited compositional model).

Gas Recovery (BCF)				
Recovery Schemes	**kv/kh Ratio**			
	0.1	**0.01**	**0.001**	**0.0001**
DEP	216.31	216.06	215.34	215.45
GI	218.63	218.63	218.63	218.63
WI	215.54	215.43	214.82	212.98
WAG	218.83	218.83	218.83	218.83
SWAG	218.72	218.72	218.72	218.72

Table 4-7:Effect of kv/kh ratio on gas recovery (limited compositional model).

Condensate Recovery (MMSTB)				
Recovery Schemes	**kv/kh Ratio**			
	0.1	**0.01**	**0.001**	**0.0001**
DEP	33.30	36.14	38.96	39.25
GI	39.67	43.33	46.85	47.42
WI	36.97	38.59	40.33	39.90
WAG	43.07	47.13	50.85	51.43
SWAG	45.07	47.50	50.04	50.65

CHAPTER FIVE: CONCLUSION AND RECOMMENDATION

The conclusions derived from this work are presented in this chapter. In addition, a set of recommendations are proposed for future studies to improve the methodology and results obtained from this research.

5.1 SUMMARY AND CONCLUSIONS

In this thesis, the fully and limited compositional simulation is used to investigate the performance of a gas-condensate reservoir in the Niger Delta. The reservoir fluid was characterized, and its phase behaviour is described with a Peng-Robinson equation of state using a commercial PVT software. Using the tuned equation of state, black-oil PVT properties are generated using Whitson and Torp method for the limited compositional model. At each step in the constant volume depletion test, the condensate is used to define the oil formation volume factor (FVF) and solution gas-oil ratio (GOR), while the gas phase was used to define the dry gas FVF and oil-gas-ratio (OGR). In the limited compositional model, equilibrium calculations are estimated using the solution gas-oil, and oil-gas ratio tables.

The five recovery schemes investigated in this study include primary depletion with no injection, water injection, gas injection, water-alternating-gas (WAG) injection, and simultaneous water-and-gas (SWAG) injection. The minimum miscibility pressure (MMP) test was conducted to determine the injection pressure at which miscibility is attained in the reservoirs. It is concluded that the limited compositional simulator can be used as a screening tool and for the rapid evaluation of reservoir performance at the early stage of condensate reservoir development when data is scarce. The results from this study can be used to assess the suitability of using limited compositional simulation to investigate the performance of condensate reservoirs.

The following conclusions can be derived from the results of this study:

- The compositional gradient method of initialization affects the performance of the limited compositional model. Hence, the fluid in place volumes predicted by the fully and limited compositional simulation are not equal.
- The fully compositional model (base case) predicts a lesser value of gas initially in place, GIIP (284.57BCF) than the limited compositional model (293.64BCF). However, the volume of oil initially in place (OIIP) estimated from the fully

compositional simulation (125.40MMSTB) is higher than that predicted by the limited compositional model (110.68MMSTB).

- The cumulative gas production for the fully and limited compositional case are identical for the gas injection (218.63BCF), WAG (218.83BCF), and SWAG (218.72BCF) recovery schemes unlike the depletion and water injection case in which the limited compositional model (216.31BCF, 216.03BCF) predicts a slightly lesser recovery of gas than the fully compositional model (216.19BCF, 215.25BCF).
- The cumulative oil production increases with increase in quantity of gas injected within the 20-year study period. The highest condensate recovery (40.91% of the volume of oil initially in place, OIIP) was obtained from the SWAG injection of 12MMSCF/D of recycled gas and 4000STB/D of water compared to the application of WAG (38.94% of OIIP); gas injection of 12MMSCF/D (37.39% of OIIP), waterflooding at 2000stb per day (36.34% of OIIP), and natural depletion (32.62% of OIIP) where no fluid was injected in the reservoir model.
- Condensate accumulates throughout the reservoir below the dewpoint pressure, especially in the lower layers. For the limited compositional model, the liquid drop-out is pressure dependent and gives lower oil production rates at the beginning of the simulation for the limited compositional model. The reservoir gas has a lower oil-gas ratio, and so, more condensate is left in the reservoir.
- During the gas cycling a miscible displacement is guaranteed in compositional model, independent of the injection gas used, even though the injected gas may not be first contact immiscible with the original reservoir gas. Miscibility develops by a simple vaporizing mechanism. However, miscibility cannot be represented by the modified black-oil (MBO) model resulting in late arrival of displacement fronts.
- Miscible displacement is improved with optimum gas injection rate. Below the dew-point pressure, a high injection rate maintains the field pressure but causes gas to bypass the condensate, leading to low recovery. Extremely low injection rates do not provide pressure maintenance, allowing further retrograde condensation or water influx from an adjoining aquifer. There is need to optimise the injection rate to maximise condensate recovery.
- Fluid Injection should be done above the MMP to ensure miscibility during the displacement process.

- It is concluded that the differences between the vaporization characteristics of the two models (fully compositional vs. limited compositional models) dictated their overall performance. In the limited compositional model, the compositional dependence in the fluid PVT properties is disregarded and consequently, the injected gas can only pick up oil as a function of pressure. With this approach, the primary compositional effect, stripping of the liquid components in inverse proportion to their molecular weights is ignored, and more oil is left in the reservoir than the fully compositional model.
- At low kv/kh ratios (i.e., reduced vertical communication), a better match between two models can be obtained in terms of gas production rates and recoveries. Reduced vertical communication gives higher pressure drop at high production rates for both models. This implies higher oil saturations in compositional model and lower oil saturations in the limited compositional model.

5.2 RECOMMENDATIONS FOR FURTHER STUDY

Further studies should be conducted in the following areas:

- The reservoir used in this research is assumed to be homogenous, which does not represent actual subsurface conditions. The effect of lateral and vertical heterogeneities (porosity and permeability) on reservoir performance and development strategy should be investigated further.
- The reservoir models should be calibrated using actual well production data. History matching should be performed to ensure accurate forecast of reservoir performance.
- It is recommended that economic analysis of the various recovery concepts be conducted to estimate the feasibility of implementing these techniques in Nigeria against a predetermined set of decision criteria such as IRR, NPV, etc. A stochastic approach can be employed to incorporate uncertainty and risk analysis.
- This study uses a peripheral pattern for the simulation of the injection schemes. Other injection patterns like regular five-spot, seven- and nine-spots and staggered line drive should be considered in future research. An extensive study on gas injection using non-hydrocarbon gases to enhance condensate recovery should be further explored.

NOMENCLATURE

a	*Attraction parameter*
°API	*API gravity*
b	*Repulsion parameter/ effective molecular volume*
BBO	*Billion barrels of oil*
BIC	*Binary interaction coefficients*
C1	*Methane*
C2	*Ethane*
C3	*Propane*
C6	*Hexane*
C7+	*Heptane-plus fraction*
CCE	*Constant composition expansion*
CGR	*Condensate-gas-ratio*
CO2	*Carbon dioxide*
CVD	*Constant volume depletion*
DEP	*Depletion*
EOR	*Enhanced oil recovery*
FC	*Fully compositional model*
GI	*Gas injection*
GOR	*Gas-oil ratio*
iC4	*Iso-butane*
iC5	*Iso-pentane*
INJ	*Injector well*
IOR	*Improved oil recovery*
krg	*Gas relative permeability*
kv/kh	*Vertical/Horizontal permeability ratio*
kro	*Oil relative permeability*
krw	*Water relative permeability*
LC	*Limited compositional model*
MBO	*Modified black oil*
MMP	*Minimum miscibility pressure*
MMSTB	*Million stock stank barrel*
nC4	*Normal-butane*
nC5	*Normal-pentane*
N2	*Nitrogen*
NPV	*Net-present-value*
OPEC	*Organization of Petroleum Exporting Countries*
Pc	*Critical pressure*
PROD	*Producer well*
R	*Ideal gas constant*
Rs	*Solution gas-oil ratio, SCF/STB*
Rv	*Oil-gas ratio, STB/SCF*
SCF	*Standard cubic feet*
SE	*South eastern region*
Sg	*Gas saturation*
*Sg**	*Effective gas saturation*
Sgc	*Critical gas saturation*
So	*Oil/Condensate saturation*
*So**	*Effective oil/condensate saturation*
Sor	*Residual oil saturation*
STB	*Stock tank barrel*
Sw	*Water saturation*
*Sw**	*Effective water saturation*
SWAG	*Simultaneous gas and water injection*
Swc	*Connate/Irreducible water saturation*
TCF	*Trillion cubic feet*
Tc	*Critical Temperature*
Tr	*Reduced temperature*
v	*Gas specific volume*
WI	*Water injection*
WAG	*Water-alternating-gas injection*
α	*component-dependent correction term*
ω	*Acentric factor*
φ	*Porosity*

REFERENCES

Ahmed, T. (2018). *Reservoir engineering handbook*. Gulf Professional publishing.

Alaigba, D., Onaiwu O., Ikponmwosa O., & Olalekan O. (2020). "Optimized Salinity Water Flooding as an Improved Oil Recovery IOR Scheme in the Niger Delta." In *SPE Nigeria Annual International Conference and Exhibition*.

Ali, F. (2014). Importance of water Influx and waterflooding in Gas condensate reservoir (Master's thesis, Norwegian University of Science and Technology, Trondheim).

Aziz, K., & Settari, A. (1979). *Petroleum reservoir simulation*. 1979. Applied Science Publishing Ltd., London, UK.

Bolling, J. D. (1987, January). Development and application of a limited-compositional, miscible flood reservoir simulator. In *SPE Symposium on Reservoir Simulation*. Society of Petroleum Engineers.

Carter, R. D., & Tracy, G. W. (1960). An improved method for calculating water influx. *Transactions of the Society of Petroleum Engineers AIME, 219*(01), 415-417.

Cason, L. D. (1989). Waterflooding increases gas recovery. *Journal of Petroleum Technology*, *41*(10), 1-102.

Coats, K. 1985. Simulation of gas condensate reservoir performance. *Journal of Petroleum Technology, 37*(10),1870–1886.

Cobanoglu, M., Shukri, I., & Omairi, R. (2018, November). Assessment of Condensate Recovery Improvement Through Gas and Water Injection: A Case Study for a Large Heavily Depleted Very Rich Gas Condensate Field in the Sultanate of Oman. In *Abu Dhabi International Petroleum Exhibition & Conference*. OnePetro.

Doust, H. (1990). Petroleum geology of the Niger Delta. *Geological Society, London, Special Publications*, *50*(1), 365-365.

Ejedawe, J. E. (1981). Patterns of incidence of oil reserves in Niger Delta Basin. *American Association of Petroleum Geologists*, *65*(9), 1574-1585.

Ejedawe, J.E., Coker, S.J.L., Lambert-Aikhionbare, D.O., Alofe, K.B., & Adoh, F.O. (1984). Evolution of oil-generative window and oil and gas occurrence in Tertiary Niger Delta Basin. *American Association of Petroleum Geologists*, *68*(11), 1744-1751.

El-Banbi, A. H., Aly, A. M., Lee, W. J., & McCain, W. D. (2000, April). Investigation of waterflooding and gas cycling for developing a gas-condensate reservoir. In *CERI Gas Technology Symposium*. Society of Petroleum Engineers.

Elkins, L. F., Brown, R. C., & Skov, A. M. (1975, January). Comparison of Performance During Cycling and Blowdown with Various Prediction Methods-Washington Cockfield "D" Gas-Condensate Reservoir. In *Fall Meeting of the Society of Petroleum Engineers of AIME*. Society of Petroleum Engineers.

Ertekin, T., Abou-Kassem, J. H., & King, G. R. (2001). *Basic applied reservoir simulation* (Vol. 7). Richardson, TX: Society of Petroleum Engineers.

Fan, L., Harris, B. W., Jamaluddin, A., Kamath, J., Mott, R., Pope, G. A., & Whitson, C. H. (2005). Understanding gas-condensate reservoirs. *Oilfield Review*, *17*(4), 14-27.

Fishlock, T. P., & Probert, C. J. (1996). Waterflooding of gas condensate reservoirs. *SPE Reservoir Engineering*, *11*(04), 245-251.

Ghahri, P. (2018). Reservoir simulation course (Heriot-Watt University).

Hernandez, I., Ali, S. M., & Bentsen, R. G. (1999). First steps for developing an improved recovery method for a gas condensate reservoir. In *CSPG and Petroleum Society Joint Convention*. OnePetro.

International Energy Agency. (2019). "Nigeria Energy Outlook: Analysis from Africa Energy Outlook." *IEA*, Paris https://www.iea.org/articles/nigeria-energy-outlook.

Karacaer, C. (2014). Mixing issues in CO2 flooding: comparison of compositional and extended black-oil simulators (Doctoral dissertation, Colorado School of Mines).

Killough, J. E., & Kossack, C. A. (1987, January). Fifth comparative solution project: evaluation of miscible flood simulators. *In SPE Symposium on Reservoir Simulation*. Society of Petroleum Engineers.

Lake, L. W. (1989). *Enhanced oil recovery*. Upper Saddle River, New Jersey 07458: Prentice-Hall Inc.

Nangacovié, H. L. M. (2012). Application of WAG and SWAG Injection Techniques in Norne E-Segment (Master's thesis, Norwegian University of Science and Technology, Trondheim).

Nwabueze, D. O. (2000, January). Condensate Production-The Nigerian Perspective. *In Nigerian Annual International Conference and Exhibition*. Society of Petroleum Engineers.

Nwonodi, C., Onwuchekwa, C., Ekong, I., Amrasa, K., & Osadjere, P. (2018). Evaluation of a Depleted Oil Reservoir for Gascap Blowdown Using 3D Simulation Models: A Case Study of Chrome Field Development. *In SPE Nigeria Annual International Conference and Exhibition*. Society of Petroleum Engineers.

Olabode, O., Alaigba, D., Oramabo, D., & Bamigboye, O. (2020). Modelling Low-Salinity Water Flooding as a Tertiary Oil Recovery Technique. *Modelling and Simulation in Engineering*, 2020.

Raghavan, R., & Jones, J. R. (1996). Depletion performance of gas-condensate reservoirs. *Journal of Petroleum Technology*, *48*(08), 725-731.

Ramachandran, K. P., Gyani, O. N., & Sur, S. (2010, January). Immiscible hydrocarbon WAG: laboratory to field. In SPE Oil and Gas India Conference and Exhibition. Society of Petroleum Engineers.

Sanusi, O. M. (2017). *Techno-Economic Feasibility of Ethane Based Enhanced Oil Recovery in Nigeria (CASE Study: Niger Delta)* (Doctoral dissertation).

Syzdykov, M. (2014). *Evaluating gas injection performance in very low permeability, thick carbonate gas-condensate reservoirs to improve ultimate liquid yield* (Doctoral dissertation, Colorado School of Mines).

Taber, J. J., Martin, F. D., & Seright, R. S. (1997). EOR screening criteria revisited-Part 1: Introduction to screening criteria and enhanced recovery field projects. *SPE Reservoir Engineering*, *12*(03), 189-198.

Todd, M.R., & Longstaff, W.J. 1972. The development, testing, and application of a numerical simulator for predicting miscible flood performance. *Journal of Petroleum Technology*, *24*(7), 874–882.

Tran, T. V., Truong, T. A., Ngo, A. T., Hoang, S. K., & Trinh, V. X. (2019). A case study of gas-condensate reservoir performance under bottom water drive mechanism. *Journal of Petroleum Exploration and Production Technology*, *9*(1), 525-541.

Tuttle, M. L., Charpentier, R. R., & Brownfield, M. E. (1999). The Niger Delta Petroleum System: Niger Delta Province, Nigeria, Cameroon, and Equatorial Guinea, Africa. *US. Department of the Interior, US Geological Survey*, 50-99.

Udie, A. C., Nwakaudu, M. S., Anyadiegwu C.I.C., Onwukwe S. I., & Enenebeaku, C. K (2014). Improving Condensate Recovery Using Water Injection Model at Dew-Point Pressure. *American Journal of Engineering Research*, *3*(02), 54-62.

Wheaton, R. J., & Zhang, H. R. (2000, January). Condensate banking dynamics in gas condensate fields: compositional changes and condensate accumulation around production wells. *In SPE Annual Technical Conference and Exhibition*. Society of Petroleum Engineers.

Whitson, C. H., & Brulé, M. R. (2000). *Phase behavior* (vol. 20, p. 233). Richardson, TX: Henry L. Doherty Memorial Fund of AIME, Society of Petroleum Engineers.

Whitson, C. H., Fevang, Ø., & Yang, T. (1999, January). Gas condensate PVT–What's really important and Why? In IBC Conference, London, UK (pp. 28-29).

Whitson, C., & Torp, S. 1983. Evaluating constant-volume depletion data. *Journal of Petroleum Technology*, 35(3):610–620.

Wijaya, Z. (2006). CO2 Injection in an Oil Reservoir with Gas Cap; Compositional Simulation Case at HEIDRUN Field Norway. Master's thesis, Norwegian University of Science and Technology, Trondheim.

Zekri, A. Y., Jerbi, K. K., El-honi, M., & Co, W. O. (2000). SPE 64727 Economic Evaluation of Enhanced Oil Recovery. *Oil Gas Science and Technology*, *57*(3), 259–267.

Zick, A. A., & Co, A. O. & G. (1986). SPE 15493 A Combined Condensing/Vaporizing Mechanism Displacement of Oil by Enriched Gases. Symposium A Quarterly Journal in Modern Foreign Literatures.

APPENDIX A

This appendix summarizes the simulation results for the fully compositional model. It includes the matched critical properties, regression process, and binary interaction parameters used in the Peng Robinson equation of state.

Table A.1: Experimental and simulated results of the dewpoint pressure of reservoir fluid

Dewpoint Pressure Experiment		
Experimental Result	Tuned Simulated Result	
	Before Lumping	After Lumping
4191 psia	4192 psia	4172.82 psia

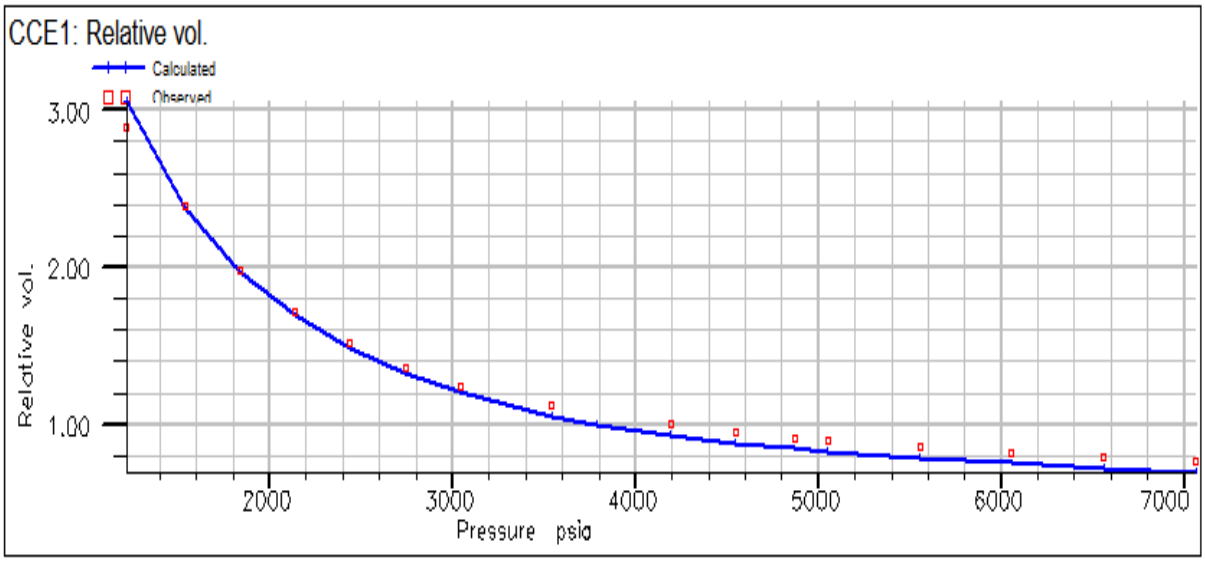

Figure A.1: Plot of the experimental and simulated relative volume (before regression)

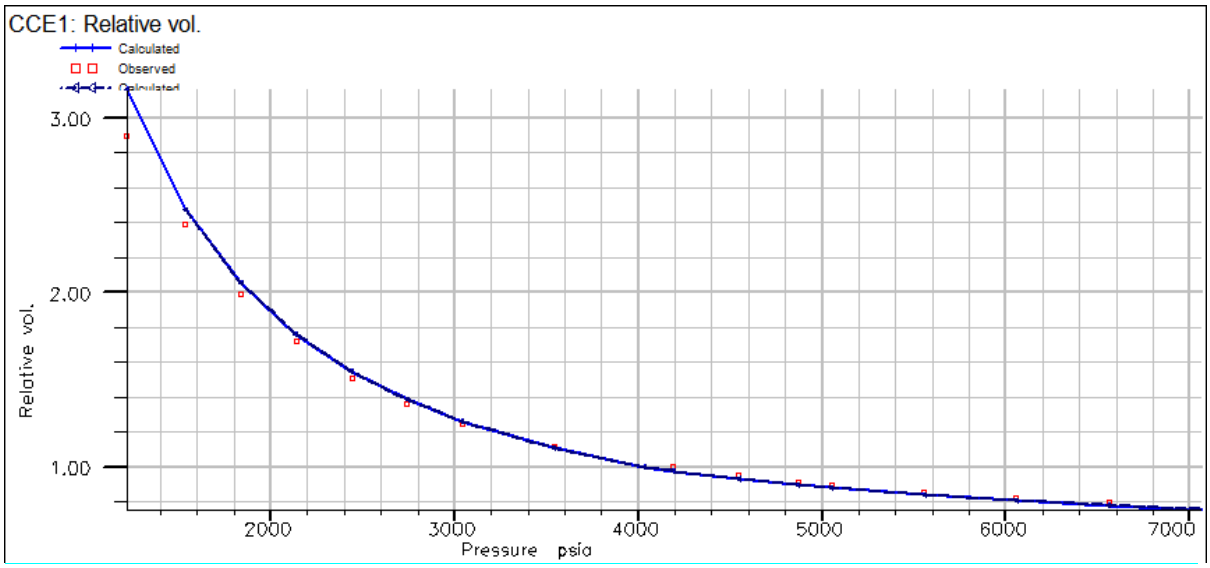

Figure A.2: Plot of the experimental and simulated relative volume (after regression).

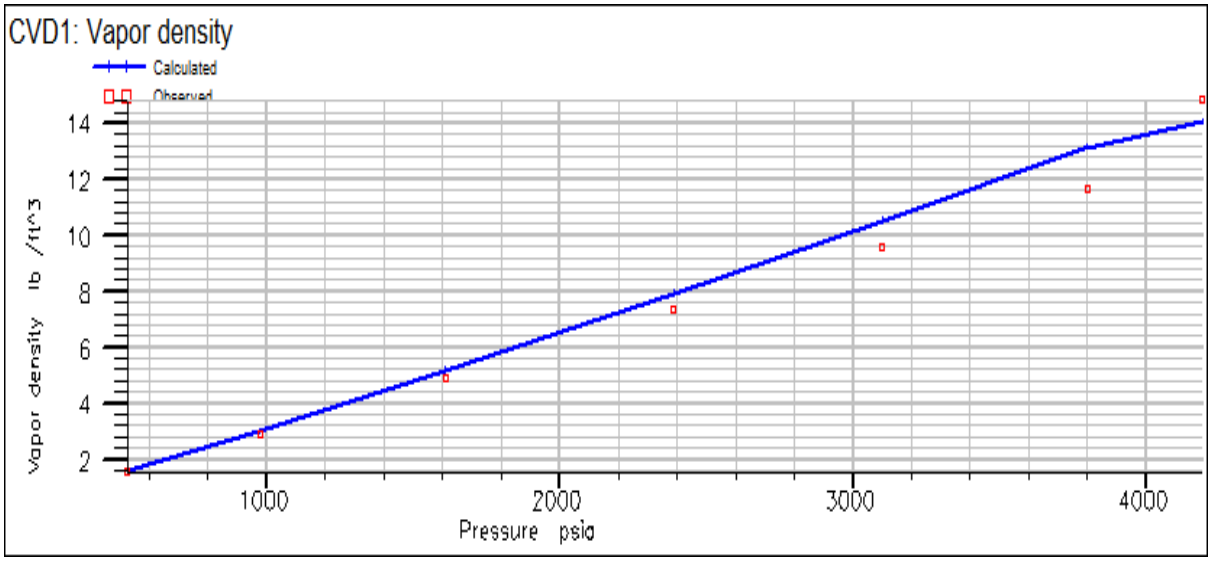

Figure A.3: Plot of experimental and simulated vapor density (after regression)

Table A.2: Critical properties of the lumped fluid.

Components	MW (lb-mole)	P_c (psia)	T_c (°R)	V_c (ft^3/lb-mole)	Z_c
N2	28.01	492. 31	227.16	1.442	0.291
CO2	44.01	1071.33	548.46	1.506	0.274
C1	16.04	667.78	343.08	1.569	0.284
C2	30.07	708.34	549.77	2.371	0.284
C3	44.097	615.75	665.64	3.204	0.276
C4C6	66.81	507.69	805.42	4.640	0.273
C7+	171.72	299.83	1218.51	10.83	0.248

Table A.3: Peng Robinson EOS parameters of the lumped reservoir fluid

Components	Ω_A	Ω_B	Acentric factor	V_{shift}	Parachor
N2	0.457235529	0.77796074	0.04	-0.131	41
CO2	0.457235529	0.77796074	0.225	-0.0427	78
C1	0.457235529	0.77796074	0.013	-0.1443	77
C2	0.457235529	0.77796074	0.0986	-0.1033	108
C3	0.457235529	0.77796074	0.1524	-0.0775	150.3
C4C6	0.457235529	0.77796074	0.2258	-0.0423	213.636
C7+	0.457235529	0.77796074	0.8575	0.0840	456.215

Table A.4: Binary interaction coefficient of the lumped reservoir fluid

Components	N2	CO2	C1	C2	C3	C4C6	C7+

N2	0	-0.012	0.1	0.1	0.1	0.1	0.1
CO2	-0.012	0	0.1	0.1	0.1	0.1	0.1
C1	0.1	0.1	0	0	0	0.00556	0.04428
C2	0.1	0.1	0	0	0	0.00199	0.01
C3	0.1	0.1	0	0	0	0.00199	0.01
C4C6	0.1	0.1	0.00556	0.00199	0.00199	0	0
C7+	0.1	0.1	0.04428	0.01	0.01	0	0

Table A.5: Relative permeability data for the oil-water system

Wyllie and Gardner (Oil- Water System)			
Sw	**Swc***	**Kro**	**Krw**
0	0	1.000	0.0000
0.1	0	1.000	0.0000
0.2	0	1.000	0.0000
0.25	0.0625	0.824	0.0002
0.3	0.125	0.670	0.0020
0.35	0.1875	0.536	0.0066
0.4	0.25	0.422	0.0156
0.45	0.3125	0.325	0.0305
0.5	0.375	0.244	0.0527
0.6	0.5	0.125	0.1250
0.65	0.5625	0.084	0.1780
0.7	0.625	0.053	0.2441
0.75	0.6875	0.031	0.3250
0.8	0.75	0.016	0.4219
0.85	0.8125	0.007	0.5364
0.9	0.875	0.002	0.6699
1	1	0.000	1.0000

Table A.6: Relative permeability data for the gas-oil system.

Wyllie and Gardner (Gas-Oil System)				
Sg	**So**	**So***	**Kro**	**Krg**
0	0.8	1	1.000	0.000
0.05	0.75	0.9375	0.824	0.005

0.1	0.7	0.875	0.670	0.036
0.15	0.65	0.8125	0.536	0.100
0.2	0.6	0.75	0.422	0.193
0.25	0.55	0.6875	0.325	0.308
0.3	0.5	0.625	0.244	0.432
0.35	0.45	0.5625	0.178	0.555
0.4	0.4	0.5	0.125	0.670
0.45	0.35	0.4375	0.084	0.769
0.5	0.3	0.375	0.053	0.850
0.55	0.25	0.3125	0.031	0.911
0.6	0.2	0.25	0.016	0.954
0.65	0.15	0.1875	0.007	0.980
0.7	0.1	0.125	0.002	0.994
0.8	0	0	0.000	1.000

APPENDIX B

In this section, additional plots of field pressure, cumulative oil recovery Np, cumulative gas recovery, gas production rate, field water cut for the limited compositional case. Also, time lapse profiles of the pressure, gas saturation, and oil saturation heatmaps for the various recovery schemes are presented here. that are not provided in the main are presented here.

B.1. LIMITED COMPOSITIONAL MODEL SIMULATION RESULTS

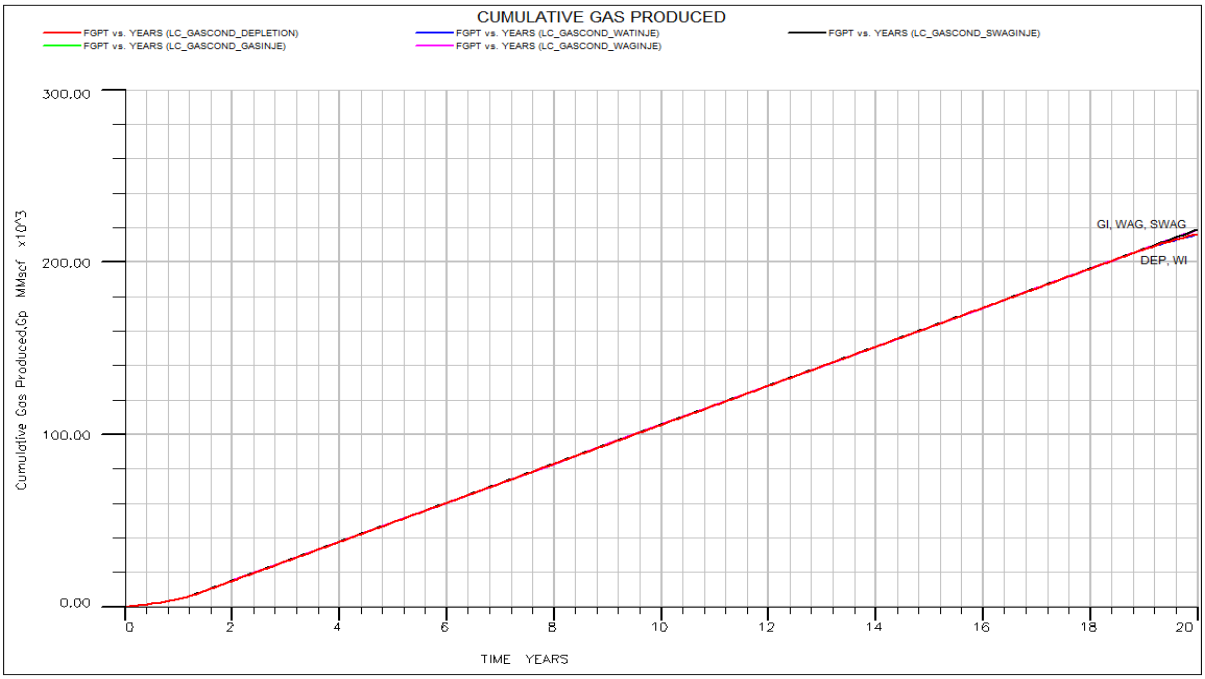

Figure B.1: Cumulative gas production (limited compositional model).

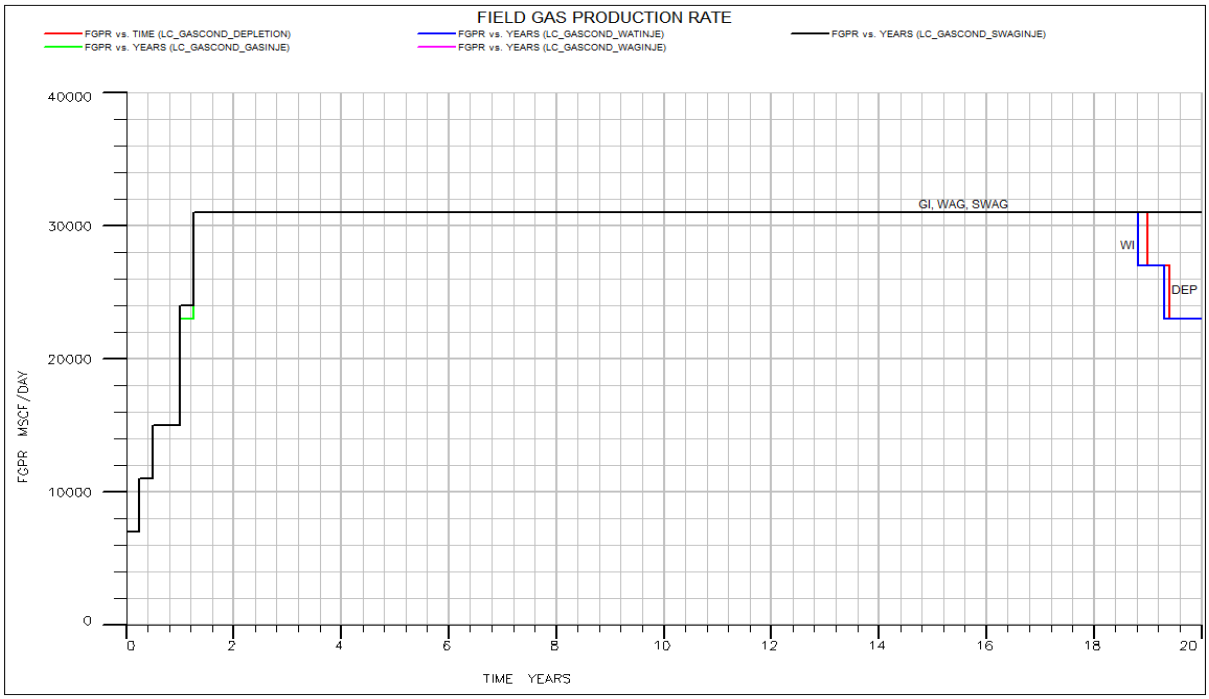

Figure B. 2. Field gas production rate (limited compositional model).

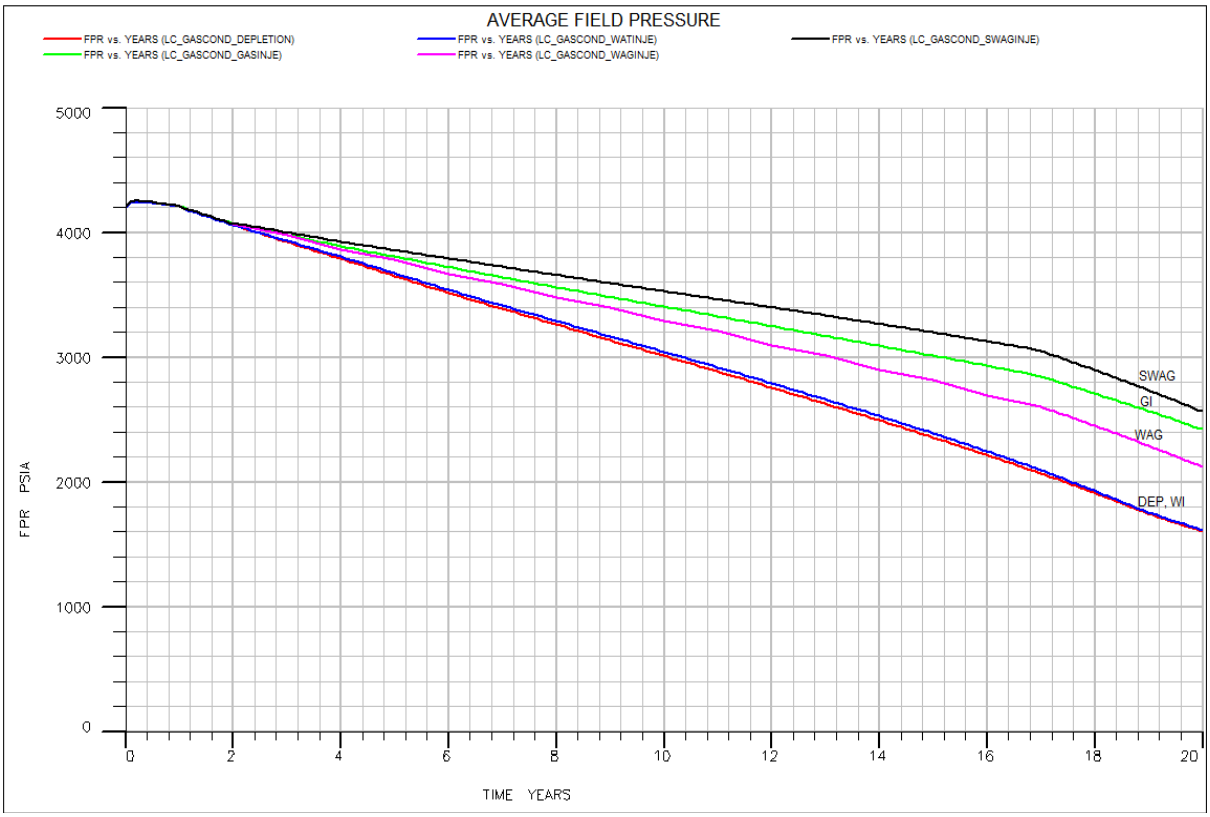

Figure B. 3. Average field pressure (limited compositional model)

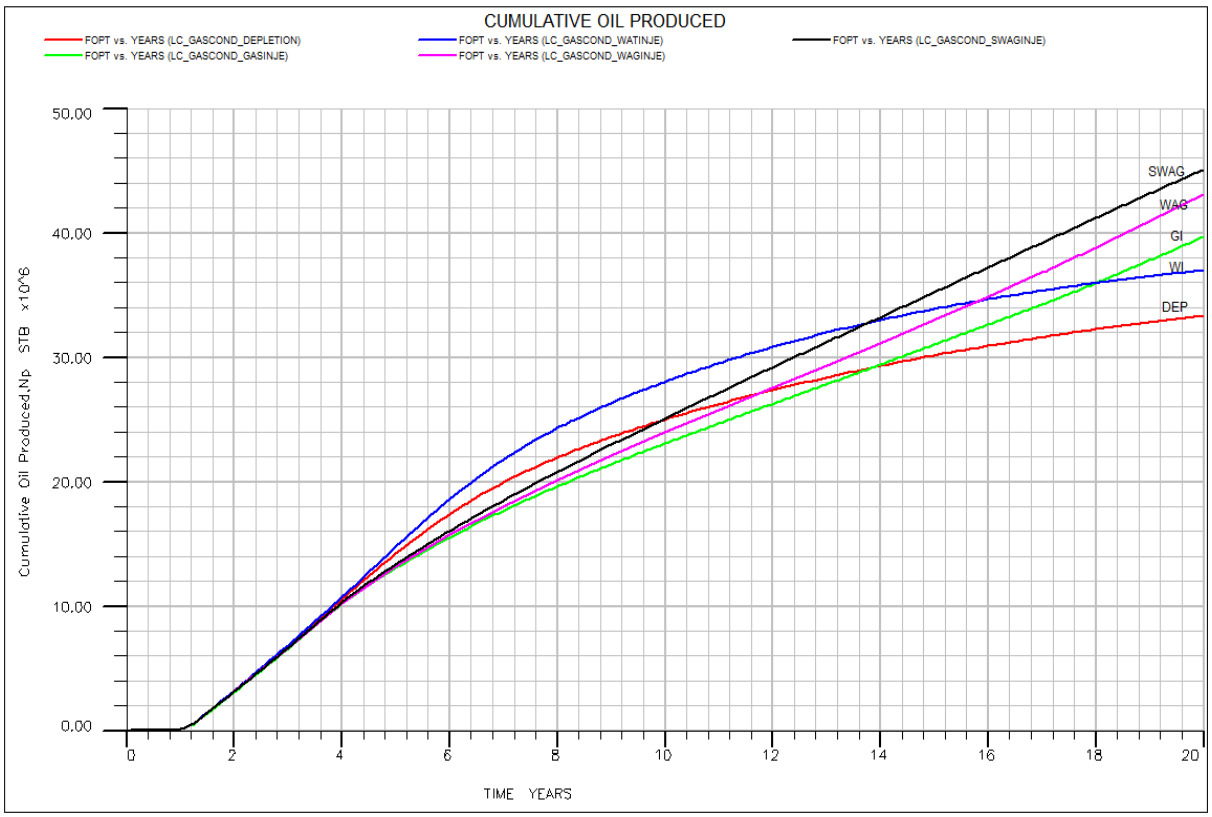

Figure B. 4. Cumulative oil production (limited compositional model).

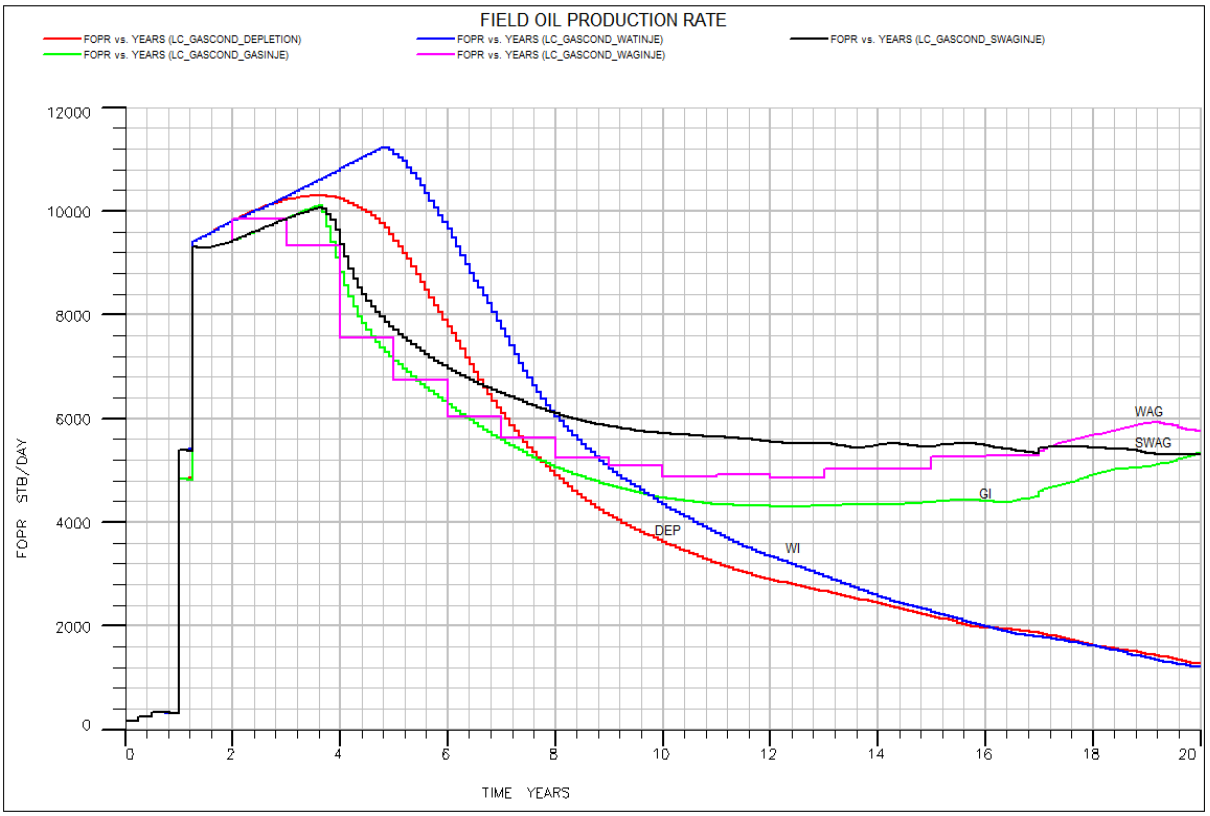

Figure B. 5. Field oil production rate (limited compositional model)

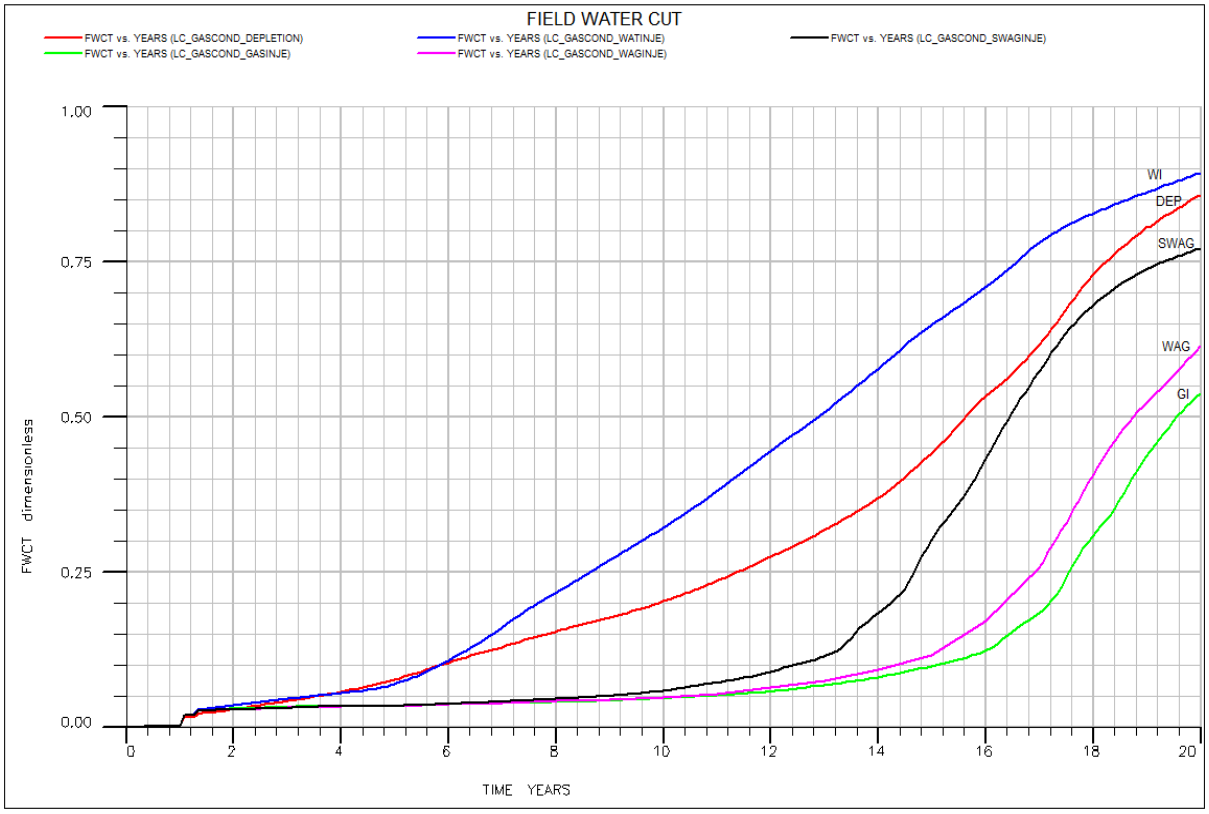

Figure B. 6. Field water cut (limited compositional model)

B.2. CONDENSATE BANKING

B.2.1. Depletion

B.2.1.1 Pressure

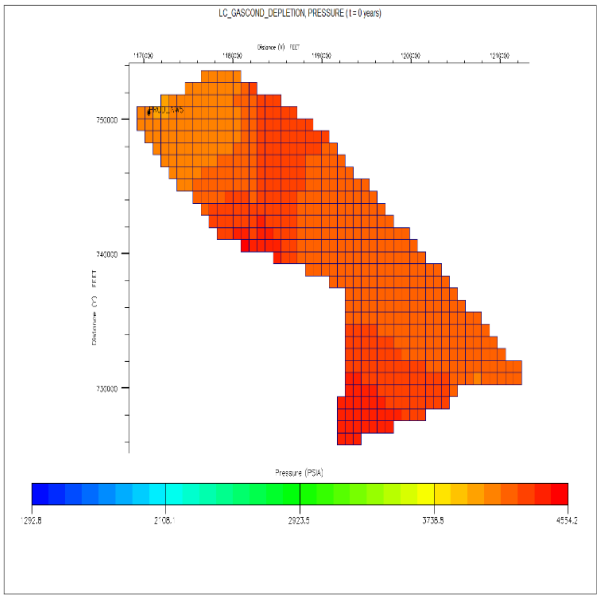

Figure B. 7. Field pressure at t=0 years (DEP).

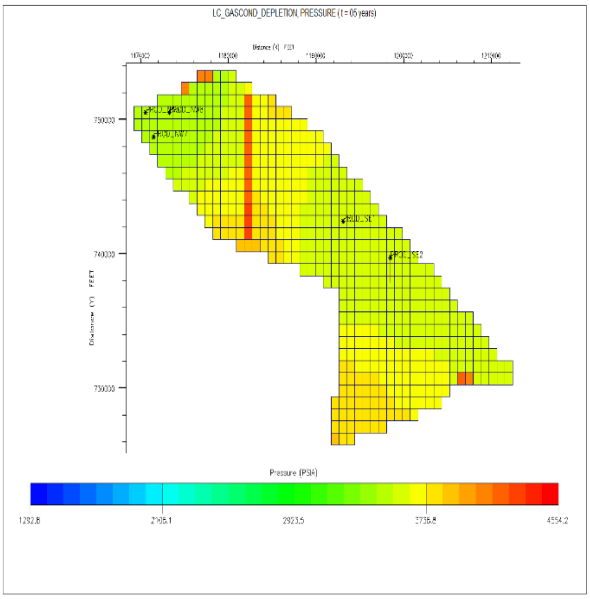

Figure B. 8. Field pressure at t=5 years (DEP)

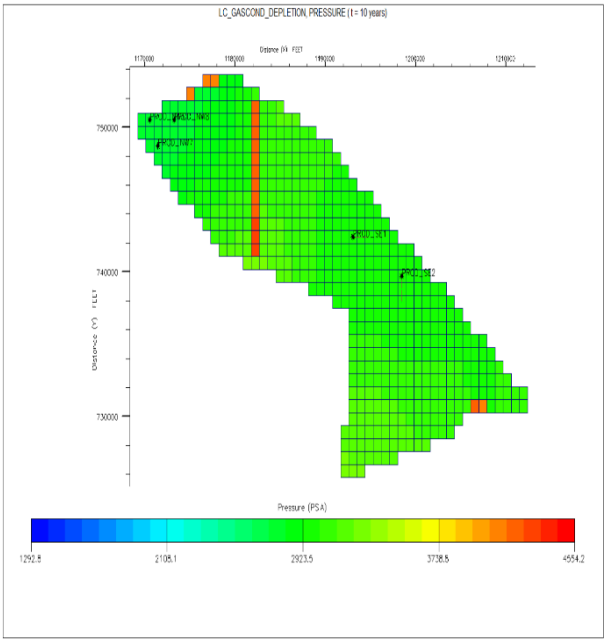

Figure B. 9. Field pressure at t=10 years (DEP).

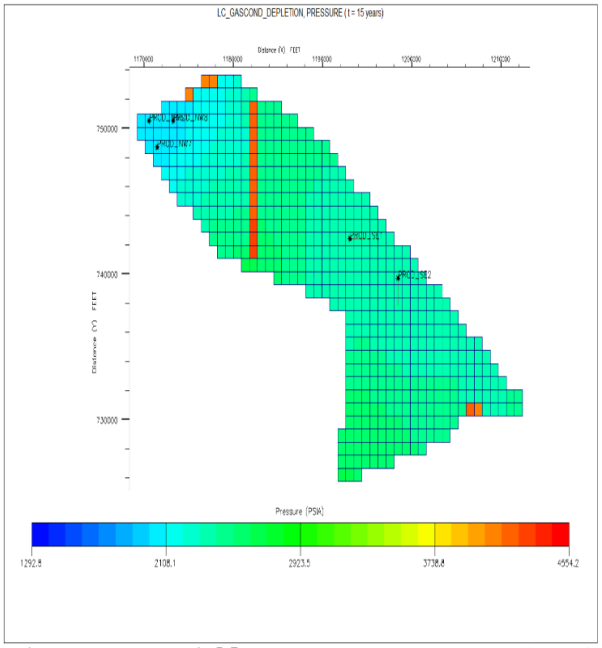

Figure B. 10. Field pressure at t=15 years (DEP)

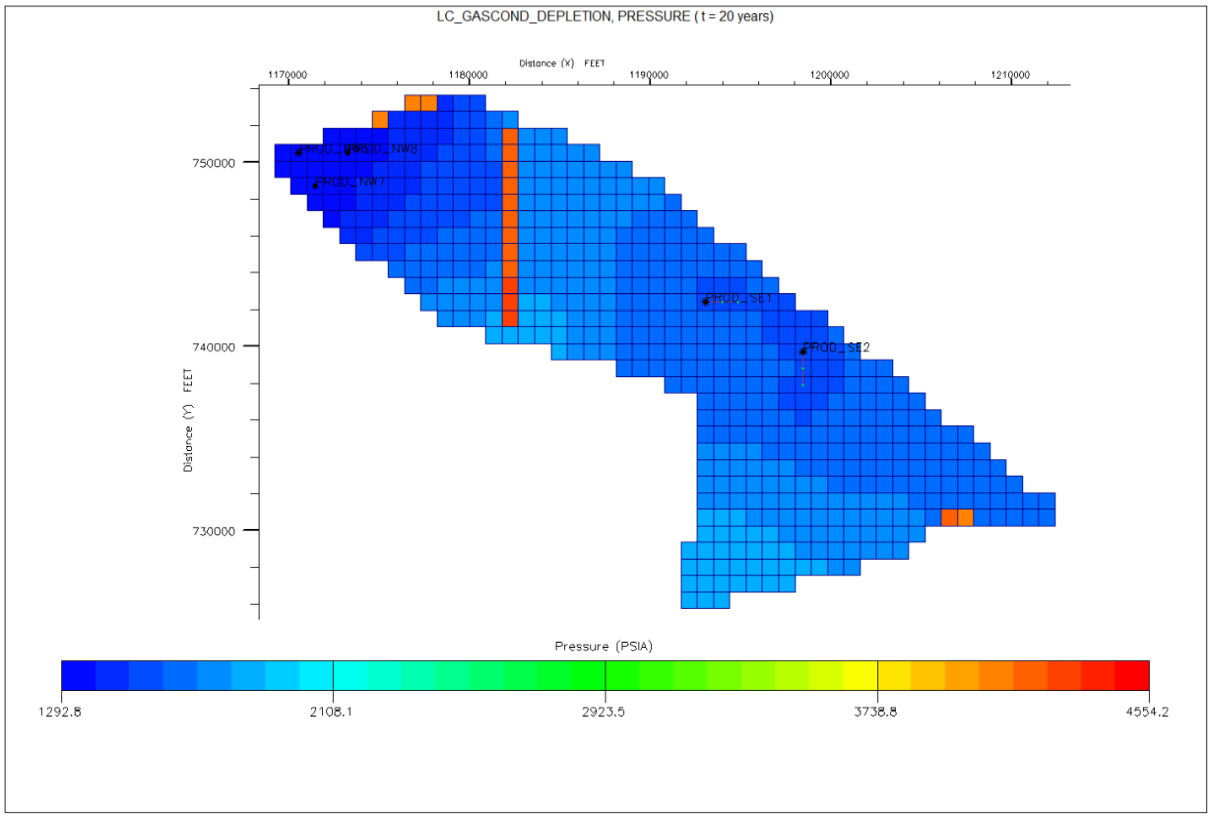

Figure B. 11. Field pressure at t=20 years (DEP).

B.2.1.2. Gas Saturation

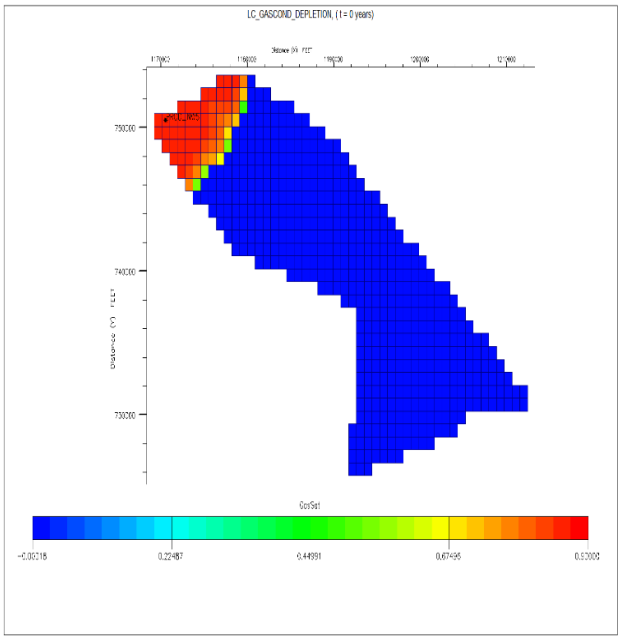

Figure B. 12:Gas saturation at t=0 years (DEP).

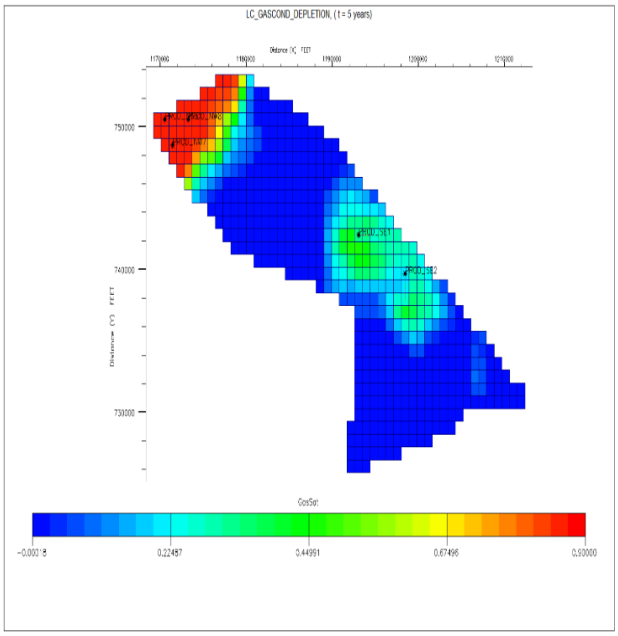

Figure B. 13:Gas saturation at t=05 years (DEP).

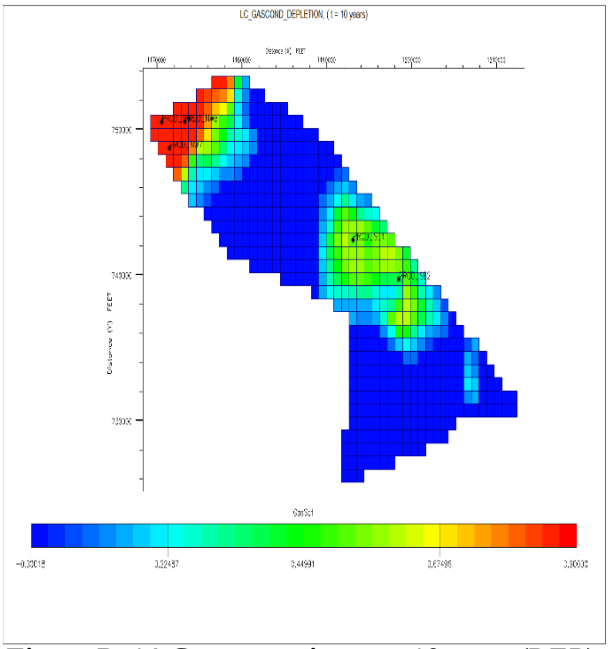

Figure B. 14:Gas saturation at t=10 years (DEP).

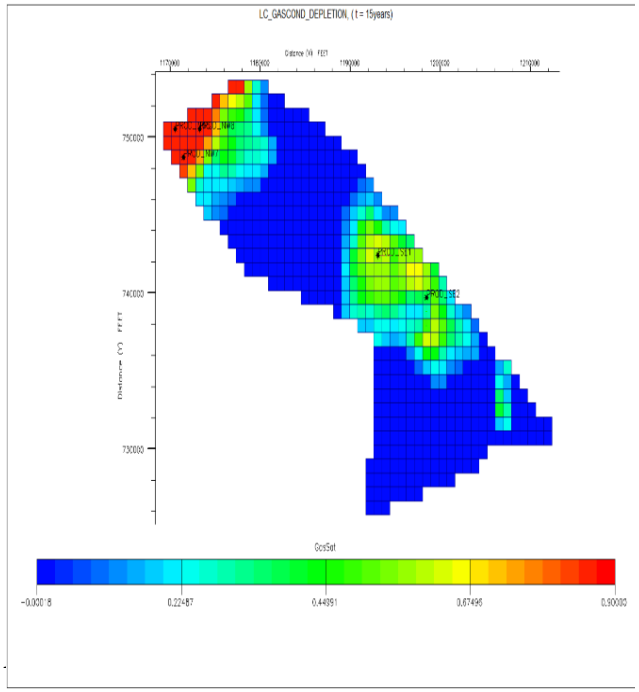

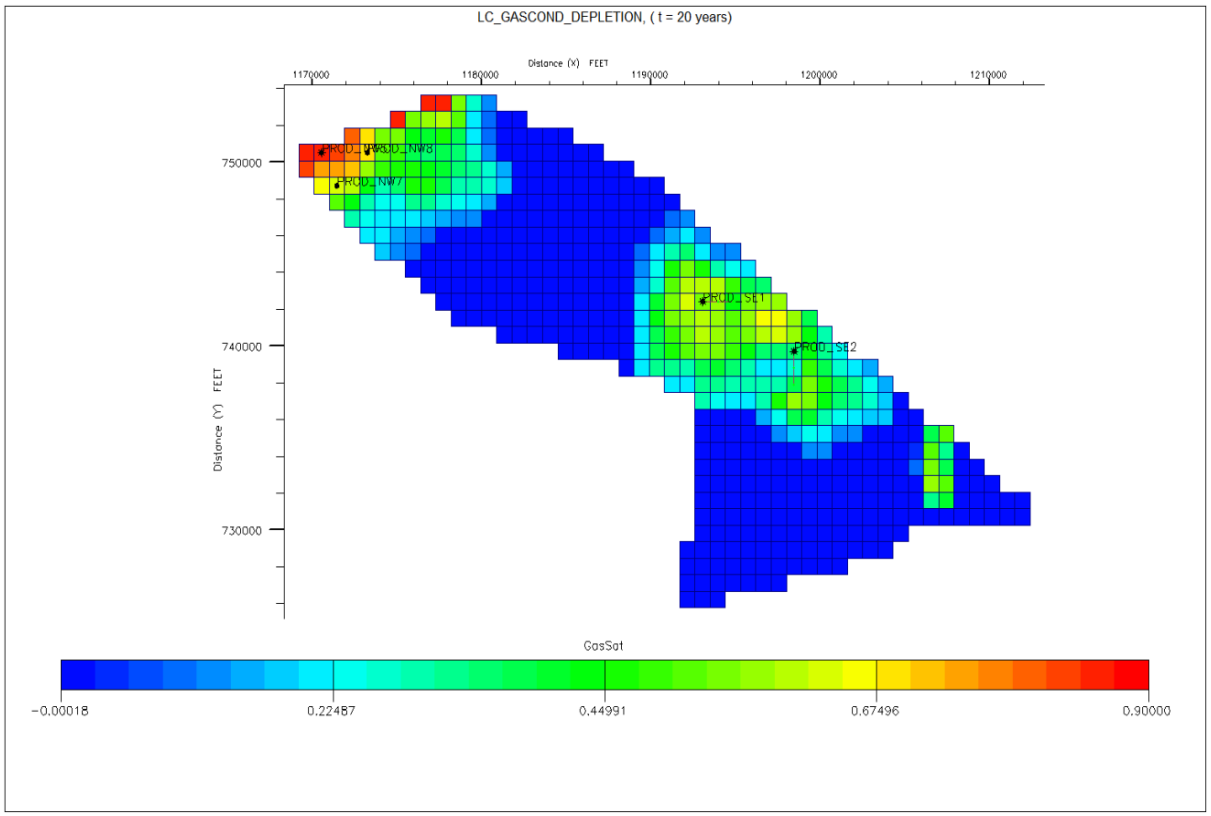

Figure B. 16:Gas saturation at t=20 years (DEP).

B.2.1.3. Oil Saturation

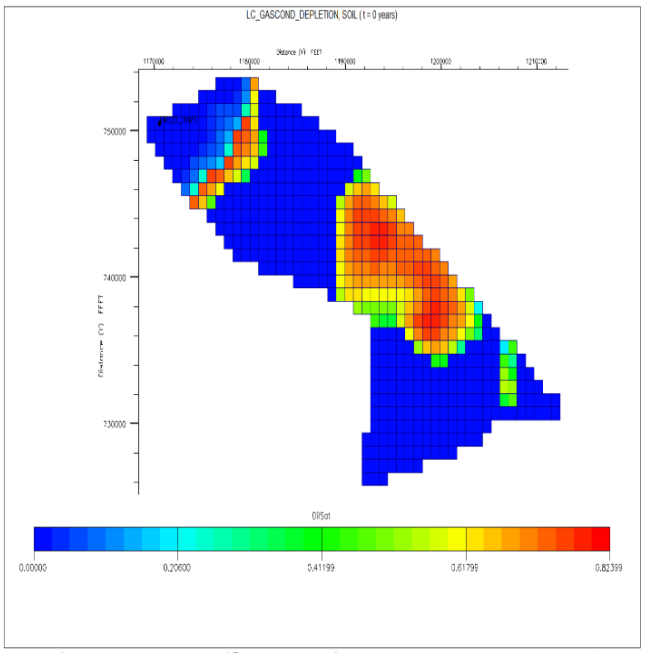

Figure B. 17:Oil saturation at t=0 years (DEP)

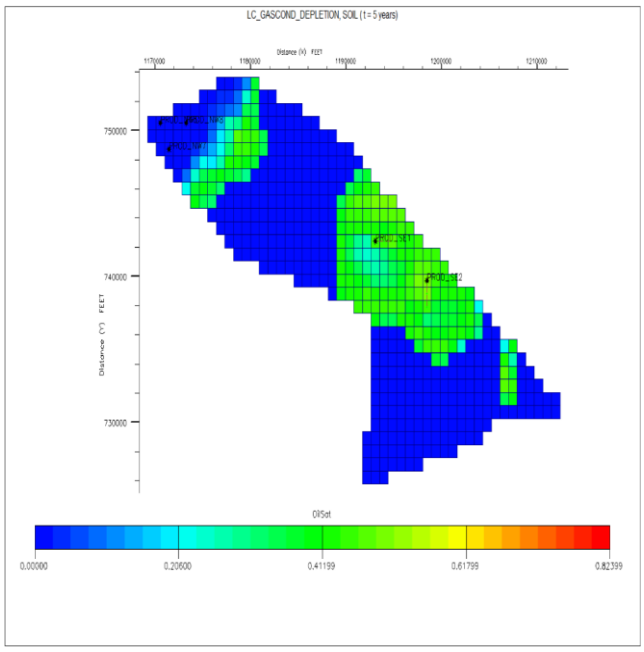

Figure B. 18:Oil saturation at t=5 years (DEP)

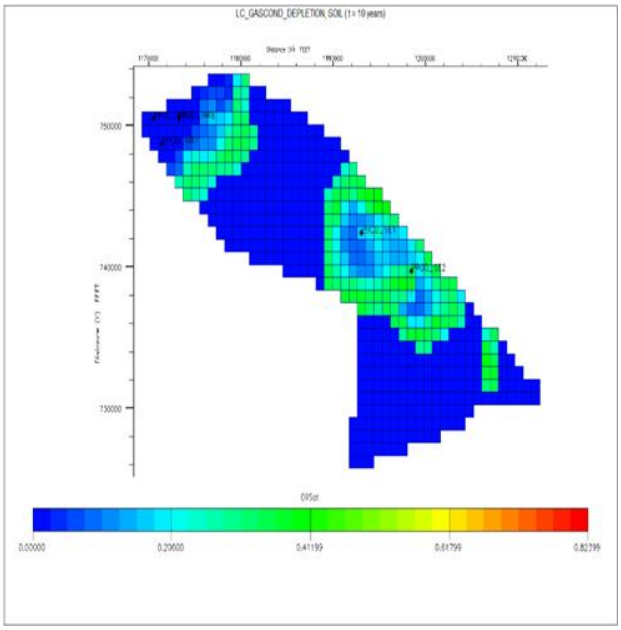

Figure B. 19: Oil saturation at t=10 years (DEP).

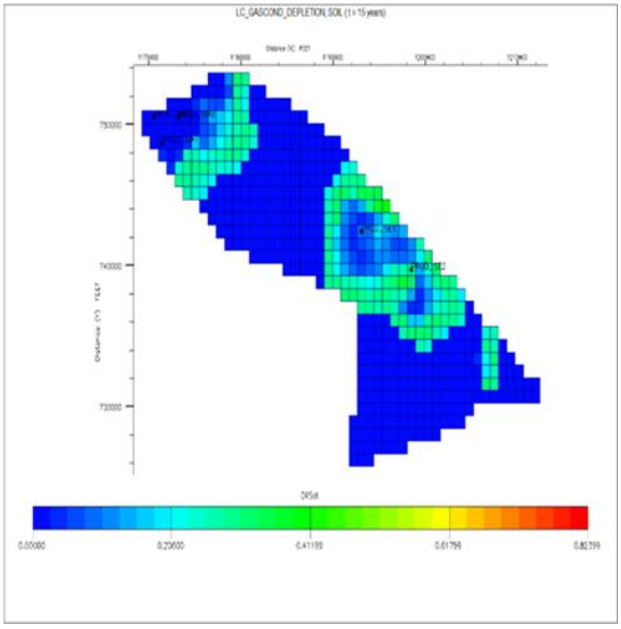

Figure B. 20: Oil saturation at t=15 years (DEP)

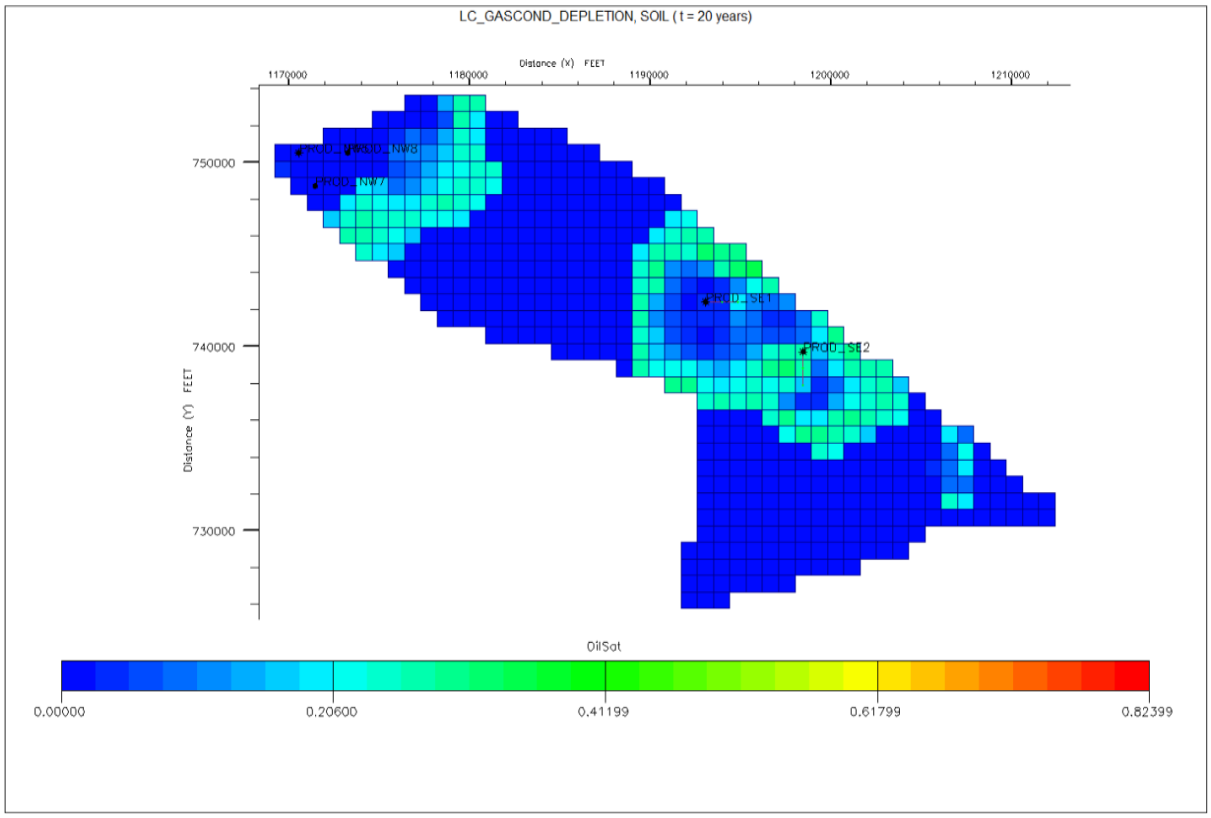

Figure B. 21: Oil saturation at t=20years (DEP).

B.2.2 Gas Injection

B.2.2.1 Pressure

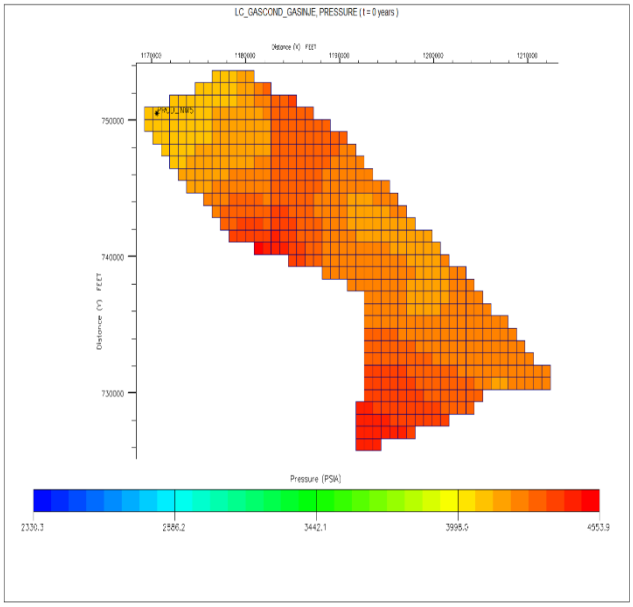

Figure B. 22:Field pressure at t=0 years (GI).

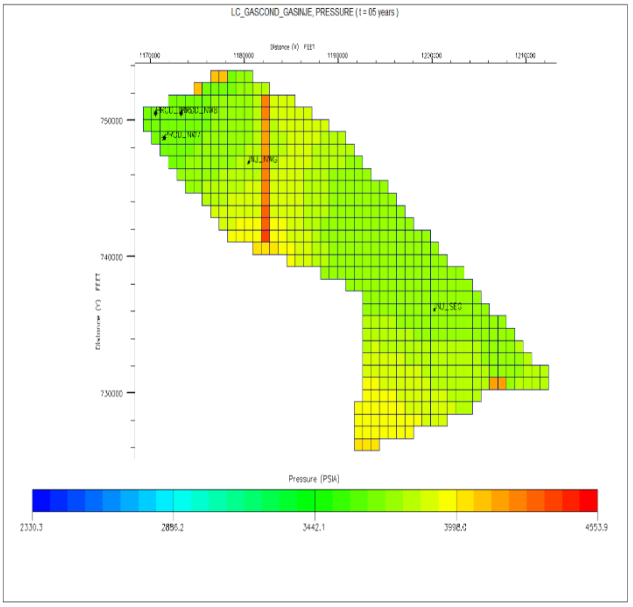

Figure B. 23:Field pressure at t=5 years (GI).

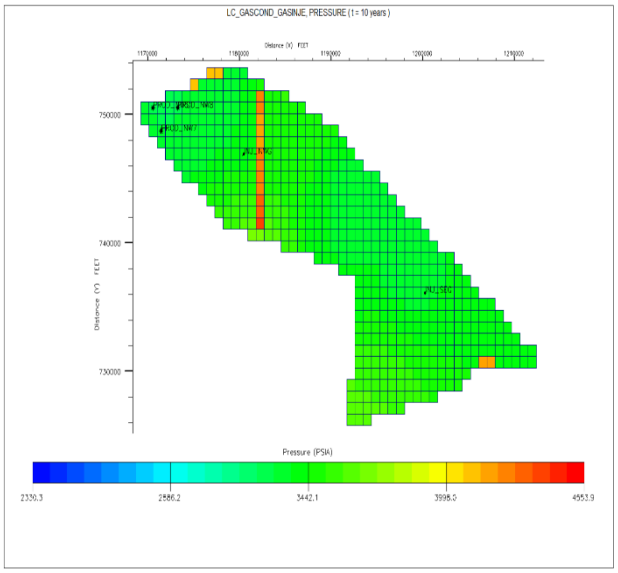

Figure B. 24:Field pressure at t=10 years (GI).

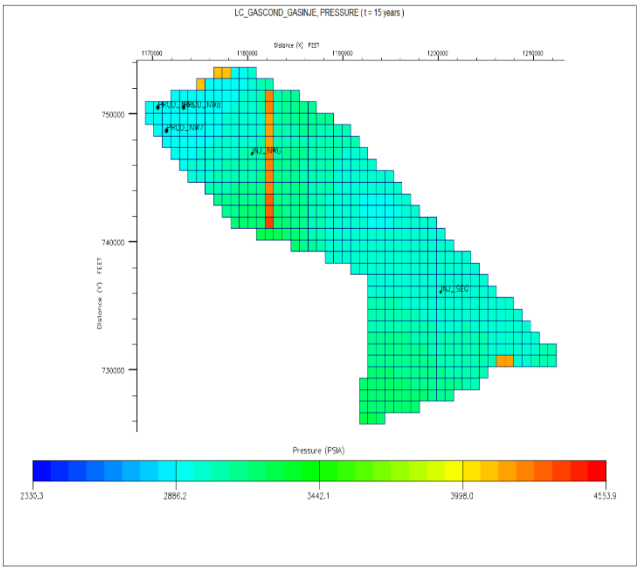

Figure B. 25:Field pressure at t=15 years (GI).

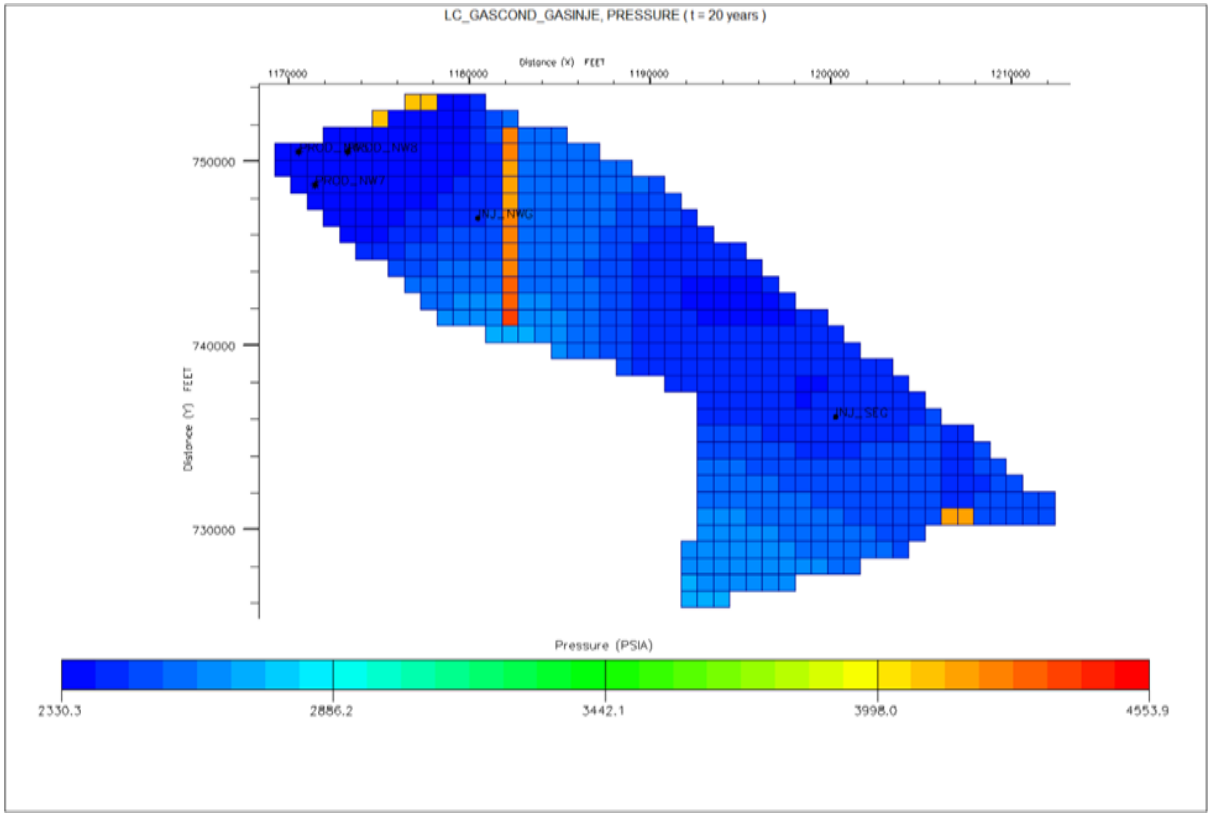

Figure B. 26:Field pressure at t=20 years (GI).

B.2.2.2. Gas Saturation

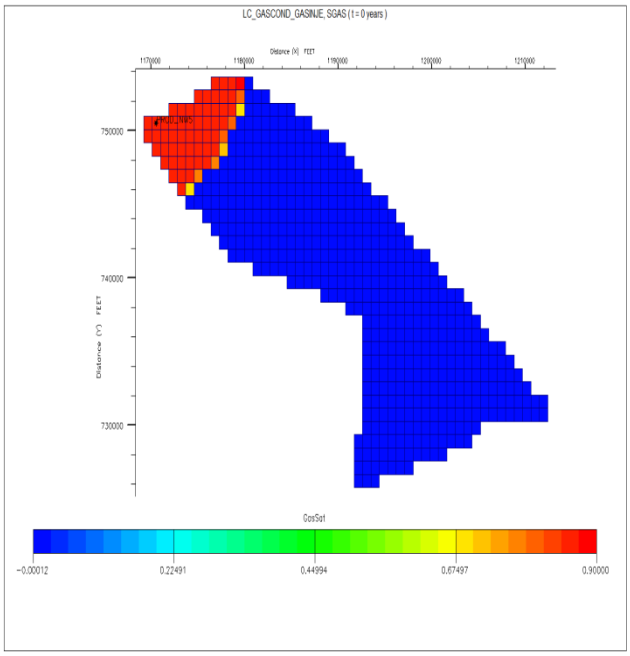

Figure B. 27:Gas saturation at t=0 years (GI).

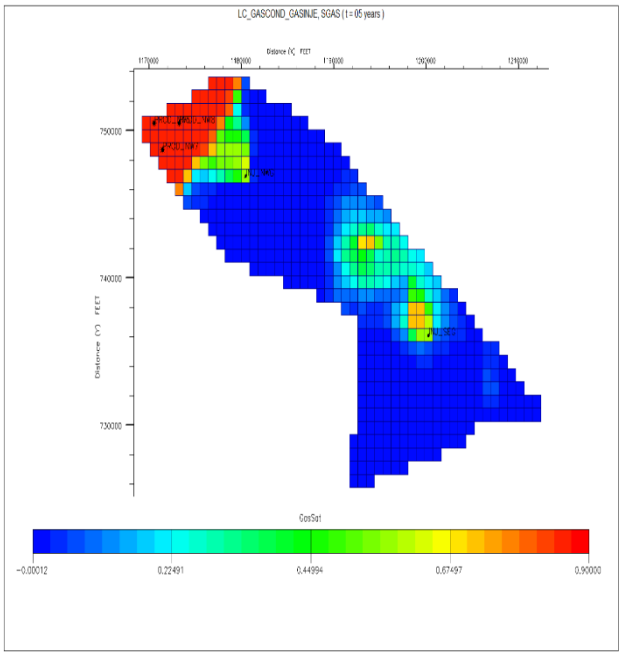

Figure B. 28:Gas saturation at t=5 years (GI).

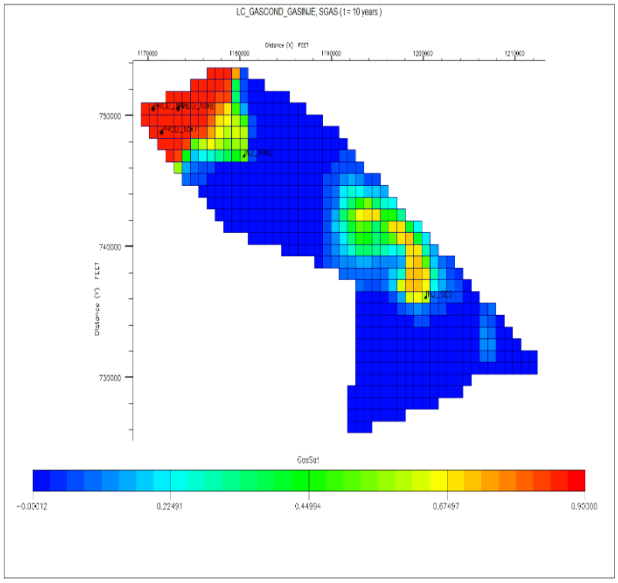

Figure B. 29:Gas saturation at t=10 years (GI).

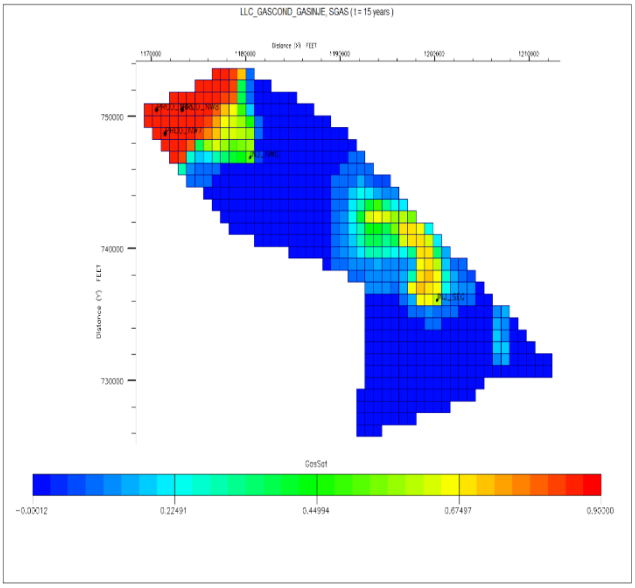

Figure B. 30:Gas saturation at t=15 years (GI).

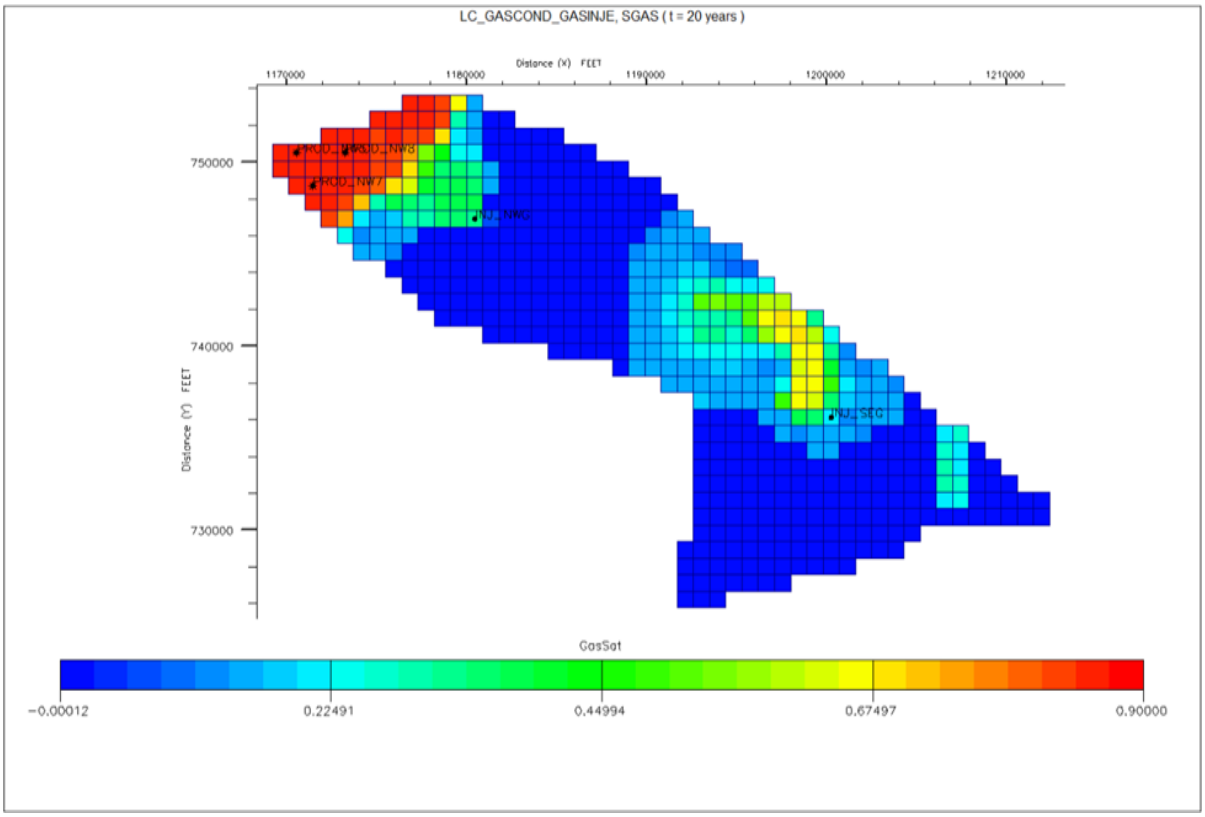

Figure B. 31:Gas saturation at t=20 years (GI).

B.2.2.3. Oil Saturation

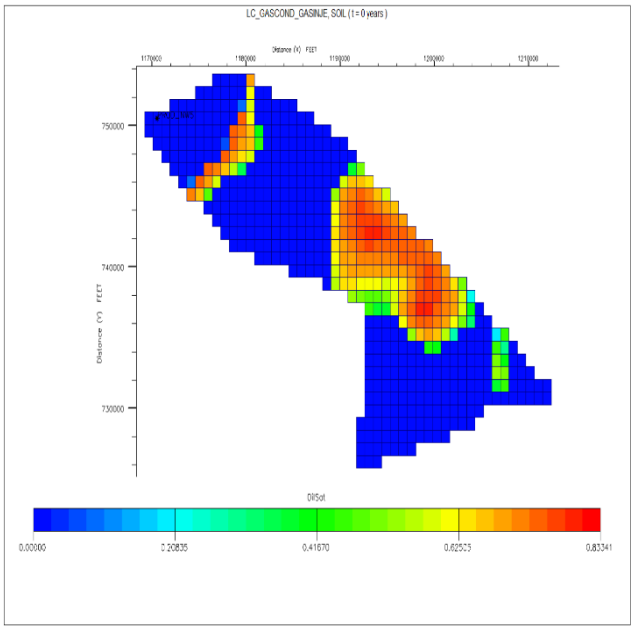

Figure B. 32:Oil saturation at t=0 years (GI)

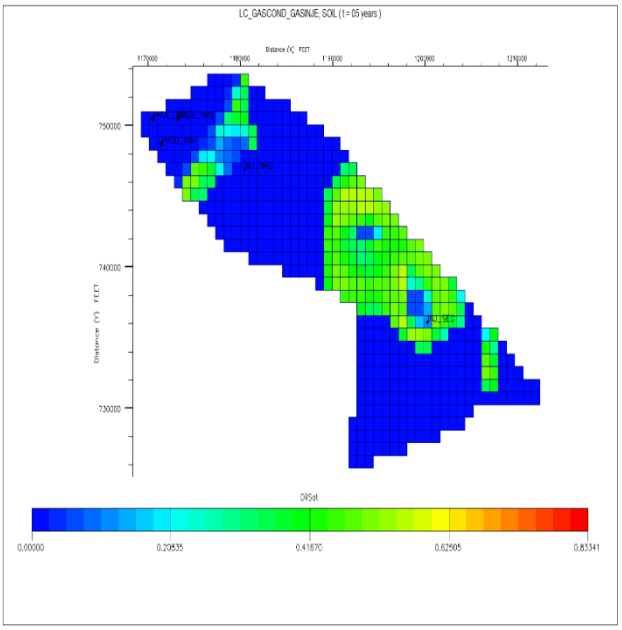

Figure B. 33:Oil saturation at t=05 years (GI)

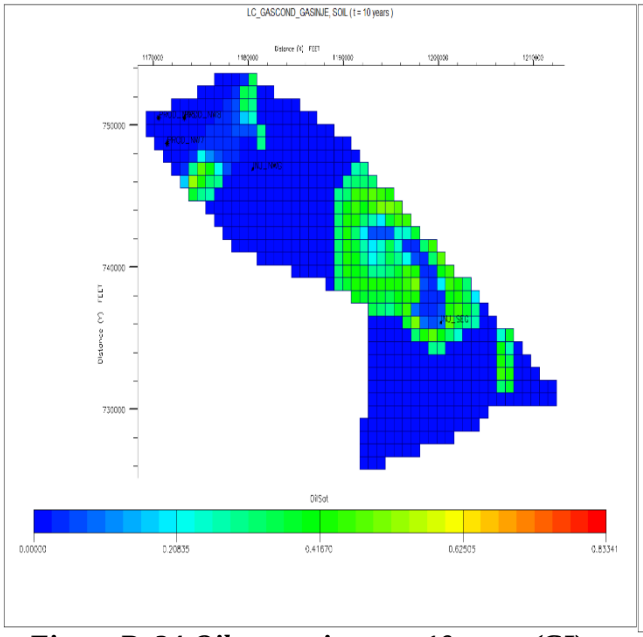

Figure B. 34:Oil saturation at t=10 years (GI)

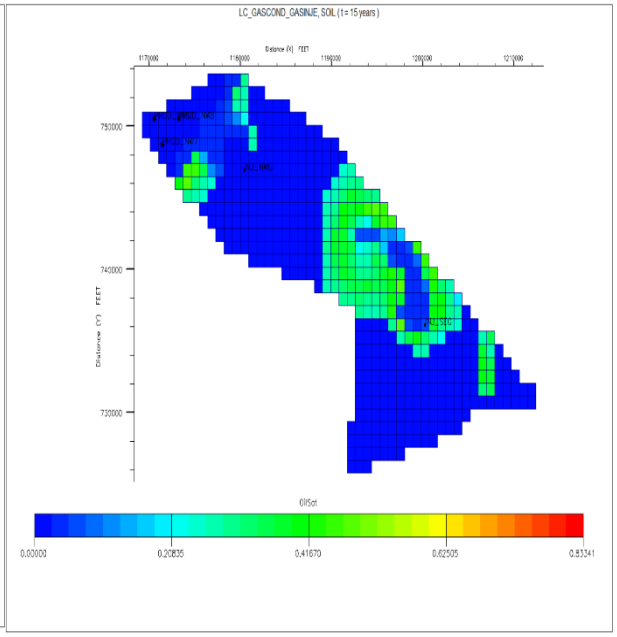

Figure B. 35:Oil saturation at t=15 years (GI)

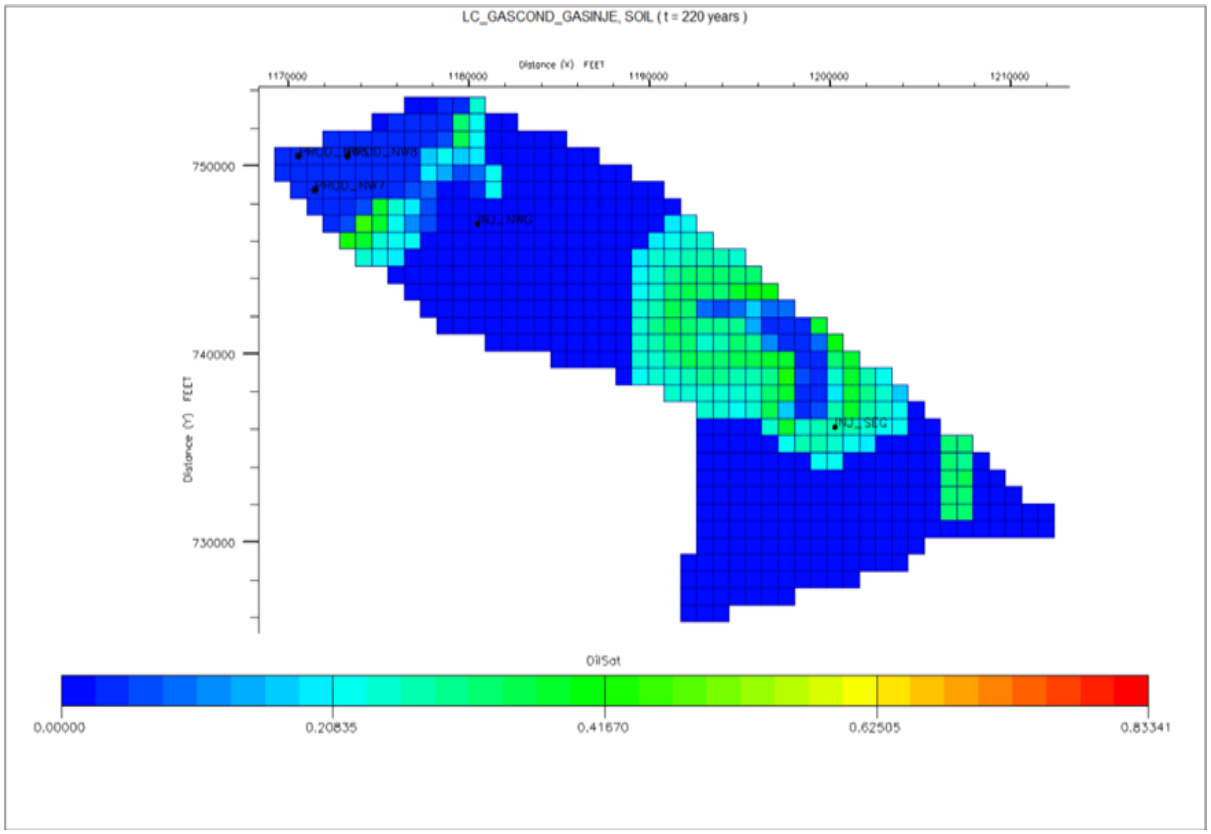

Figure B. 36::Oil saturation at t=20 years (GI).

B.2.3WAG Injection

B.2.3.1Pressure

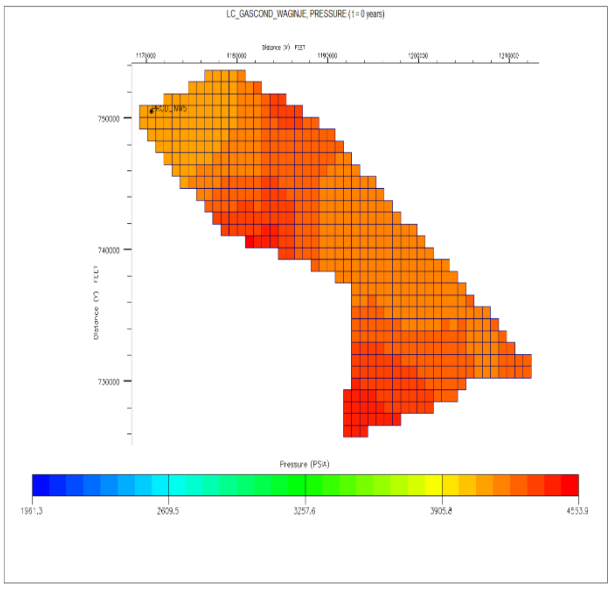

Figure B. 37:Field pressure at t=0 years (WAG)

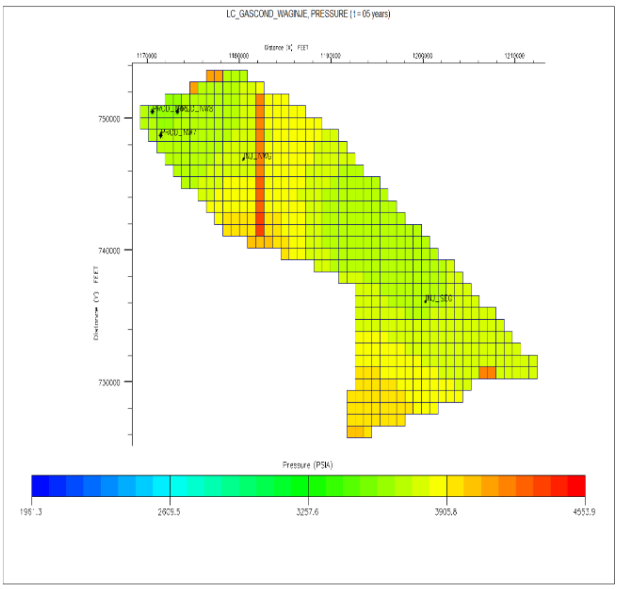

Figure B. 38:Field pressure at t=05 years (WAG)

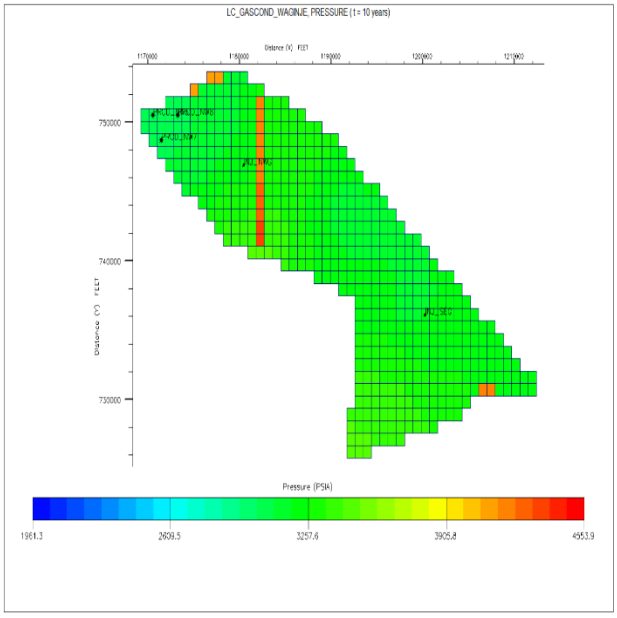

Figure B. 39:Field pressure at t=10 years (WAG)

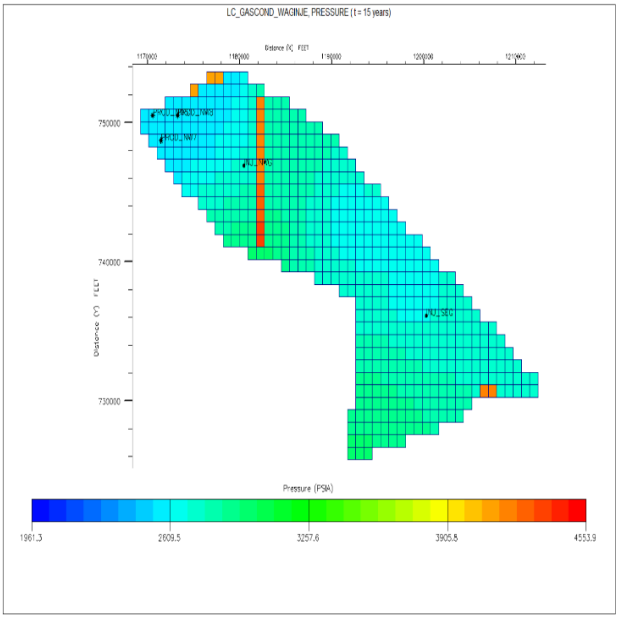

Figure B. 40:Field pressure at t=15 years (WAG)

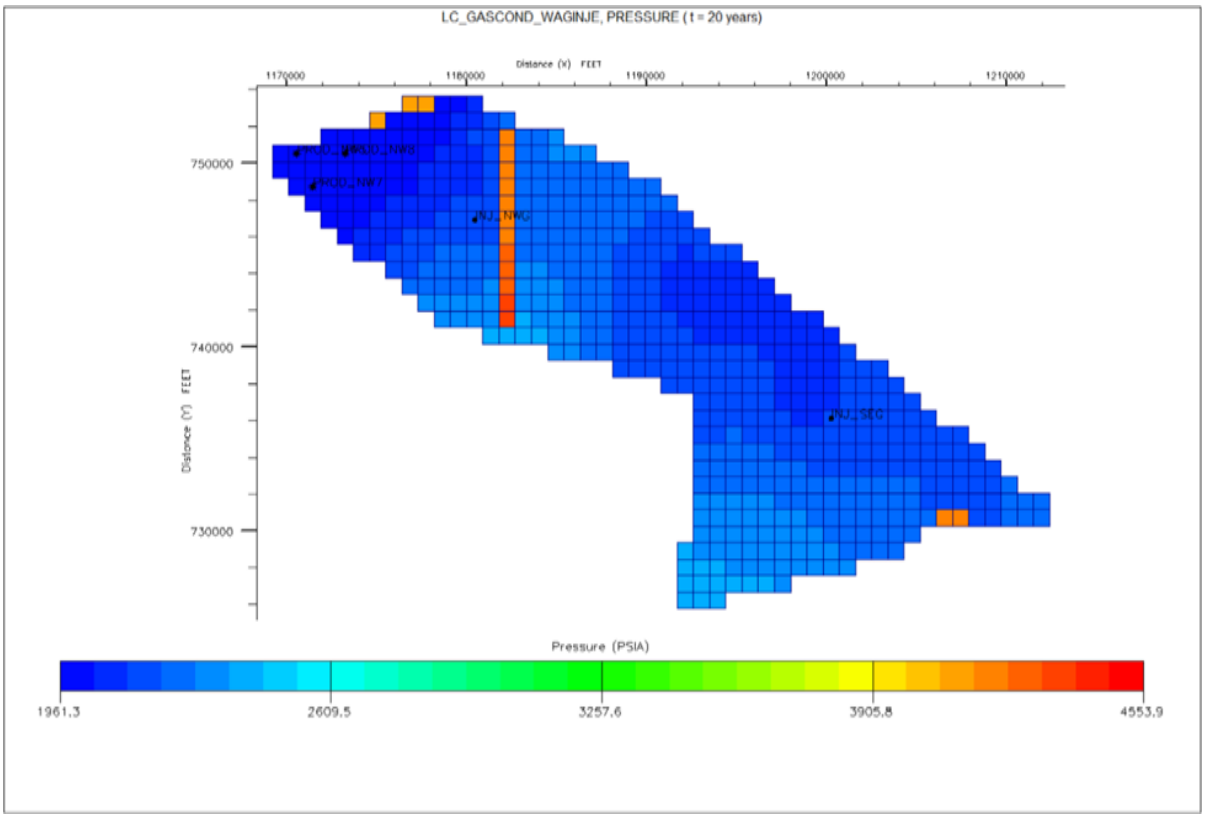

Figure B. 41:Field pressure at t=20 years (WAG)

B.2.3.2. Gas Saturation

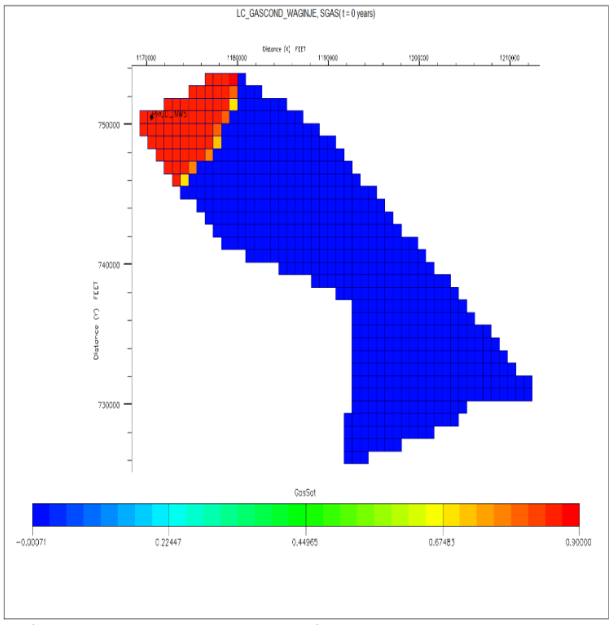

Figure B. 42:Gas saturation at t=0 years (WAG).

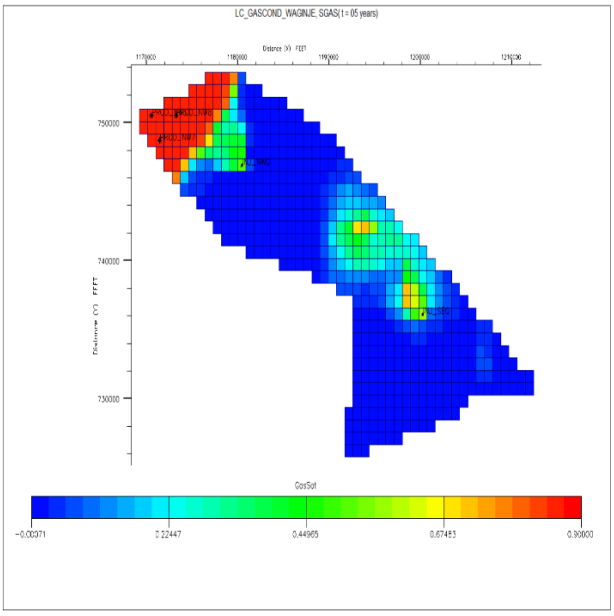

Figure B. 43:Gas saturation at t=05years (WAG).

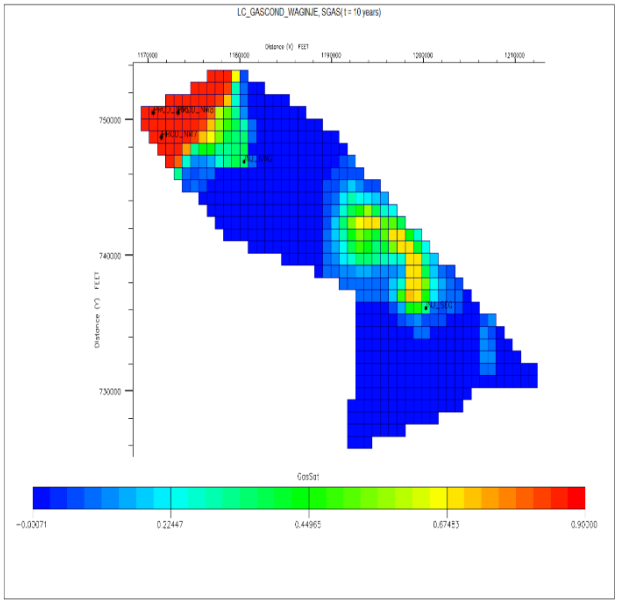

Figure B. 44:Gas saturation at t=10 years (WAG)

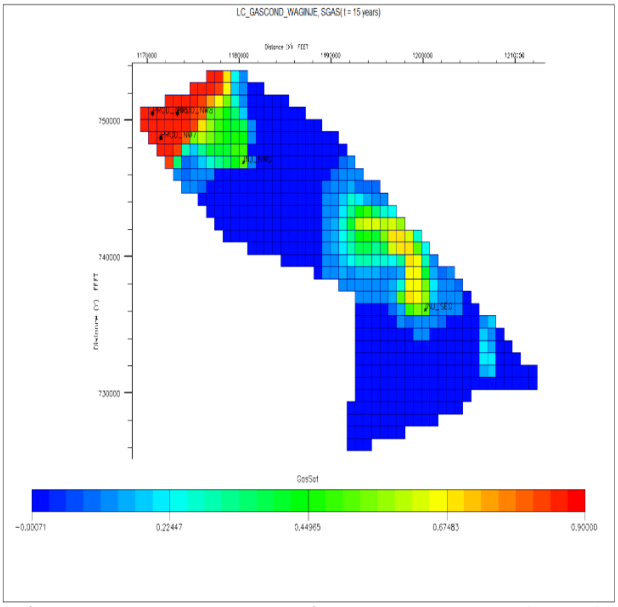

Figure B. 45:Gas saturation at t=15 years (WAG)

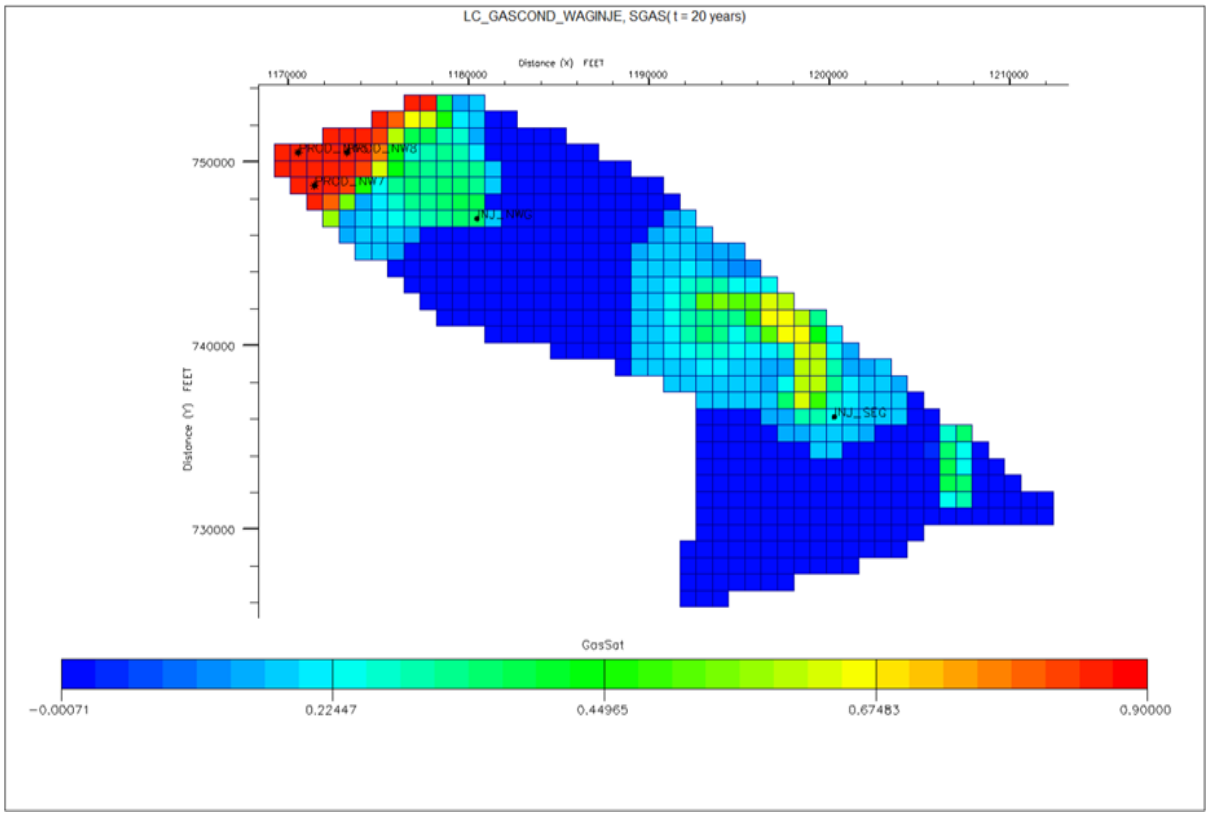

Figure B. 46:Gas saturation at t=20 years (WAG).

5.2.1.1 B.2.3.3. Oil Saturation

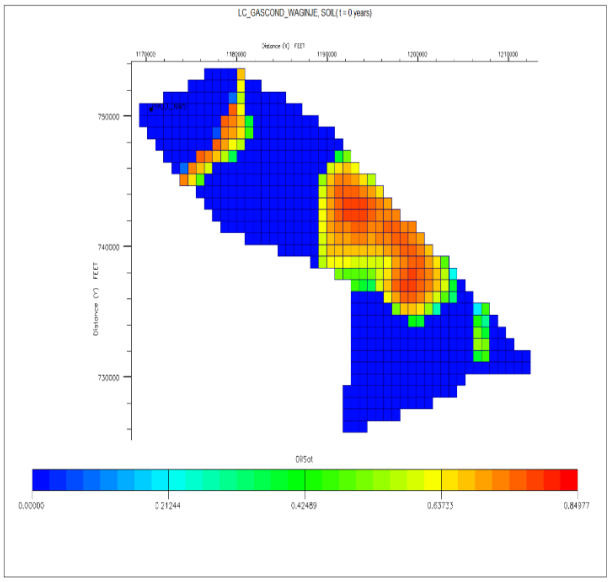

Figure B. 47:Oil saturation at t=0 years (WAG)

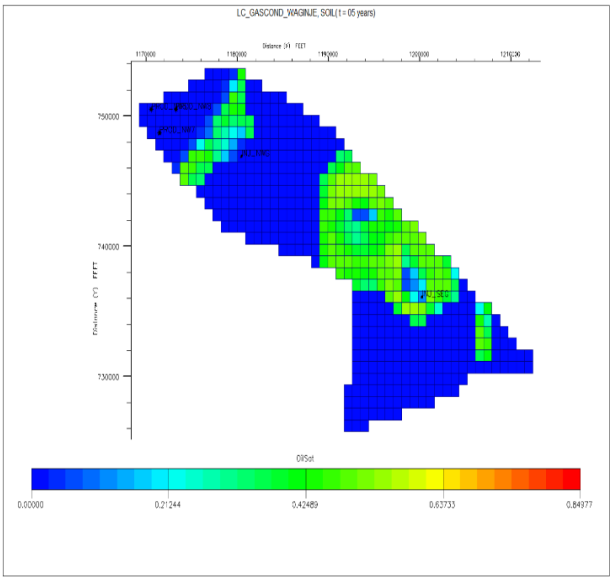

Figure B. 48:Oil saturation at t=5 years (WAG).

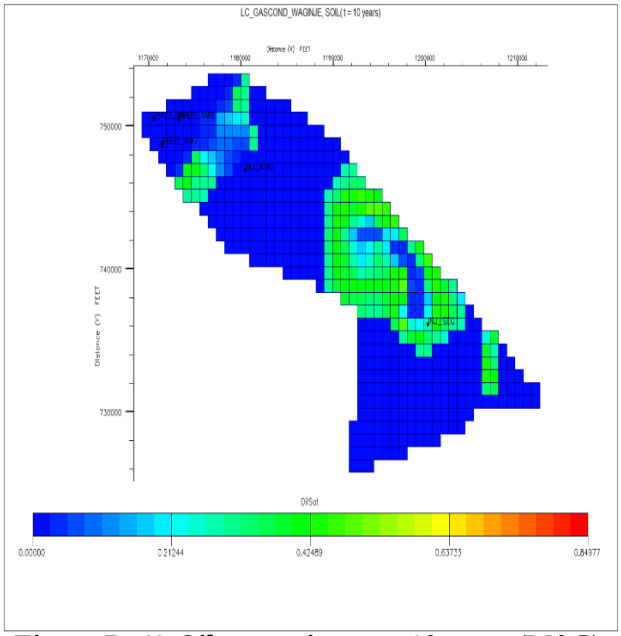

Figure B. 49:Oil saturation at t=10 years (WAG)

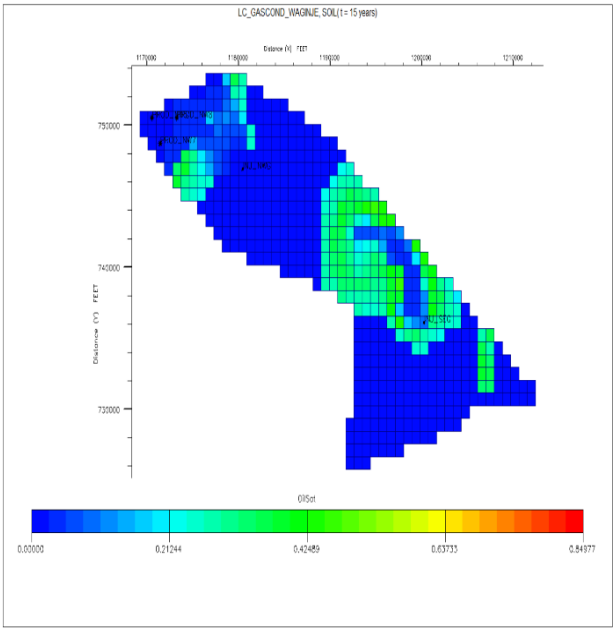

Figure B. 50:Oil saturation at t=15 years (WAG)

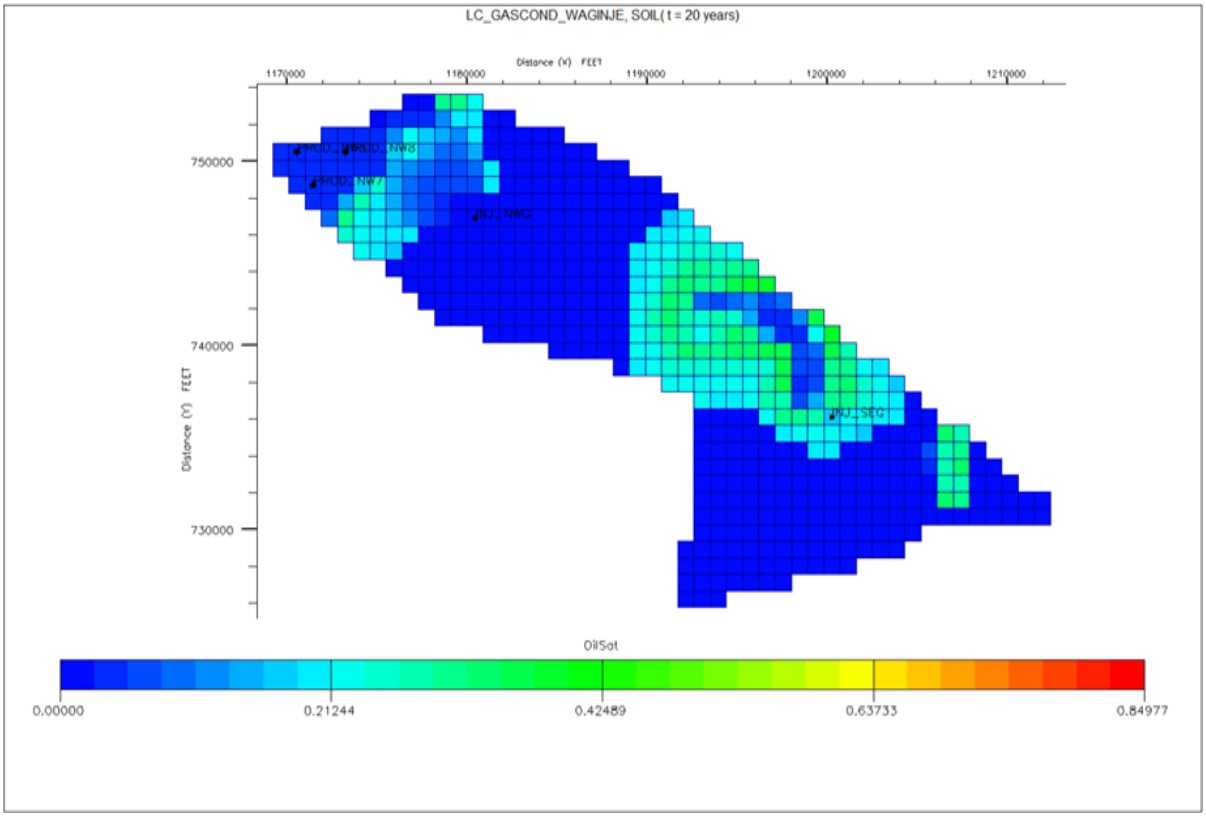

Figure B. 51:Oil saturation at t=20 years (WAG)

B.2.4. SWAG Injection

B.2.4.1. Pressure

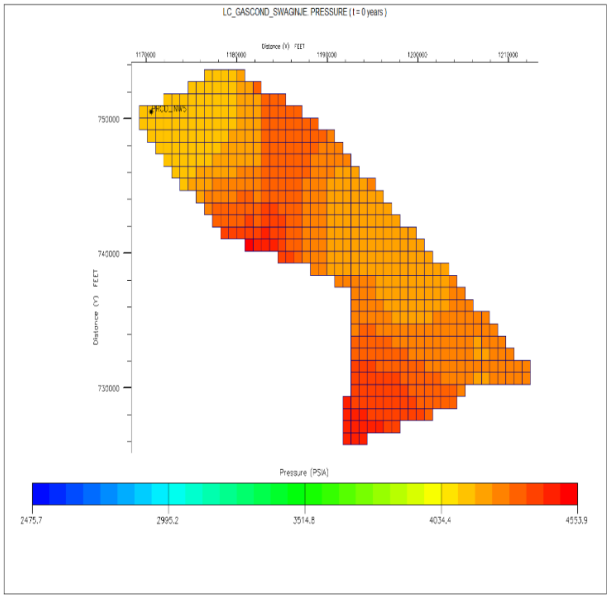

Figure B. 52:Field pressure at t=0 years (SWAG).

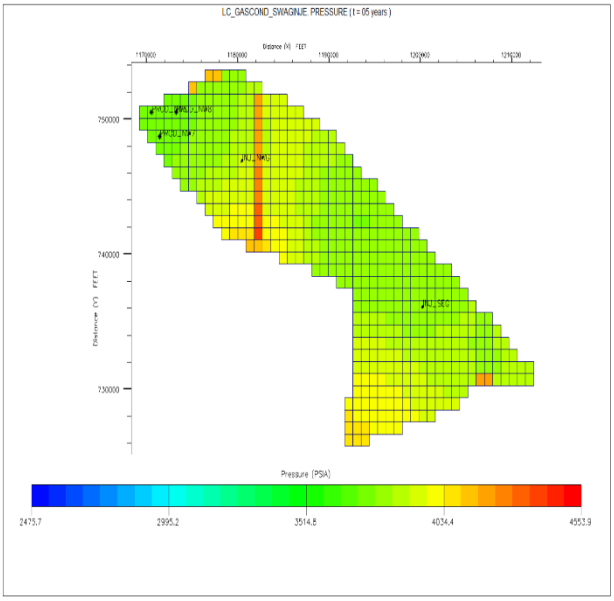

Figure B. 53:Field pressure at t=5 years (SWAG).

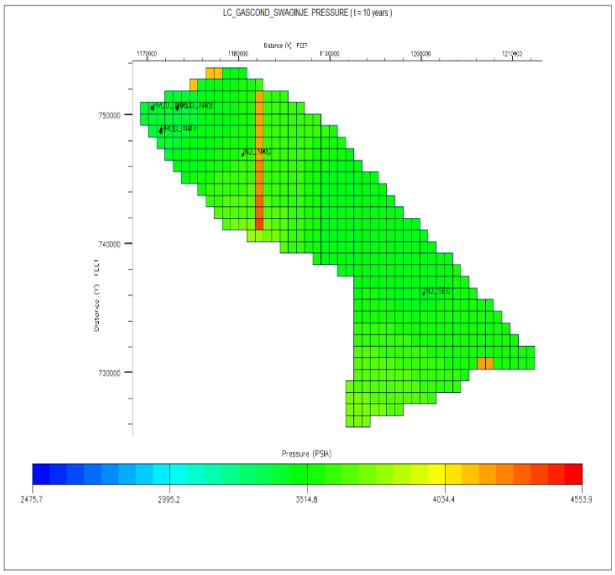

Figure B. 54:Field pressure at t=10 years (SWAG).

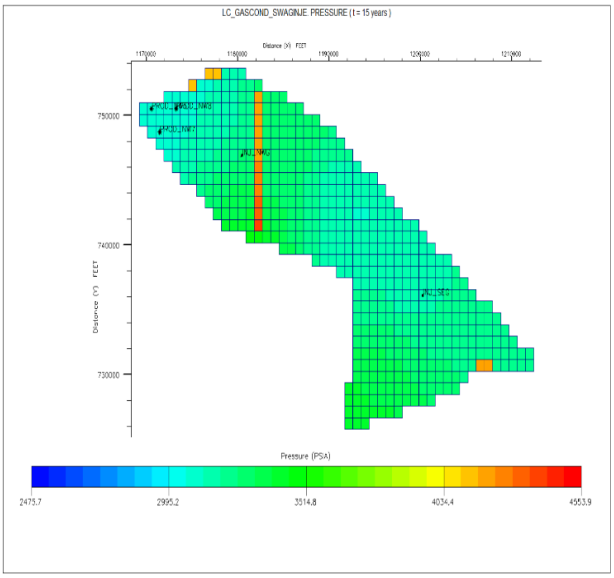

Figure B. 55:Field pressure at t=15 years (SWAG).

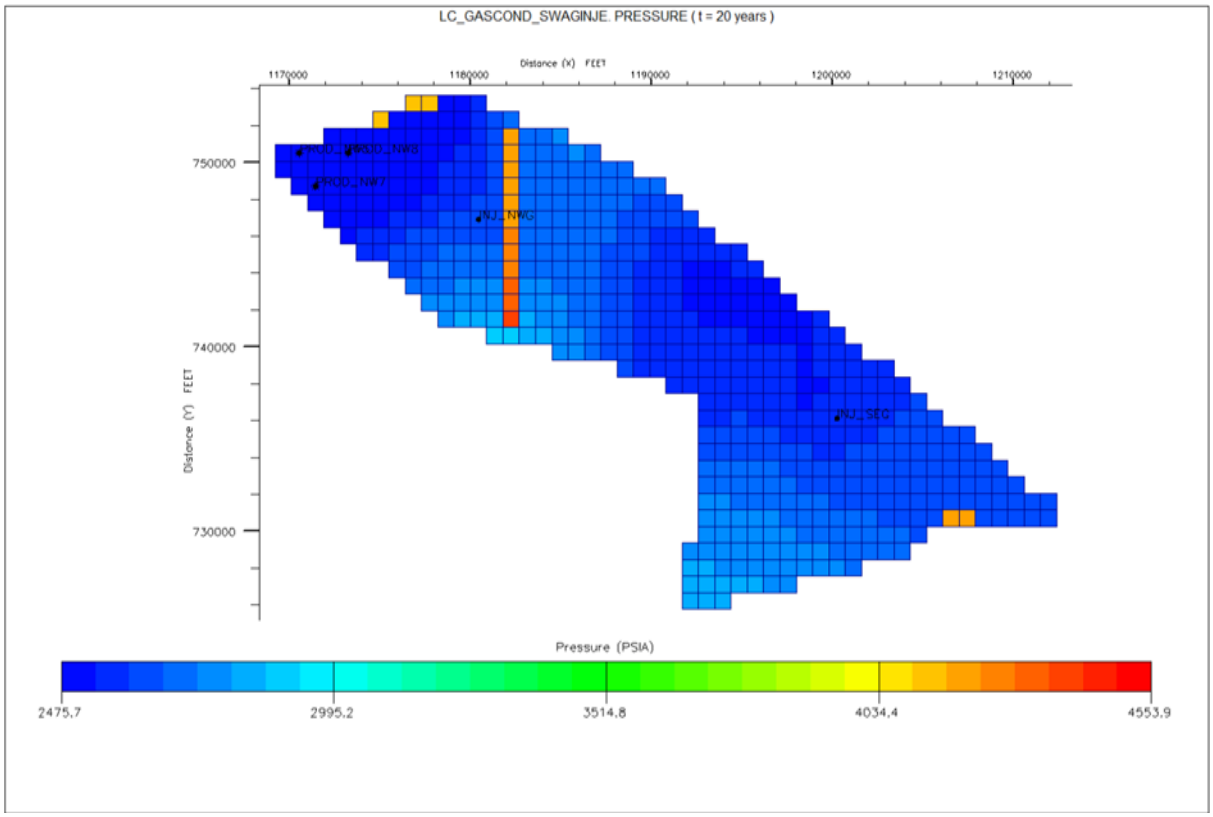

Figure B. 56:Field pressure at t=20 years (SWAG).

B.2.4.2. Gas Saturation

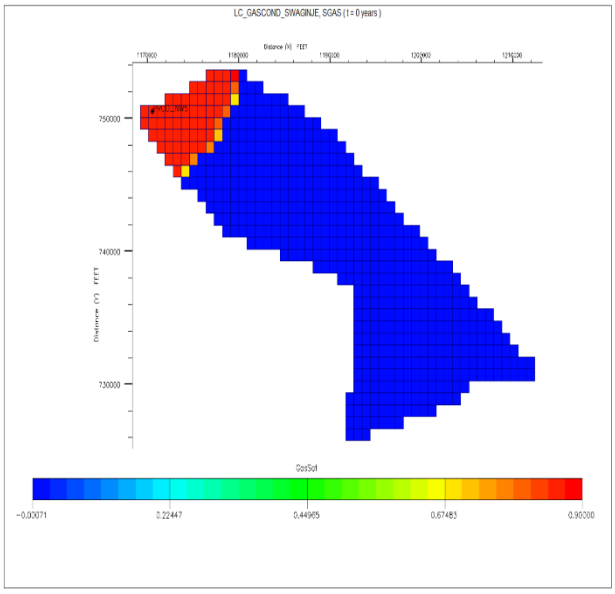

Figure B. 57:Gas saturation at t=0 years (SWAG)

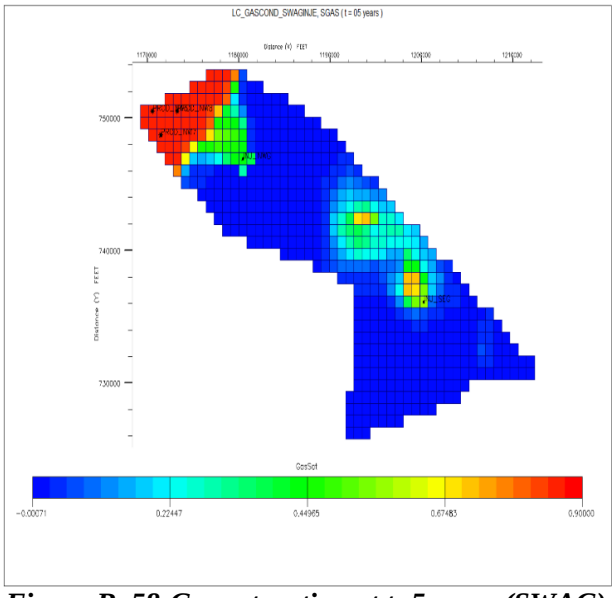

Figure B. 58:Gas saturation at t=5 years (SWAG)

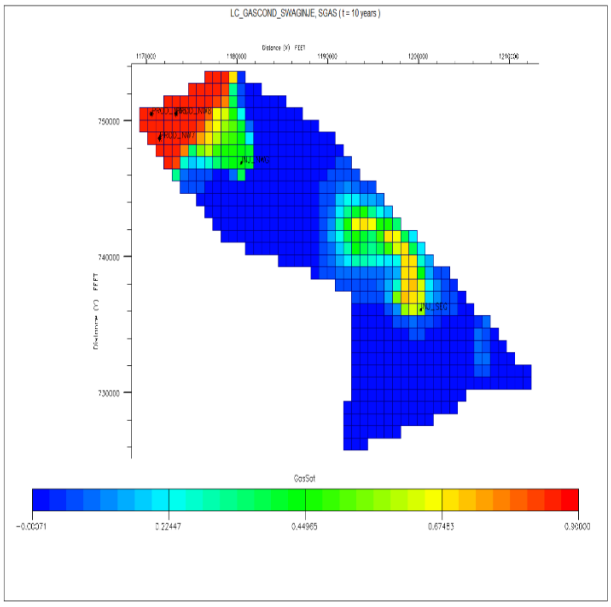

Figure B. 59:Gas saturation at t=10 years (SWAG)

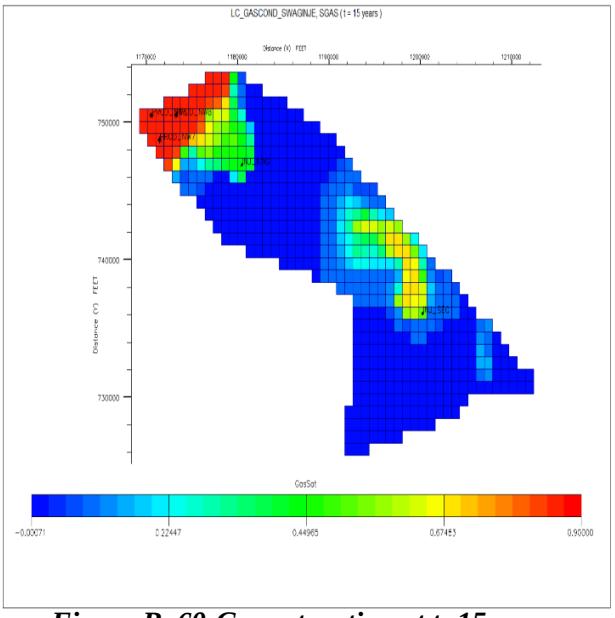

Figure B. 60:Gas saturation at t=15 years (SWAG)

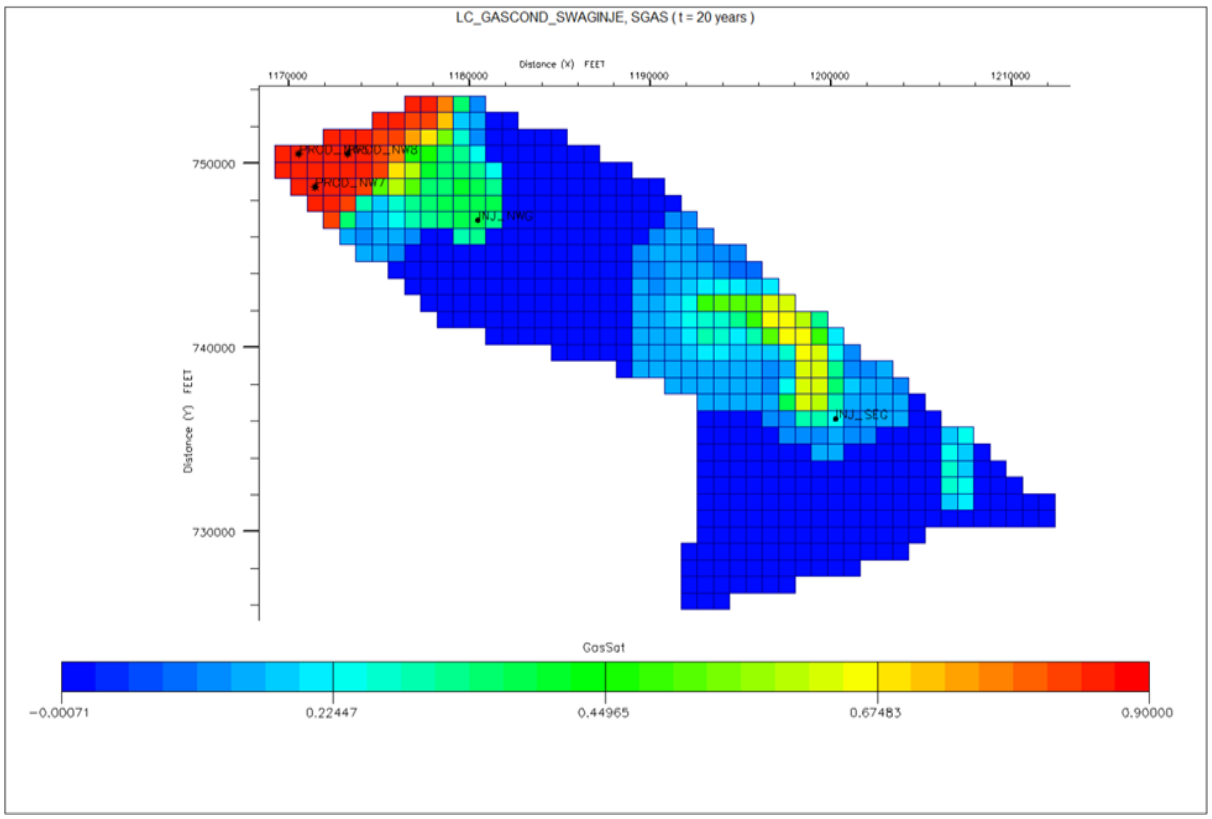

Figure B. 61:Gas saturation at t=20 years (SWAG)

5.2.1.2 B.2.4.3. Oil Saturation

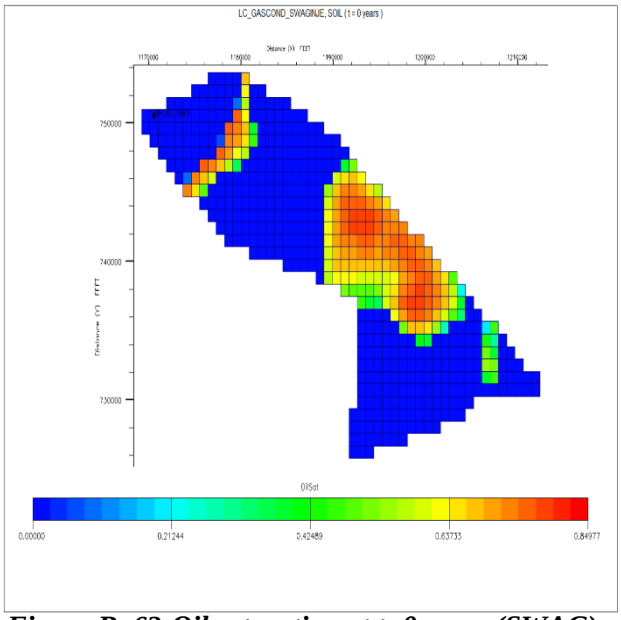

Figure B. 62:Oil saturation at t=0 years (SWAG).

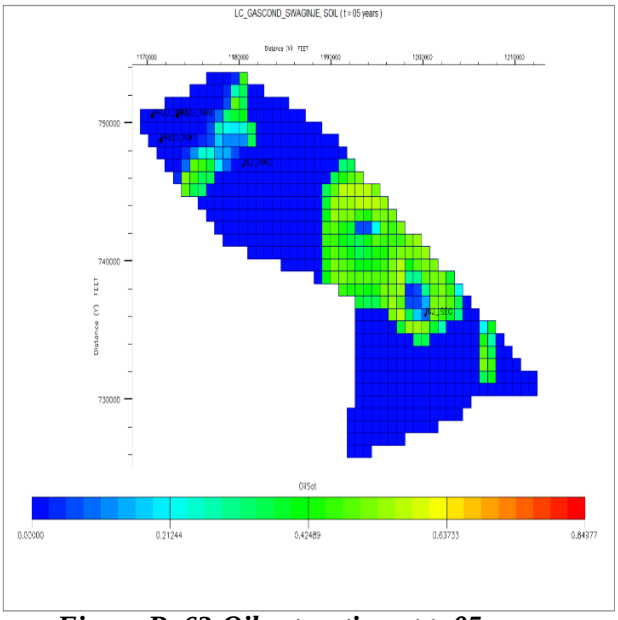

Figure B. 63:Oil saturation at t=05 years (SWAG).

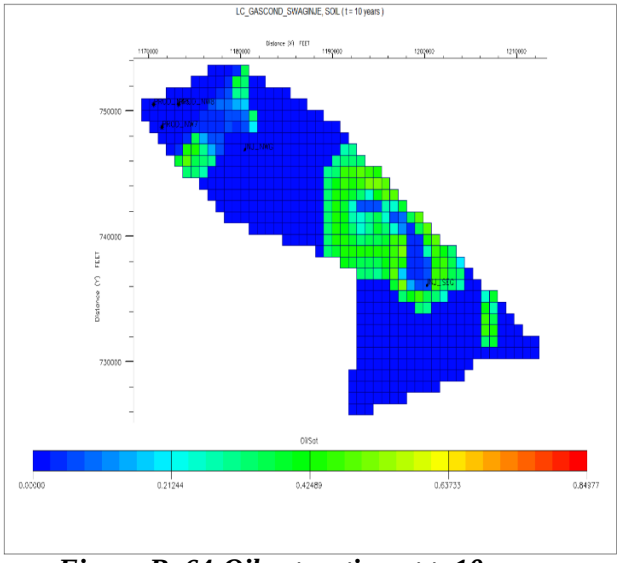

Figure B. 64:Oil saturation at t=10 years (SWAG).

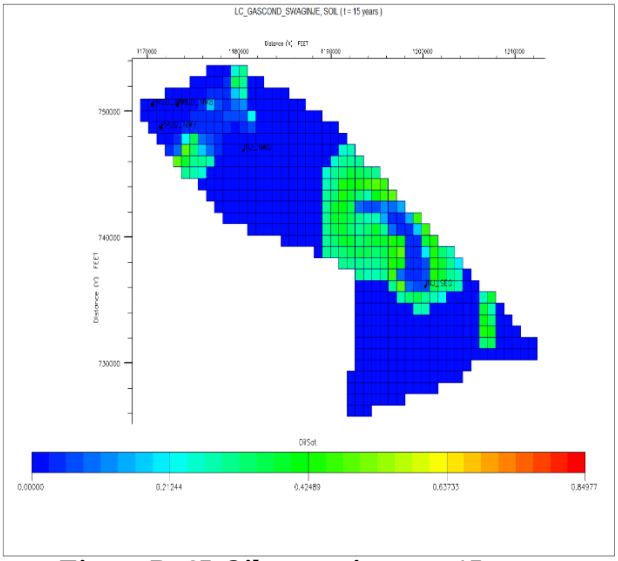

Figure B. 65:Oil saturation at t=15 years (SWAG).

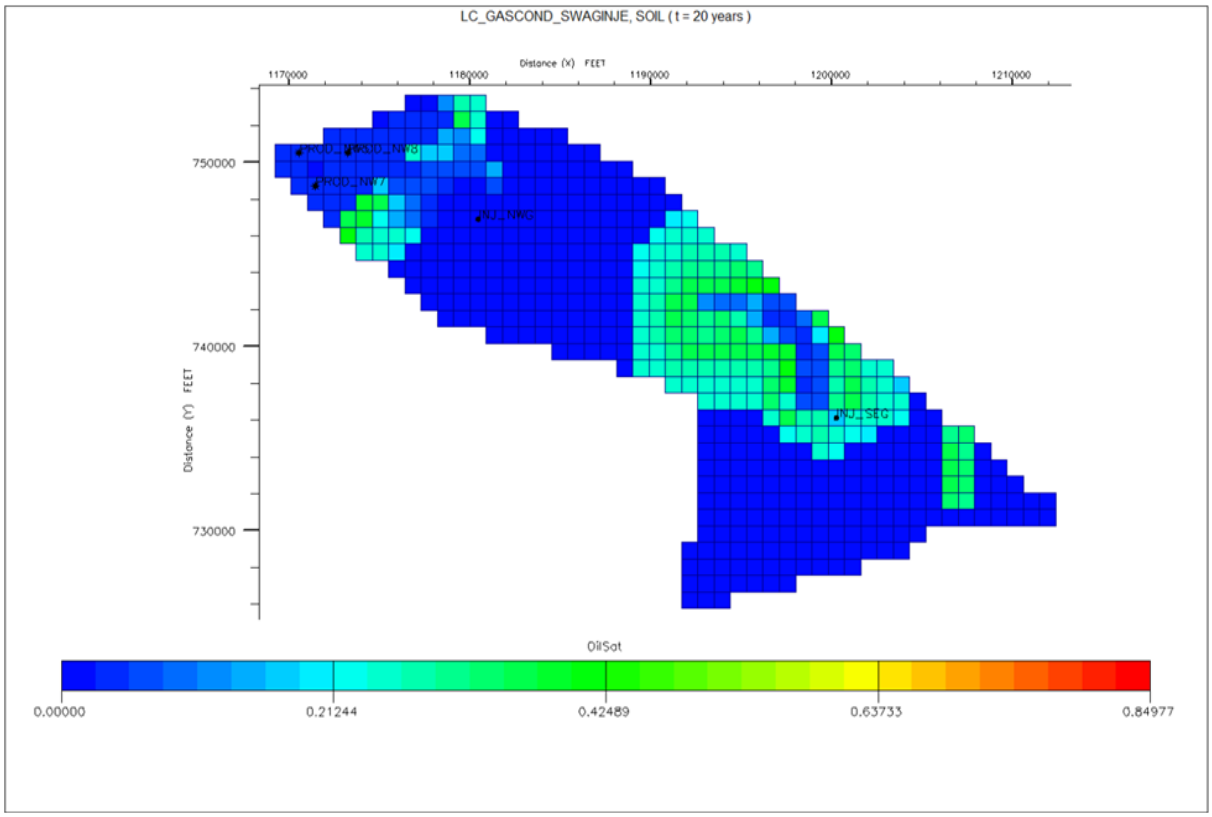

Figure B. 66:Oil saturation at t=20 years (SWAG).

APPENDIX C

In this section, results for the sensitivity analyses carried out in this thesis for the limited compositional model are presented. It includes gas injection sensitivity, water injection sensitivity, and kv/kh ratio sensitivity for the recovery schemes that are not discussed in the main body.

Multi-rate Gas Injection (Limited Compositional Modelling)

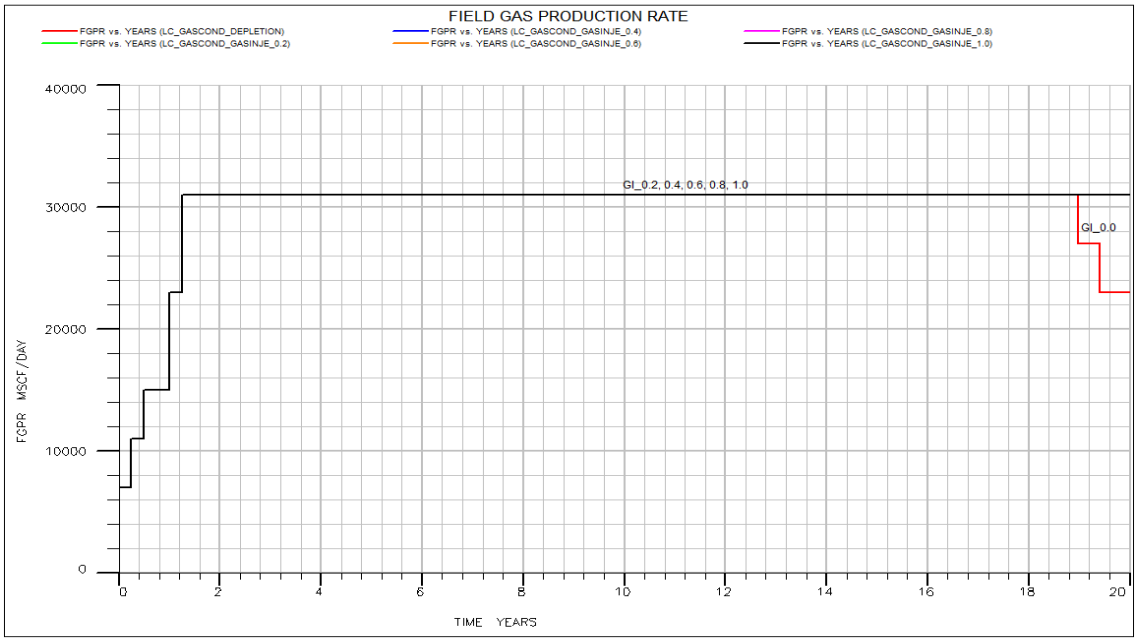

Figure C. 1:Field gas production rate (limited compositional model).

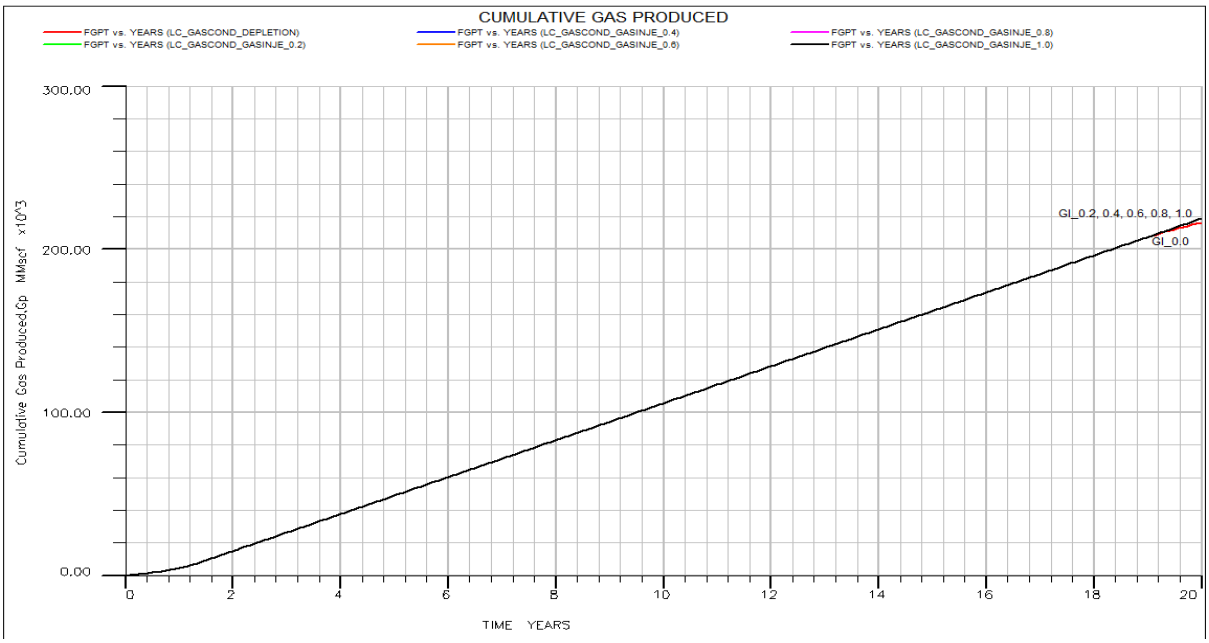

Figure C. 2:Cumulative gas production (limited compositional model).

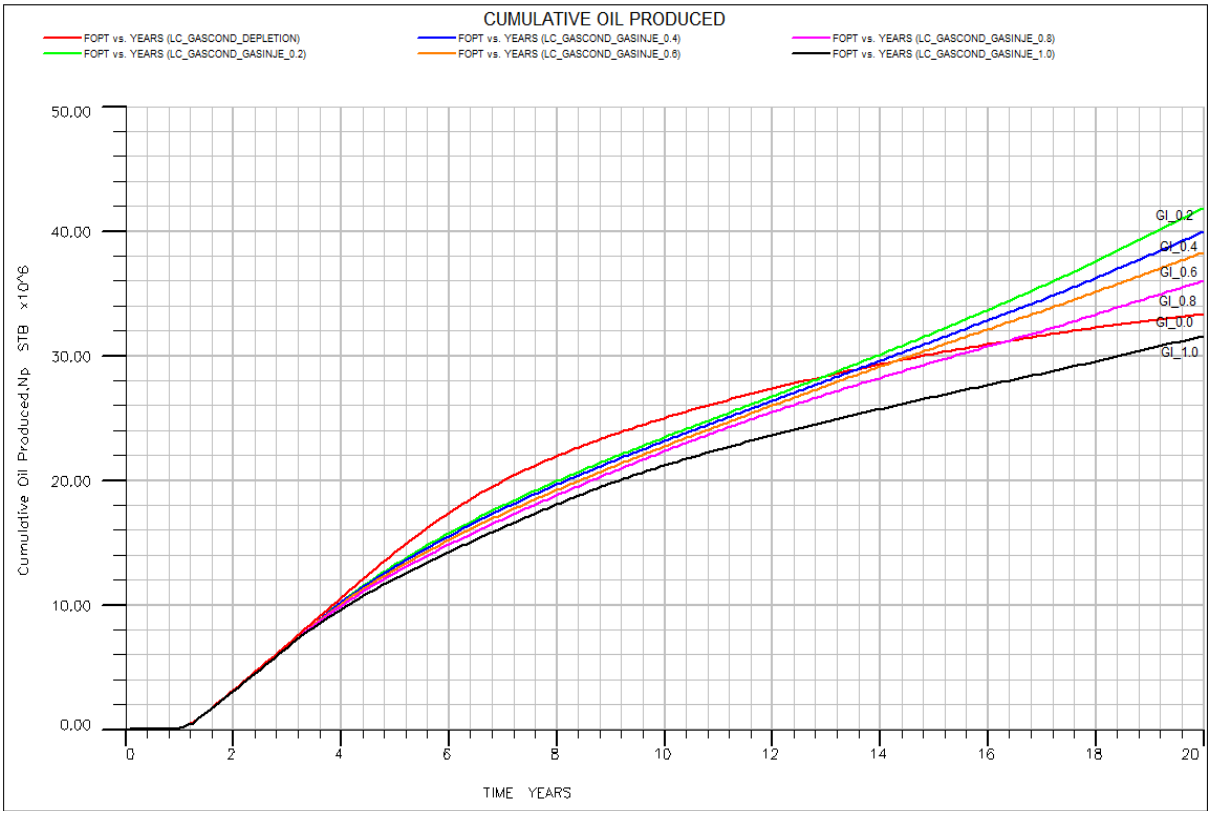

Figure C. 3:Cumulative Oil production (limited compositional model)

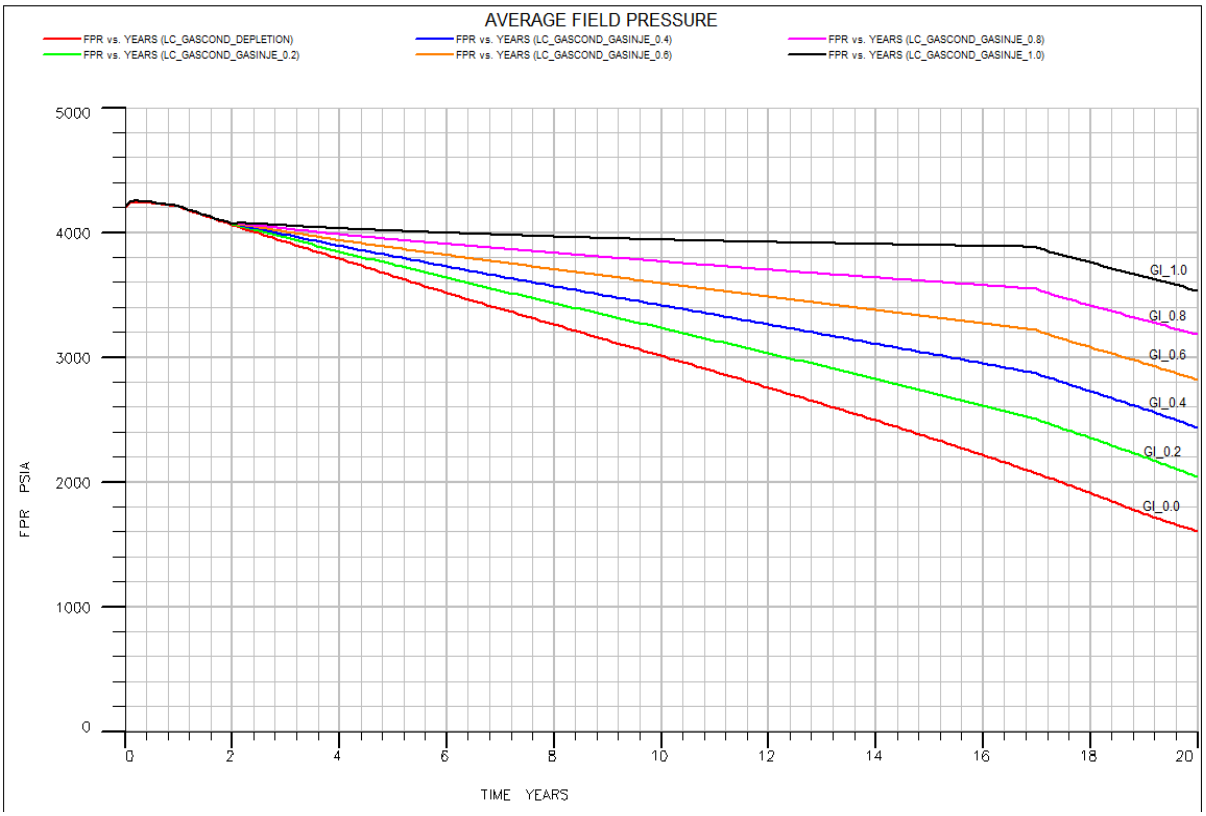

Figure C. 4: Average reservoir pressure (limited compositional model)

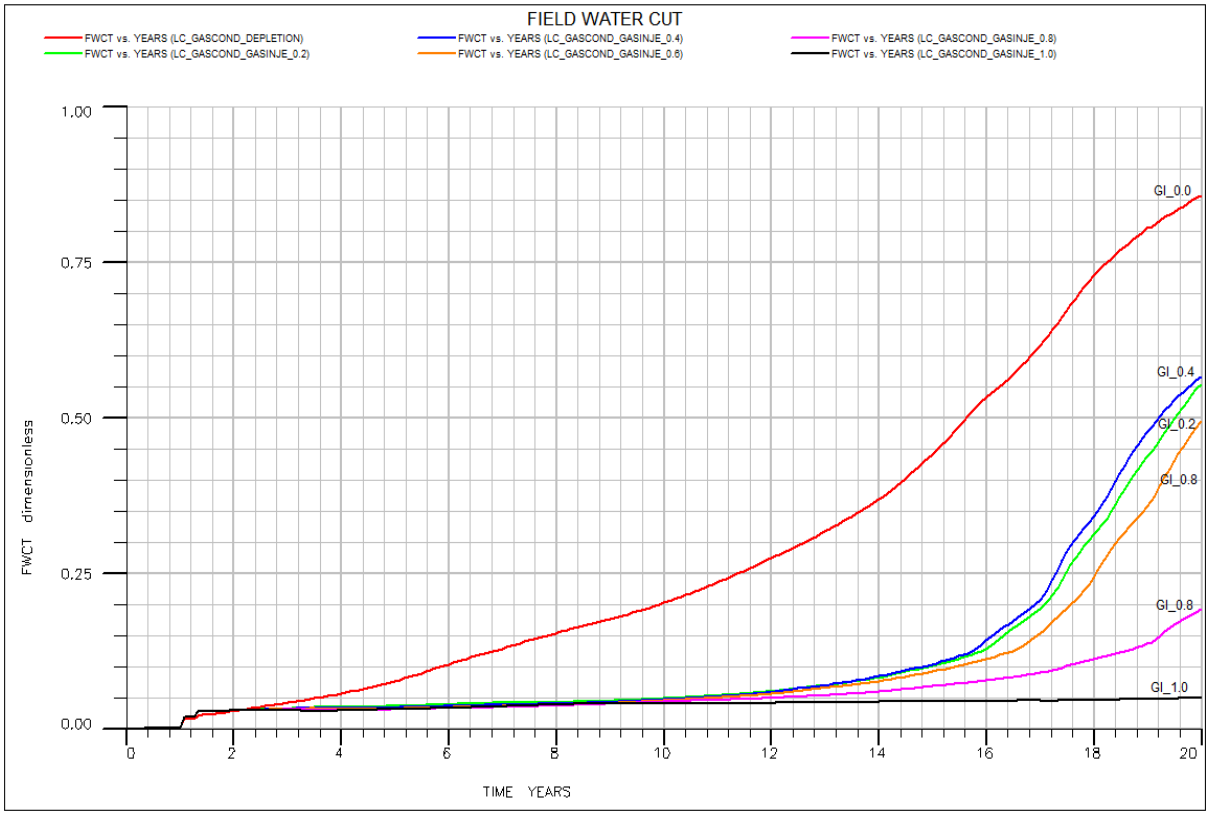

Figure C. 5:Field water cut (limited compositional model)

WAG Cycle Sensitivity

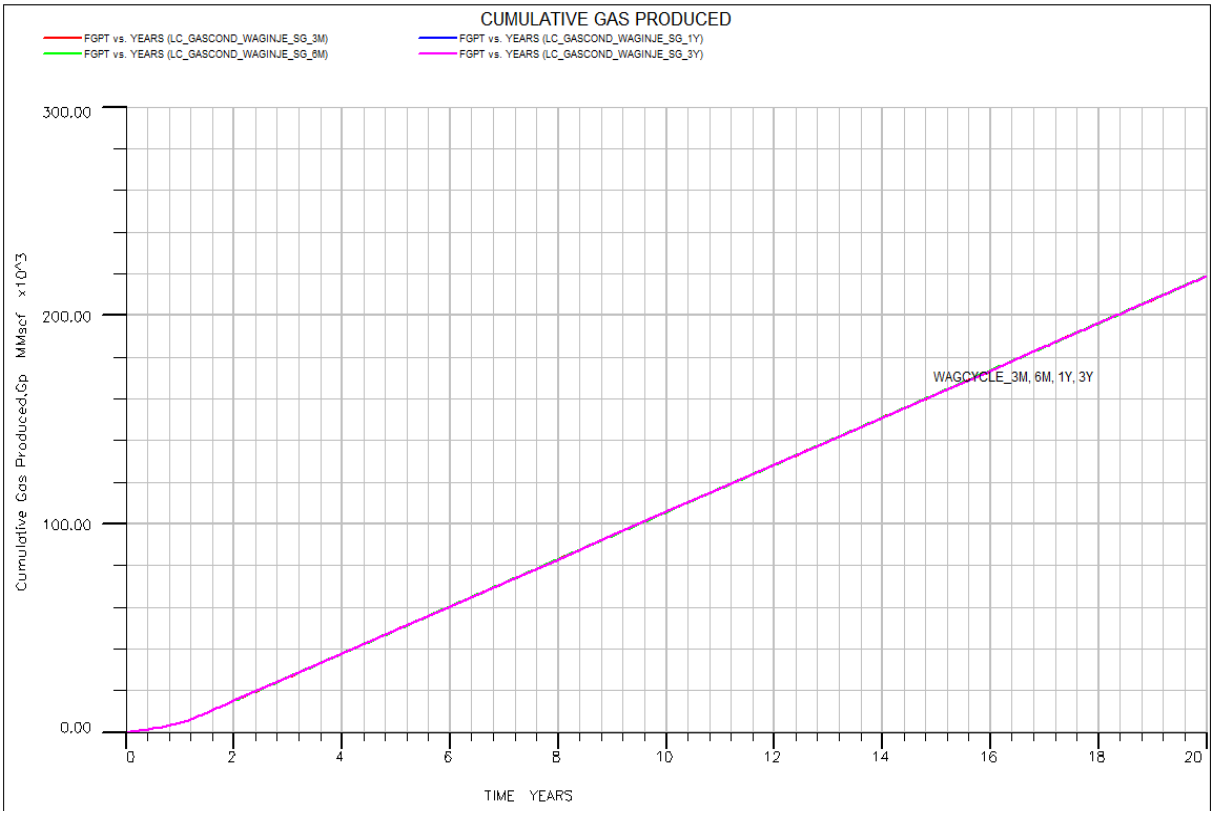

Figure C. 6:Cumulative gas produced (limited compositional model)

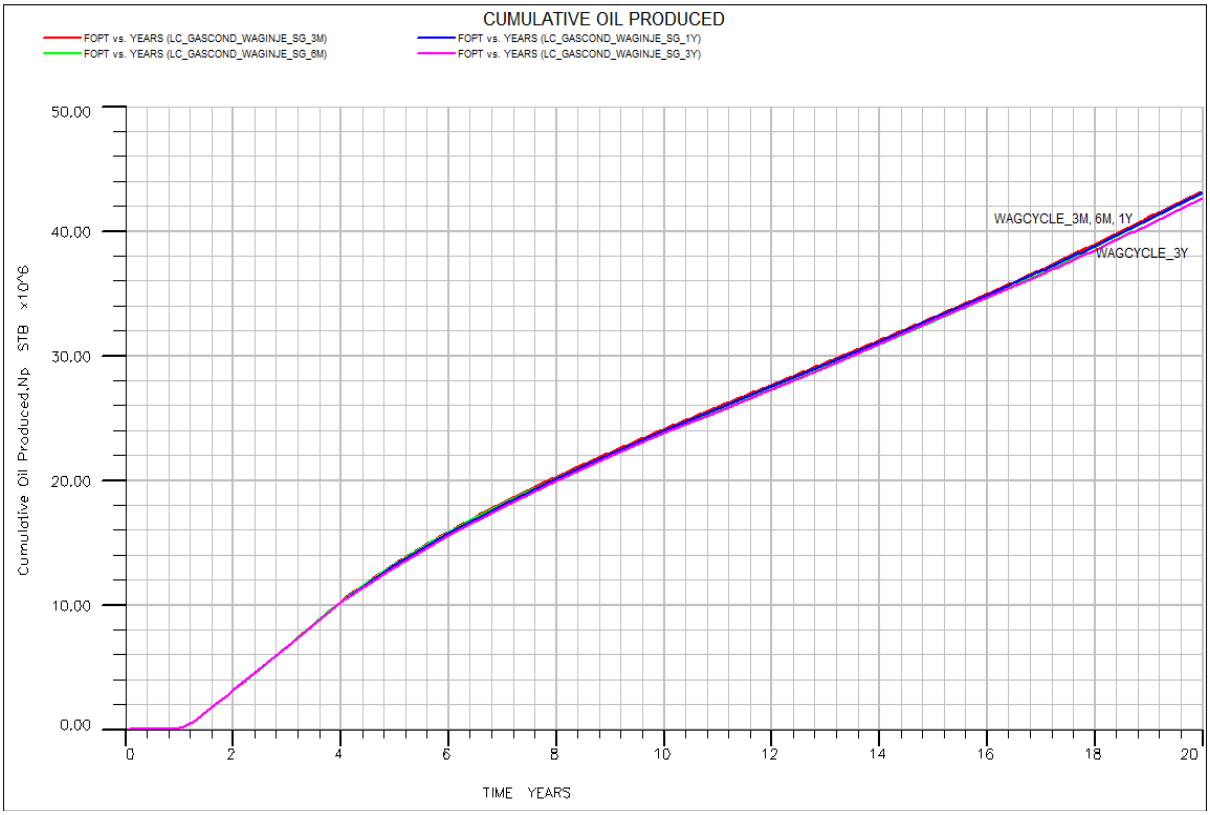

Figure C. 7:Cumulative oil production (limited compositional model)

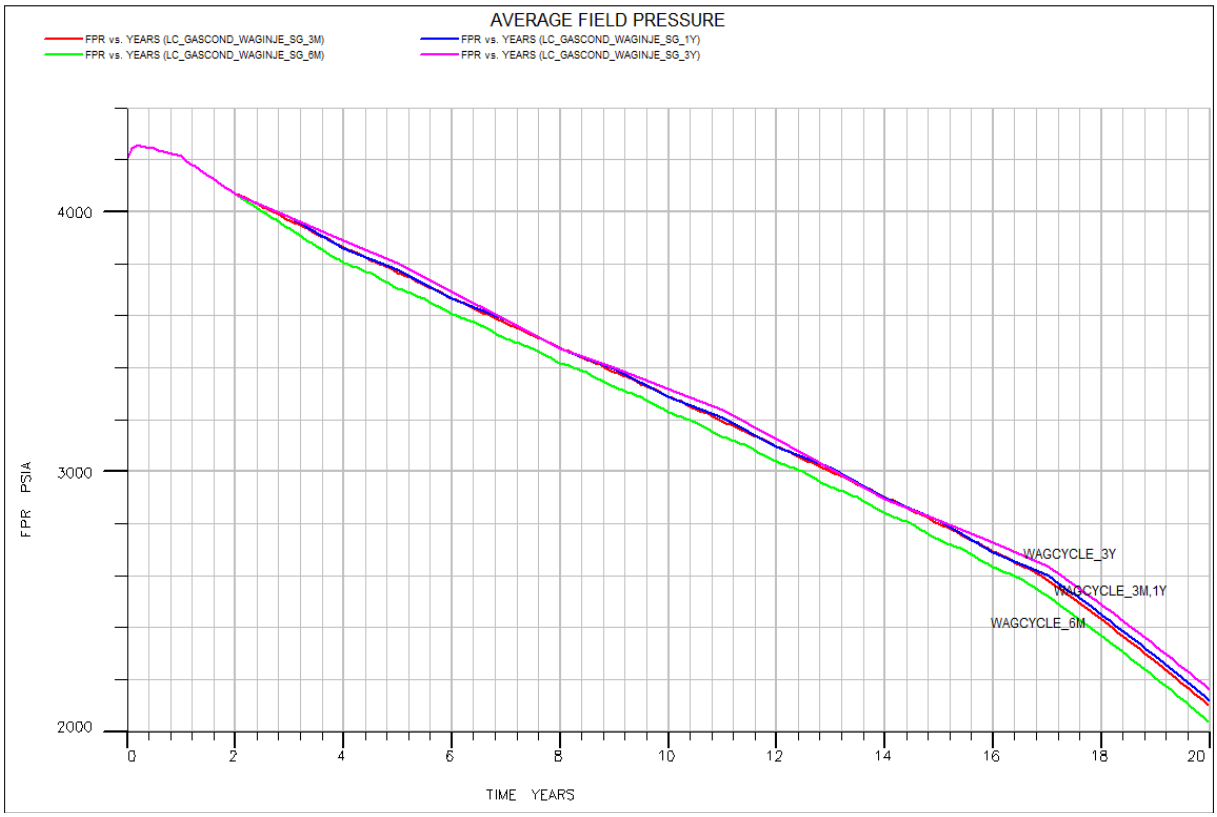

Figure C. 8:Average reservoir pressure (limited compositional model)

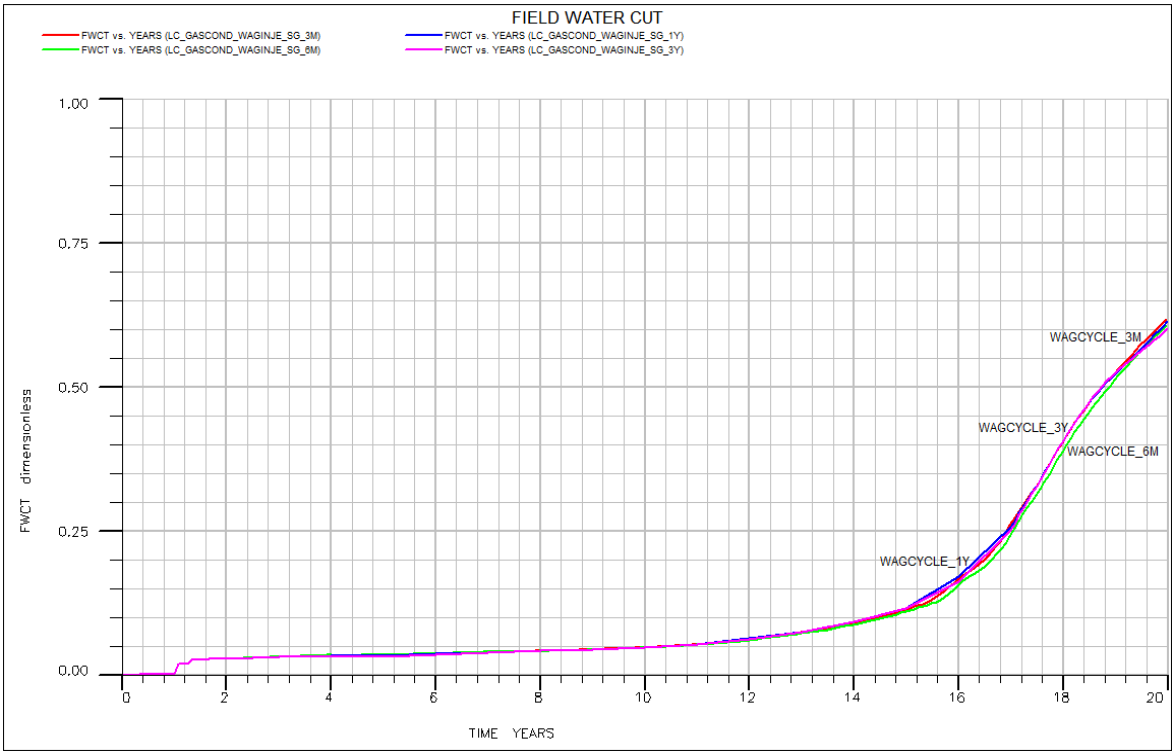

Figure C. 9:Field water cut (limited compositional model)

Vertical Communication Sensitivity (kv/kh Ratio)

A series of plots illustrating the effect of reduced vertical communication on cumulative condensate recovery, field pressure, and water cut are presented here for the SWAG scheme.

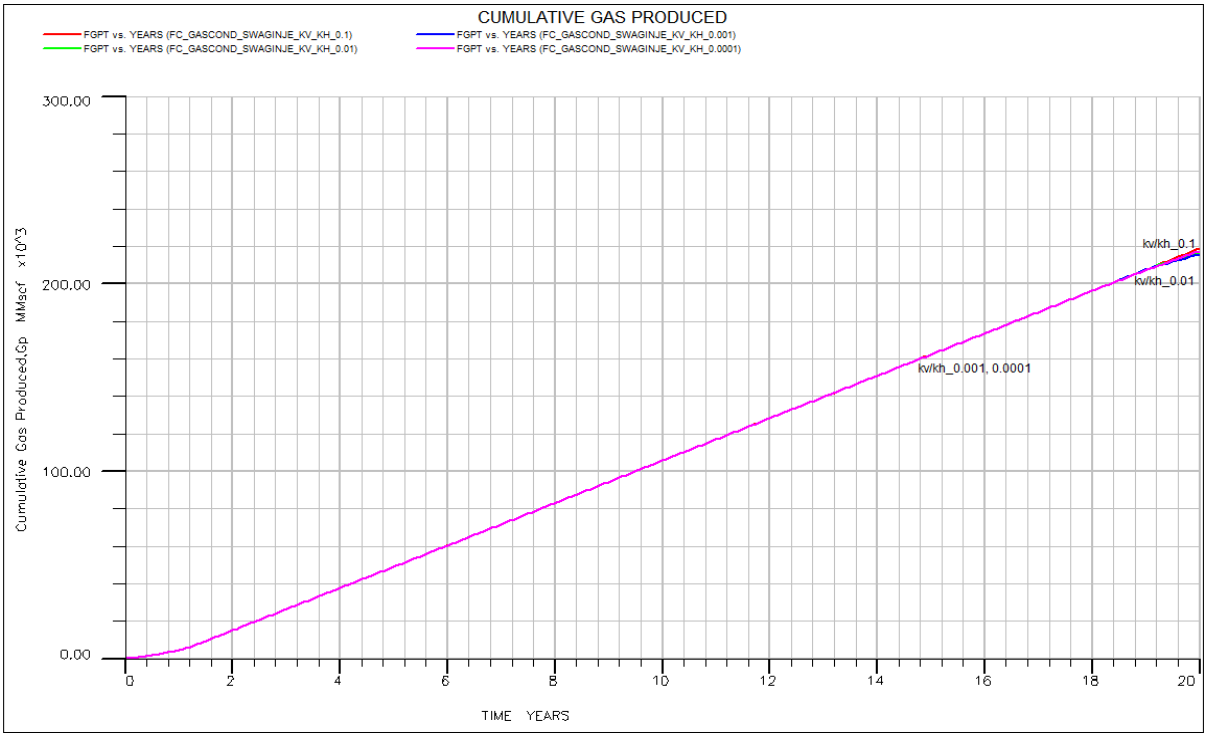

Figure C. 10:Cumulative gas production for SWAG injection (fully compositional model)

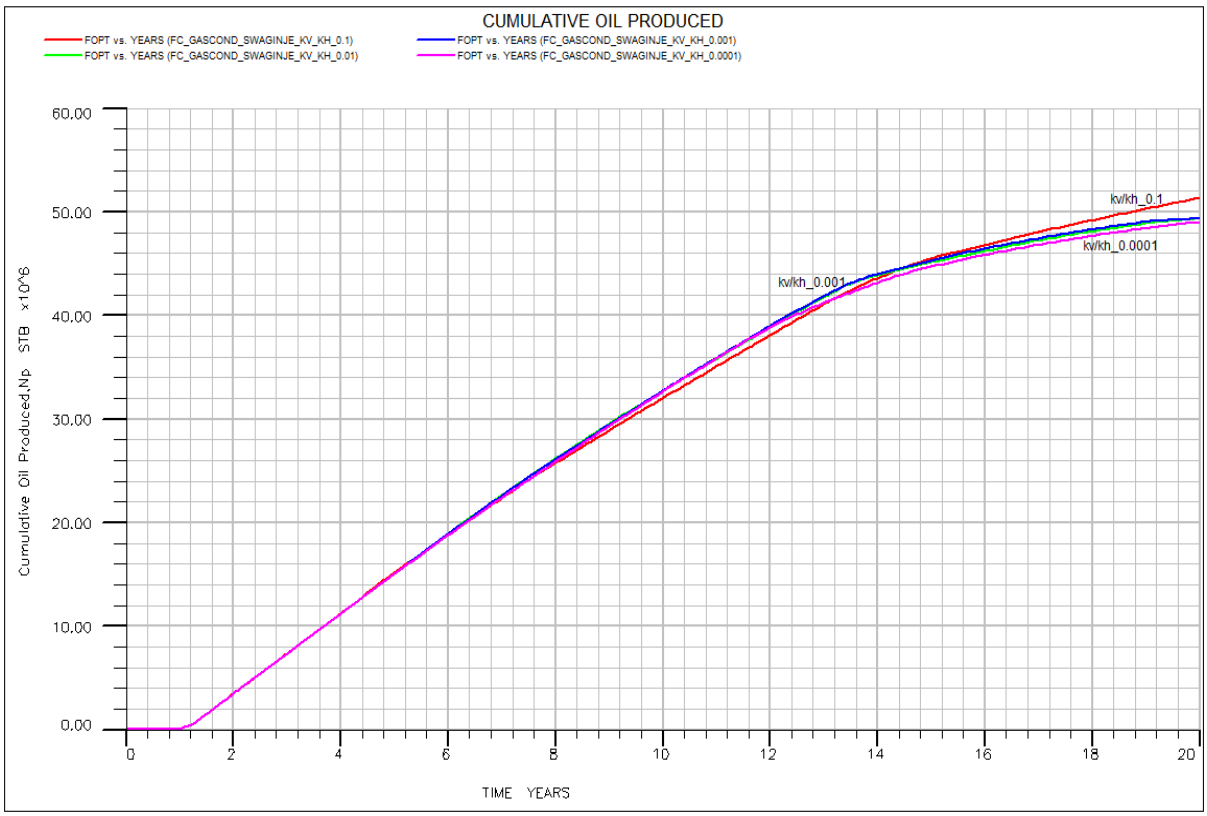

Figure C. 11:Cumulative oil production for SWAG injection (fully compositional model).

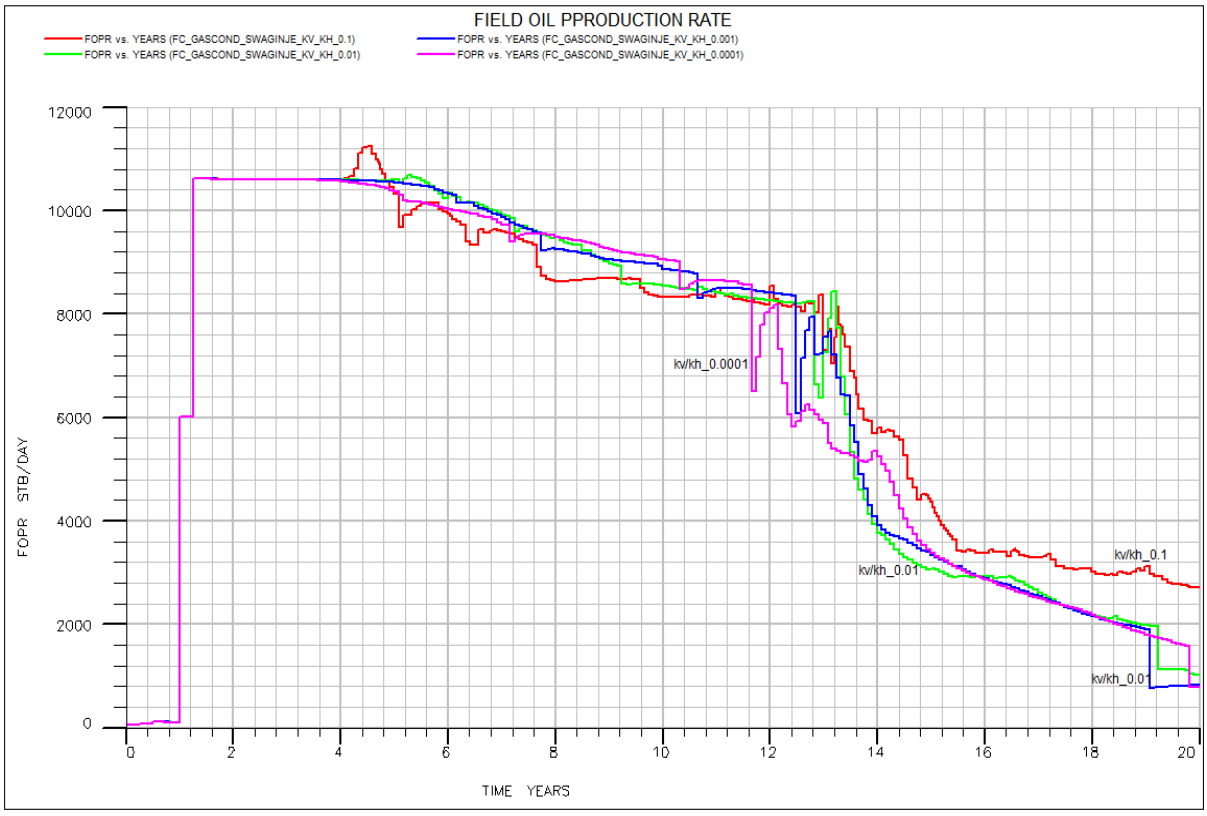

Figure C. 12:Oil production rate for SWAG injection (fully compositional model).

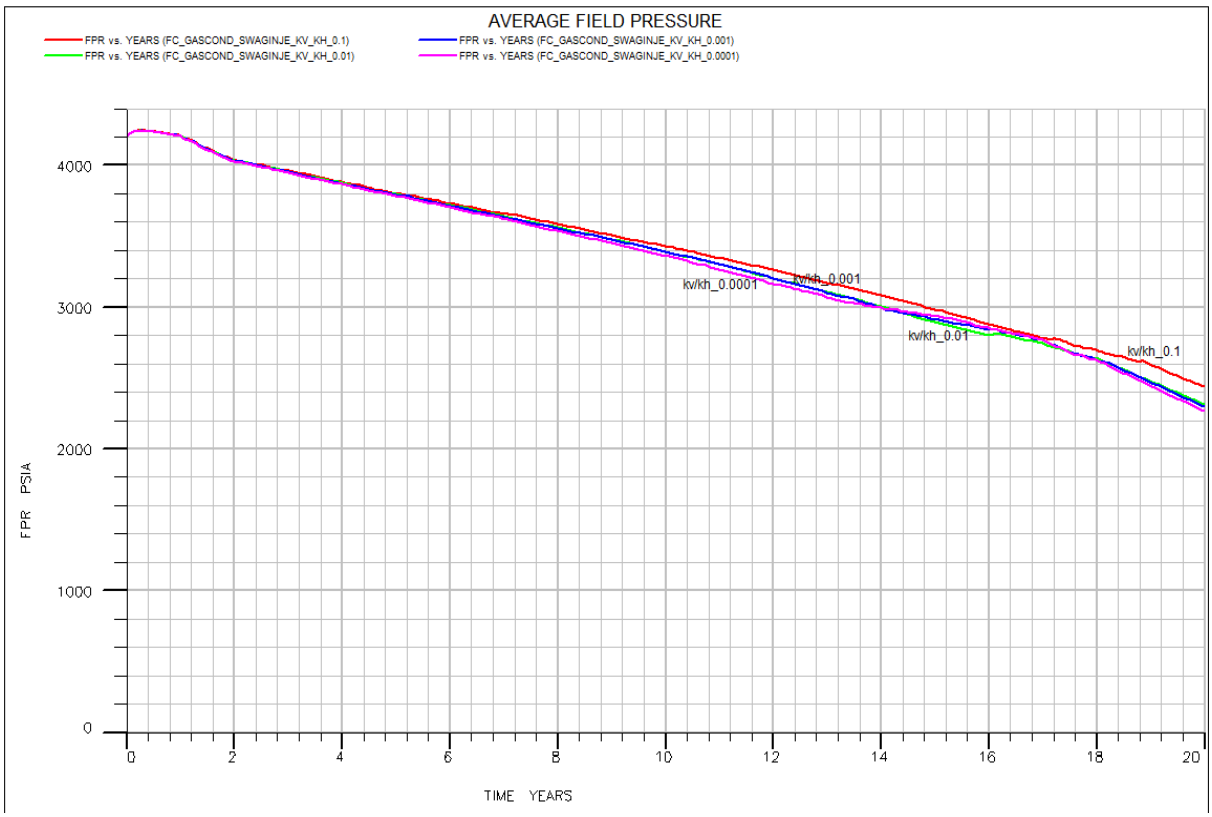

Figure C. 13:Field pressure for SWAG injection (fully compositional model).

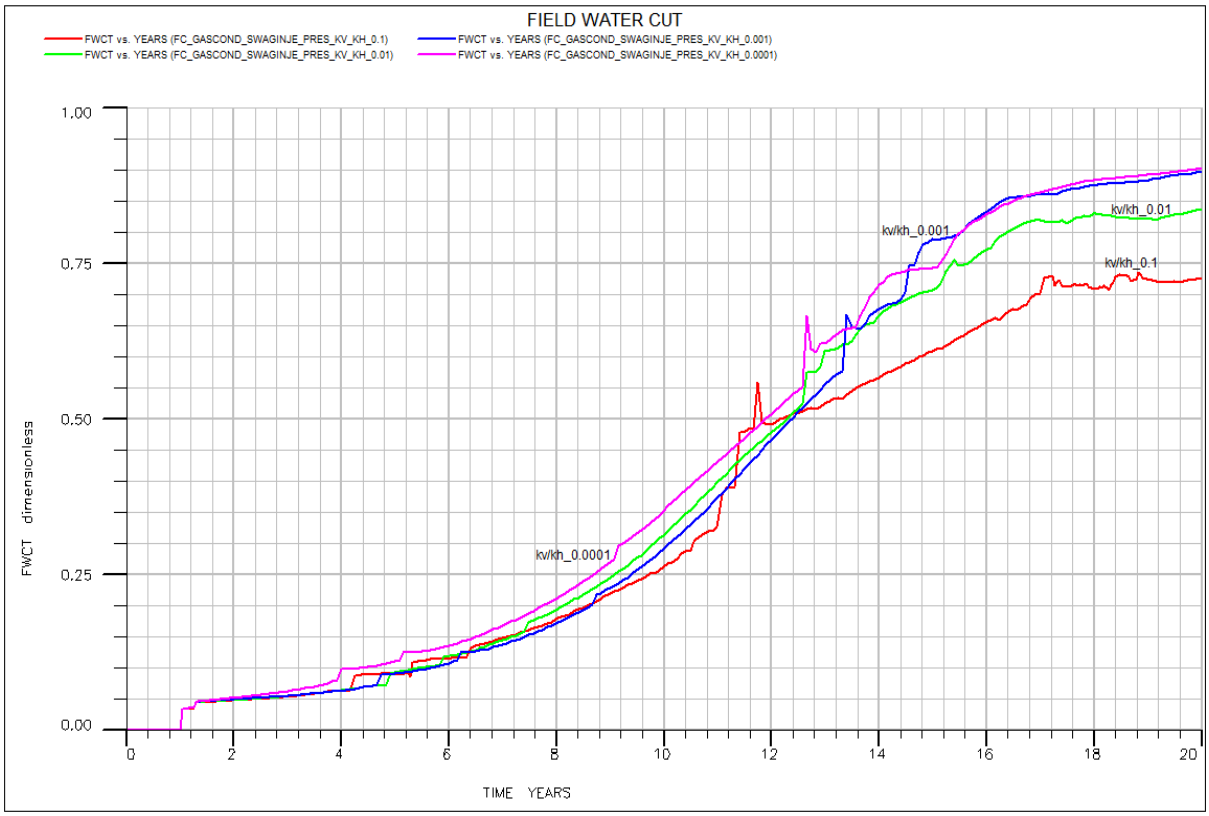

Figure C. 14:Field water cut for SWAG injection (fully compositional model).